School of Medicine and Surgery

Ph.D. program in Neuroscience, XXXIII cycle

Curriculum in Clinical Neuroscience

Motivation gone awry: investigations on aberrant reward processing in obesity and substance use disorder.

Thesis by:

Francantonio Devoto

835085

Tutor: Prof. Eraldo Paulesu

Supervisor: Dr. Laura Zapparoli

Coordinator: Prof. Rosa Maria Moresco

Academic year: 2019/2020

"Nova artificia docuit fames"

Seneca (Ep. 15,7)

Index

Abstract

Obesity and Substance Use Disorder (SUD) are chronic relapsing disorders characterized by pathological craving. Evidence suggests that craving can be prompted by the exposure to food or drug-related cues, and that current non-invasive brain stimulation techniques can be used to down-regulate craving. However, there is limited available information about (i) the influence of internal and external factors on the neural responses to food and drug cues, and (ii) on the neurobiological mechanisms beyond non-invasive brain stimulation applied to obesity.

In my thesis, I provide a systematic meta-analytical and fMRI investigation of these issues, demonstrating that several internal and external factors modulate the neural correlates of craving in obesity and SUD, and that excitatory deep TMS induces plastic changes in the neurofunctional brain organization in sample of obese individuals.

In the general introduction (**Chapter 1**), I describe the core neural networks involved in food and drug craving, within a unitary framework that accounts for the influence of several internal and external factors that modulate the neural responses to cues, in both obesity and SUD.

In **Chapter 2**, I combine a novel toolbox based on hierarchical clustering algorithm (Clustering the Brain, CluB) with the Activation Likelihood Estimation method to meta-analyze 22 studies on the influence of <u>weight-status</u> (healthy-weight vs. obese), <u>sensory modality of stimulus presentation</u> (visual vs. gustatory), and <u>satiety state</u> (hungry vs. satiated) on the neural responses to food cues. In particular, evidence from such main and interaction effects are taken as a benchmark to test the validity of the main neurocognitive theories of overeating and obesity.

In **Chapter 3**, I use the same method to meta-analyze 64 neuroimaging studies on the influence of <u>addiction severity</u> (addiction to legal vs. illegal substances) and <u>treatment status</u> (treatment-seeking vs. not-seeking treatment) on the neural drug cue-reactivity in SUD. Evidence from the main and interactive effects will be taken as a benchmark to discuss one of the most influential theories on the influence of treatment status and drug availability on the neural responses to drug cues.

An in-depth analysis of the meta-analytical method employed in Chapter 2 and Chapter 3 is reported in **Appendix A**, where I describe two validation studies demonstrating that CluB can (i) reliably extract a set of spatially coherent clusters of activations from a database of stereotactic coordinates, and (ii) test for factor-specific clusters of convergent activation within designs that cannot be usually implemented in a meta-analytical study.

In **Chapter 4**, I assess the neurofunctional changes associated with a 5-weeks deep rTMS treatment targeting the bilateral insular and prefrontal cortices to induce weight-loss and reducing food craving in a sample of 17 obese individuals undergoing excitatory (N=9) versus sham (N=8) stimulation. In particular, I apply a novel data-driven method on resting-state fMRI data to test that hypothesis that real, compared to sham, deep rTMS can induce plastic changes in the brain functional organization of key areas involved in food craving. Finally, I conclude with **Chapter 5**, where I integrate my findings into a unitary theoretical framework for the disorders of the motivation, discussing their implications for basic research and translational medicine.

Chapter 1 – General Introduction

1.1. "Bad habits" share a common neurobiological basis

It may be surprising that seemingly distant actions, such as eating a slice of pizza and smoking a cigarette, share largely overlapping neural substrates. However, the remarkable overlap between feeding and addiction is ancient, and it can be dated to about 1000 million years ago, when some of the neurotransmitters that mediate incentive behaviors evolved (Walker et al., 1996). Of those, dopamine (DA) is a major neurotransmitter of an highly preserved neurobiological mechanism that mediate the feeding behavior in different species, including humans (Gelperin, 1986).

DA-containing neurons project from the midbrain (ventral tegmental area, or VTA, and substantia nigra, or SN) to the ventral (nucleus accumbens or NAc) and dorsal striatal (caudate, putamen) complex (Butler and Hodos, 2005), and they likely evolved to facilitate the repetition of behaviors that sustain life and that result in a rewarding outcome, such as primary rewards (e.g., water, food, sex). To promote these adaptive behaviors, mesocorticolimbic DA neurons send ascending projections to, and receive projections from, brain regions involved in autonomic responses (hypothalamus, brainstem), memory (hippocampus), emotional reactivity and salience processing (amygdala, insula), and cognitive control (prefrontal cortex or PFC, anterior cingulate cortex or ACC). This collection of brain structures and neural pathways constitutes the so-called human "reward system" (Figure 1.1). If this neurobiological mechanism promotes adaptive behaviors, what has to do with maladaptive conditions such as addiction to drugs of abuse?

Crucially, both food and drugs have the capability of stimulating DA increase in key nodes of the reward system (Di Chiara and Imperato, 1988, Di Chiara et al., 1993, Bassareo and Di Chiara, 1999). Drugs of abuse, including heroin, cocaine, amphetamine, alcohol, and marijuana, exert their pharmacological effects on the reward system, activating mesolimbic DA neurons and their associated opioid receptors (Koob, 1992, Koob, 1996, Wise, 1996): by mimicking the neurobiological mechanisms that mediate the incentive motivation to pursue primary rewards, drugs of abuse can "hijack" the brain by signaling the presence of a huge benefit for the organism, facilitating the repetition of drug-seeking behaviors (Nesse and Berridge, 1997). As a consequence, drugs of abuse exert their pharmacological and motivational effects *via* the same neurobiological mechanism that evolved to reinforce the behaviors that are useful to address primary biological needs, such as eating.
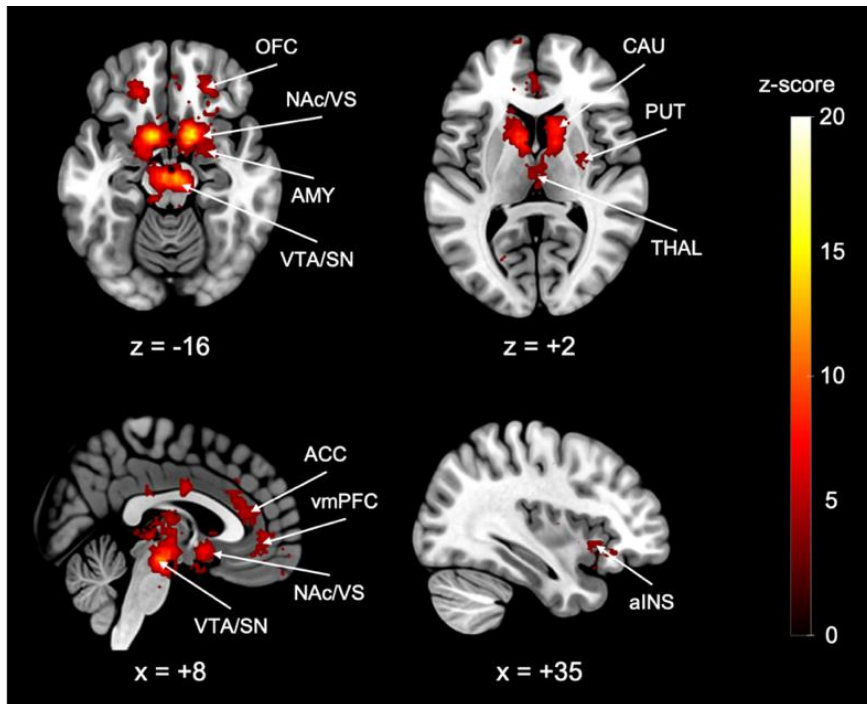
Figure 1.1. Brain areas involved in reward processing | The main subcortical and cortical structures of the reward system are displayed on an anatomical brain template. The statistical map is the result of an automated neuroimaging meta-analysis (association test, p > .01 FDR-corrected) of reward-related studies performed by means of Neurosynth (www.neurosynth.org/analyses/topics/v4-topics-400/332). Slice coordinates are reported in MNI stereotaxic space. ACC, Anterior Cingulate Cortex; aINS, anterior insula; AMY, amygdala; CAU, caudate nucleus; NAc/VS, Nucleus accumbens/ventral striatum; OFC, orbitofrontal cortex; THAL, thalamus; vmPFC, ventromedial prefrontal cortex; VTA/SN, ventral tegmental area/substantia nigra.

Perhaps unsurprisingly, the dysregulation of both food and drug intake is linked, at least in part, to an aberrant functioning of the reward system. In humans, one of the earliest evidence pointing to a shared pathophysiology between obesity and substance-use disorder (SUD) comes from a seminal paper by Wang and colleagues (Wang et al., 2001). By means of Positron Emission Tomography (PET) and [C-11]raclopride (a radioligand for the D2 DA receptors), the authors observed a marked reduction of D2 receptor availability in the striatum of obese compared to healthy-weight individuals; further, in obese subjects, D2 receptor availability correlated with the Body-Mass Index (BMI, an indirect measure of adiposity) such that the higher the BMI, the lower the availability of D2 receptors (Wang et al., 2001). Because lower striatal D2 receptor availability was also observed in SUD, including heroin (Wang et al., 1997), cocaine (Volkow et al., 1993), and alcohol dependence (Hietala et al., 1994), the authors suggested that a D2 receptor deficiency is associated with the addictive behavior, irrespective of the type of reward (Wang et al., 2001).

Indeed, accumulating evidence suggests that reward system malfunctions are not only observed in obesity and SUD, but they are also present in other disorders of the motivation,

including, for example, internet pornography addiction (Brand et al., 2016), and gambling disorder (Limbrick-Oldfield et al., 2017). In other words, reward system dysfunctions seem to be involved in every situation where "habits", whether they are directed toward biologically relevant (e.g., food, sex) or irrelevant stimuli (e.g., drugs, gambling), become "bad" and out of control.

Since the publication of the seminal work by Wang and colleagues in 2001 (Wang et al., 2001), there has been an explosive growth in the number of neuroimaging studies, including PET and functional Magnetic Resonance Imaging (fMRI), published on obesity and addiction (Figure 1.2). As the reader shall see in the next sections, much of the neuroscientific research in these fields focused on the study of the neural correlates of *craving*, that is a strong and compelling desire to seek, and to consume, a reward. In particular, human neuroimaging research has been dominated by the use of the "cue-reactivity" paradigm: a simple experimental procedure that consists in the examination of the physiological, behavioral, and subjective responses to the controlled exposure to food or drug-related stimuli.
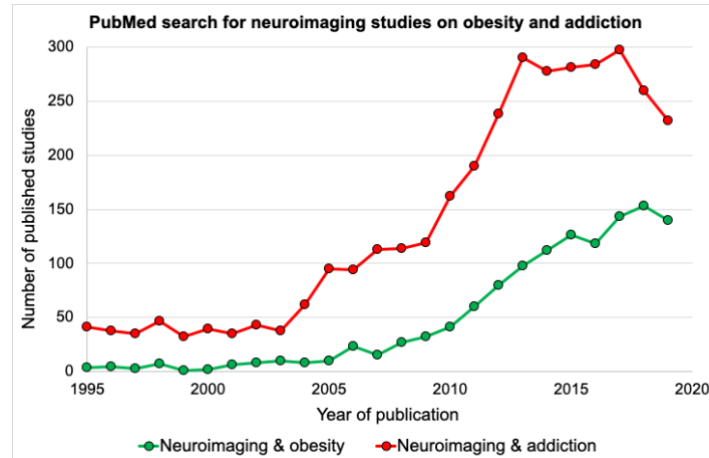
Figure 1.2. PubMed search for neuroimaging studies on obesity and addiction | Number of neuroimaging studies published from year 1995 to 2019 for the two queries: "neuroimaging AND obesity" (green) and "neuroimaging AND addiction" (red). PubMed search performed on September 28th, 2020.

In what follows, I will first describe the major brain circuits underlying cue-reactivity in obesity and SUD. Then, based on the available neuroimaging literature, I will discuss the influence of the main internal and external factors that modulate the neural reactivity to cues in obesity and SUD, in light of a unitary model. In particular, I will focus on the use of meta-

analytical approaches: these are making it possible the testing of complex effects according to factorial designs (e.g., the interaction between drug cues, treatment status and nature of the drug of abuse), by combining information coming from disparate sources in ways that single prospective studies cannot afford.

Finally, I will discuss the role of brain-centred treatments in the management of obesity and addiction, with particular reference to the effects of non-invasive brain stimulation and modulation techniques, such as the Transcranial Magnetic Stimulation (TMS) and the transcranial Direct Current Stimulation (tDCS), in the reduction of craving.

1.2. Images of desire: the neural correlates of cue-reactivity

An effective description of the experience of the cue-induced craving, and of its real-life consequences, is reported in Childress et al. 1993, page 1: "Jimmy[1] pulls out of the graveled driveway onto the smooth asphalt surface of the road. It feels so good to drive again after the long months in "rehab." No heroin use in over 6 months. 'Not bad', he congratulates himself. But as he takes the exit into the old neighborhood, his bowels begin to growl. He breaks out in sweat, gripping the steering wheel and trying to ignore the raw, acid taste in the back of his throat. Yawning, eyes watering, he feels mounting panic, and the desire for drugs begins to burn in the pit of his stomach. 'So much for good intentions', he mutters, turning toward a familiar alley and the drug that will make everything right again." (Childress et al., 1993). The mere sight, or spontaneous thought, of a cue (e.g., the street) associated with a reward (e.g., heroin) can be a powerful trigger of craving, and it can override long-term goals (e.g., quitting heroin use), leading to relapse (Niaura et al., 1988, Courtney et al., 2016). Notwithstanding the obvious differences between the two rewards, it is reasonable to expect a similar scenario in individuals who try to stick on a diet: the simple sight of a fast-food sign near home may frustrate the efforts to lose weight. The cue-reactivity paradigm, combined with neuroimaging techniques, offers a window into the neural circuits that mediate those processes. These include, of course, not only the sensory, hedonic, and motivational reactions to such cues, but also higher-order attentional, decision-making, and inhibitory control processes.

Dovetailing with the complexity of the phenomenon, several reviews (Dagher, 2012, Garrison and Potenza, 2014, Giuliani et al., 2018) and meta-analyses (Chase et al., 2011,

---

[1] Not the real name of the patient, as the authors specified in their manuscript.

Kühn and Gallinat, 2011, van der Laan et al., 2011, Engelmann et al., 2012, Brooks et al., 2013, Schacht et al., 2013, Huerta et al., 2014, Kennedy and Dimitropoulos, 2014, Pursey et al., 2014, van Meer et al., 2015) have highlighted the role of a distributed network of brain regions that are recruited during endogenous (e.g., spontaneous thoughts, mental imagery) and exogenous (e.g., perceptual) cue-reactivity. From a functional point of view, these can be broadly categorized into two main circuits: those underlying the sensory, hedonic, and motivational reactions to cues (cue-reactivity), and those supporting the regulation and valuation of such cue-reactivity (cue-regulation) through higher-order attentional, decision-making, and inhibitory control processes (Figure 1.3). Even if the former is more tightly related with "bottom-up" processes prompted by the exposure to cues, and the latter is more tightly linked to "top-down" control processes, it is important to underline that these two circuits do not always operate in antithesis and, as such, they do not represent a dual "go/no-go" system.
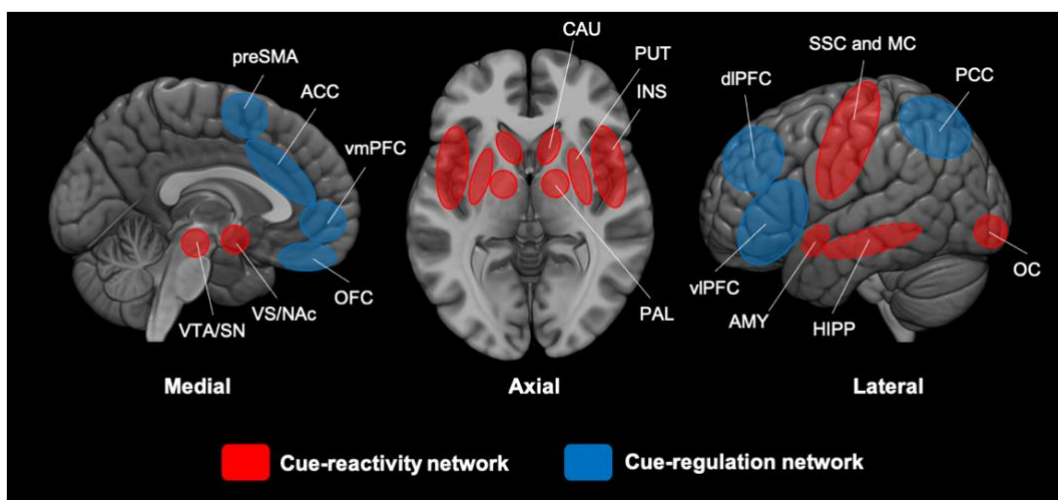
Figure 1.3. Schematic representation of the main brain circuits involved in the reactivity and regulation of food and drug cues | The major brain networks identified in cue-reactivity studies can be broadly categorized into a "cue-reactivity" network, subserving sensory, hedonic, and motivational reactions to cues (red), and into a "cue-regulation" network, involved in also higher-order attentional, decision-making, and inhibitory control processes (blue). Dotted circles represent medial structures on lateral surface. ACC, anterior cingulate cortex; AMY, amygdala; CAU, caudate; dlPFC, dorsolateral prefrontal cortex; HIPP, hippocampus; INS, insula; MC, motor cortex; NAc, nucleus accumbens; OC, occipital cortex; OFC, orbitofrontal cortex; PAL, pallidum; preSMA, pre supplementary motor area; SN, substantia nigra; SSC, somatosensory cortex; VS, ventral striatum; VTA, ventral tegmental area.

Both networks play a crucial role in the regulation of food and drug intake, as demonstrated by prospective neuroimaging studies linking neural cue-reactivity to different behavioral and clinical outcomes. In human overweight/obese individuals, activity in several brain regions, including the striatum, sensory cortices, insula, and PFC (Stice et al., 2010b, Murdaugh et al., 2012, Yokum et al., 2014), can predict weight-change at different follow-ups, suggesting that food cue-reactivity may be employed to predict weight trajectory and the outcome of weight-loss interventions. These findings can be extended to addiction, where similar brain activation patterns in response to drug cues were found to predict subsequent relapse (Grüsser et al., 2004), reinforcing the notion that neural responsivity to reward-related cues can be used as a predictive biomarker also in SUD (Janes et al., 2010, Li et al., 2015, Courtney et al., 2016). Overall, this is evidence that neural cue-reactivity inside the scanner can be a reliable proxy of the real-life brain dynamics that may contribute to the enduring of obesity and addiction.

Nevertheless, real-life encounters with food or drug-related cues occur in a variety of forms, and reactions to such cues also depend on as many contingencies. Watching food-related commercials after dinner is different from watching the same advertisement when dinner is approaching; similarly, watching alcohol-related commercials may feel different for alcohol-dependent individuals who are under treatment compared to those who are not. In what follows, I will provide a brief survey of the empirical studies investigating the factors that modulate the neural reactivity to food and to drug cues.

These findings will be discussed in light of a unitary model, with particular reference to the most studied factors for obesity and addiction.

1.3. Factors modulating the neural reactivity to food and drug cues

Recently, Jasinska and colleagues, based on a survey of neuroimaging studies, proposed a model of the factors that modulate the neural drug cue-reactivity in addiction research (Jasinska et al., 2014). In particular, the authors suggested that a variety of individual-specific (e.g., addiction severity, treatment status, abstinence/withdrawal status, length and intensity of drug use, stressor exposure) and study-specific factors (e.g., drug availability, sensory modality and length of cue presentation, implicit/explicit regulation of craving) can either up or down-regulate the neural responses to drug cues. I adapted this model[2] to provide

---

[2] I acknowledge that the present model is far from being complete, as it does not include many other factors that can modulate the neural reactivity to food and to drug cues (e.g., gender, developmental

a unitary framework that accommodates the factors that modulate the neural reactivity to food cues in obesity within a drug-related model (Figure 1.4).

These factors are expected to act in isolation, by up or down-regulating the responses of the cue-reactivity and cue-regulation networks, or in interaction, giving rise to specific brain activation patterns. Below, I will review the most relevant internal (genetic and developmental, cognitive and physiological) and external (cue-specific, environmental) factors that are known to modulate the neural reactivity to food and to drug cues: whenever possible, studies on obesity and SUD will be discussed in parallel.
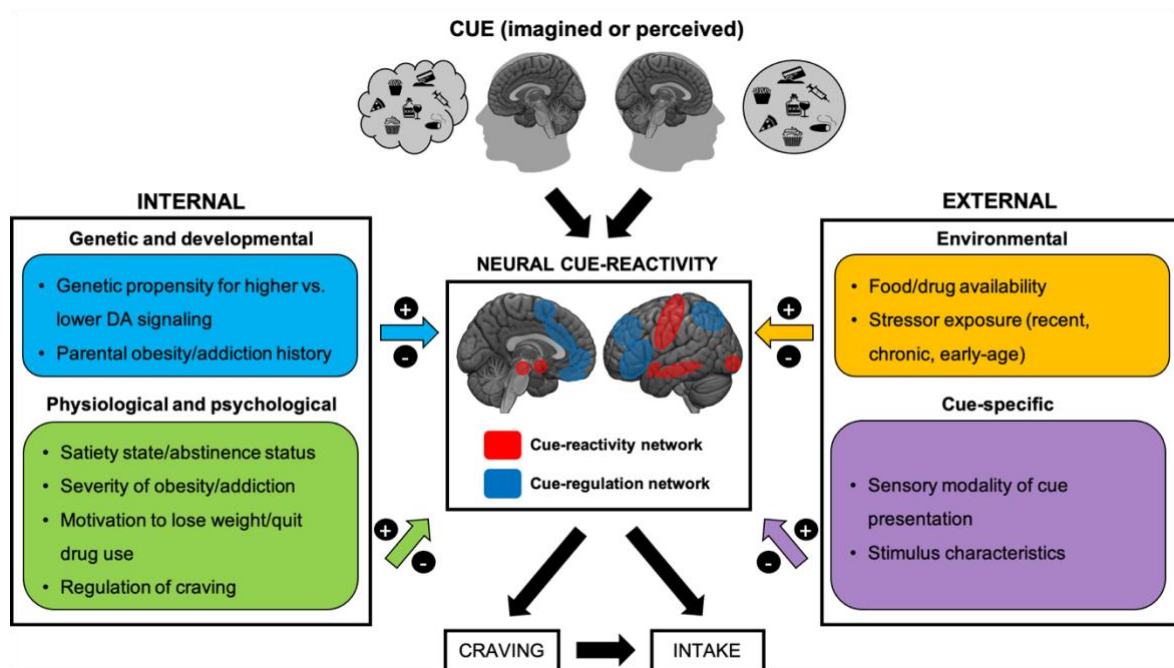
Figure 1.4. Factors modulating the neural cue-reactivity to food and/or drug cues | This simplified model, adapted from Jasinska et al., 2014, displays the main internal (genetic and developmental, physiological and psychological) and external factors (cue-specific, environmental) that modulate the neural response to food and/or drug cues in obesity and SUD. These factors are expected to act in isolation, by up (+) or down-regulating (-) the responses of the cue-reactivity and/or cue-regulation network, or in interaction, giving rise to specific brain activation patterns. These, in turn, are expected to influence craving and, ultimately, food or drug intake.

---

stage, length of cue-presentation, duration of the disease, just to name a few). Such an in-depth review would be beyond the scope of the present introduction: conversely, I hope that a unitary, yet incomplete, model will prove useful to ease the interpretation of the vast and heterogeneous literature on the neural cue-reactivity.

The purpose of the current review is twofold: first, to provide an overview of the major factors that modulate the activity of the cue-reactivity and cue-regulation networks, in light of a unitary neurocognitive framework that may guide future research on the neural cue-reactivity in obesity and SUD; second, to highlight the need of empirical and meta-analytical studies aimed at assessing complex factorial designs, in order to explore the main and the interactive effects of the factors under examination.

Specific attention will be directed to the most studied factors in the domain of obesity (e.g., obesity severity or weight status, sensory modality of stimulus presentation, satiety state) and SUD (e.g., addiction severity, treatment status or drug availability).

1.3.1. Internal factors: genetic and developmental

Genetic differences can account up to the 70% of the vulnerability to obesity (Baessler et al., 2005) and addiction (Uhl et al., 2002), and the genetic make-up can also account for the inter-subject variability in the neural responses to food and drug cues. For example, the TaqIA (rs1800497) polymorphism in chromosome 11 is associated with greater DA signaling capacity: subjects with A2/A2 genotype seem to have 30–40% more dopamine D2 receptors (Pohjalainen et al., 1998, Ritchie and Noble, 2003). Interestingly, higher caudate activity in response to milkshake cues predicted future weight gain in a sample of adolescents, but only in those possessing the TaqIA A2/A2 allele, whereas the opposite was found in those adolescents possessing one or more TaqIA A1 allele (i.e., lower caudate activity in response to the same gustatory cue predicted weight gain) (Stice et al., 2008a, Stice et al., 2015a). Similar results were found in adults with respect to amygdala activation in response to milkshake gustatory cues (Sun et al., 2015).

Genes associated with the regulation of DA neurotransmission are also found to influence the neural reactivity to drug cues. The dopamine receptor 4 variable number tandem repeat (DRD4 VNTR) polymorphism codes the dopamine 4 (D4) receptor: individuals possessing the 7-repeat (or longer, DRD4 L) allele display greater cue-induced craving for smoking (Hutchison et al., 2002) and heroin (Shao et al., 2006); further, compared to those without one or two longer DRD4 VNTR allele, those possessing the DRD4 L allele exhibit greater responses of the cue-reactivity and cue-regulation networks, such as the insula and the superior PFC, in response to visual cigarette-related cues (McClernon et al., 2007). Similarly, alcohol-dependent subjects having the DRD4 L allele showed greater activity of the anterior cingulate cortex (ACC), orbitofrontal cortex (OFC), and striatum in response to alcohol taste cues compared to litchi juice (Filbey et al., 2008).

With respect to **developmental factors**, it suffices to mention that pre-natal exposure to nicotine increase the risk of nicotine dependence (Buka et al., 2003), and obesity (Toschke et al., 2003), in the offspring. Few studies investigated the modulatory role of parental obesity/SUD status on the neural responses to food or drug cues in the offspring. One study showed that healthy-weight adolescents with two obese or overweight parents exhibit greater activity of the striatum and OFC in response to milkshake taste cues compared to healthy-weight adolescents with two lean parents (Stice et al., 2011a). Likewise, another study showed that non-substance using adolescents with one or two parents with an history of substance use/dependence, compared to those without parents with drug use/dependence history, showed greater midbrain responsivity to milkshake taste receipt (Stice and Yokum, 2014), suggesting that family history of obesity and addiction both modulate the neural reactivity to food cues.

A schematic representation of the hypothetical modulation (up or down-regulation) of the genetic and developmental factors reviewed here on the cue-reactivity and cue-regulation networks is given in Figure 1.5.
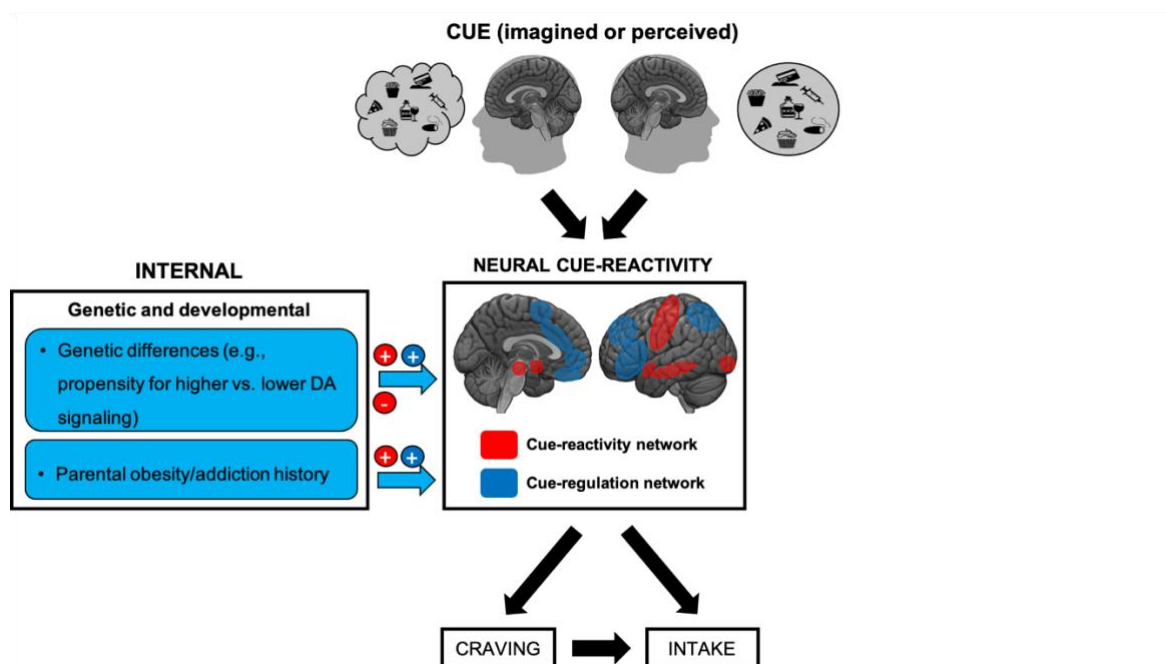
Figure 1.5. Genetic and developmental factors modulating the neural cue-reactivity | Hypothetical model describing the up (+) and down-regulation (-) of the cue-reactivity (red circle) and cue-regulation networks (blue circle) as a function of the genetic and developmental factors considered.

1.3.2. Internal factors: physiological and psychological

A number of physiological (e.g., satiety and abstinence status, disease severity) and psychological factors (e.g., motivation to lose weight/quit drug use, explicit or implicit regulation of craving) modulate the neural responses to food and drug cues. Of particular interest are the roles of **satiety and abstinence** in modulating the neural responses to food and drug cues, respectively. Compared to healthy weight individuals, obese patients exhibit greater activity of the ACC and medial PFC in response to visual food cues prior to a meal (Martin et al., 2010), supporting the notion that hunger potentiates the neural responses to food cues, and even more so in obesity. Critically, in the same study, activity in the medial PFC in response to food cues decreased after a meal only in healthy weight participants, suggesting that altered satiety signaling may contribute to the enduring of obesity. Indeed, obese compared to healthy weight individuals display greater activity of several brain regions, including the PFC, OFC, insula, amygdala, and striatum in response to visual drug cues, even when they are satiated (Dimitropoulos et al., 2012, Holsen et al., 2012, Cornier et al., 2013, Martens et al., 2013). These results are broadly confirmed by two neuroimaging meta-analyses that addressed the role of satiety in modulating the neural response to food cues in obesity (Kennedy and Dimitropoulos, 2014, Pursey et al., 2014). Similarly, short-term abstinence was shown to up-regulate the neural reactivity to drug cues in nicotine (McClernon et al., 2005), alcohol (Fryer et al., 2013), and heroin addiction (Li et al., 2013a), and it has been associated with increased responses in the thalamus, hippocampus, striatum, insula, and the PFC, including the ACC. Greater PFC and cerebellar activity in smoking-deprived individuals exposed to smoking cues was also reported by a meta-analysis of neuroimaging studies on nicotine SUD (Engelmann et al., 2012). Conversely, long-term compared to short-term abstinence is usually associated with a decreased neural cue-reactivity, in line with the idea that long-term abstinence can decrease the motivational salience of drug-associated stimuli (Lou et al., 2012, Li et al., 2013a).

The **severity of obesity or addiction** status is another factor capable of modulating the neural reactivity to food and drug cues. The BMI, an indirect index of adiposity and severity of obesity, is positively associated with the neural response to drug cues in regions involved in the sensory, hedonic, and motivational responses to food cues (e.g., striatum, somatosensory cortex, insula), as well as in brain regions involved in the regulation and evaluation of food-related cues (e.g., OFC, PFC) (Rothemund et al., 2007, Martens et al., 2013). Accordingly, neuroimaging meta-analyses on food cue-reactivity show that obese

compared to healthy weight individuals exhibit convergent hyper-activity of limbic and frontal regions in response to food cues, as well as convergent hypo-activity of the left dlPFC and insular cortex (Dimitropoulos et al., 2012, Brooks et al., 2013, García-García et al., 2014, Pursey et al., 2014). Dovetailing with the evidence that obesity severity is associated with an up-regulation of the neural substrates of cue-reactivity, neuroimaging studies on SUD have shown that addiction severity, measured via self-reported questionnaires and clinical interviews, is positively associated with DA release in the striatum (Volkow et al., 2006), and with the neural response to drug cues in the cue-reactivity network, including the striatum, amygdala, insula, and in the cue-regulation network, including the ACC, the supplementary motor area, and the parietal cortex (Smolka et al., 2006, Claus et al., 2011). Results of neuroimaging meta-analyses on drug cue-reactivity in SUD are largely in line with the notion that exposure to drug-associated cues, in individuals with SUD compared to light users or healthy controls, is associated with an up-regulation of key regions of the cue-reactivity (e.g., striatum, insula, amygdala, hippocampus) and cue-regulation networks (e.g., vmPFC, OFC, ACC) across different populations of SUD (heroin, cocaine, alcohol, nicotine) (Chase et al., 2011, Kühn and Gallinat, 2011, Engelmann et al., 2012, Tang et al., 2012a, Schacht et al., 2013, Hanlon et al., 2014). Overall, disease severity is associated with an up-regulated response to food and drug cues, in key areas of the cue-reactivity and cue-regulation networks.

Finally, two other internal psychological factors can modulate the neural activity to food and/or drug cues: the regulation of craving and treatment status, or motivation to quit drug use. **Explicit regulation of craving**, associated with different cognitive reappraisal strategies (i.e., mindful attention, thinking about long-term costs of eating high-calories palatable food/drug use, thinking about long-term benefits of not eating/using it, and actively suppressing food/drug craving) have been associated with increased activity of cue-regulation regions (e.g., ventrolateral PFC or vlPFC, dorsolateral PFC or dlPFC) and a concurrent decrease in activity of cue-reactivity and attention-related regions (e.g., VTA, ventral striatum, amygdala, precuneus, posterior cingulate cortex, parietal regions) during food-related (Kober et al., 2010, Scharmüller et al., 2012, Siep et al., 2012, Yokum and Stice, 2013, Tuulari et al., 2015) and drug-related stimulation (Volkow et al., 2010, Hartwell et al., 2011, Westbrook et al., 2013). The overall evidence supports the view that **explicit cognitive regulation of craving down-regulates** the **cue-reactivity network** in favor of an up-regulation of the **cue-regulation network**.

A schematic representation of the hypothetical modulation (up or down-regulation) of the physiological and psychological factors reviewed here on the cue-reactivity and cue-regulation networks is given in Figure 1.6.
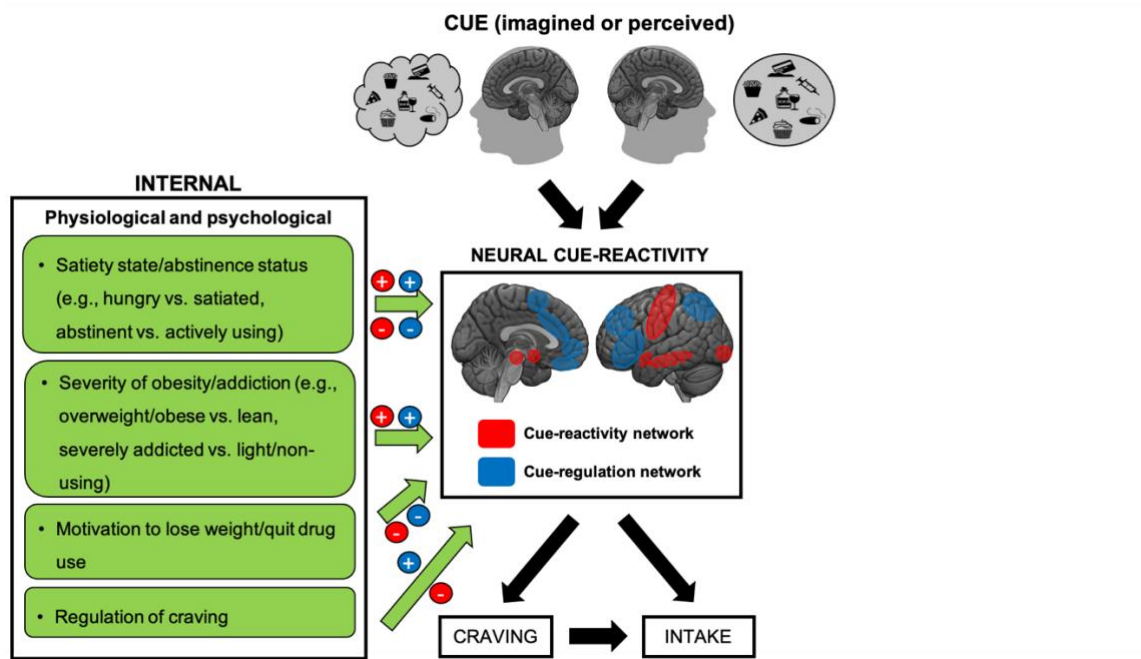
Figure 1.6. Physiological and psychological factors modulating the neural cue-reactivity | Hypothetical model describing the up (+) and down-regulation (-) of the cue-reactivity (red circle) and cue-regulation networks (blue circle) as a function of the physiological and psychological factors considered.

In SUD, there is also evidence that an explicit **motivation to change s**ubstance use, as reported by a self-reported questionnaire, is associated with a decreased reactivity to cocaine-related versus neutral pictures in a wide network of brain regions comprising the frontal, temporal, and occipital cortices (Prisciandaro et al., 2014). To the best of my knowledge, no studies investigated the neural correlates of the explicit motivation to change food intake in obesity. Still, studies on treatment-seeking obese individuals (i.e., individuals who are motivated to alter their eating habits) examining the neural predictors of future weight-loss can provide some insights. In one study, lower responses to food cues in key regions of the cue-reactivity (e.g., striatum, insula, occipital cortex) and cue-regulation networks (e.g., PFC, parietal cortex) predicted greater weight-loss at a 12-weeks follow-up in a sample of treatment-seeking overweight and obese individuals (Murdaugh et al., 2012). Similarly, decreases in striatal (caudate, putamen, pallidum) activity in response to food cues

after 1-month of weight-loss intervention were associated with greater total weight-loss at 6-months at the end of the intervention, in a sample of obese individuals (Hermann et al., 2019). Overall, these findings suggest that explicit and implicit (as indexed by the treatment status) motivation to change is associated with a lower reactivity to food-cues, particularly in the cue-reactivity network.

It is worthy to note that the effect of treatment status is mediated by at least two different aspects: the motivation to change, and the expectation to consume food or drug soon after cue exposure, or food/drug availability (Wilson et al., 2005, McBride et al., 2006, Blechert et al., 2010). As the availability of the reward is here considered as an external factor, its influence over the neural reactivity to food and drug cues will be discussed below.

1.3.3. External factors: environmental

Treatment status, conceived as a proxy of **drug availability** and expectancy to consume the substance, is one of the most studies factors that modulate the neural cue-reactivity in SUD (Grant et al., 1996, Wilson et al., 2004, Wilson et al., 2005, McBride et al., 2006, Wilson et al., 2012, Hayashi et al., 2013, Prisciandaro et al., 2014). In particular, Wilson and colleagues, based on the review of nineteen neuroimaging studies on drug cue-reactivity, proposed that activity of the cue-regulation network (in particular, of the dorsolateral PFC, or dlPFC, and of the OFC) is modulated by the availability and expectancy to consume the substance after cue-exposure (Wilson et al., 2004). Given the role of the OFC in integrating stimulus values (Lim et al., 2013) and in representing the expected value of rewards (Kahnt et al., 2010), and given the involvement of the dlPFC in planning and executing actions aimed at achieving the reward (Goldstein and Volkow, 2002), the authors proposed that frontal activity in individuals not-seeking treatment reflects, at least in part, the expectation to obtain the drug after the experimental session. These findings have been mainly replicated in studies on cocaine SUD (Grant et al., 1996, Garavan et al., 2000), whereas results from studies on nicotine and alcohol SUD are more mixed, with studies reporting increased activity in dlPFC (Claus et al., 2011) and OFC (McBride et al., 2006) when participants are seeking for a treatment, or when they are explicitly told to not expect drug-consumption soon after the experiment. Interestingly, preliminary evidence suggests that the effect of drug availability is independent by the motivation to quit. In one study on patients with nicotine SUD, both quitting-motivated and quitting-unmotivated subjects exhibited PFC activity in response to smoking cues, but only when they were expected to smoke within seconds,

compared to hours, after cue-exposure (Wilson et al., 2012). To date, only one neuroimaging meta-analysis tested the influence of treatment status on the neural response to reward-related cues, in a set of heterogenous studies including substance and non-substance addiction, as well as unisensory and multisensory cue presentation (Chase et al., 2011). In particular, the authors performed two separate meta-analyses on treatment-seeking and not-seeking treatment individuals with addiction: they observed that treatment-seeking individuals show convergent activity in the cue-reactivity network, comprising the ventral striatum, amygdala, and occipital cortex, whereas not-seeking treatment individuals display convergent activity in both the cue-reactivity (e.g., ventral striatum, occipital cortex) and cue-regulation (e.g., OFC, dlPFC) networks, partially in line with Wilson's et al. predictions[3] (Wilson et al., 2004).

Initial evidence points to a similar modulation of food availability on the neural responses to food cues. In particular, one study examined the influence of actual food availability on neural responses to food cues in a sample of healthy weight individuals (Blechert et al., 2016): consistent with Wilson's hypothesis (Wilson et al., 2004), high and low-calories available foods, compared to those unavailable after the experiment, induced greater activity of the cue-reactivity (amygdala, striatum) and cue-regulation networks, including the ACC and the OFC. In the same study, a significant cue (high vs. low-calories) by availability (available vs. unavailable) interaction was also observed in the caudate nucleus: this was more active in the high compared to the low-calories condition, when the high-calories food was available. In sum, treatment status and drug availability modulate the neural reactivity to drug cues also outside the cue-regulation network, and initial evidence in healthy weight volunteers point to similar effects of food availability and further interactions with other factors (e.g., stimulus characteristics).

With respect to the other external factor taken into account here, it suffices to mention that **stress exposure**, either recent, chronic, or occurred in early-age, is associated with an increased vulnerability to both obesity (Torres and Nowson, 2007) and addiction (Sinha, 2008) (see (Sinha, 2008) for a review). Further, experimental manipulation of stress (e.g., anticipation of stress delivered by the experimenter) and stressful early-age events (e.g.,

---

[3] It is worthy to note that, in the study by Chase et al. (2011), no direct statistical comparison was made between the two groups. As a consequence, the OFC activity they observed in the not-seeking treatment group may be a by-product of the higher number of foci that entered the meta-analysis on not-seeking treatment patients (222 foci), compared to the one on treatment-seeking individuals (161 foci).

history of abuse) can both influence the neural reactivity to drug cues, mainly by up-regulating the cue-reactivity network and down-regulating the cue-regulation network (Dagher et al., 2009, Feldstein Ewing et al., 2010, Elton et al., 2015).

The relationship between stress and the neural responses to food cues is less clear. One study, in a sample of lean-to-obese individuals (mean BMI = 25.6 ± 0.9 kg/m^2), showed that self-reported chronic stress is associated with increased activity of the amygdala, striatum, and ACC in response to high vs. low-calories food pictures, and a concurrent decreased activation of the left dorsolateral (dlPFC), in line with the evidence in SUD. In another study, brain reactivity to visual food cues was compared between obese individuals with high versus low self-reported levels of stress: contrary to what expected (higher activity in obese individuals with high levels of stress), the authors did not find any significant difference in the activity of the pre-defined regions-of-interest (amygdala, hippocampus, ACC, insula, OFC). A schematic representation of the hypothetical modulation (up or down-regulation) of the environmental factors reviewed here on the cue-reactivity and cue-regulation networks is given in Figure 1.7.
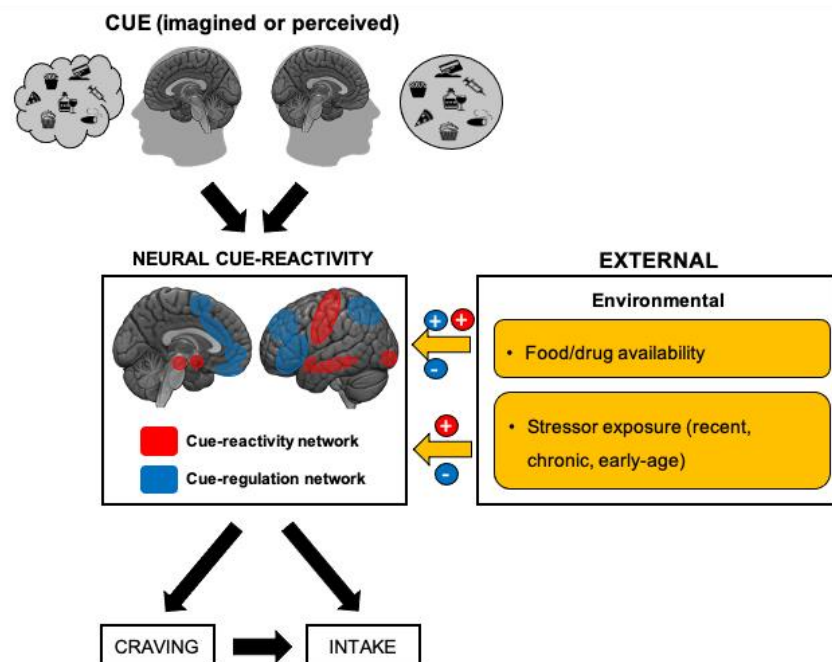
Figure 1.7. Environmental factors modulating the neural cue-reactivity | Hypothetical model describing the up (+) and down-regulation (-) of the cue-reactivity (red circle) and cue-regulation networks (blue circle) as a function of the environmental factors considered.

1.3.4. External factors: cue-specific

Among the cue-specific factors, the sensory modality of cue presentation and the stimulus characteristics are the most studied in obesity and SUD cue-reactivity research. With respect to the **sensory modality of cue presentation**, studies on obesity and overeating usually focused on the visual (Holsen et al., 2012; Martin et al., 2010; Rothemund et al., 2007; Stoeckel et al., 2008) and gustatory (Stice et al., 2010a, Green et al., 2011, Szalay et al., 2012) modalities, with few exceptions concerning the olfactory modality (Bragulat et al., 2010, Eiler et al., 2012, Jacobson et al., 2019). For evident reasons, cue-reactivity studies on SUD have been dominated by the visual modality of stimulation (Garavan et al., 2000, Li et al., 2005, Li et al., 2012, Li et al., 2013a, Li et al., 2013b, Wang et al., 2014, Zhang et al., 2018, Wei et al., 2019), except for alcohol SUD studies, where alcohol taste stimulation was also employed (Filbey et al., 2008, Claus et al., 2011), and for studies on nicotine SUD, where the administration of haptic and multisensory stimuli (e.g., holding a cigarette vs. a pen while exposed to a cigarette picture) is receiving increased attention (Yalachkov et al., 2010, Yalachkov et al., 2013).

The impact of the sensory modality of cue presentation on the neural responses to food cues in obesity is particularly relevant, since the major neurocognitive theories have their own anatomofunctional predictions with respect to anticipatory (e.g., visual food cues) versus consummatory processing (e.g., taste cues) (see (Stice and Yokum, 2016) and Chapter 3 of the present work for a review and meta-analysis on the topic). For example, the reward surfeit hypothesis (Davis et al., 2004) suggests that obesity is associated with heightened responses of the cue-reactivity network during consummatory processing, whereas the incentive sensitization theory (Robinson and Berridge, 1993, Berridge et al., 2010) predicts an up-regulation of the cue-reactivity network during anticipatory processing. In other words, the sensory modality of cue presentation can be used as a proxy of the underlying anticipatory (e.g., visual, olfactory, haptic) and consummatory (e.g., gustatory) reward processing[4].

In line with this reasoning, neuroimaging studies on SUD have shown that brain activity in response to unisensory haptic and multisensory drug cues, compared to unisensory visual cues, is more frequently associated with clinical variables such as craving and addiction severity (Yalachkov et al., 2009, Yalachkov et al., 2010, Yalachkov et al., 2012, Yalachkov et al., 2013),

---

[4] Tackling the issue by another perspective, it is possible that the effect of the sensory modality of cue presentation is partially mediated by the perceived availability associated with the specific sensory channel. In our everyday life, touching or even smelling an object means that the object is close and available to us. Conversely, visual cues may be present in the environment even if the actual object is not physically around us (e.g., tv commercials).

particularly in brain regions involved in habit formation (caudate nucleus), interoception and awareness of craving (insula), somatosensory processing and motor control (somatosensory and motor cortices). With this respect, haptic and multisensory cues can be employed as a proxy to unravel anticipatory processes related to the sensory-motor aspects of addiction, including, for instance, drug-taking motor skills (Yalachkov et al., 2010). In sum, whereas brain activity in response to unisensory visual stimuli may reflect a rather general anticipatory processing associated with the incentive and motivational value of drug-cues, brain responses to haptic and multisensory stimuli are more tightly associated with the sensory-motor aspects of SUD, thus suggesting an alternative yet complementary pathway to the enduring of addiction (Yalachkov et al., 2010, Yalachkov et al., 2012).

Preliminary evidence in heroin SUD suggests that unisensory visual cues can also elicit greater responses of a cue-reactivity network involved in sensory and motor, when specific **characteristics of the stimulus** are considered (Zeng et al., 2018). For example, visual cues depicting drug-taking actions, compared to pictures of drug and pictures of drug tool use, elicited greater activity of the posterior central gyrus, para-hippocampus, supra marginal gyrus, superior and inferior parietal cortices in a sample of heroin-dependent individuals (Zeng et al., 2018), suggesting that specific characteristics of the stimuli can modulate the neural reactivity to drug cues. To the best of my knowledge, there is no study investigating whether visual food cues depicting eating actions, compared to pictures of food and pictures of kitchen tools, elicit greater sensory and motor processing in obese individuals. However, other relevant characteristics of food stimuli can modulate the neural responses to cues in obesity. For example, high-calories food pictures usually induce greater activity of the cue-reactivity (e.g., dorsal striatum, parahippocampal gyrus) and cue-regulation (e.g., ACC) networks in overweight and obese individuals (Stoeckel et al., 2008, Blechert et al., 2016), and initial evidence points to higher order interactions between stimulus characteristics (e.g., high vs. low-calories food) and food availability (e.g., available vs. available) (Blechert et al., 2010). Interestingly, a recent line of evidence suggests that the level of transformation of foods (e.g., unprocessed vs. processed) may be another important factor that modulates the neural responses to food cues (Coricelli et al., 2019). In their electroencephalogram (EEG) study, Coricelli and colleagues recorded visually evoked potentials (VEPs) while healthy individuals watched pictures of processed versus unprocessed foods equated for energy content. The authors showed that, as early as 130 ms after stimulus onset, brain activity discriminates between processed versus unprocessed foods, irrespectively of calorie-content; further, estimation of the sources of neural activity suggested that processed vs. unprocessed foods lead to the recruitment of the

cue-reactivity network, including the occipital cortices bilaterally, whereas unprocessed vs. processed foods lead to the activation of a widespread network of brain regions, including the inferior frontal and temporal cortices, and the motor cortex (Coricelli et al., 2019). With this respect, it might be interesting to investigate whether weight status interacts with the level of food transformation (regardless of the caloric content), and whether this effect converges in discrete neuroanatomical structures of the cue-reactivity and cue-regulation networks.

In sum, the sensory modality of stimulus presentation modulates the neural reactivity to cues in obesity and SUD, and their modulatory effect may also depend on the weight status of the participants, as far as studies on obesity are concerned, and on the severity of the dependence, when studies on SUD are considered. A schematic representation of the hypothetical modulation (up or down-regulation) of the cue-specific factors reviewed here on the cue-reactivity and cue-regulation networks is given in Figure 1.8.
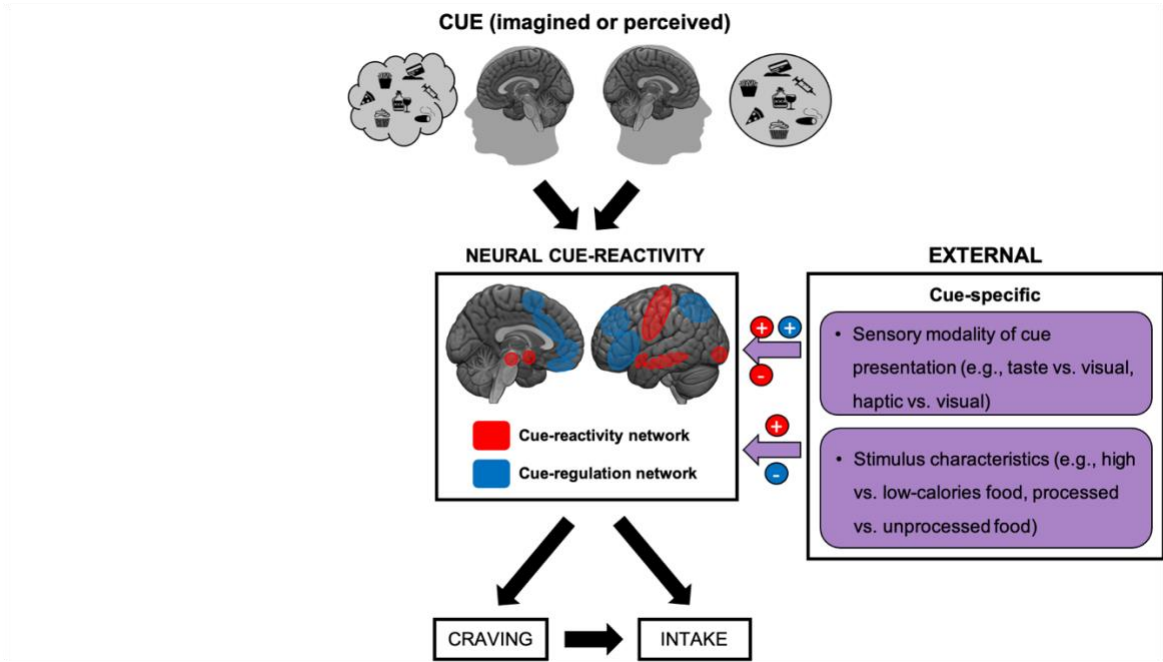
Figure 1.8. Cue-specific factors modulating the neural cue-reactivity | Hypothetical model describing the up (+) and down-regulation (-) of the cue-reactivity (red circle) and cue-regulation networks (blue circle) as a function of the cue-specific factors considered.

As the above review suggests, the neuroimaging literature on the cue-reactivity paradigm in obesity and SUD is vast, and heterogenous. The compelling evidence that numerous internal and external factors modulate the neural reactivity to such cues makes it even harder to translate empirical knowledge into clinical practice (e.g., translational medicine), identifying reliable biomarkers of disease severity that might be used to predict, or to assess, treatment outcomes. Moreover, it is reasonable to expect that different internal and external factors interact with each other, giving rise to specific brain activation patterns as a function of the factors under examination.

The study of such higher-order interactions is not only critical for basic research, but also for translational and personalized medicine, as it can guide future cognitive and brain-centred treatments through the identification of the neural circuitry that should be up or down-regulated under specific circumstances, or for a particular population of patients.

In what follows, I will describe the main clinical implications of the literature reviewed above, with respect to (i) cognitive-behavioral interventions, and (ii) brain-centred (neuromodulation and neurostimulation) treatments aimed at reducing food and drug craving.

1.4. Translational implications for cognitive-behavioral interventions

Unraveling the neural underpinnings of food and drug craving is the *conditio sine qua non* of designing effective treatment approaches. The overall evidence reviewed above indicates that obesity and SUD are both associated with heightened activity of brain regions involved in sensory, hedonic, and motivational processes, which can also be accompanied by diminished activity of key nodes of the cue-regulation network involved in (top-down) cognitive control (e.g., vlPFC, dlPFC). Cognitive-behvioral interventions aimed at empowering cognitive control strategies, while suppressing the hedonic and motivational processes prompted by food and drug cues, aim at fixing this unbalance by modulating the activity of the dys-functional brain regions through specific cognitive strategies.

As already pointed out in section 1.3.2, different cognitive reappraisal strategies (i.e., mindful attention, thinking about long-term costs of eating high-calories palatable food/drug use, thinking about long-term benefits of not eating/using it, and actively suppressing food/drug craving) operate via the activity of the cue-regulation network, by down-regulating the activity of the cue-reactivity network in response to food (Kober et al., 2010, Scharmüller et al., 2012, Siep et al., 2012, Yokum and Stice, 2013, Tuulari et al., 2015) and to drug cues (Volkow et al.,

2010, Hartwell et al., 2011, Westbrook et al., 2013). This is an area where cognitive-behavioral interventions can be directly informed by basic research on cue-reactivity.

Preliminary results suggest that cognitive-behavioral interventions aimed at empowering cognitive reappraisal strategies (Stice et al., 2015b), or attentional and inhibitory processes (Stice et al., 2017), induce significant weight-loss, and they are associated with diminished reactivity to food cues in brain areas involved in reward (e.g., putamen) and attention (e.g., cingulate cortex, inferior parietal lobe), and augmented activity of regions involved in inhibitory control (e.g., inferior frontal gyrus). Despite not being associated with long-lasting changes in eating habits (Stice et al., 2015b, Stice et al., 2017), these results provide a proof of concept that cognitive behavioral interventions, which can be often delivered costless and at patients' house, can be used in isolation or in combination with other extant treatments to improve their efficacy.

The study of the internal and external factors that modulate the neural activity to food and drug cues has also some translational potential, and it can help improving the efficacy of existing approaches. Cognitive-behavioral interventions aimed at empowering cognitive reappraisal and control strategies in obesity may be tailored to accommodate the effects of satiety, for example by focussing on the down-regulation of hedonic and motivational responses to visual cues that persist beyond satiety. Similarly, the evidence that treatment status and drug availability modulate the neural reactivity to drug cues is *per se* sufficient to justify tailor-made interventions that take into account not only the individuals' motivation to quit drug use, but also the perceived availability of the substance.

In sum, cognitive-behavioral interventions attempt to modulate the neural activity of the cue-reactivity and cue-regulation network from the "inside", by empowering those cognitive processes that rely on the brain circuits that show aberrant responses to food or drug cues. As the reader shall see below, neuromodulation and neurostimulation approaches allow to tackle this issue the other way around, from the "outside": through the direct modulation and stimulation of the cortical areas implied in cognitive control processes.

1.5. Translational implications for brain-centered treatments
During the last two decades, there has been an increasing interest into the application of non-invasive brain stimulation and modulation techniques for the management of obesity and addiction. In particular, the two most commonly used brain stimulation and modulation techniques are, respectively, TMS and tDCS.

The first is based on the application of rapidly changing magnetic fields (delivered with a coil encased in plastic that is placed over the scalp of the subject), that cause an induction of secondary currents in the adjacent cortex that can be strong enough to trigger neuronal action potentials (Barker, 1991). In repetitive TMS (rTMS), train of pulses are delivered to the cortical surface, leading to a sustained alteration of the neural excitability; this alteration can be induced by high-frequency "excitatory" stimulation (> 5 Hz), or by low-frequency "inhibitory" stimulation (< 1 Hz). In the case of the second technique, tDCS, mild currents (typically in the order of 1–2 mA) are applied directly over the head through a pair of saline-soaked electrode pads connected to a battery-like device. Approximately 50% of the current delivered by tDCS penetrates the scalp and can raise or decrease the resting membrane potential of neurons in underlying areas (anodal or cathodal tDCS stimulation, respectively), causing changes in spontaneous firing (Nitsche et al., 2008).

To date, the brain region that is most frequently the target of tDCS and TMS is the dlPFC. This choice is motivated, on the one hand, by the evidence that the cue-regulation network (particularly, the dlPFC) plays a crucial role in the inhibition of behavioral responses, and in the explicit regulation of craving, in both obesity and SUD (Batterink et al., 2010, Hartwell et al., 2011, Yokum and Stice, 2013); on the other hand, by the fact that the dlPFC lies close to the scalp, and common TMS and tDCS techniques act only on the cortical surfaces. Converging evidence from two meta-analysis indicate that excitatory non-invasive brain stimulation of the dlPFC (by means of rTMS and anodal tDCS) is effective in reducing craving (Jansen et al., 2013), and consumption (Song et al., 2019) across different populations of patients with eating disorder, including obesity, and with SUD (individuals addicted to legal and illegal substances). Preliminary evidence suggests that the insular cortex might be a promising neuroanatomical target of stimulation for the management of obesity (Ferrulli et al., 2019b) and SUD (Dinur-Klein et al., 2014). Based on the evidence that damage to the insular cortex is associated with the disruption of cigarette smoking (Naqvi et al., 2007), Dinur-Klein and colleagues designed a rTMS treatment aimed at targeting the bilateral insular and prefrontal cortices (Dinur-Klein et al., 2014), by means of an H-coil specifically design to reach deeper cortical structures, also known as deep rTMS (Zangen et al., 2005). The authors showed that high-frequency (10 Hz), but not low-frequency (1 Hz), deep rTMS led to an abstinence rate of 44% at the end of the three-weeks treatment, and to an estimated 33% of abstinence rated at 6-months follow-up (Dinur-Klein et al., 2014). Recently, the efficacy of excitatory (18 Hz) over inhibitory (1 Hz) deep rTMS targeting the bilateral PFC and insular cortices has been also demonstrated in obesity (Ferrulli et al., 2019b). In particular, the authors showed that real excitatory deep rTMS

induced greater weight-loss at the end of the treatment, and for up to 1 year (Ferrulli et al., 2019b), supporting the idea that the insular cortex may be another transdiagnostic target for the management of obesity and SUD.

Perhaps surprisingly, the neurobiological mechanisms beyond the efficacy of these brain stimulation treatments remain almost completely unexplored, as few studies investigated the neurofunctional changes associated with a rTMS treatment in obesity and SUD (Herremans et al., 2015, Kim et al., 2019b), and no study, to the best of my knowledge, involved deep rTMS. Several underlying mechanisms have been proposed to explain the efficacy of non-invasive brain stimulation approaches: (i) excitatory stimulation of the dlPFC empowers patients' ability to exert cognitive control over food or drug consumption; (ii) since deep TMS influence cross-hemispheric cortical and subcortical activity, including the insula and anatomically-connected regions (Zangen et al., 2005, Roth et al., 2007, Fiocchi et al., 2018), another mediating mechanism may be related to a generalized disruption of the neural circuits associated with craving, which involve a wide network of cortical and subcortical brain regions described in the current Chapter; (iii) finally, in line with the evidence that stimulation of the PFC induce DA release in the mesocorticolimbic circuitry (Strafella et al., 2001, Kanno et al., 2004), stimulation-induced DA release may "mimic" the neurochemical effects of food or drugs in absence of actual consumption.

It is important to note that, in the vast majority of cases, neurostimulation is delivered "offline", *after* the exposure to food or drug-related cues. Alternatively, "online" PFC stimulation, delivered while the patient is actively trying to suppress cue-elicited craving, may also prove effective in reducing craving, by directly acting on those brain circuits that are recruited during the exposure to cues. With this regard, neurocognitive models of craving, and of the internal and external factors that modulate the neural cue-reactivity (Jasinska et al., 2014, Figure 1.4), are crucial for the identification of the brain areas that are recruited by a particular stimulus (visual, tactile, olfactory, gustatory), in a certain population of patients (obese patients, legal or illegal SUD), and/or under specific contingencies (satiety or abstinence/withdrawal state, treatment status and drug availability).

However, before basic research on cue reactivity can be translated into tailor-made "online" stimulation schemes, the effect of PFC neurostimulation on the functional brain activity, connectivity, and organization should be carefully addressed, and elucidated. If anything, a model such as the one proposed in Figure 1.4 may be a valuable framework to ease this

endeavor, guiding the neurocognitive interpretation of the neurofunctional changes induced by the treatment.

1.6. Aims

The present thesis was designed to address two general purposes: first, to assess the individual, and interacting, effects of different factors that modulate the neural reactivity to cues in obesity and SUD, by adopting a novel meta-analytical approach based on hierarchical clustering analysis (Clustering the Brain, CluB; (Cattinelli et al., 2013b, Berlingeri et al., 2019)); second, to evaluate the neurofunctional changes associated with a deep rTMS treatment aimed at inducing weight-loss in a sample of obese individuals (Ferrulli et al., 2019b), by adopting a novel data-driven approach to the analysis of resting-state fMRI data (rs-fMRI) (Martuzzi et al., 2011).

In Chapter 2, I will use the CluB method to test the main and interactive effects of three of the main factors that modulate the neural reactivity to food cues in obesity: weight status (healthy weight vs. obese), sensory modality of stimulus presentation (visual vs. gustatory), and satiety state (hungry vs. satiated). In particular, evidence from such main and interactive effects will be taken as a benchmark to test the validity of the main neurocognitive theories of overeating and obesity.

In Chapter 3, I will employ the same approach to test the main and interactive effects of addiction severity (individuals addicted to legal vs. illegal substances) and treatment status (treatment-seeking vs. not-seeking treatment individuals) on the neural reactivity to drug cues. Again, evidence from such main and interactive effects will be taken as a benchmark to test the validity of one of the most influential neurocognitive theories on the influence of treatment status on the neural drug cue-reactivity (Wilson et al., 2004).

An in-depth analysis of the methodology employed in Chapters 2 and 3 is given in Appendix A, where I will demonstrate, by means of two validation studies, that CluB can (i) reliably extract a set of spatially coherent clusters of activations from a database of stereotactic coordinates, and (ii) test for factor-specific clusters of convergent activation within designs that cannot be usually implemented in a meta-analytical study.

In Chapter 4, I will assess the neurofunctional changes associated with a deep rTMS treatment targeting the bilateral insular and prefrontal cortices aimed at inducing weight-loss and reducing food craving in a sample of 17 obese individuals. In particular, I will employ a novel data-driven method to test that hypothesis that excitatory, compared to sham, deep rTMS over the

bilateral insular and prefrontal cortices is associated with changes in the brain functional organization in key areas of the cue-reactivity and/or cue-regulation networks.

Finally, in Chapter 5, the results of the single studies will be presented within a unitary neurocognitive framework (Figure 1.4) through a general discussion.

Since much of the present work is already published (Devoto et al., 2018, 2020, Berlingeri et al., 2019), or it is currently submitted to peer-reviewed journals (Devoto, Ferrulli et al., *submitted*[5]), some sections (e.g., methods, results) are taken from the papers, whereas others (e.g., introduction, discussion) will be adapted to reflect the narrative structure expected from a PhD thesis. Shared comments across the studies (e.g., comparison of food vs. drug cue-reactivity) will be pointed out in the general discussion (Chapter 5).

---

[5] Devoto F. & Ferrulli A., Zapparoli L., Massarini S., Banfi G., Paulesu E., and Luzi L. "Repetitive deep TMS for the reduction of body weight: bimodal effect on the functional brain connectivity in obese individuals".

Chapter 2 – Hungry Brains: A Meta-analytical Review of Brain Activation Imaging Studies On Food Perception and Appetite in Obese Individuals

2.1. Introduction

In the previous Chapter, I reviewed the neuroimaging literature about the cue-reactivity paradigm, and I described a unitary model (adapted from (Jasinska et al., 2014)) of the factors that modulate the neural reactivity to food and to drug cues, in obesity and SUD (Chapter 1). In the present Chapter, I reassess the available task-based imaging activation evidence on the neural cue-reactivity to food in obese individuals, by means of a new meta-analytical approach that combines hierarchical clustering analysis, as implemented in the software CluB (Clustering the Brain, (Berlingeri et al., 2019); see Appendix A for an in-depth description and validation of the tool), with the Activation Likelihood Estimation (ALE) method implemented in the GingerALE software (Eickhoff et al., 2009, Eickhoff et al., 2012, Turkeltaub et al., 2012).

This is not, of course, the first meta-analysis on the subject: yet, as the reader shall see, for the first time I explicitly assess the mutual relationship between three factors that modulate the neural reactivity to food cues: (i) weight status (healthy weight, or HW vs. obese, or OB), (ii) sensory modality of cue-presentation (visual vs. gustatory), and (iii) satiation state at the time of testing. Importantly, the effects exerted by the aforementioned factors on the neural reactivity to food cues in obese individuals have been taken as benchmarks for the discussion of the main neurocognitive theories of obesity and overeating (see (Stice and Yokum, 2016) for a detailed, paper by paper, review).

In what follows I first introduce, briefly, the main theories on the neural vulnerability factors associated with obesity, with particular reference to visual and gustatory processing; then, I rather summarize evidence derived by previous studies about the effect of satiety, and I spell-out the methodological and historical justifications for the present new meta-analysis.

2.1.1. How and why, we may become overweight or even obese? Neurocognitive theories of long-term phenomena

Obesity has become a major health concern. A recent study on different European countries estimated that 47.6% of adults are overweight ($25 \text{ Kg/m}^2 \leq \text{BMI} < 30 \text{ Kg/m}^2$) or even obese (Gallus et al., 2015) ($\text{BMI} \geq 30 \text{ Kg/m}^2$); furthermore, pediatric obesity is also increased at alarming rates, hence representing a significant medical and economic burden (Wang and Lobstein, 2006). Several approaches have been adopted to minimize the economic and health

consequences of this condition; yet, most treatments, from physical activity and lifestyle interventions to bariatric surgery (Colquitt et al., 2009), often result in only a transient weight loss (Jeffery et al., 2000), as much as it happens in chronic relapsing conditions like Substance Use Disorder (McLellan et al., 2000).

Despite the causes of overweight and obesity may seem straightforward (i.e., an individual's intake of food exceeds the homeostatic energy needs), the mechanisms underlying the overeating behavior remain largely unknown. As pointed out in Chapter 1, eating is a complex and multisensory experience that calls into play different interrelating factors, at either the peripheral (homeostatic) level, with the long-term and circadian fluctuations of signaling molecules (e.g., ghrelin, insulin, leptin; see (Burger and Berner, 2014) for a review), and central (neurocognitive) level. The hypothalamus and reticular formation, represent, of course, the interface between the humoral and the neurocognitive levels (Hussain and Bloom, 2013, Liu and Kanoski, 2018). With that said, it follows that any treatment or approach to the study of the normal and pathological eating behavior "cannot remain brainless", to use the wording of Schmidt and Campbell (Schmidt and Campbell, 2013).

According with this principle, there are several theories that try to give neurocognitive explanations of the development of obesity. These all, one way or the other, associate the dysregulation of food intake with alterations within either the reward system (mostly overlapping with the cue-reactivity network, Figure 1.3, in red) or the cognitive control system (mostly overlapping with the cue-regulation network, Figure 1.3, in blue). Initial evidence (Stice et al., 2008a, Stice and Dagher, 2010, Stice et al., 2010b, Stice et al., 2011b) permits to combine these theories with the genetic makeup that determines the expression of greater DA signaling capacity. This is associated with the TaqIA (rs1800497) polymorphism, as subjects with A2/A2 genotype seem to have 30–40% more DA D2 receptors (Volkow et al., 2008, Baik, 2013).

The theories focusing on the sensory, hedonic, and motivational responses to food (i.e., the cue-reactivity network), such as the **Reward Surfeit Theory of Obesity** (Davis et al., 2008, Stice et al., 2008b), postulate that subjects become obese because of their permanently increased reward signaling for food-related stimuli. In other words, it suggests that subjects would keep overeating because this gives them a strong permanent reward during the intake of high-calorie, palatable food.

A refinement of this theory can be found in the **Incentive Sensitization Theory of Obesity** (Robinson and Berridge, 1993, Berridge et al., 2010) which posits that, after repeated pairings between visual food-cues and the hedonic impact of food consumption, anticipatory food cues

would come to elicit strong responses of the cue-reactivity network. This theory echoes similar concepts from the domain of drug abuse and chronic addiction ((see for example Everitt et al., 1999, Everitt and Robbins, 2013)): instrumental in the making of these modifications within the reward system would be variations in dopaminergic and endorphin neurotransmission (Ambrose et al., 2004, Berridge et al., 2010, Tuominen et al., 2015).

Conversely, the **Reward Deficit Theory of Obesity** suggests that obese people keep overeating because "they would never get satisfied enough by their eating", their reward circuitry being less sensitive to dopaminergic signals (Wang et al., 2002); grounded on the initial evidence that blocking D2 dopaminergic receptors leads to obesity (Wang et al., 2001), the theory has been questioned by the evidence that atypical neuroleptics (with less effect on D2 receptors) have a higher obesogenic effects compared to haloperidol (Krakowski et al., 2009). A U-shaped response of the ventral striatum to too high, or too low, levels of dopamine in obese may still keep the theories mentioned so far under the same conceptual umbrella.

In a different vein, an **Inhibitory Control Deficit Theory** (Nederkoorn et al., 2006a) calls into play higher-level control functions (the cue-regulation network): these would be not as good in obese patients who would over-react to food-related cues, a behavior related to a more general trait of impulsivity. Consistent with this notion, obese individuals are more prone to temporal discounting phenomena, hence preferring short-term food rewards over the long-term ones (Bonato and Boland, 1983, Sobhany and Rogers, 1985, Epstein et al., 2008). Nonetheless, while the supposed inhibitory control deficit does correlate with a general impulsiveness (Aiello et al., 2018), to date only few neuroimaging studies have shown a relationship between lower activity in inhibitory regions during delay-discounting and future weight gain (Kishinevsky et al., 2012, Weygandt et al., 2013): this makes it difficult to draw firm conclusions about the role of inhibitory control regions in overeating.

Two other theories try to achieve an integration of these different neurocognitive accounts of obesity: the **Dynamic Vulnerability Model of Obesity** ((DVM, Burger and Stice, 2011, Stice et al., 2011a)) and its refined form, the **R-DVM** (Stice and Yokum, 2016). The refined form of the theory brings together, in a sequential fashion, the most solid aspects of those discussed before conceding that the predisposition to obesity starts with a hyper-responsivity of the cue-reactivity network to taste, which in turn leads to overeating also in combination with genetic factors related to dopamine signaling (Stice et al., 2008a, Stice and Dagher, 2010, Stice et al., 2015a). This hyper-responsivity to taste is thought to contribute to greater cue-reward learning and faster habituation to food of the reward system (reinforcer satiation), both of which have been shown to predict overeating independently (Burger and Stice, 2014). Further, enhanced

cue-reward learning is believed to trigger incentive motivational processes in subjects exposed to anticipatory food cues, as suggested by the comparison of brain activity in HW and OB individuals exposed to food pictures (Rothemund et al., 2007, Stoeckel et al., 2008, Stice et al., 2010b). Stice and Yokum (2016) also propose that a bias for immediate reward is a further factor behind overeating and weight gain, since immediate reward bias predicts weight gain in children (Seeyave et al., 2009, Evans et al., 2012) even over a 30-year follow-up (Schlam et al., 2013). Finally, the R-DVM predicts that the repeated overeating, leading to weight gain, contributes to the blunted responses of the reward system to palatable high-calorie food intake. It is important to underline that the R-DVM is based on evidence coming from prospective studies on the neurofunctional predictors of weight gain. Yet, it is unclear whether the neurofunctional predictors of weight gain map into the brain functional abnormalities associated with chronic obesity.

2.1.2. Hungry brains: how satiety interacts with food-related behavior in obese and healthy weight individuals

One missing link between obesity and the brain mechanisms behind the aforementioned models is the one related to short-term circadian regulatory phenomena, such as those implied by the varying levels of satiety during the day (Burger and Berner, 2014), and how the sense of satiety interacts with the factors mentioned so far (Gautier et al., 1999, Gautier et al., 2000, Gautier et al., 2001, Martin et al., 2010, Holsen et al., 2012) in obesity or in lean weight subjects.

Despite the growing evidence pointing to altered brain responses to hunger and satiety in OB individuals, the effect of the internal factor satiety on the neural responses to food cues has not been fully implemented in all the neurocognitive models of obesity: yet, it is reasonable to expect that an impaired sense of satiety may contribute to the maintenance (or to the worsening) of the obese weight status. The incentive sensitization theory is the only model that took into account the satiety state as a modulator of the reward system reactivity (Berridge et al., 2010). In its translation to computational models (Zhang et al., 2009), hunger is expected to multiply the incentive salience process, boosting "liking" and "wanting" reactions to food intake and associated cues. On the contrary, satiety is expected to blunt hedonic reactions to food consumption and anticipation, leading to diminished "liking" and "wanting" reactions and to down-regulated activity of the cue-reactivity network in response to food intake and to anticipatory food cues.

Cross-sectional studies comparing HW and OB individuals during fasting (i.e., hunger state) and fed (i.e., satiety state) conditions suggest that OB show persistent brain activations to food

intake and to food cues even when satiated. For instance, PET studies using measures of regional cerebral blood flow reported increased neuronal activity in the PFC and decreased activity in limbic, paralimbic and striatal regions in OB compared to HW individuals during the feeding to satiety of a liquid meal (Gautier et al., 2000, Gautier et al., 2001).

There is also evidence that OB, compared to HW individuals, exhibit greater activation of the hypothalamus and the dorsolateral PFC (dlPFC) (Holsen et al., 2012), in addition to greater responses of striatal, medial and superior frontal regions, in response to food images in a satiety condition (Martin et al., 2010). Taken together, previous studies suggest that obesity is associated with a persistent brain activation in response to food even in a condition of satiety, which highlights the on-going motivational and reward processes in the absence of homeostatic energy needs (Ho et al., 2012). Conversely, hunger has been associated with increased activation of key regions of the cue-reactivity network involved in reward, motivation (insula, hypothalamus, striatum), and memory (hippocampus, amygdala) in HW individuals exposed to simple tastes (Haase et al., 2009), whereas higher self-reported impaired satiety was associated with reduced responses of the cue-regulation network (dlPFC) in response to food images in OB individuals (Ho et al., 2012).

So far, neuroimaging studies have provided evidence suggesting that the appetitive and motivational states exert a different influence on the neurofunctional responses to food in HW and OB individuals, thus suggesting an impaired central satiety signaling. Despite not being directly associated with future weight gain in previous studies, I argue that an impaired central satiety signaling might have a role in overeating and/or in the maintenance of the unhealthy weight.

To summarize the two previous sections, as it should be clear by now, there are multiple theories on the neurocognitive underpinnings of obesity, in its making and in its maintenance over time. Besides the testing in animal models, a substantial part of the evidence taken in support to each and every theory rests, at least in part, on functional neuroimaging activation data on the cue-reactivity paradigm in the visual and gustatory sensory modalities. Given the complexity of the matter at stake, no single experiment has had the potential to address all the relevant issues with a single paradigm. However, to date there have been no less than twenty functional imaging brain activation studies, to make a conservative estimate, that have attacked these issues from different perspectives. This is a suitable situation to address, using the meta-analytical technique described in Appendix A (CluB), the available functional imaging

evidence and to assess the relative explanatory power of the "three factors" cited at the beginning of this introduction.

2.1.3. Aims of the study

This study was motivated, on the one hand, by the evidence that there is sufficient empirical data from several different brain activation studies on obesity to define a replicable underlying (dys)functional anatomy of the internal (weight status, satiety) and external factors (sensory modality of cue-presentation) under examination; on the other hand, by the desire of testing the different neurocognitive theories of obesity in the light of the three factors discussed before: weight status, sensory modality of cue-presentation, and satiety.

By design, I restricted the meta-analysis to the evidence coming from fMRI/PET activation studies on adults in two fixed states, obese or lean[6]. To the best of my knowledge, this is the first meta-analytical attempt to summarize the previous neuroimaging literature in light of the principal neurocognitive theories of overeating and obesity while classifying the available data according to a factorial design suitable for reflecting both anticipatory (e.g., visual) and consummatory (i.e., gustatory) processing of food stimuli. With this respect, Table 2.1 shows to what extent the three factors and their interactions were tested by the previous meta-analyses on the topic, most of which have been mentioned in the General Introduction (Chapter 1).

To this aim, I re-assessed the previous activation literature by combining the CluB toolbox with the GingerALE approach: as illustrated in Appendix A, the HCA implemented in CluB provides reproducible meta-analytical results, whereas the CCA permits a *post-hoc* statistical assessment of the association of a given cluster with a factor, or indeed the interactions between factors.

In fact, the theories summarized above have different predictions on the neurofunctional responses to food in function of the sensory modality of cue presentation and of the weight status, something that was not assessed in previous meta-analyses. I also speculated on how, and whether, an impaired central satiety signaling may interact with the factors above.

---

[6] I did not include in our meta-analysis data coming from PET molecular imaging studies mapping neurotransmitter receptor density of displacement. It is not clear to what extent this information is biologically consistent with the one carried by changes in BOLD signal, or regional cerebral blood flow. I felt methodologically not acceptable to bias the identification of brain clusters using information derived from multiple heterogeneous sources. Moreover, ligand-based PET studies are typically analyzed using regions of interest, an approach not suited for coordinate-based meta-analyses, as in the present case.

Table 2.1 | Summary of previous meta-analyses on food perception in obesity. Overview of meta-analytical studies on visual-anticipatory and gustatory-consummatory perception of food in healthy weight and obese individuals varying in satiety state. OB, obese partcipants; HW, healthy-weight participants. Taken from: Devoto et al. 2019.

	Visual-Anticipatory Food Cues		Gustatory-Consummatory Food Cues	
	Fasting	*Fed*	*Fasting*	*Fed*
HW	• Pursey et al. 2014 • Huerta et al. 2014 • Kennedy & Dimitropoulos 2014 • Tang et al. 2012 • van der Laan et al. 2011 • van Meer et al. 2015	• Pursey et al. 2014 • Kennedy & Dimitropoulos 2014 • van der Laan et al. 2011	• Huerta et al. 2014 • Veldhuizen et al. 2011	• Yeung et al. 2016 (participants with mixed weight status)
OB	• Pursey et al. 2014 • Kennedy & Dimitropoulos 2014	• Pursey et al. 2014 • Kennedy & Dimitropoulos 2014		• Yeung et al. 2016 (participants with mixed weight status)

2.1.4. Predictions

Differently to what can be done in a fresh empirical experiment, in which the variables under examination are controlled by the experimenter, meta-analyses are more observational in nature. Still, the factorial approach implemented in CluB permitted, at the very least, to test to what extent various neurocognitive theories on overeating are justified by the available imaging literature (for the application of the same logic in a different domain see (Paulesu et al., 2014)). As it can be appreciated by the inspection of Table 2.2, where models are somewhat arranged in order of complexity[7], simple theories compete with each other (e.g., reward surfeit and reward deficit theories); other theories can be integrated together more easily (e.g., the inhibitory control theory can be added to any other theory), while the R-DVM, with its integration of the most robust aspects of other theories, represents the most complex and dynamic scenario, providing predictions for both anticipatory (e.g., visual food cues) and consummatory (e.g., actual receipt of taste in the mouth) brain responses to food.

---

[7] For consistency with the narrative of the present thesis, the original table of the published manuscript was adapted to reflect the modulation (hyper or hypo-reactivity) of the cue-reactivity and cue-regulation network. Indeed, except for the OFC which underlies higher-order reward-related processes, all the other brain regions considered in the original publication fit well into the gross categorization provided in Chapter 1: brain regions involved in sensory, hedonic, and motivational aspects of reward (cue-reactivity network), and brain regions involved in higher-order cognitive control processes (cue-regulation network).

Table 2.2 | Anatomo-functional predictions of the main neurocognitive theories of obesity. For each neurocognitive theory, the neurofunctional predictions are expressed as up (upward arrow) or down-regulation (downward arrow) of the cue-reactivity and cue-regulation networks. The R-DVM is not explicitly tested in this meta-analysis based on cross-sectional studies in adult obese subjects. Adapted from: Devoto et al. 2018.

	Reward Surfeit Theory	Reward Deficit Theory	Incentive Sensitization Theory	Inhibitory Control Deficit Theory	Refined – Dynamic Vulnerability Model
Anticipatory Food Cues			↑ **Cue-reactivity network** (midbrain, striatum, insula, OFC)	↓ **Cue-regulation network** (vmPFC, dlPFC)	↑ **Cue-reactivity network** (midbrain, striatum, insula, OFC)
Consummatory Food Intake	↑ **Cue-reactivity network** (midbrain, striatum, insula, OFC)	↓ **Cue-reactivity network** (midbrain, striatum, insula, OFC)			↓ **Cue-reactivity network** (midbrain, striatum, insula, OFC)

Indeed, throughout the Chapter, I will refer to the "visual" and "gustatory" levels of the "sensory modality" factor as reflecting *anticipatory* and *consummatory* brain responses to food, respectively, in agreement with previous neurocognitive theories.

Despite not committing to any of the aforementioned models from the outset – I consider these not to be necessarily mutually exclusive -, and despite the limitations of meta-analyses as far as the possibility of making strong predictions, I had a series of educated guesses in mind at least about what theory would be supported by a given finding[8] (see Table 2.2).

Starting from a very easy one, the **Reward Surfeit Theory** (Davis et al., 2004) suggests that a predisposing factor to excessive food intake in some individuals is the fact that food ingestion has a particular rewarding value. Thus, the main prediction of the Reward Surfeit Theory is that OB individuals display an up-regulation of the cue-reactivity network in response to food intake (i.e., gustatory modality of cue presentation).

On the other hand, the **Incentive Sensitization Theory** (Robinson and Berridge, 1993, Berridge et al., 2010) would be supported if obese individuals, who have experienced repetitive pairings of visual cues with the hedonic sequelae of food ingestion, show an up-regulation of the cue-reactivity network in response to anticipatory food cues (Rothemund et al., 2007, Stoeckel et al., 2008, Martin et al., 2010, Stice et al., 2010b, Dimitropoulos et al., 2012, Holsen et al., 2012).

Further, a down-regulation of dopamine-mediated reward regions in OB, consistent with studies on overfeeding in animal models of obesity (Fulton et al., 2006, Roseberry et al., 2007, Davis et al., 2008, Koyama et al., 2013, Cook et al., 2017) and some neuroimaging studies in humans (Wang et al., 2001, Wang et al., 2002, Volkow et al., 2008, Volkow et al., 2013), would be in line with the idea that, rather than being an initial vulnerability factor to overeating, the down-regulation of the cue-reactivity network in response to gustatory cues is the main consequence of weight gain (Stice et al., 2010a), in accordance with the **Reward Deficit Theory** (Wang et al., 2001, Wang et al., 2002).

Finally, the **Inhibitory Control Deficit Theory** (Nederkoorn et al., 2006a, Nederkoorn et al., 2006b) highlights the role of the neural circuits underlying the inhibition of inappropriate behavior and pathological temporal discounting (Kishinevsky et al., 2012), mainly involving

---

[8] It should be noted that the nominal report, from several sources, of the involvement of a given anatomical structure in a given process does not guarantee by itself that the findings, once the stereotactic coordinates are used, will converge anatomically in a meta-analysis. This is particularly true the less specific it is the anatomical definition originally used (e.g., prefrontal cortex; insular cortex).

the PFC and particularly its dorsolateral subdivisions. On the basis of this theory, I would expect that OB individuals had exhibited a down-regulation of the cue-regulation network compared to HW during the perception of food images, to suggest a limited inhibitory processing in the OB population.

It is worthy to note that all the above-mentioned models, but the incentive sensitization theory have not taken into great account the role of circadian fluctuations of satiation and hunger on overeating. Yet, the demonstration of a strong effect of the level of hunger and its interaction with the various systems would not only call for a further refinement of some of the models discussed, but it would also contribute to enrich available models of the factors that modulate the neural reactivity to food cues in obese individuals, as the one described in Chapter 1 (Figure 1.4).

Having spelled out the main benchmarks for the different theories considered and the ensuing educated guesses, what it important here is that I did put myself in a sufficiently good position to test them and to provide quantitative answers to the issues described.

2.2. Materials and methods

The meta-analytical approach employed here involves a series of analytical steps starting from the identification of the raw data (data collection and preparation), followed by hierarchical clustering analysis (HCA) (see Appendix A, section 2.1, for the validation study for the HCA), and statistical inferences on the clusters which comprise a cluster composition analysis (CCA) (see Appendix A, section 2.2, for the validation study for the CCA) and a validation of the spatial relevance of each cluster by means of the GingerALE method. These procedures are described in detail below.

2.2.1. Data collection and preparation

I identified neuroimaging studies exploring the neural correlates of food cue-reactivity (presented in either the visual-anticipatory[9] or gustatory-consummatory modality) in HW and OB individuals across different motivational states using the following procedures.

---

[9] As I was interested in comparing the anticipatory versus consummatory responses to food, cue-reactivity studies using mental imagery were included as reflecting anticipatory processes. This choice was motivated by the fact that (i) food craving can be also elicited by the spontaneous thoughts about food, and by the belief that (ii) mental imagery tasks model well this anticipatory experience.

First, I entered the following queries in PubMed (https://www.ncbi.nlm.nih.gov/pubmed/): "obesity and fMRI", "obesity and PET" "obesity and functional magnetic resonance imaging", "obesity and positron-emission tomography" and "obesity and neuroimaging". The initial set of studies included 7391 papers, updated to February 2017 (see Figure S1.1 in Supplementary File 1).

Second, after removal of duplicates, I ran a preliminary selection based on the titles and abstracts of the papers, through which I excluded the studies that did not match the following criteria:

- Data reported using stereotactic coordinates (either MNI or Talairach atlases);
- Activation protocol on food-related stimuli limited to passive visual/imagery (i.e., reflecting the anticipation and not the actual food intake) or gustatory (i.e., reflecting the actual taste/food in the mouth) stimulation (only simple effects related to stimuli or between-group comparisons for the factor obesity were considered). For example, studies employing delay-discounting tasks (Kishinevsky et al., 2012, Weygandt et al., 2013) or requiring explicit inhibitory processes (Hendrick et al., 2012, Hsu et al., 2017), not reflecting simple anticipatory processing, have been excluded.
- When studies contrasted or collapsed together different sensory modalities or satiety states, I considered only foci coming from contrasts derived from stimulation in a single sensory modality (visual or gustatory) and satiety state (foci coming from contrasts in which fasting and fed conditions were merged (Führer et al., 2008, De Silva et al., 2011) have been excluded);
- Adult subjects;
- Populations involved: either obese subjects, or healthy weight, or both;
- For studies with obese subjects, I considered only populations with BMI above or equal to 30 (World Health Organization, 2000);
- For comparative studies of obese versus control subjects, I considered only studies that employed a standard BMI cut-off to dichotomize groups (i.e., correlation studies were not considered);
- Whole brain analyses (no region-of-interest analyses);
- When studies assessed the effects of hormonal or drug treatments, I considered only studies that reported foci belonging to the pre-treatment condition.

This selection, initially primarily based on titles and then on abstracts, yielded to the identification of 37 papers candidates for the meta-analysis (Figure S1.1 in Supplementary File 1).

Third, I made a further selection by inspecting the entire manuscripts and applying the aforementioned inclusion criteria in detail.

The final dataset included 22 papers (Gautier et al., 1999, Killgore et al., 2003, Rothemund et al., 2007, Cornier et al., 2009, Martin et al., 2010, Haase et al., 2011, Cornier et al., 2012, Dimitropoulos et al., 2012, Murdaugh et al., 2012, Nummenmaa et al., 2012, Szalay et al., 2012, Cornier et al., 2013, Geliebter et al., 2013, Jastreboff et al., 2013, Karra et al., 2013, Lundgren et al., 2013, Luo et al., 2013, Murray et al., 2014, St-Onge et al., 2014, van Bloemendaal et al., 2014, Blechert et al., 2016, Puzziferri et al., 2016), 70 contrasts and 660 activation foci (see Table S1.1 in the Supplementary File 1 for a detailed description of the paradigms).

To arrange the dataset for the subsequent Cluster Composition Analysis (CCA), each focus was classified according to the three factors of interest: group (HW vs. OB), sensory modality (visual vs. gustatory) and satiety (fasting vs. fed). Further, all the Talairach coordinates were converted to MNI space through the Talairach to MNI (SPM) transformation implemented in GingerALE (Eickhoff et al., 2009, Turkeltaub et al., 2012), version 2.3.6. Ten out of 660 foci were excluded from the dataset because they fell outside even from the less conservative brain boundary mask of the GingerALE software.

In the end, the dataset was based on 556 participants, 329 HW, and 227 OB (mean BMI = 22.4 vs. 35.6; mean age = 32.6 vs. 36.9 years), with an average of 8.6 hours of fasting for the fasting condition. Subjects in the fed condition were by default those who just have had a meal.

2.2.2. Hierarchical Clustering Analysis (HCA) and Cluster Composition Analysis (CCA)

To identify anatomically coherent regional effects, I first performed a HCA using the unique-solution clustering algorithm developed by Cattinelli et al. (2013b), implemented in CluB (Clustering the Brain) (Berlingeri et al., 2019). In brief, CluB takes into account the squared Euclidian distance between each couple of foci included in the dataset; the clusters with minimal dissimilarity are then recursively merged using Ward's criterion (Ward, 1963), to minimize the intra-cluster variability and maximizing the between-cluster sum of squares (Cattinelli et al., 2013b). To impose a suitable *a priori* spatial resolution to the analyses, I set

to be 5 mm the maximum mean spatial variance within each cluster in the three directions[10]. The centroid coordinates of each resulting cluster were then labeled according to the Automatic Anatomic Labelling (AAL) (Rorden and Brett, 2000), and then controlled by visual inspection on the MRIcron (Rorden and Brett, 2000) visualization software.

The output of the HCA was then entered as an input for the subsequent CCA. This procedure allows a post-hoc statistical exploration of each cluster by computing, within each cluster, the proportion of foci belonging to different levels of a variable of interest. Such proportion is then compared with a target proportion, which, in this case, is extracted from the overall distribution of foci classified according to our factors of interest in the whole dataset (Prior Likelihood, PL). First, I ran a CCA to explore the main effects of group, sensory modality, and satiety. This composition analysis was done by running a binomial test on the proportion of foci associated with each level of the three factors within each cluster. For example, if a cluster X had a cardinality of $N = 20$ and included 15 foci associated with the level "HW" of the "group" factor, CluB computes the proportion 15/20 (i.e., 0.75) and compares it with the theoretical proportion computed over the entire dataset (e.g., $PL_{HW} = 377/650 = .58$). Hence, (a) the Prior Likelihood represents the probability of success under the null hypothesis and (b) a significant binomial test ($p < .05$) indicates that the proportion of activation peaks included in that specific part of the brain is higher than the proportion computed all over the brain.

Then, to test for interaction effects (sensory modality-by-satiety, group-by-sensory modality, and group-by-satiety), I performed a series of Fisher's exact tests (Fisher, 1970) on the empirical peak-distribution within each cluster. Finally, with the aim to interpret the directionality of the second-level interactions, I employed the following method: for each cell of the 2 x 2 crosstab, I calculated the ratio between the proportion of observed foci and the total number of foci within the cluster (OP, observed probability). Then, I divided this value for the proportion of foci belonging to the same factors considering the entire dataset (PL). This computation (i.e., OP/PL) results in an index that indicates the degree to which the distribution of activation peaks belonging to a specific combination of factors within a cluster exceeds the expected probability. Values greater than one indicate a higher probability for the cluster to be specific for that particular combination of factors.

---

[10] This choice was motivated by the interest into small and discrete subcortical structures, such as the ventral (nucleus accumbens) and dorsal striatum.

Despite not being associated with a formal statistical test, the same procedure was applied to explore, descriptively, eventual three-way interaction effects (i.e., group-by-sensory modality-by-satiety interactions).

To limit the impact of any given study, I considered for further discussion only clusters with at least 3 contributing studies; moreover, clusters with cardinality (i.e., number of peaks) inferior to the 25th percentile (< 3) of the total cardinality of clusters were discarded.

2.2.3. Validation of the spatial relevance of each cluster using the ALE procedure

As pointed out in Appendix A, the HCA does not provide a statistical test of the spatial significance of the resulting clusters: this can be compensated for by searching for spatial convergence between the clustering solution and the results of an Activation Likelihood Estimate (ALE)-based meta-analysis on the same overall dataset (see, for example (Paulesu et al., 2014)). For the spatial cross-validation ALE, I employed the Turkeltaub Non-Additive method (Turkeltaub et al., 2012), with the general statistical threshold set to $p < 0.05$ FDR corrected. For the small subcortical structures, I accepted as significant also clusters converging on an ALE map thresholded at the slightly more liberal $p < 0.001$ uncorrected threshold. The resulting maps were overlapped with the HCA map with the "intersection" function in the software MRIcron (https://www.nitrc.org/projects/mricron). Only the clusters that fell in this intersection map were then taken into account for further analyses (the CCA) and discussion.

2.3. Results

2.3.1. Hierarchical Clustering Analysis (HCA)

The HCA returned 119 clusters, each composed by 3 to 16 peaks; mean standard deviation along the three axes was 4.98 mm (x-axis), 4.89 mm (y-axis) and 4.86 mm (z-axis). Of these, 38 were retained following the intersection analysis procedure with the ALE map. On average these clusters contained 8 foci (range: 3-16). The full list of clusters overlapping with the ALE map is available in the Supplementary File 1 (Table S1.2). These clusters were then submitted to a cluster composition analysis (CCA) to test for association with group, stimulation modality and satiety.

The following group, modality or satiety associations imply a more frequent detection of an activation effect in the specified level for each factor (e.g., obese, visual-anticipatory modality, etc.).

2.3.2. Cluster Composition Analysis (CCA)

2.3.2.1. Group-specific clusters

The binomial CCA performed to test whether each cluster was significantly associated with either group revealed that three clusters were significantly associated with HW individuals (i.e., clusters containing a significantly smaller number of peaks from obese individuals), and three with OB subjects (i.e., clusters containing more peaks from obese subjects) (Table 2.3, Figure 2.1).

The HW-specific clusters were located in the left midbrain (CL45), right thalamus (CL103) and right Rolandic operculum (CL113). As only two studies contributed to this cluster (Haase et al., 2011, Cornier et al., 2013), CL113 will not be discussed further. The centroid coordinates of the OB-specific clusters were located in the left ventral striatum (VS, CL43), right superior frontal gyrus (CL23) and the left anterior insula/frontal operculum (CL116).
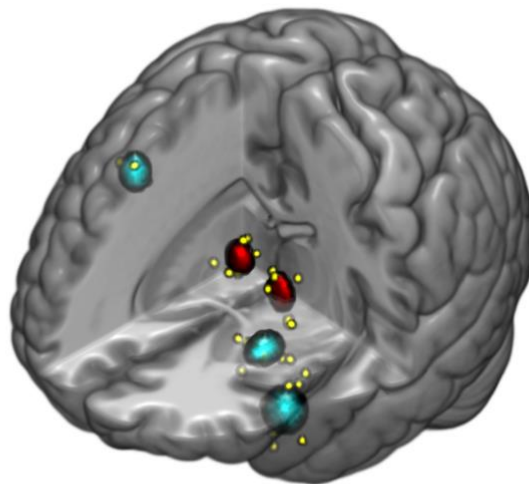
Figure 2.1 | Distribution of clusters showing a significant main effect of group. Clusters associated with obese individuals are depicted in cyan, whereas clusters specific for healthy weight subjects are depicted in red. Yellow dots re-present the cloud of peaks that generated the cluster. Taken from: Devoto et al. 2018.

2.3.2.2. Sensory modality-specific clusters

There was one cluster, located in the left anterior insula/frontal operculum (CL116), that was also significantly associated with the visual modality, while six clusters were specific for the gustatory modality (Table 2.3, Figure 2.2): these were located in the right pallidum (CL29), right anterior insula (CL41), left ventral striatum (CL43), left postcentral gyrus/Rolandic operculum (CL101) and right thalamus (CL103).

Table 2.3 | Results of the Cluster Composition Analysis. For each cluster the following information is reported: the anatomical label according to the AAL; the cluster ID; the centroid coordinates in the MNI stereotaxic space (standard deviation of the distance from the centroid along the three axes); the number of foci falling within the cluster (N); the p-values associated with the binomial and Fisher's tests. Significant main and interaction effects are shown in bold. FA, fasting state; FE, fed state; G, gustatory modality; GR, group; GRxS, group-by-satiety interaction; GRxSM, group-by-sensory modality interaction; HW, healthy weight; OB, obese; S, satiety; SM, sensory modality; V, visual modality. Adapted from: Devoto et al. 2018.

Anatomical Label	ID	Left Hemisphere			Right Hemisphere			N	GR-specific		SM-specific		S-specific		GRxSM	GRxS	SMxS
		X (SD)	Y (SD)	Z (SD)	X (SD)	Y (SD)	Z (SD)		HW	OB	V	G	FA	FE			
Superior Frontal Gyrus	23				22 (3.5)	25 (3.8)	51 (6.1)	4	1	**0.031**	0.199	1	0.997	**0.044**	1	1	1
Globus Pallidus	29				14 (4.5)	6 (6.2)	-1 (5)	15	0.737	0.453	0.992	**0.03**	0.098	0.983	0.093	1	1
Orbitofrontal Cortex	31				34 (6.2)	30 (2.6)	-15 (4.4)	12	0.804	0.389	0.396	0.817	0.989	**0.043**	0.516	0.608	1
Insula	41				38 (3.9)	18 (4.9)	-3 (4)	14	0.636	0.575	1	**0.001**	0.779	0.432	0.225	0.244	0.221
Ventral Striatum	43	-19 (4)	5 (5.8)	-9 (3.5)				11	0.999	**0.009**	1	**0.001**	0.051	1	**0.002**	1	1
Midbrain (ventral tegmental area/substantia nigra)	45	-5 (3.8)	-15 (2.1)	-4 (6.2)				9	**0.007**	1	0.653	0.62	0.088	1	1	1	1
Superior Medial Frontal Cortex	72				2 (2.1)	59 (3.8)	21 (8.3)	6	0.792	0.497	0.353	0.911	0.996	**0.031**	1	0.097	1
Caudate Head/Nucleus Accumbens	99	-7 (5.5)	14 (8.6)	-9 (6.4)				8	0.937	0.206	0.981	0.087	0.903	0.289	0.505	1	**0.031**
Postcentral Gyrus/Rolandic Operculum	101	-50 (7)	-16 (4.4)	18 (4.3)				7	0.883	0.329	0.993	**0.045**	0.478	0.849	1	1	1
Thalamus	103				14 (4.1)	-14 (3.4)	0 (5.5)	9	**0.007**	1	0.999	**0.008**	0.637	0.667	1	1	0.107
Posterior Insula	104	-39 (4)	-4 (5.6)	6 (5.4)				16	0.92	0.183	0.168	0.94	**0.013**	1	1	1	1
Anterior Insula/Frontal Operculum	116	-38 (5.7)	13 (6.4)	-19 (7.2)				10	0.997	**0.017**	**0.018**	1	0.565	0.725	1	0.509	1
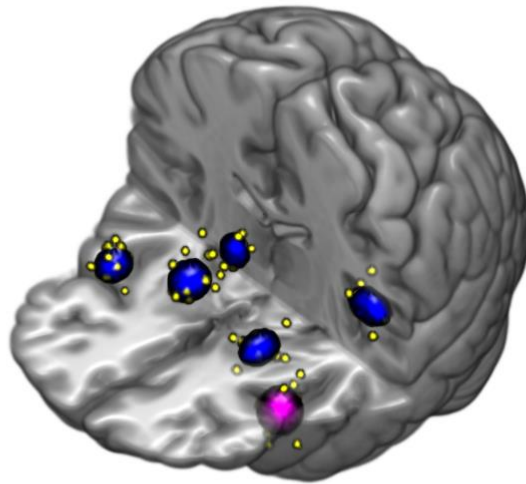
Figure 2.2 | Distribution of clusters showing a significant main effect of sensory modality. The cluster associated with the visual modality is depicted in purple, whereas clusters specific for the gustatory modality are depicted in blue. Yellow dots represent the cloud of peaks that generated the cluster. Taken from: Devoto et al. 2018.

2.3.2.3. Satiety-specific clusters

Only one cluster in the left posterior insula (CL104) was significantly associated with the fasting condition. Three clusters, located in the right superior frontal gyrus (CL23), right caudolateral orbitofrontal cortex (CL31) and in the right superior medial prefrontal cortex (CL72) were associated with the fed condition (Table 2.2, Figure 2.3).
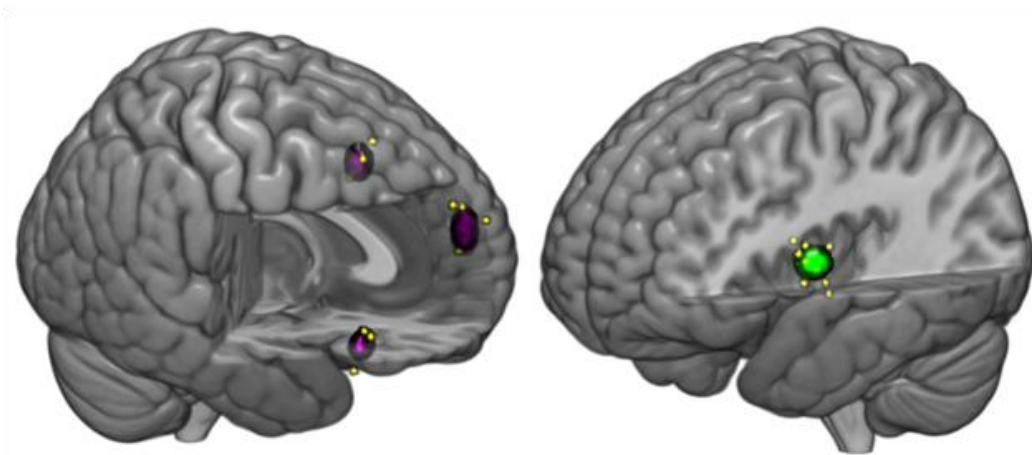
Figure 2.3 | Distribution of clusters showing a significant main effect of satiety. Clusters associated with the fed condition are depicted in dark purple, whereas the cluster specific for the fasting state is depicted in green. Yellow dots represent the cloud of peaks that generated the cluster.Taken from: Devoto et al. 2018.

2.3.2.4. Group-by-sensory modality interaction

I identified one significant *group-by-sensory modality* interaction effect (Table 2.3, Figure 2.4), and it was located in the left ventral striatum (CL43). The inspection of the graph in Figure 2.4 (top right) shows that the VS was more likely to be recruited by OB individuals during gustatory stimulation.

2.3.2.5. Group-by-satiety interaction

No cluster displayed a significant group-by-satiety interaction effect.

2.3.2.6. Sensory modality-by-satiety interaction

Only one cluster, located in the left caudate head/nucleus accumbens (CauH/NAc, CL99) displayed a significant interaction effect (Table 2.3, Figure 2.4). The inspection of the graph in the Figure 2.4 (top left) shows that the left CauH/NAc was more likely to be associated with gustatory stimulation in a fasting state and with the visual stimulation in a fed state.
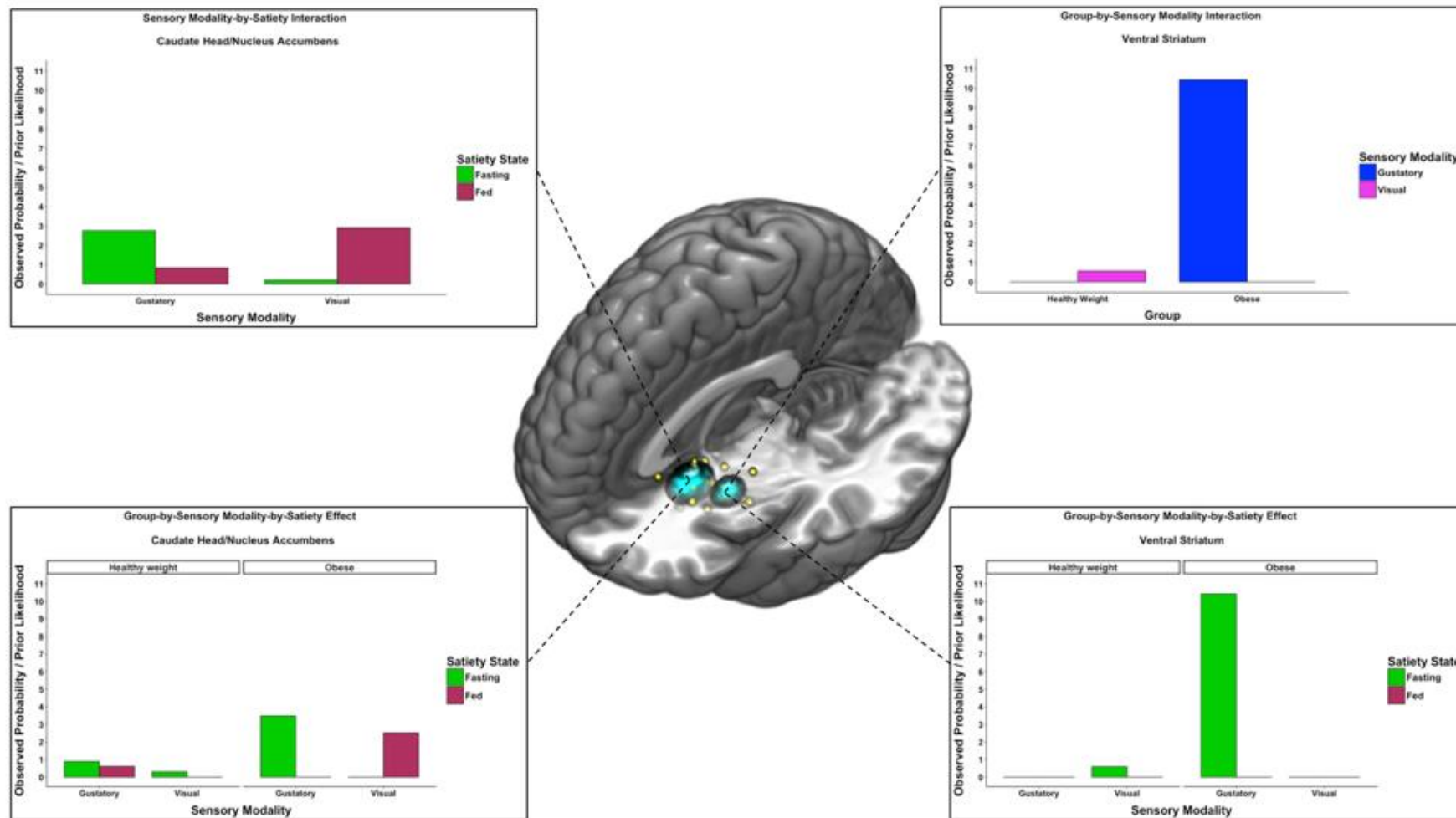
Figure 2.4 | Distribution of clusters showing a significant interaction effect. Yellow dots represent the cloud of peaks that generated the cluster. Top: bar plot for the significant group-by-sensory modality interaction in the left ventral striatum (top right) and for the significant sensory modality-by-satiety interaction in the left caudate head/nucleus accumbens (top left). Bottom: bar plot for further visual inspection of group-by-sensory modality-by-satiety interactions in the left ventral striatum (bottom right) and in the left caudate head/nucleus accumbens (bottom left). Values greater than one indicate a higher probability for the cluster to be specific for that particular combination of factors. Taken from: Devoto et al. 2018.

2.3.2.7. Group-by-sensory modality-by-satiety effects

Given the numerosity of the peaks in the clusters commented below, a formal estimate of the significance of this level of interaction by means of the Mantel-Haenszel test (MANTEL and HAENSZEL, 1959) was not possible. Yet, I thought it was interesting to illustrate the origin of the effects in CL43 and CL99, considering the factors "Satiety" and "Group", respectively. To this end, I plotted the OP/PL ratio for each combination of the three factors (Figure 2.4, bottom row). The inspection of the graph in Figure 2.4 (bottom left) shows that the left CauH/NAc (CL99) were coming essentially from OB individuals during the visual stimulation in a fed state and during the gustatory stimulation in the fasted state. Similarly, the bottom graph in Figure 2.4 (bottom right) shows that the left ventral striatum (CL43) was determined by activations in OB individuals during gustatory stimulation in the fasting state.

2.4. Discussion

Before entering into a detailed discussion of the results, I wish to point out my position with respect to the "food addiction" hypothesis (Davis, 2014). Admittedly, this work was inspired by theories developed to explain substance abuse, and one may be led to conclude that with the present findings I will root for a plain explanation of obesity as a case of food addiction: I am not doing so in any deterministic manner. I am aware that the concept of obesity as a food addiction has been recently criticized on theoretical, empirical, and even ethical considerations (Ziauddeen et al., 2012, Finlayson, 2017). However, I believe that this does not weaken the potential value of showing that one or more theories, originally developed for explaining substance abuse, may fit, as a whole or in part, the available activation imaging literature on obesity. Since the literature considered here has not covered all possible aspects of the brain physiology in obesity (e.g., fMRI has little if anything to tell about neurotransmission), it follows that the present evidence should not be treated as a strict case for the concept of obesity as caused by food addiction[11].

---

[11] Another word of caution is needed here: brain activation data by no means can offer a complete picture of the complex phenomena under examination. Molecular brain imaging using PET and specific ligands are offering important complementary ways to address the neural bases of obesity. However, the available corpus of data from this literature in humans is more limited and dominated by "resting state" measures of receptor binding potentials and their relation with BMI: this set of data would not permit the testing of the neurocognitive hypotheses of obesity along a factorial design as it was possible for the activation data. For a comprehensive review of this literature, I refer the reader to the article by Van Galen et al. (2017).

Having made clear my position with respect to the concept of food addiction, I now attempt to answer three questions about the dysfunctional anatomy associated with obesity, as described by functional imaging activation studies: (1) do the patterns of functional and dysfunctional anatomy converge anatomically in a replicable manner, surviving to a formal meta-analysis and can be specific for a particular modality of stimulus presentation (visual-anticipatory vs. gustatory-consummatory), satiety level (fasting vs. fed), and group (healthy weight vs. obese)? (2) Do the aforementioned patterns reflect the interactive effect of the three factors that we examined (BMI, sensory modality of cue presentation and satiety), particularly for obese individuals? (3) Do these findings allow us to support in part or full a particular neurocognitive theory on the making and maintenance of obesity discussed in the introduction?

The first hypothesis is not as trivial as it might seem. Anatomical replications in functional neuroimaging are such if they go beyond the mere observation of recurrent anatomical names: indeed, a nominal reference to a given brain structure and the ensuing discussions are deprived of much value unless the precise stereotactic locations of a statistical effect are used and their convergence is submitted to a quantitative meta-analytical assessment[12].

Of course, the testing of the second and third hypotheses was the central motivation of the present meta-analysis, and the answers will be discussed in detail below. For clarity, and for consistency with the framework introduced at the beginning of this thesis, the discussion will be broken down into paragraphs concerning the simple, or interaction effects, on the cue-reactivity and cue-regulation networks. Following an incremental logic, the main effects of sensory modality and satiety will be presented first, followed by the discussion of the main effect of group. Then, I will discuss the interaction among the factors taken into consideration, with particular reference to the effects related to obese individuals. Finally, I will try to integrate the abovementioned findings and spell-out the implications for the neurocognitive theories of obesity described in the introduction.

2.4.1. Hypothesis one: anatomical convergence of functional effects across studies
The HCA and CCA identified two main classes of spatially significant clusters: the first is less interesting, as these spatially significant clusters were not associated with group, nor with sensory modality or level of satiety. There were 38 such clusters (Table S1.2 in Supplementary File 1). Not surprisingly, this broad network of brain regions is compatible with both the

---

[12] As argued before, the lack of PET ligand data reported with stereotactic coordinates makes it impossible a formal meta-analysis of ligand work with the PET/fMRI activation data.

exteroceptive (visual) and the interoceptive (gustatory, somatosensory) processing of food-related information, in keeping with the activation paradigms that generated such observations. These effects were also captured by previous meta-analyses (van der Laan et al., 2011, Veldhuizen et al., 2011, Dimitropoulos et al., 2012, Brooks et al., 2013, Huerta et al., 2014, Kennedy and Dimitropoulos, 2014, Pursey et al., 2014, van Meer et al., 2015).

Of major interest was the second class of clusters, for which the post-hoc CCA revealed significant main effects and interactions between the factors under examination.

2.4.1.1. Sensory modality of cue-presentation

Across groups and satiety conditions, both the visual-anticipatory and the gustatory-consummatory sensory modalities of cue presentation were mainly associated with more frequent activity within the cue-reactivity network.

Visual modality. Among the clusters significantly associated with a specific sensory modality of cue presentation, only one cluster was specific for the visual modality: the left anterior insula. As a right insular cluster was specific for gustatory stimuli (see below), these findings suggest *asymmetrical processing* of food-related stimuli for the insular cortex (Figure 2.2, in purple). Neurofunctional patterns of activation during food perception in different sensory modalities have been shown to overlap in the left insula, whereas olfactory and gustatory stimuli were found to elicit more bilaterally distributed responses (Huerta et al., 2014). Notably, in the latter study, exposure to food images selectively evoked responses in the left, rather than the right, insular cortex (Huerta et al., 2014). My result hence dovetails with findings of previous independent[13] fMRI studies (Small et al., 1997a, Small et al., 1997b, Frey and Petrides, 1999, Small et al., 1999, Barry et al., 2001, Cerf-Ducastel et al., 2001), supporting an asymmetrical information processing in the insular cortex as a function of the sensory modality of cue presentation.

Gustatory modality. The majority of the clusters was specifically associated with the gustatory modality (Figure 2.2, in blue), revealing a network of brain regions typically involved in reward (ventral striatum) (Berridge et al., 2010, Berridge and Kringelbach, 2015) and sensory processing (right thalamus, right insula, postcentral gyrus/Rolandic operculum) of gustatory stimuli, much as it was found in a previous meta-analysis on the topic (Veldhuizen et al., 2011).

---

[13] The fMRI studies cited are independent in that the data of those studies did not enter in our meta-analysis.

2.4.1.2. Satiety state

Across groups and sensory modalities of cue presentation, hunger was associated with more frequent activity within the cue-reactivity network, whereas satiety was associated with more frequent activity within the cue-regulation network.

Satiety. I found that three clusters were significantly associated with the fed condition, in the prefrontal cortex: the right SFG, the right caudo-lateral OFC, the superior medial PFC (Figure 2.3, in dark purple). The prefrontal cortex plays an important role in several higher-order processes such as attention control (Knight et al., 1995), working memory and decision-making (Bechara et al., 1998), and its over-activation in OB seems a consistent result across meta-analyses and imaging studies on satiety (Gautier et al., 2000, Gautier et al., 2001, Kennedy and Dimitropoulos, 2014, Pursey et al., 2014). More specifically, this result may be in keeping with the role of the prefrontal cortex in meal termination (Tataranni et al., 1999, Del Parigi et al., 2002).

Hunger. On the contrary, only the left middle insular cortex was specific for the fasting (i.e., hunger) condition, in a region posterior to the one involved in visual perception of food (Figure 2.3, in green). This portion of the insular cortex has been linked to the subjective experience of several types of *cravings*, such as craving for food (Gordon et al., 2000, Pelchat et al., 2004), for substances of abuse such as cocaine (Breiter et al., 1997, Bonson et al., 2002) and even for air (Liotti et al., 2001); more importantly, lesions to the insula disrupt addiction to cigarettes smoking (Naqvi et al., 2007, Naqvi and Bechara, 2009), thus suggesting that the region plays a pivotal role in craving and in addiction-like behaviors.

As discussed below, the sensory modality of cue presentation and the satiety state interact in a meaningful way, revealing distinct dysfunctional brain responses in obese individuals.

2.4.1.3. Group

As much as this can be reflected by measures of the BOLD response, obesity is associated, across sensory modalities of cue presentation and satiety conditions, with both up and down-regulation of key regions of the cue-reactivity and cue-regulation networks.

Obese. Overall, I confirm one of the most frequently reported findings in imaging studies and meta-analyses on cue-reactivity in OB individuals: the higher recruitment of regions involved in reward and motivation (dorsal and ventral striatum), salience (insula and superior frontal gyrus) and gustatory processing (anterior insula) in response to food-related stimulation (Brooks et al., 2013, Kennedy and Dimitropoulos, 2014, Pursey et al., 2014). Indeed, most of the clusters associated with HW or OB individuals were also specific for a given sensory

modality or satiety condition, to suggest that OB individuals show hyper-activation of areas that usually respond to the visual or the gustatory sensory modality (anterior insula/frontal operculum and ventral striatum, respectively), or when satiated (right superior frontal gyrus). In particular, persistent PFC activations in response to food in OB individuals have been linked to the deployment of attentional resources by a taste input (Kringelbach et al., 2004) or increased inhibitory efforts to contrast striatal and limbic hyper-activations (Gautier et al., 2000, Gautier et al., 2001). This latter hypothesis is particularly intriguing, because it would frame the striatal (cue-reactivity network) and PFC (cue-regulation network) association with obesity under the same conceptual umbrella.

Lean. In obese individuals, I also identified less frequent activation of the thalamus and the midbrain, in a region compatible with the dopaminergic nuclei: the ventral tegmental area (VTA) and the substantia nigra (SN). Hypoactivation of the midbrain in humans has gone largely unnoticed by previous functional imaging studies and meta-analyses on the topic, despite the quite compelling evidence pointing to dysregulation of VTA activity in animal models of obesity (Fulton et al., 2006, Roseberry et al., 2007, Davis et al., 2008, Koyama et al., 2013). Given the nature of the data submitted to meta-analysis (focal changes of the BOLD response), any discussion on the possible mechanisms behind the brainstem signals remains a matter of educated guesses at best. However, it has been recently found that obesity induced by a cafeteria diet[14] leads to increased D2 receptors auto-inhibition of the VTA dopaminergic neurons in mice (Cook et al., 2017), while obesity was found to decrease the excitability of GABAergic neurons in the VTA (Koyama et al., 2013). Accordingly, it may be tempting to hypothesize that a down-regulation of the VTA, particularly if this involves GABAergic neurons, may lead to a disinhibition of ventral striatal activity in response to food. Furthermore, the increased response to food in the ventral striatum and a reduced VTA response might represent the two sides of the same coin of a dysregulated reward system.

---

[14] Consisting of bacon, potato chips, cheesecake, cookies, breakfast cereals, marshmallows, and chocolate candies.

2.4.2. Hypothesis two: are there anatomo-(dys)functional interactions between BMI, sensory modality and satiety?

I expected that the interaction between the sensory modality of food presentation (visual-anticipatory vs. gustatory-consummatory) and the satiety state (hungry vs. sated) would unveil specific patterns of dysfunctional responses to food in obese individuals, thus favoring a quantitative assessment of the current neurocognitive theories of obesity. To test my second hypothesis, I first explored the directionality of the significant two-way interactions in the VS and the CauH/NAc; second, I looked for a further modulation of the satiety state and the BMI status in the VS and CauH/NAc, by exploring the origin of what may represent a higher-level interaction.

Group-by-sensory modality interaction. Beyond the main effects of group and sensory modality, the left VS showed a significant group-by-sensory modality interaction; the post-hoc analysis of the interaction showed that, in obese individuals, there are more convergent activations in the gustatory versus the visual sensory modality, whereas in healthy weight subjects there is no difference between sensory modalities (Figure 2.4, top right). A further inspection of the cluster composition revealed that the more frequent response to taste was mainly driven by studies in the fasting condition, thus suggesting more potent reward-related responses to taste in fasting obese individuals (Figure 2.4, bottom right). With this respect, as the duration of fasting time for healthy weight and obese individuals was identical, one may hypothesize that fasting could be perceived more threatening to an obese organism, that is used to higher availability of short-term and long-term energy resources, compared with a normal weight organism. Accordingly, more frequent activation of regions involved in the motivational/hedonic aspects of food perception such as the ventral striatum, might represent the way of the obese organism to defend the new status of positive energy balance (Berthoud et al., 2017), reinforcing the action of eating (noteworthy, the interaction involves the gustatory – consummatory – rather than the visual – anticipatory – sensory modality). Also, a stronger response to hunger-related peripheral signals (e.g., ghrelin) may also be hypothesized.

Sensory modality-by-satiety interaction. The sensory modality-by-satiety effect observed in the CauH/NAc points to another dysfunctional interaction that might account for overeating: a persistent over-reaction to visual food cues in regions typically involved in reward and motivation(Martin et al., 2010). As shown by the inspection of the plot in Figure 2.4 (top left), satiety seems to modulate in opposite directions the neurofunctional response to food in the CauH/NAc, as a function of the sensory modality of cue presentation. As the specificity for the

gustatory stimulation during fasting strongly resembled the effect that we observed in the left VS, I further explored the composition of the cluster with respect to the weight status (healthy weight vs. obese), to assess whether the effect was mainly driven by obesity. The inspection of the plot in Figure 2.4 (bottom left) suggests that obese individuals show more frequent activation of the left CauH/NAc in the gustatory stimulation condition during fasting, and for visual food stimuli when fed.

Taken as a whole, my results suggest that: (i) the up-regulation of the cue-reactivity network, in obese individuals, interacts with the sensory modality and the level of satiety; (ii) the way they interact is compatible with enhanced reward processing to taste (particularly when fasting), and with continued reward processing in response to anticipatory visual food cues even when well fed; (iii) current neurocognitive theories are not mutually exclusive, but might tap onto different aspects or timing (onset vs. maintenance) of obesity. This is what I discuss next.

2.4.3. Hypothesis three: do the available data permit to identify a best fitting neurocognitive theory of obesity?
In Table 2.2 I tried to summarize the benchmarks that one could take in favor of any given neurocognitive theory of obesity. Among the theories there are some that clearly did not receive any support: for example, the Inhibitory Control Deficit Theory of obesity (Nederkoorn et al., 2006a, Nederkoorn et al., 2006b), as I did not observe any reduced frontal lobe activity in obese subjects. Nonetheless, I acknowledge the possibility that the lack of support to an Inhibitory Control Deficit Theory might be a by-product of the fact that the hypothesis has been tested only occasionally or indirectly[15]. In fact, evidence suggests that obese compared to healthy weight individuals show altered activity of inhibitory control regions during Go/No-Go tasks (Hendrick et al., 2012), and during delay-discounting tasks (Kishinevsky et al., 2012, Weygandt et al., 2013) involving food stimuli; further, this alteration is related to weight-loss maintenance (Weygandt et al., 2013) and to future weight gain (Kishinevsky et al., 2012). However, since the neural activation during those tasks could not be attributed to simple anticipatory processing, I had to exclude them by the meta-analysis (please refer to inclusion criteria in the methods section). More importantly, the predictions for the Inhibitory Control Deficit Theory

---

[15] One possible benchmark would have been a reduced prefrontal activation when viewing food-related cues in a fed state. However, a group by feeding state interaction was not observed in the prefrontal cortex.

mainly stemmed by previous meta-analytical (Brooks et al., 2013, Kennedy and Dimitropoulos, 2014, Pursey et al., 2014) and preliminary fMRI evidence suggesting that obesity is associated with lower recruitment of brain regions associated with inhibitory control in response to the simple exposure to food-related stimuli (Gearhardt et al., 2014, Silvers et al., 2014). Since the simple exposure to anticipatory food cues might not be sufficient to detect a deficient activity in inhibitory control regions, specific paradigms are needed to further explore the Inhibitory Control Deficit account, particularly if this has to be framed within the context of an altered predisposition to temporally discounted rewards (Evans et al., 2012, Kishinevsky et al., 2012). If deciding on the less fitting explanations was perhaps an easy task, deciding on a best fitting theory may be more complicated. This is why in what follows we take an Occam's razor-like approach[16] and exclude the need of more theories if one can explain most of the results.

Let's consider the Reward Surfeit Theory and Reward Deficit Theory. The first is supported by the fact that obese individuals showed more frequent activation in regions involved in reward and motivation (ventral and dorsal striatum) in response to taste, in particular when fasting; the second would find support by the less frequent activation of the brainstem in a region compatible with the dopaminergic nuclei of the midbrain, and in agreement with animal models (Roseberry et al., 2007, Koyama et al., 2013, Cook et al., 2017) pointing to a blunted reward system activity in chronic obesity. However, as discussed, if the brainstem down-regulation in obesity was involving specific populations of VTA GABAergic neurons, this may lead to a dysregulated and increased response of the ventral striatum. As this, in turn, would make the data still compatible with the Reward Surfeit Theory, I abandon the Reward Deficit Theory and retain the Reward Surfeit Theory for further discussion.

The next theory to be compared with the Reward Surfeit Theory is the Incentive Sensitization Theory. The latter is clearly more articulated and dynamic compared to the former: by assuming repeated pairings between visual anticipatory cues and the hedonic impact of food consumption, the theory is supported by the evidence of an enhanced response for visual food cues in regions usually involved in salience and reward processing. Accordingly, I retain the Incentive Sensitization Theory as the provisional best fit of the data of the present meta-analysis. In fact, my data show that obese individuals, after their prolonged period of overeating, exhibit hyper-responsivity of regions involved in gustatory and salience processing (insula), reward and motivation (nucleus accumbens, caudate head) in response to food cues, which witnesses the

---

[16] Strictly speaking, the Occam's razor approach posits that one should prefer simpler over more articulated explanations. Here I favour best fitting explanations.

process of incentive sensitization to anticipatory visual cues. Nonetheless, the composition of the cluster in the CauH/NAc suggests that OB individuals exhibit persistent reward and motivational processing in response to food images, as if the incentive salience of food cues could override the peripheral signals of satiety, motivating the eating behavior in absence of homeostatic energy needs. It is worthy to note that the theory accommodates the impact of physiological body signals like hunger. According to Berridge and colleagues (Berridge et al., 2010), "normal hunger acts as a physiological "drive" signal to magnify the incentive "wanting" and hedonic "liking" triggered by tasty foods and their associated cues whereas satiety dampens the multiplicative impact of cues and foods" (Figure 1, page 32). Therefore, the interaction of hunger with a sensitized reward system would lead to powerful activity of the mesocorticolimbic circuitry in response to visual food cues and to food consumption, which could be also interpreted in favor of a Reward Surfeit Theory of obesity.

It is important to underline that while satiety should normally dampen the impact of food cues, it seems to do so to a lesser extent in obese patients. In the data meta-analyzed here, the level of satiety seems to have a different impact on the functional brain patterns of obese subjects in response to food cues or to tastes. The differential response observed within the cue-reactivity network (more frequent activations for visual cues even in a satiated state in obese) sets the rationale for new empirical studies in which these factors are explicitly manipulated and modeled. In addition, obesity is associated with more frequent activations within the cue-reactivity network in response to taste cues while starving, suggesting that hunger is a particularly powerful signal for obese individuals, their hyperactivation in such condition representing, perhaps, the result of a greater reward value of food.

To summarize, I believe that my data confirm that any complete theory of eating behavior in obesity should incorporate the differential weight that the level of satiety has for obese subjects. The combination of different levels of satiation with cognitive control task in lean and obese subjects may also revitalize the Inhibitory Control Deficit Theory in a more context-dependent manner.

2.4.4. Obesity in its making and the vulnerability factors for obesity

There is one other aspect in which Incentive Sensitization Theory seems not sufficiently explicit: the making of obesity and the connection if its making with vulnerability factors leading certain individuals to have a greater likelihood of becoming obese. These are aspects that our meta-analysis was unable to capture as the studies on obese individuals submitted to meta-analysis were cross-sectional. There is one candidate theory in the literature that that tries

to integrate diachronically an initial reward surfeit followed by enhanced value to food related cues and the blunting of the hedonic system, particularly when subjects are exposed to high-calories foods. This is the Refined Dynamic Vulnerability Model (Stice and Yokum, 2016). Much of the model is based on considerations derived from longitudinal studies (an aspect not considered here because there are no such studies in the selected imaging literature) and from observations to the response to high-calories food intake. This last aspect was also impossible to assess with the present meta-analysis as a mere 7% of the total gustatory foci came from studies employing high-calorie liquid meals (Gautier et al., 1999, Szalay et al., 2012), whereas the remaining foci came from studies employing pure tastes as gustatory stimuli (Gautier et al., 1999, Haase et al., 2011, Szalay et al., 2012, Cornier et al., 2015).

2.4.5. Implications for brain-centered treatments of obesity

Having shown that the Incentive Sensitization Theory is a likely candidate to provide a neurocognitive explanation of obesity, at least in its steady adult state, it is natural to wonder to what extent this has been or could be conceptually useful to plan therapeutic interventions. Unfortunately, the available evidence of a translation of these principles into clinical practice is limited. The long-lasting temporal characteristics of sensitization suggest that the suppression of the relevance of food cues and their interaction with the level of satiation might be a particularly difficult route to pursue. Clearly this is one area where cognitive behavioral therapy may have an impact.

As far as a more directly brain-based approach, neurostimulation and neuromodulation techniques, such as repetitive transcranial magnetic stimulation (rTMS) and transcranial direct-current magnetic stimulation (tDCS), have been tested in obesity and eating disorders (for a review see (Val-Laillet et al., 2015)). So far, all the studies employing these techniques have targeted the prefrontal cortex (Uher et al., 2005, Fregni et al., 2008, Barth et al., 2011, Goldman et al., 2011, Montenegro et al., 2012, Jauch-Chara et al., 2014, Kekic et al., 2014, Lapenta et al., 2014) providing mixed results. As shown by our quantitative meta-analysis and by a recent review of Stice and colleagues (Stice and Yokum, 2016), the evidence in support of an inhibitory control deficit explanation behind overeating and obesity is scarce. One other approach could be to target brain regions involved in salience (insula), reward and motivation (nucleus accumbens and caudate nucleus) as these appear more frequently active in obese individuals exposed to food pictures. Given the role of the insular cortex in the subjective feeling of craving (Pelchat et al., 2004) and in nicotine addiction (Dinur-Klein et al., 2014) and the recent advances in neurostimulation techniques in reaching deep cortical structures (Zangen

et al., 2005), the insular cortex stands out as a promising target for future neurostimulation treatments of overeating and obesity (see (Ferrulli et al., 2019b) and Chapter 4).

Finally, there has been a recent revival of neuro-pharmacological interventions in obesity beyond amphetamine-like drugs: for example, a combination of naltrexone, an opioid antagonist, and bupropion, an antidepressant, which inhibit dopamine and norepinephrine reuptake seems effective in appetite suppression and weight loss promotion by acting on both the hypothalamus and the ventral tegmental area (review in (Subramaniapillai and McIntyre, 2017)).

Whether these interventions, in isolation or combined, could reverse the incentive sensitization of the reward system to food and its cues, promoting weight loss and long-term healthier eating, remains to be seen and demonstrated explicitly. If so, this would provide a further support to the Incentive Sensitization Theory.

2.4.6. Strengths, limitations and future directions

By adopting a factorial approach, I tried to test the major neurocognitive theories in the field while also taking into account the modulatory role of the motivational state of the participants, to consider satiety-specific effects or interactions. I combined the ALE method (Eickhoff et al., 2009), which reveals the brain regions with most convergent activation across the whole dataset, with hierarchical clustering (Cattinelli et al., 2013b) and *post-hoc* statistical characterization of the clusters concerning the factors of interest, both implemented in the CluB toolbox (Berlingeri et al., 2019). An undoubted advantage of this approach was the possibility to include a heterogeneous set of studies without renouncing to a functional characterization of the meta-analytic clusters (see Appendix A for further information about the toolbox).

Yet the present study has some limitations. I already commented upon the issue of considering obesity as the end point of an addiction to food. I am not rooting for this hypothesis in any deterministic and simplistic manner: I am only showing that many aspects of one theory are supported by the existing activation imaging literature. Future studies will help to decide on whether the concept of food addiction should be abandoned or retained. For the time being, I remark that there are intriguing similarities between the two domains of substance abuse and excessive food intake in already obese subjects.

2.4.6.1. Further limitations

I cannot exclude that the disproportion between male and female participants of the reviewed studies may have left some effects overlooked. In fact, there is evidence of gender-specific differences in the brain responses towards food (Haase et al., 2011, Geliebter et al., 2013). Similarly, it was impossible to take into account data associated with altered levels of appetitive hormones in OB individuals. This is an important issue, as altered hormone levels are known to influence the neural responses to food stimuli (see (Burger and Berner, 2014) for a review). Not least, the evaluation of the highest order interactions remained at a descriptive level by observation of which of eight possible levels was pulling in the direction of the higher-level interaction (the group-by-sensory modality-by-satiety interactions). While more data are needed to attach a significance to such higher order effects, at the very least, the present evidence provides the rationale for future experiments in which body weight, sensory modality of cue presentation, and satiety are manipulated in a controlled manner. Nonetheless, this study provides the first evidence that different internal and external factors can modulate the neural reactivity to food cues not only in isolation, but also in interaction.

Another issue that remains unaddressed here is the importance of subjective "liking" and "wanting" ratings of food stimuli in (i) shaping the neurofunctional responses to food and (ii) providing support to a neurocognitive theory over the other, as assessed by our meta-analysis. The Reward Surfeit Hypothesis implies that the highly hedonic experience of food ingestion may prompt for future overeating, suggesting that people who overeat will show enhanced "liking" reactions to food intake. On the contrary, the Incentive Sensitization Theory focuses on the "wanting" reactions elicited by food cues, suggesting that overeating is triggered by excessive "wanting" that can be accompanied by normal "liking" of food stimuli. As shown in Supplementary Table S2.1, only half of the studies included in our meta-analysis collected and reported subjective ratings for the stimuli employed. More importantly, the ratings required to the participants are quite heterogeneous across studies, each focusing on a slightly different quality of the stimuli (e.g., pleasantness of the image, palatability or liking of a food). Despite not being a limitation of the meta-analysis per se, the lack of such data has made it impossible to assess how good is the fitting of the theories considered in the light of "liking" and "wanting" components of reward processing: this remains an issue for future studies.

Finally, as I reviewed data comparing adult OB and HW, I cannot draw any conclusion about the temporal and causal dynamics of the phenomena described. Inevitably, given the cross-sectional nature of the studies included in this meta-analysis, my results cannot but provide a relatively "static" picture of the neurofunctional correlates of food perception in obese versus

healthy weight individuals, making it impossible to disentangle causes from consequences in chronic overeating over the brain patterns described.

Furthermore, it would be tempting to try and connect the relative less frequent activation of the midbrain in obese individuals and their striatal hyper-responsivity for taste and food cues. However, this is impossible at this stage with the present data and it remains to be empirically tested whether i) the midbrain down-regulation is causally linked to disinhibited striatal activity and ii) whether it is associated with overeating before the individuals become obese. With this respect, it is important to emphasize that the genetic make-up linked to higher or lower dopamine signaling capacity seems crucial in determining increased versus decreased striatal activity in response to food cues (Stice et al., 2008a, Stice and Dagher, 2010, Stice et al., 2010b, Stice et al., 2011b, Stice et al., 2012, Stice et al., 2015a). As a consequence, the genetic make-up of the individuals is also expected to interact with other factors, such as weight status and sensory modality of cue-presentation, giving rise to specific brain activation patterns.

The field is much in need of prospective studies examining the differences (and similarities) between the neurofunctional predictors of overeating in HW and OB individuals, and whether a differential response to satiety or hunger may represent a vulnerability factor with respect to future weight gain. To the best of my knowledge, I am not aware of any prospective study that explored whether, and how, "hungry" or "insatiable" brains can predict future overeating and weight gain, something left for future studies.

Summary of Chapter 2

In this Chapter, I combined the CluB method with the GingerALE algorithm to perform a meta-analysis of 22 neuroimaging studies on food cue-reactivity in obesity. In particular, I explored the simple and interactive effect of three factors that modulate the neural reactivity to food cues: weight status, sensory modality of cue-presentation. These effects were taken as benchmarks to assess the validity of the major neurocognitive theories of obesity and overeating.

The results showed that obesity is associated with altered activity of key regions of the cue-reactivity and cue-regulation networks, being both up (left anterior insula, right SFG) and down-regulated (midbrain, right thalamus) in response to food cues, across modalities of cue-presentation and satiety conditions. The two sensory modalities of cue-presentation were associated with the activity of discrete clusters localized within the cue-reactivity network: whereas the visual-anticipatory modality was associated with left anterior insula activity, the gustatory-consummatory modality was associated with the activity of a wider network of

subcortical (right thalamus, globus pallidus, left VS) and cortical (right insula, postcentral gyrus/Rolandic operculum). Interestingly, hunger was associated with activity within the cue-reactivity network (left mid-posterior insula), while satiety was associated with an up-regulation of the cue-regulation network (right SFG, superior medial PFC, caudolateral OFC). Consistent with a Reward Surfeit Hypothesis, obese individuals exhibit a ventral striatum hyper-responsivity in response to pure tastes, particularly when fasting (group-by-sensory modality-by-satiety interaction). Furthermore, I found that obese subjects display more frequent ventral striatal activation for visual food cues when satiated: this continued processing within the reward system, together with the aforementioned evidence, is compatible with the Incentive Sensitization Theory. On the other hand, I did not find univocal evidence in favor of a Reward Deficit Hypothesis, nor for a systematic deficit of Inhibitory Control Deficit Theory. I concluded that: (i) internal (weight status, satiety) and external factors (sensory modality of cue presentation) operate in isolation and in interaction, modulating the neural responses to food cues in key regions of the cue-reactivity and cue-regulation networks; (ii) the available brain activation data on the dysregulated food intake and food-related behavior in chronic obesity can be best framed within an Incentive Sensitization Theory.

The extent to which internal and external factors, in isolation and/or in interaction, modulate the neural response to drug cues in SUD is what will be addressed in the next Chapter.

Chapter 3 – How the Harm of Drugs and Their Availability Affect Brain Reactions to Drug Cues: a Meta-analysis of 64 Neuroimaging Activation Studies

3.1. Introduction

In the previous Chapter, I have performed a meta-analysis of 22 neuroimaging studies on food perception in healthy weight and obese individuals, by combining the CluB approach with the GingerALE method. I have shown that different internal and external factors, such as weight status, sensory modality of cue presentation, and satiety, modulate the neural response to food cues in key areas of the cue-reactivity and cue-regulation networks. I have also observed that these factors act not only in isolation, but also in interaction, prompting specific neural cue-reactivity patterns. Crucially, the results revealed that the available neuroimaging literature on food perception in obese individuals mostly aligns with the prediction of the Incentive Sensitization Theory (Robinson and Berridge, 1993, Berridge et al., 2010), a neurocognitive model that was originally proposed for the study Substance Use Disorders.

In the present Chapter, I will use the same combined approach to perform a meta-analysis of 64 neuroimaging studies on drug cue-reactivity in SUD. In particular, for the first time I explicitly assess the mutual relationship between two different internal and external factors that modulate the neural reactivity to drug cues: addiction severity, indexed by the addiction by legal versus illegal substances (Nutt et al., 2007), and drug availability, indexed by the treatment status (Wilson et al., 2004).

Though a general summary of the topic is given in Chapter 1, in what follows I first provide a more detailed review of the neuroimaging literature on drug cue-reactivity, contextualizing the key findings in terms of activity within the cue-reactivity and cue-regulation networks, whenever possible. Then, I will provide an overview of the evidence on the modulatory effects of addiction severity and treatment status, and I will introduce the reader to the aims and methods of the present study.

3.1.1. The neurobiology of drug craving

Substance use disorder (SUD) is a chronically relapsing condition. Animal and human research provided converging evidence that SUD, for either legal (alcohol, nicotine) and illegal (cocaine, heroin) substances, is linked to long-lasting neuroadaptations at the molecular, cellular, and circuitry level, which mediate the transition from goal-directed to habitual and compulsive drug intake (Everitt and Robbins, 2005, Koob and Volkow, 2016). As already pointed out in Chapter 1, another crucial aspect of SUD is drug *craving*, defined as an intense desire for the substance;

this can be triggered by the presence of the drug itself or by the presence of drug-related stimuli, and it is often accompanied by changes in physiological responses such as heart rate, sweating, and skin temperature (Carter and Tiffany, 1999). As the enhanced response to drug-related cues may be a key factor contributing to the persistence of addiction (Courtney et al., 2016), the controlled exposure to the drug and drug-related stimuli (cue-reactivity) has been widely used for the study of the physiological (Rajan et al., 1998) and neurofunctional (Tapert et al., 2004, Karoly et al., 2019) correlates of drug craving.

As it should be clear by now, the exposure to drug-associated cues triggers motivational and emotional responses that influence decision-making and the ensuing motor plans (Childress et al., 1993). These are tightly linked to the nature of the substance, of its rewarding and reinforcing effects, as well as its availability. Neuroimaging studies (McClernon et al., 2008, Li et al., 2012, Tomasi et al., 2015) and previous meta-analyses (Chase et al., 2011, Kühn and Gallinat, 2011, Engelmann et al., 2012) have shown that individuals with SUD exhibit altered neural responses in brain areas involved in different relevant aspects for craving.

People with SUD show altered activity in early visual cortices when exposed to drug-related cues versus neutral objects (Hanlon et al., 2014), presumably mediating the attentional bias towards the substance. They also exhibit increased activity in regions involved in incentive motivational processes (Robinson et al., 2014, Warlow et al., 2017) of the mesocorticolimbic system (Li et al., 2013a, Tomasi et al., 2015, Kaag et al., 2018), in the ventral tegmental area (VTA) and its dopaminergic afferents to the ventral striatum, limbic structures (amygdala, hippocampus), and the prefrontal cortex (PFC). SUD is also associated with heightened responses in brain regions involved in the expression of habits (Everitt and Robbins, 2005) and in processing knowledge about tool use (Calvo-Merino et al., 2006, Lewis, 2006), such as the dorsal-striatal circuits and the inferior temporal, parietal, and motor cortices. This aberrant activity may favor drug-taking through the automatic activation of the semantic and motor representations associated with drug use (Yalachkov et al., 2010).

Taken together, previous empirical and meta-analytical evidence suggests that exposure to drug-related cues is mainly associated with an up-regulation of key regions of the cue-reactivity network, such as the striatum, and the sensory and motor cortices, in line with the notion that SUD is characterized by heightened motivational processing.

Recently, increasing efforts have been dedicated to the study of factors that can modulate the neural response to drug cues such as, among others, addiction severity and drug availability or treatment status (Wilson et al., 2004, Jasinska et al., 2014). However, as the reader shall see, previous empirical and meta-analytical studies have focused on one factor at a time, often by

collapsing together different populations of individuals with SUD: hence, a systematic investigation of these effects in different populations with SUD is lacking.

3.1.2. Factors modulating the neural drug cue-reactivity: addiction severity and treatment status

Not many years ago Jasinska and colleagues (2014), based on a systematic review of the neuroimaging literature, proposed a model on the factors that modulate the neural reactivity to drug cues in substance-dependent individuals addicted to either cocaine, alcohol or nicotine (Jasinska et al., 2014), the one I adapted in Chapter 1 to accommodate the role of the factors that modulate the neural reactivity to food cues. Among others (see Figure 1.4 in Chapter 1), **addiction severity** (i.e., intensity, frequency of drug use, and drug-related problems) and **treatment status** (i.e., whether participants are seeking for a treatment or not) emerged as powerful factors that can modulate the neural circuits involved drug craving across the three substances (Jasinska et al., 2014).

Addiction severity, which is mainly assessed through self-reported questionnaires, correlates with the activity of several brain regions belonging to the cue-reactivity (e.g., VTA, ventral and dorsal striatum, pallidum, amygdala, hippocampus, insula, sensory and motor cortices) and cue-regulation network (ACC, ventromedial PFC or vmPFC, OFC, and parietal cortices) in response to drug cues in cocaine (Volkow et al., 2006), alcohol (Smolka et al., 2006, McClernon et al., 2008), and nicotine SUD (Claus et al., 2011). It is worthy to note that the direction of these effects (up or down-regulation) varies consistently within, and across, studies involving different populations with SUD, which led the authors to hypothesize that the influence of other uncontrolled factors may contribute to the variability of the findings (see (Jasinska et al., 2014) for an in-depth review). These inconsistencies may be also partially explained by the well-known, intrinsic limitations of self-report measures, such as the social desirability effect (e.g., when response patterns reflect the desire of the respondent to project a positive image to others (Fisher, 1993a)).

Another approach to assess to what extent addiction severity modulated the neural reactivity to drug cues may be comparing brain activity across different populations of SUD. Indeed, it is reasonable to hypothesize that the reinforcing properties of the substance *per se* may be a crucial aspect that determines addiction severity. Substances are not equally addictive and harmful, and they can be classified based on the harm and dependence induced (Nutt et al., 2007), and based on their reinforcing properties (Volkow and Wise, 2005): due to these differences, a great deal of variability in the neuroimaging literature may be explained by the particular population

of substance-dependent individuals under examination which, in turn, is associated with a certain degree of addiction severity.

Recently, for the first time, Hanlon and colleagues examined the neural correlates of PFC activity in a large sample of cocaine-only, alcohol-only or nicotine-only substance-dependent individuals, using a standardized visual cue-reactivity fMRI task (Hanlon et al., 2018). Their analyses, restricted to the cue-regulation network – the PFC and the anterior cingulate cortex (ACC) -, showed that a cluster in the medial orbitofrontal cortex (mOFC) was consistently activated by all the three groups of substance-dependent individuals, thus suggesting the mOFC as a common neural correlate of craving across legal and illegal substances. Interestingly, cocaine-dependent individuals exhibited also activity in the pars opercularis of the inferior frontal gyrus and the precentral gyrus, bilaterally, suggesting that cue-induced craving in substances that induce a severe addiction, such as cocaine or heroin (Nutt et al., 2007), is characterized by the recruitment of additional cortical areas compared to substances that induce a moderate addiction, such as, for example, alcohol and nicotine (Nutt et al., 2007).

Treatment status (TR), indexing the perceived possibility of consuming a substance in the near future, has also been proposed to modulate the activity of key regions within the cue-regulation network (dlPFC, OFC) during drug cue-reactivity (Wilson et al., 2004). In a first attempt to explain inconsistencies across neuroimaging studies on cue-reactivity, Wilson and colleagues reviewed 19 neuroimaging studies in individuals addicted to cocaine, heroin, alcohol, and nicotine: they observed that activity in the PFC – in particular, in the dorsolateral (dlPFC) and the orbitofrontal (OFC) subdivisions – was consistently reported in studies with not-seeking treatment (NST) individuals, whereas it was not in studies involving treatment-seeking (TS) participants. Given the role of the OFC in integrating stimulus values (Lim et al., 2013) and in representing the expected value of rewards (Kahnt et al., 2010), and the involvement of the dlPFC in planning and executing actions aimed at achieving the reward (Goldstein and Volkow, 2002), the authors proposed that PFC activity in NTS individuals represents the expectation to obtain the drug after the experimental session (Wilson et al., 2004). Their model was recently supported by the evidence that NTS cocaine-dependent subjects, compared with TS participants, exhibit greater activity of the lateral OFC and the dlPFC in response to drug cues (Prisciandaro et al., 2014). Nonetheless, OFC and dlPFC activation in NTS was accompanied by additional cortical activity in the posterior cingulate cortex and the occipital cortex. Another study on cigarette smokers reported similar results: only substance-dependent individuals expecting to smoke after the experimental session showed activity in the mOFC, but not in the dlPFC, in response to cigarette cues compared to neural objects (Wilson

et al., 2005). It is important to note that preliminary evidence suggests that the effect of drug availability is independent by the motivation to quit. In one study on patients with nicotine SUD, both quitting-motivated and quitting-unmotivated subjects exhibited PFC activity in response to smoking cues, but only when they were expected to smoke within seconds, compared to hours, after cue-exposure (Wilson et al., 2012). The involvement of the mOFC in NTS individuals has also been recently supported by the only formal meta-analysis addressing this issue, in which additional brain regions – such as the inferior frontal gyrus, the ventral striatum, and the occipital cortex – were identified in studies with NTS participants (Chase et al., 2011). Crucially, the authors pooled together studies from substance (e.g., cocaine, heroin, alcohol, nicotine, marijuana) and non-substance addiction (e.g., gambling, gaming addiction), and no direct contrast study between the two groups of NST and TS participants was performed: as a consequence, it is impossible to determine to what extent other factors, such as addiction severity, contributed to their findings. As recently argued in Jasinska et al. (2014) model (Jasinska et al., 2014), and as demonstrated in the previous Chapter in the domain of food cue-reactivity, factors that modulate the neural reactivity to drug cues are likely to interact with each other, giving rise to specific brain-activation patterns.

These factors have never been considered together in a single study. Given the complex nature implied by such design [a 2 x 2 x 2 factorial design with four different groups of patients, two groups for each of two types of substances, and two kinds of visual stimuli (drug cues and control stimuli)] it would be beyond the strength of most to produce a study with this structure and sufficiently large samples on this matter. Moreover, to date only few studies have explicitly investigated the modulatory role of treatment status and/or drug availability on the neural reaction to drug cues (Wilson et al., 2005, Claus et al., 2011, Wilson et al., 2012, Prisciandaro et al., 2014).

In what follows, I present my attempt to assess the influence of treatment status on the neural responses to drug cues in individuals addicted to substances that induce a moderate (legal substances: alcohol, nicotine) versus severe (illegal substances: cocaine, heroin) addiction, through a formal meta-analysis of previous imaging data considering sixty-four papers on the subject. The details of the rationale of the present study and the methodologies employed are presented below.

3.1.3. Aims and predictions

The goal of the current study is two-fold: first, to identify common and distinct neural correlates of craving triggered by visual anticipatory cues[17] across different populations of legal (alcohol, nicotine) and illegal (cocaine, heroin) substance abusers; second, to study the modulatory effect of treatment status on the neural drug cue-reactivity, *per se* and in interaction with the type of substance.

I hypothesized that differences in the neural drug cue-reactivity patterns between the two classes of substances might reflect the different severity of addiction that they can induce (Nutt et al., 2007); in particular, I expected that the use of illegal substances would have been associated with stronger activation of brain regions involved in incentive salience and motivation, mainly within the cue-reactivity network, much in line with the evidence that activity of these regions correlate with the severity of addiction and can predict relapse (see, for example, (Grüsser et al., 2004, Kosten et al., 2006, Janes et al., 2010, Li et al., 2015)). I further anticipated that treatment status could exert a modulatory effect over the brain responses within the cue-regulation network (Wilson et al., 2005, Wilson et al., 2012, Prisciandaro et al., 2014), according to the role of the OFC and dlPFC in encoding reward expectations and action planning in NST subjects (Wilson et al., 2004).

However, it remained a matter of empirical investigation whether such effects would be the same for legal and illegal substances: if not, this would suggest a complex interaction between biological and environmental factors not explicitly investigated so far in the imaging literature.

3.2. Materials and methods

Similarly to Chapter 3, the meta-analytical approach employed here involves a series of analytical steps starting from the identification of the raw data (data collection and preparation), followed by hierarchical clustering analysis (HCA), and statistical inferences on the clusters which comprise a cluster composition analysis (CCA) and a validation of the spatial relevance of each cluster by means of the GingerALE method.

These procedures are described in detail below.

---

[17] I concentrated on anticipatory drug visual cues because experiments based on other sensory modalities (e.g., taste) are not sufficiently represented in the literature, nor they would permit to test the effects of interest over the entire spectrum of drugs, as the oral route is not the prevalent administration route for the illegal drugs considered, heroin or cocaine.

3.2.1. Data collection and preparation

Records were retrieved through the following query in PubMed: "[cocaine OR heroin OR alcohol OR nicotine] AND [functional magnetic resonance imaging OR fMRI OR positron emission tomography OR PET OR neuroimaging] AND [addiction OR craving]". The initial set of studies included 4240 papers, updated to March 2019.

Papers were included when fulfilling the following inclusion criteria:

- Populations involved: adult (mean group age $\geq$ 18 years) substance-dependent individuals according with the DSM-IV and DSM-5 criteria or similar, heavy drinkers (Vollstädt-Klein et al., 2010) or regular and abstinent drug users (Kober et al., 2016); no minimum sample size was required; given the heterogeneity of abstinence time across studies, no consideration for the abstinence status was made;

- Anatomical conventions: we considered only data reported using MNI (Mazziotta et al., 1995) or Talairach (Talairach and Tournoux, 1988) coordinates exclusively from whole-brain analyses;

- Activation protocols: we considered only drug cue-reactivity paradigms based on both passive unimodal visual perception (with supraliminal stimuli) or mental imagery; this choice was motivated by our interest into anticipatory processing and by the need of curtailing the effect of potential confounds (e.g., sensory modality of stimulus presentation (Jasinska et al., 2014));

- Statistical comparisons (linear contrasts) included: drug cue > control stimulus or baseline; data describing "deactivations" (drug cue < control stimulus) were not considered; only data from univariate analyses were considered (minimum threshold: $p < 0.05$ uncorrected); only contrasts related to simple effects of the group of substance-dependent individuals or interaction effects were included. For the interaction effects we considered only those testing a comparison like [drug cue > control]$_{SUD}$ > [drug cue > control]$_{normal\ controls}$;

- The regional effects were considered providing that they were measured from homogeneous populations (e.g., all treatment seekers);

- For studies assessing the effect of drug or drug treatments, we considered only studies that reported foci belonging to the pre-treatment and/or placebo condition (Myrick et al., 2008) or analyses corrected for treatment effects (Courtney et al., 2014).

This selection, initially primarily based on titles and then on abstracts, yielded to the identification of 192 papers candidates for the meta-analysis (Figure S3.1 in Supplementary File 2).

Third, I made a further selection by inspecting the entire manuscripts and applying the aforementioned inclusion criteria in detail. The final dataset included 64 studies (Garavan et al., 2000, George et al., 2001, Kilts et al., 2001, Grüsser et al., 2004, Myrick et al., 2004, Li et al., 2005, Hermann et al., 2006, Kosten et al., 2006, McBride et al., 2006, Xiao et al., 2006, David et al., 2007, Park et al., 2007, Wrase et al., 2007, Myrick et al., 2008, Janse Van Rensburg et al., 2009, Yalachkov et al., 2009, Zijlstra et al., 2009, Goudriaan et al., 2010, Volkow et al., 2010, Vollstädt-Klein et al., 2010, Vollstädt-Klein et al., 2011, Li et al., 2012, Lou et al., 2012, Potenza et al., 2012, Tang et al., 2012b, Goudriaan et al., 2013, Lee et al., 2013, Li et al., 2013a, Li et al., 2013b, Prisciandaro et al., 2013a, Prisciandaro et al., 2013b, Courtney et al., 2014, Holla et al., 2014, Kim et al., 2014, Krienke et al., 2014, Mann et al., 2014, Prisciandaro et al., 2014, Tabatabaei-Jafari et al., 2014, Wang et al., 2014, Cortese et al., 2015, Elton et al., 2015, Hassani-Abharian et al., 2015, Janes et al., 2015, Li et al., 2015, Ray et al., 2015, Tomasi et al., 2015, Wang et al., 2015a, Zanchi et al., 2015, Falcone et al., 2016, Kober et al., 2016, Hong et al., 2017, De Pirro et al., 2018, He et al., 2018, Huang et al., 2018b, Kaag et al., 2018, Liberman et al., 2018, Moran et al., 2018, Zeng et al., 2018, Zhang et al., 2018, Bach et al., 2019, Koopmann et al., 2019, Li et al., 2019, Wei et al., 2019), 90 statistical comparisons and 1006 activation foci (see Table S3.1 in Supplementary File 2 for further details on the studies included).

Then, to arrange the dataset for the subsequent Cluster Composition Analysis (CCA), each focus of activation was classified according to two factors of interest: (i) **class of substances** (*legal* vs. *illegal*) and (ii) **treatment status** of the participants (*treatment-seeking* (TS) vs *not-seeking treatment* (NST)). In particular, foci coming from studies with individuals addicted to alcohol or nicotine were classified as *legal,* whereas foci from studies with individuals addicted to cocaine or heroin were labeled as *illegal*. Accordingly, this labeling encoded a between-group factor that we call **class of substances**. Activation foci were also classified according to the **treatment status** of the participants: only the activation foci belonging to studies with treatment-seeking participants as specified in the manuscript (Kosten et al., 2006, Zhang et al., 2018), with participants involved in clinical trials(Prisciandaro et al., 2013a, Prisciandaro et al., 2013b, Mann et al., 2014) or admitted/to-be-admitted to inpatient (Lou et al., 2012, Bach et al., 2019) or outpatient treatment (Lee et al., 2013, Wang et al., 2014) or recruited from drug services or rehabilitation centers (De Pirro et al., 2018, Wei et al., 2019) were classified as

treatment-seeking (TS – participants whose drug use is limited by the willingness to quit and/or by the restricted access to the substance); by contrast, activation foci generated by participants that are not involved in any treatment nor clinical (Kaag et al., 2018) or that are active users recruited from the community (Garavan et al., 2000, Park et al., 2007) were classified as *not-seeking treatment* (NST – participants that are not motivated to quit and whose access to the substance is not restricted).

All the Talairach coordinates were converted to MNI space using the TAL2ICBM_SPM function (Lancaster et al., 2007, Berlingeri et al., 2019). Thirteen activation foci fell outside the less conservative mask of the GingerALE software (version 3.0.2 (Eickhoff et al., 2009, Turkeltaub et al., 2012)) and were excluded. The final dataset comprised 993 foci, based on 1620 substance-dependent individuals (mean age: 36.9 years) with an average history of abuse of 11.56 years (information about the history of abuse was not available for 20 studies). Further details on the populations of the 64 studies are reported in the Supplementary File 2 (paragraph 1.1).

3.2.2. Hierarchical Clustering Analysis (HCA) and Cluster Composition Analysis (CCA)

To identify anatomically coherent regional effects, I first performed a HCA using the unique solution clustering algorithm (Cattinelli et al., 2013b) implemented in the software CluB (Berlingeri et al., 2019), as described in the previous Chapter. In brief, CluB takes into account the squared Euclidian distance between each couple of foci included in the dataset; the clusters with minimal dissimilarity are then recursively merged using Ward's criterion (Ward, 1963), to minimize the intra-cluster variability and maximizing the between-cluster sum of squares (Cattinelli et al., 2013b). To impose a suitable *a priori* spatial resolution to the analyses, I set to be 5 mm the maximum mean spatial variance within each cluster in the three directions[18]. The centroid coordinates of each resulting cluster were then labeled according to the Automatic Anatomic Labelling (AAL) (Rorden and Brett, 2000), and then controlled by visual inspection on the MRIcron (Rorden and Brett, 2000) visualization software.

The output of the HCA was then entered as an input for the subsequent CCA. This procedure allows a post-hoc statistical exploration of each cluster by computing, within each cluster, the proportion of foci belonging to different levels of a variable of interest. Such proportion is then

---

[18] This choice was motivated by two main reasons: first, by the interest into small and discrete subcortical structures, such as the ventral (nucleus accumbens) and dorsal striatum; second, for consistency with regard to the meta-analytical studies on food perception illustrated in Chapter 2.

compared with a target proportion, which, in this case, is extracted from the overall distribution of foci classified according to our factors of interest in the whole dataset (Prior Likelihood, PL). First, I ran a CCA to explore the main effects of class of substances and treatment status. This composition analysis was done by running a binomial test on the proportion of foci associated with each level of the three factors within each cluster. For example, if a cluster X had a cardinality of N = 20 and included 15 foci associated with the level "legal" of the "class of substances" factor, CluB computes the proportion 15/20 (i.e., 0.75) and compares it with the theoretical proportion computed over the entire dataset (e.g., PL_{legal} = 377/650 = .58). Hence, (a) the Prior Likelihood represents the probability of success under the null hypothesis and (b) a significant binomial test ($p < .05$) indicates that the proportion of activation peaks included in that specific part of the brain is higher than the proportion computed all over the brain.

Then, to test for interaction effects (class of substances-by-treatment status), I performed a series of Fisher's exact tests (Fisher, 1970) on the empirical peak-distribution within each cluster. Finally, with the aim to interpret the directionality of the second-level interactions, I employed the following method: for each cell of the 2 x 2 crosstab, I calculated the ratio between the proportion of observed foci and the total number of foci within the cluster (OP, observed probability). Then, I divided this value for the proportion of foci belonging to the same factors considering the entire dataset (PL). This computation (i.e., OP/PL) results in an index that indicates the degree to which the distribution of activation peaks belonging to a specific combination of factors within a cluster exceeds the expected probability. Values greater than one indicate a higher probability for the cluster to be specific for that particular combination of factors.

To limit the impact of any given study, I considered for further discussion only clusters with at least 4 contributing studies (equal or greater than the 25th percentile of the total contributing studies); moreover, I discarded those clusters with cardinality (the number of peaks) inferior to the 25th percentile (< 5) of the total cardinality.

Clusters whose one-tailed p-value was greater than or equal to 0.5 for both levels of the factor Class of substances were considered as of high chance of being genuinely *undifferentiated* (Paulesu et al., 2014).

3.2.3. *Validation of the spatial relevance of each cluster using the ALE procedure*

To validate the results of the HCA, we assessed the spatial significance of the HCA solutions by comparison with a standard Activation Likelihood Estimate meta-analysis of the same raw data. Here I used the Turkeltaub Non-Additive method (Turkeltaub et al., 2012), with the

cluster-forming statistical threshold of p < 0.05 FWE-corrected and corrections for contrasts coming from the same study (Turkeltaub et al., 2012, Müller et al., 2018). Only clusters surviving the spatial intersection between the HCA and ALE maps were then taken into account for additional analyses and discussion.

3.2.4. Further methods of interpretation of the results

Besides typical forward inferences based on the experimental design and interaction of factors, I also relied on quantitative reverse inference when needed. Each CCA map representing the effect of the factor of interest was loaded into the Neurosynth database and analyzed by means of the "decoder" function (http://neurosynth.org/decode/). As illustrated in Chapter 2, the decoder function of Neurosynth allows one to retrieve the Pearson correlation of the key-words that are most associated with the input image, containing the clusters identified by the meta-analysis, based on the NeuroVault repository. The r-value associated with each key-word reflects the correlation across all voxels between the input map and the map associated with a particular key-word in NeuroVault. I considered the first 15 words associated with each CCA map, after excluding anatomy-related terms and duplicate terms.

3.3. Results

3.3.1. Hierarchical Clustering Analysis (HCA)

The HCA identified 117 clusters, each composed by 2–24 peaks; the mean standard deviation along the three axes was 4.96 mm (x-axis), 4.93 mm (y-axis) and 4.92 mm (z-axis). Thirty-five clusters were retained following the intersection procedure with the ALE map (the results of the ALE analysis are reported in the Supplementary File 2, Figure S3.2). One cluster was excluded because its cardinality fell below the 25th percentile of the total cardinality of the clusters (cardinality < 5 foci).

On average, these clusters contained 13 foci (range: 5–24), with 3 to 17 studies (mean: 8) contributing to each cluster. The full list of clusters overlapping with the ALE maps is available in the Supplementary File 2 (Table S3.2). The results of the CCA are reported in Table 3.1, whereas the full list of terms identified by Neurosynth for each CCA map is reported in Table S3.3 in the Supplementary File 3.

3.3.2. Cluster Composition Analysis (CCA)

3.3.2.1. Undifferentiated clusters

There were 4 undifferentiated clusters, that is spatially significant clusters, consistently activated in the basic drug-cue paradigm, yet with no association with a specific drug class: these were located in the left lingual gyrus, anterior cingulate cortex (ACC), left inferior occipital gyrus and right middle occipital gyrus (Figure 3.1). The 15 terms with the higher r-values, according to Neurosynth, are reported in Figure 3.1 caption; the top five were *traits (personality), mentalizing, beliefs, craving, visual stimuli.*
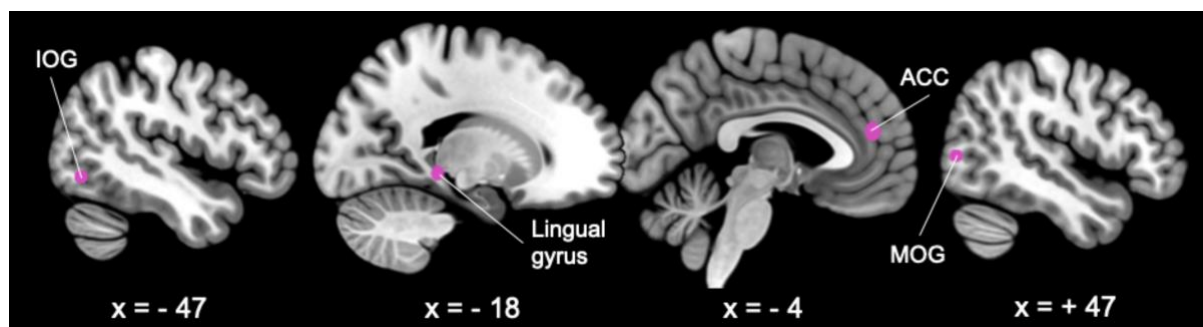
Figure 3.1 | Clusters undifferentiated with respect to the factor class of substances. The clusters that resulted as reliably undifferentiated across legal and illegal substances are depicted in violet. The decoder function of Neurosynth returned the following 15 terms with the highest association with the CCA map (decreasing order): traits (personality), mentalizing, beliefs, craving, visual stimuli, contexts, autobiographical, moral (decision-making), emotion regulation, oscillations, object recognition, placebo, attended, abuse. Slice coordinates are reported in MNI stereotaxic space. ACC, anterior cingulate cortex; IOG, inferior occipital gyrus; MOG, middle occipital gyrus. Taken from: Devoto et al. *Transl. Psych*.

3.3.2.2. Class of substances-specific clusters

The binomial CCA performed to test whether each cluster was significantly associated with either class of substances revealed 5 clusters significantly associated with illegal substances, and one cluster associated with legal substances.

Illegal substance abusers showed more frequent activity the left posterior inferior temporal gyrus (pITG), anterior hippocampus/amygdala, in calcarine cortex and precuneus, the right caudate/nucleus accumbens and the midbrain (VTA) (Figure 3.1, in red). Legal substance abusers showed more frequent activity of the left dorsal anterior cingulate cortex (dACC) (Figure 3.1, in yellow). The 15 Neurosynth terms with the higher r-values are reported in Figure 1 caption; the top five were: *tools, motivational, anticipation, addiction, reward anticipation.*
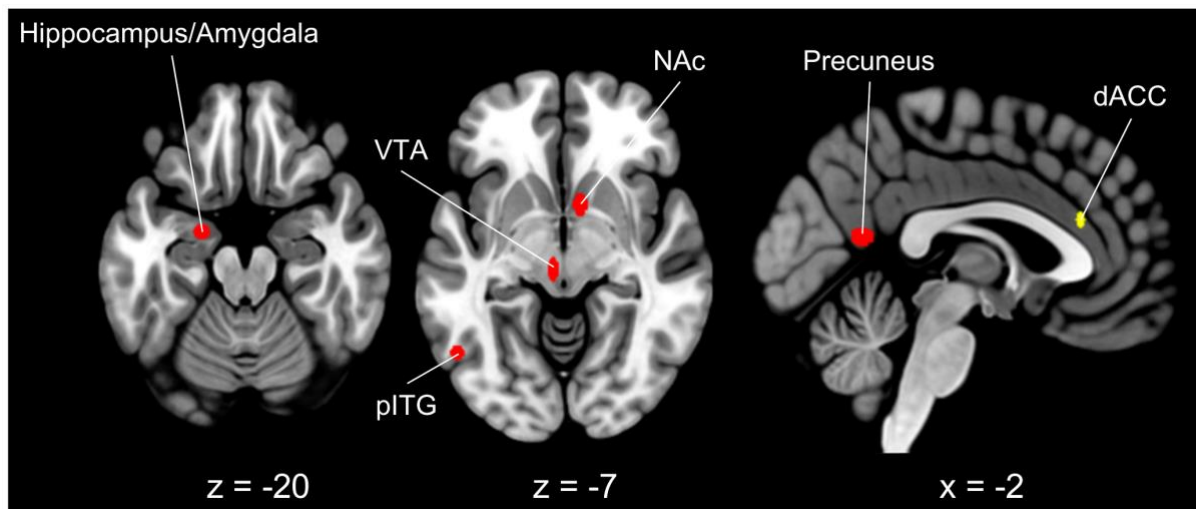
Figure 3.2 | Distribution of clusters showing a significant main effect of class of substances. Clusters more frequently activated by individuals addicted to legal substances are depicted in yellow, whereas clusters more frequently activated by individuals addicted to illegal substances are depicted in red. Slice coordinates are reported in MNI stereotaxic space. The decoder function of Neurosynth returned the following 15 terms with the highest association with the CCA map (decreasing order): tools, motivational, anticipation, addiction, reward anticipation, outcome, subjective, behavior, monetary reward, complex, probabilistic, objects, incentive delay, form, sighted. dACC, dorsal anterior cingulate cortex; pITG, posterior inferior temporal gyrus; VTA, ventral tegmental area. Taken from: Devoto et al. *Transl. Psych.*

Table 3.1 | Results of the Cluster Composition Analysis. For each cluster the following information is reported: the cluster ID; the anatomical label according to the AAL (Brodmann Area); the centroid coordinates in the MNI stereotaxic space (standard deviation of the distance from the centroid along the three axes); the number of foci falling within the cluster (N); the number of contributing studies; the p-values associated with the binomial and Fisher's tests. Significant main and interaction effects are shown in bold. Undifferentiated clusters are marked by *. CoS, class of substances; CoSxTR, class of substances-by-treatment status interaction; NST, not-seeking treatment participants; TR, treatment status; TS, treatment-seeking participants; IL, illegal substances; L, legal substances. Adapted from: Devoto et al. *Transl. Psych*.

Cluster ID	Centroid label (BA)	Left hemisphere			Right hemisphere			N	# of contributing studies	CoS		TR		CoSxTR
		X (SD)	Y (SD)	Z (SD)	X (SD)	Y (SD)	Z (SD)			L	IL	TS	NST	
21	Inferior occipital gyrus (19)	-46 (4.5)	-70 (3.8)	-8 (3.9)				17	4	**.616***	**.583***	.552	.645	.102
22	Inferior temporal gyrus (37)	-51 (3.4)	-63 (4.2)	-5 (5.8)				17	8	.995	**.027**	.076	.977	1
28	Caudate nucleus	-13 (6.7)	17 (3.8)	2 (4)				9	7	.687	.582	.794	.441	**.032**
30	Nucleus accumbens				8 (3.4)	8 (5.6)	-6 (6.1)	19	10	.986	**.049**	.597	.59	1
47	Middle occipital gyrus (19)				49 (3.7)	-77 (4.9)	4 (4.3)	6	5	**.7 ***	**.626 ***	.607	.716	1
62	Calcarine scissure/precuneus (17/30)	0 (6.3)	-59 (5.1)	15 (4)				12	6	.995	**.036**	**.032**	.996	1
68	Lingual gyrus (27)	-15 (5.3)	-35 (4.8)	-6 (5.3)				10	9	**.515 ***	**.728 ***	.461	.779	1
69	Midbrain (ventral tegmental area)	-5 (2.8)	-23 (6.7)	-9 (4.7)				12	9	.995	**.036**	**.032**	.996	.438
92	Medial orbitofrontal gyrus (10)	-5 (5.6)	52 (4.7)	-4 (4.9)				15	11	.47	.726	.701	.5	**.006**
96	Supragenual anterior cingulate cortex (32)	-5 (5.9)	45 (4.5)	18 (5.8)				20	9	**.622 ***	**.562 ***	.087	.97	.54

#	Region	x	y	z	x	y	z							
97	Hippocampus/amygdala (35/28)	-21 (4.2)	-5 (3.7)	-21 (3.3)				17	9	1	**.005**	.076	.977	1
103	Perigenual anterior cingulate cortex (32)				2 (4.5)	40 (3.5)	5 (7)	16	12	.344	.817	.908	.204	**.045**
114	Dorsal anterior cingulate cortex (24)	0 (2.3)	29 (4.2)	22 (6.1)				13	7	**.003**	1	.999	**.004**	1
116	Thalamus				1 (3.6)	-11 (3.7)	4 (4.7)	24	10	.913	.181	.158	.927	**.04**

3.3.2.3. Treatment status-specific clusters

The binomial CCA performed to test whether each cluster was significantly associated with either treatment status revealed 2 clusters significantly associated with TS individuals, and one cluster associated with NST individuals.

TS patients activated more frequently the calcarine cortex and the precuneus and the midbrain, in a region compatible with the ventral tegmental area (VTA) (Figure 4.3, in green), whereas NST patients activated more frequently the dACC (Figure 2, in blue). The 15 terms with the higher r-values are reported in Figure 4.3 caption; the top five were: *aversive, reversal (learning), anticipatory, heart (rate), intense (emotion).*
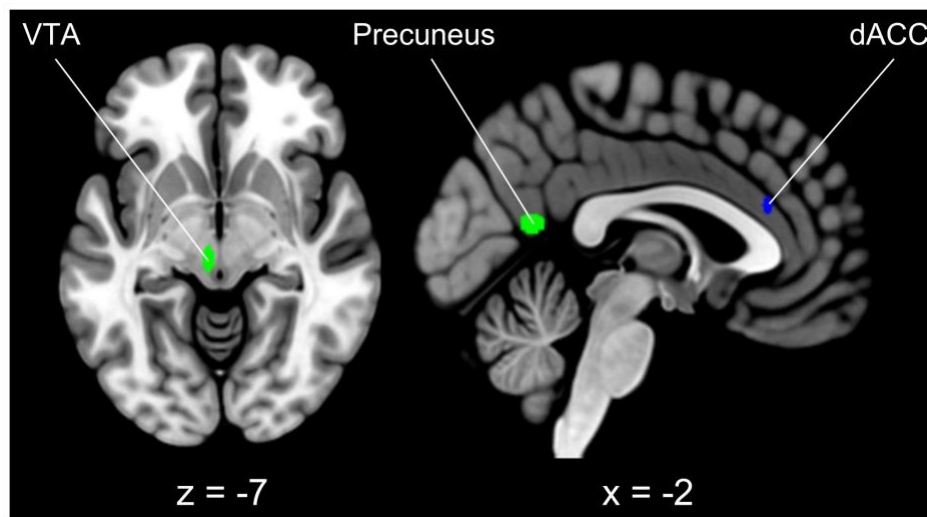
Figure 4.3 | Distribution of clusters showing a significant main effect of treatment status. Clusters specific for treatment-seeking individuals are depicted in green, whereas the cluster specific for not-seeking treatment subjects is depicted in blue. The decoder function of Neurosynth returned the following 15 terms with the highest association with the CCA map (decreasing order): aversive, reversal (learning), anticipatory, heart (rate), intense (emotion), episodic memory, autobiographical, cognitive emotional, force, fear, reward, mild cognitive, pain, personal, sensation. Slice coordinates are reported in MNI stereotaxic space. dACC, dorsal anterior cingulate cortex. Taken from: Devoto et al. *Transl. Psych.*

3.3.2.4. Class of substances-by-treatment status interactions

The Fisher's Exact test revealed 4 clusters with a significant interaction between class of substances and treatment status of the participants. These clusters were located in the left medial orbitofrontal gyrus (mOFC), in the right perigenual ACC (pgACC), in the right thalamus and the left caudate nucleus (Figure 3.4).

The interaction plots show that the mOFC and the ACC were more frequently activated by TS subjects addicted to legal substances, and by NST individuals addicted to illegal substances.

On the other hand, the caudate nucleus was more frequently activated by TS compared with NST individuals, specifically for legal substances. Conversely, the right thalamus was associated with TS compared with NST subjects, particularly for individuals addicted to illegal substances. The 15 terms with the higher r-values are reported in Figure 3.4 caption; the top five were: *engagement, referential (self), value, reward, traits (personality).*
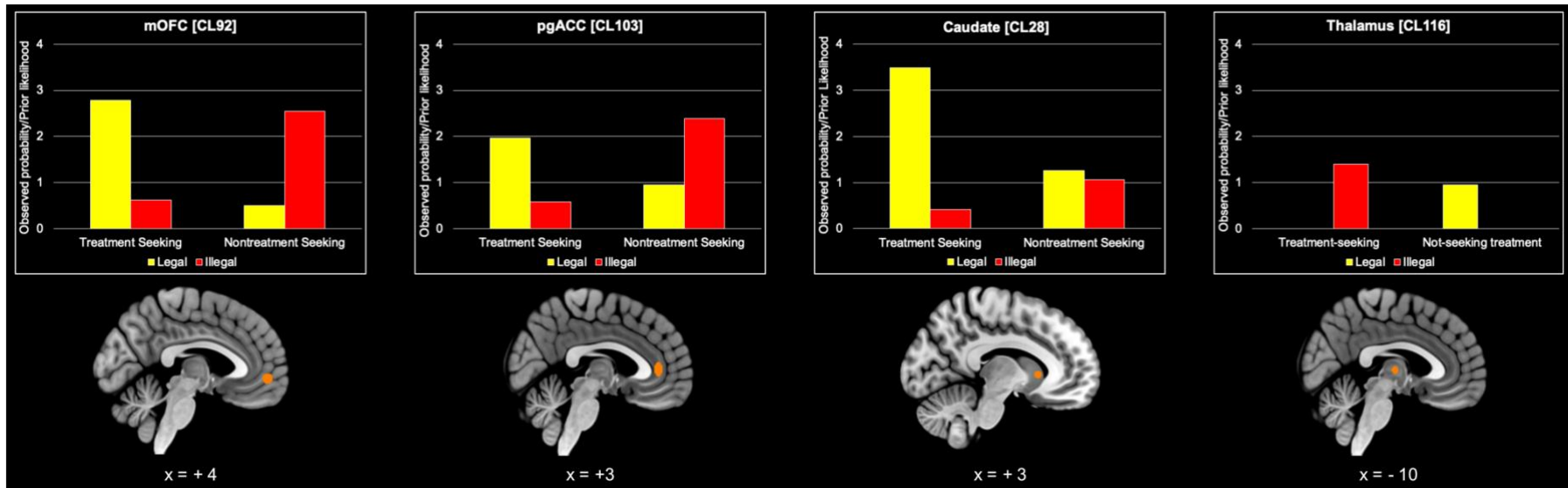
Figure 4.4 | Distribution of clusters showing a significant class of substances-by-treatment status interaction. Clusters with a significant class of substances-by-treatment status interaction are shown in orange, along with their respective plot. On the y-axis of the bar-plots is represented the ratio between the observed probability and the prior likelihood: the more this value exceeds 1, the more the cluster is associated with that combination of factors. The decoder function of Neurosynth returned the following 15 terms with the highest association with the CCA map (decreasing order): engagement, referential (self), value, reward, traits (personality), choose, arousal, task positive, autobiographical, monetary, moral (decision-making), contexts, monetary incentive, expectations, valence. Slice coordinates are reported in MNI stereotaxic space. pgACC, perigenual anterior cingulate cortex; mOFG, medial orbitofrontal gyrus. Taken from: Devoto et al. *Transl. Psych.*

3.4. Discussion

Legal and illegal drugs differ in several respects. Alcohol and tobacco/nicotine are freely available in the environment: they can be found 24/7 in shops at a low-to-moderate monetary cost. Conversely, illegal drugs like cocaine and heroin are less widely available, they are associated with a severe degree of harm and dependence(Nutt et al., 2007), they are usually sold at very high prices per unit weight in the illegal market(Caulkins and Reuter, 1998), and their trading implies the risks associated with a criminal action. The present meta-analysis of neuroimaging studies on drug cue-reactivity, for the first time assessed whether, and how, nature of these drug and treatment status can interact at the neurobiological level, giving rise to specific brain activation patterns in response to drug cues.

In what follows, I will first discuss the effect of addiction severity, by identifying the common and distinct neural substrates of drug craving across legal and illegal substances. Then, I will discuss the influence of treatment status and, finally, the interaction effects.

3.4.1. Common neural correlates of craving across legal and illegal substances

I found that a frontal-occipital network, comprising three clusters located in the occipital cortex (IOG, MOG, lingual gyrus) and one in the PFC, in the ACC, was activated in response to drug cues regardless of the type of substance, suggesting the existence of a core brain circuit underlying cue-induced drug craving.

Occipital cortex activity in response to drug-cues has been consistently reported in previous meta-analyses of neuroimaging studies (Chase et al., 2011, Kühn and Gallinat, 2011, Engelmann et al., 2012), and it has been associated with craving (McClernon et al., 2009) and meta-cognitive processes, such as awareness of problematic drug use (Prisciandaro et al., 2014), in previous experimental studies. In a recent ALE meta-analysis, Hanlon and colleagues demonstrated the replicability of the occipital cortex finding (Brodmann areas 19 and 17) across legal and illegal substance abusers, suggesting that occipital activity may reflect the attentional bias towards drug-related stimuli or the rewarding properties of the substance per se (Hanlon et al., 2014). If one accepts that the legal and illegal substances included here vary with respect to reinforcing properties (Volkow and Wise, 2005) and to the degree of dependence induced (Nutt et al., 2007), our finding does not support the idea that occipital cortex activity reflects the reinforcing properties of the substance itself: indeed, they are more compatible with the hypothesis that occipital cortex activity reflects bottom-up attentional phenomena towards drug-associated stimuli, a process that might be shared across abusers of different substances;

similar findings have been observed for visual stimuli evoking other rewarding contingencies, like erotic and sexual images (Montorsi et al., 2003, Voon et al., 2014).

Another cluster, located in the ACC, was undifferentiated with respect to the class of substances. Activity of the ACC in response to drug cues has been previously associated with reinforcement-guided decision-making (i.e., integration of information including previous experiences with the reward) (Kennerley et al., 2006), cognitive control (Kühn and Gallinat, 2011, Engelmann et al., 2012), and reward value representation (Schacht et al., 2013). Further, based on the evidence that intact glutamatergic projections from the PFC – which includes the ACC – to the NAc and the ventral pallidum are necessary to trigger drug-seeking in animal models (McFarland and Kalivas, 2001, McLaughlin and See, 2003), this network has been considered as a "final common pathway" mediating the initiation of drug-seeking (Kalivas and Volkow, 2005). Relevant to this interpretation, a qualitative analysis of the terms identified by Neurosynth is consistent with the idea that this pattern of activation reflects the deployment of attention to rewarding visual stimuli and, ultimately, to craving.

In other words, across different populations with SUD, exposure to visual-anticipatory drug cues versus neutral objects is associated with an up-regulated activity of discrete portions within the cue-reactivity network (occipital cortices), linked to a share attentional bias toward the substance, and within the cue-regulation (ACC) network, linked to higher-order attentional and top-down processes.

3.4.2. Distinct neural correlates of craving across legal and illegal substances

Consistent with the fact that cocaine or heroin can be severely addictive inducing extreme craving, we found a more frequent activation of the subcortical reward pathway (the VTA, NAc, the amygdala) in illegal drugs abusers. This evidence is also in agreement with a large body of animal and human studies suggesting that aberrant activity of the mesocorticolimbic pathway may be responsible for this phenomenon: the VTA, the NAc and the amygdala are crucial structures for the expression of cue-elicited reward-seeking behaviors(Everitt et al., 1999, Warlow et al., 2017). In humans, the activity of the ventral striatum (which includes the NAc) during cue-reactivity predicts relapse in heroin (Li et al., 2015) and alcohol-dependent individuals (Reinhard et al., 2015), and NAc resting-state functional connectivity with the dlPFC predicts relapse in cocaine-dependent individuals (Berlingeri et al., 2017). These findings also align with the evidence that measures of addiction severity correlate with cue-induced activity in these regions (Smolka et al., 2006, Volkow et al., 2006, Claus et al., 2011).

Unexpectedly, two other brain regions outside the mesocorticolimbic system were more frequently activated in addicted to illegal substances, the inferior temporal cortex and the precuneus. The precuneus is part of the default mode network: all the well-known associated behavioral dimensions may apply (Cavanna and Trimble, 2006), including enhanced attentional anticipation for external stimuli (Schacht et al., 2013, DeWitt et al., 2015). The inferior temporal cortex is part of a network that stores and processes knowledge about object manipulation and tool use (Lewis, 2006, Yalachkov et al., 2010): its involvement may reflect automatic bottom-up phenomena representing, in a broad sense, the "affordances" for the particular substance of abuse. Such bottom-up phenomena would be stronger the more severe the condition of abuse (Jasinska et al., 2014).

Interestingly, the only brain region that was more frequently activated in legal substance abusers was the dACC. In nicotine addiction, the dACC activity was tentatively associated with the effort of directing the attention away from the stimulus to suppress craving, as immediate consumption was impossible (Kühn and Gallinat, 2011, Engelmann et al., 2012): indeed, cognitive control over craving may be especially required when the possibility of consuming the substance is a more concrete one, as in the case of legal substances, alcohol and nicotine. All these interpretations were broadly confirmed by the quantitative semantic associations made by Neurosynth.

In sum, whereas individuals addicted to illegal substances are mainly characterized by an up-regulated activity of key nodes within the cue-reactivity network (VTA, NAc, amygdala/hippocampus), presumably due to the deeper neural sensitization and to the enhanced incentive salience attribution, SUD patients addicted to legal substances are characterized by more frequent activity of the cue-regulation network (dACC), possibly linked to emotion (craving) regulation.

3.4.3. The effect of treatment status in legal and illegal substances

Contrary to what one could have predicted according with previous investigations and theoretical models (Wilson et al., 2004, Wilson et al., 2005), the brain activation patterns of TS and NST differed only for a small number of regions, all outside prefrontal cortex: these included the VTA and the precuneus (associated with TS *and* illegal substances) and the dACC (associated with NST *and* legal substances). Exploration of the *Neurosynth* database showed that the clusters associated with treatment status, as a main effect, are linked to cognitive emotional processes and reward anticipation. Of great interest is the association of these regions also with reverse learning paradigms: one can imagine that seeing a drug-cue in a treatment-

seeking status may trigger processes needed to change the associated value with the cue and the actions typically involved.

On the other hand, I observed two cortical regions where the nature of the substance of abuse and the treatment status of a participant did interact: the perigenual ACC (pgACC) and the medial OFC (mOFC). More specifically, these two regions were more frequently activated in NST consumers of illegal substances and in TS consumers of legal substances. Interestingly, these include the same cortical region, the OFC, that according to Wilson et al (2004) (Wilson et al., 2004) should display an association with NST. Our data show that this is not the case and that its association with treatment status is modulated by the nature of the drug.

The medial and ventral portion of the OFC (also called ventromedial PFC), together with the ACC, is part of a network that mediates intertemporal decision-making, as suggested by neuroimaging meta-analyses on temporal discounting phenomena (these are tested in experimental situations in which an individual is forced to choose between a later - but larger - or an earlier - but smaller – reward (Carter et al., 2010, Wesley and Bickel, 2014)), and by clinical evidence on patients with OFC lesions, whose decisions are characterized by the insensitivity to future consequences and by the preference for immediate reward (Bechara et al., 2000). Further, OFC (in particular, Brodmann area 10) activity correlates with the ease and difficulty of the choice (Rolls et al., 2010), and it is functionally connected with the pgACC (Yu et al., 2011), a region that is thought to represent action-reward associations (Rolls, 2019). The interpretations of the role of these regions in temporal discounting (key-words: *expectations*, *value*) and decision making (key-word: *choose, moral (decision-making)*) is also consistent with a Neurosynth analysis.

In keeping with the above interpretation of our data, I acknowledge that the direction of the interactions observed here may be driven by a number of internal and environmental factors that reflect the intrinsic differences between classes of substances and treatment types. First, it is worth recalling that illegal substances, here heroin and cocaine, are associated with more profound brain reactions to drug cues in general and they are, by definition, less widely available or even not available or affordable at times, if compared with legal substances, here alcohol and tobacco. Second, the availability of substances of abuse differs depending on the status of treatment seeking and the nature of the substance: for example, a treatment seeker, abuser of illegal substances, is frequently an inpatient submitted to a forced regimen of withdrawal from the drug (of the studies reviewed here, at least 10 out of 23 studies involved inpatients for the illegal drugs groups). Third, getting illegal substances exposes to the risk of

dealing with crime, often leading to enforced treatment, while legal substances can be obtained without such risk.

Following these considerations, one may argue that the interaction effects seen in regions concerned with the representation of reward value and decision making (here, the pgACC and the mOFC) may reflect conflictual situations in which internal predispositions and drug availability clash when subjects are exposed to drug cues: as illustrated in Figure 4.4, this is exactly what may happen when one is determined to quit and/or under treatment and yet he is exposed to an easily available drug (legal drugs here) or when one is not determined to quit and at the mercy of limited availability (in quantity and/or price) typical of the illegal drug market. The way time is represented in these brain regions, with respect to reward and the variable delay whereby this is gained, may be an important factor here. For example, for a cigarette smoker seeking for treatment (low internal predisposition to consumption and high environmental availability) or for a crack-cocaine abuser not seeking for treatment (high internal predisposition to consumption and low environmental availability), a drug cue represents (i) a substance that should be not consumed soon - the patient is under treatment - but that is highly available in the environment or (ii) a substance that one may want to consume soon - the patient is not under treatment - but that is costly and poorly available in the environment, thus making the outcome less predictable (Figure 3.4).

As a consequence, the interaction effects seen for class of substances and treatment status in the pgACC and mOFC may reflect the recruitment of additional reward evaluation and decision-making processes, which are required to form, and stressed by, the expectations about the potential delay of drug consumption after exposure to drug cues.
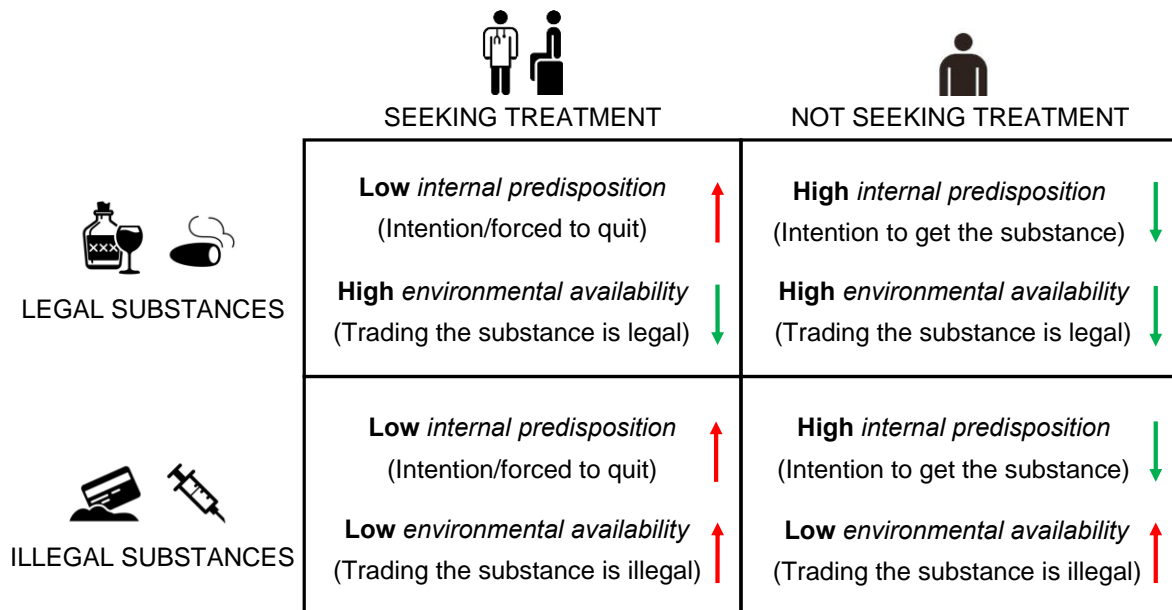
Figure 3.4 | Internal and environmental determinants in drug cue-reactivity. A simplified model of the interaction between class of substances and treatment status in the PFC. More frequent activity in regions involved in inter-temporal decision-making and reward evaluation may reflect the incongruency between determinants that signal shorter delay/immediate reward (downward green arrows) versus longer delay/absence of reward (upward red arrows): when these contingencies signal conflicting information about the potential time-frame of the reward (represented by the arrows pointing in different directions), additional decision-making and reward evaluation processes may be required to form an expectation about the delay of drug consumption. The interaction effect observed here may be in part mediated by the different drug availability implied by the type of treatment usually considered for legal (outpatient - getting the substance soon is still possible) versus illegal (inpatient – getting the substance soon is less likely) substance abusers. Taken from: Devoto et al. *Transl. Psych.*

Unexpectedly, two subcortical structures - whose activity is usually not observed in studies where treatment status/drug availability is explicitly manipulated (Wilson et al., 2005, Wilson et al., 2012, Prisciandaro et al., 2014) - showed a significant interaction between class of substances and treatment status: the caudate nucleus and the thalamus. In particular, both regions were more frequently activated by TS participants, but the caudate nucleus was more frequently activated by legal substance abusers, the thalamus by illegal substance abusers.

The caudate nucleus is functionally and structurally connected to multiple brain areas involved in emotion, cognition, and action (Robinson et al., 2012), and it supports efficient goal-directed actions through the selection of appropriate behavioral schemata (Grahn et al., 2008). Goal-oriented versus habitual behavior is indeed crucial for those individuals that are seeking for a treatment, not for those NST. Conversely, activity of the thalamus has been associated with drug craving and with addiction severity in previous animal and human neuroimaging studies

(Claus et al., 2011, Huang et al., 2018a), even if its precise contribution to the experience of drug craving is still unclear. If anything, our results show that subcortical structures such as the caudate nucleus and the thalamus are modulated by some aspects of treatment status and/or drug availability that are specific for a particular class of substances.

To summarize, the interaction between addiction severity and treatment status gives rise to specific brain activation patterns in subcortical structures within the cue-reactivity network (caudate, thalamus), and in cortical areas within the cue-regulation network (pgACC, mOFC). Whereas the contribution of subcortical structures such as the caudate nucleus and thalamus might be more difficult to unravel, the interaction effect observed within the PFC suggests that brain activity within the cue-regulation network reflects, at least in part, the integration between different internal and contextual contingencies aimed at forming an expectation about future drug consumption.

3.4.4. Likely causes of the differences with the observations of Wilson et al. (2004)

Contrary to what described by Wilson et al. (2004), a systematic association with prefrontal cortex activation and the not-seeking treatment status, we did not find such main effect, nor in dorsolateral prefrontal cortex, nor in orbitofrontal cortex. We rather found that this association was dependent on the nature of the substance of abuse in orbitofrontal cortex. While it was impossible to replicate with a coordinate based meta-analysis Wilson's et al. (2004) results because 8 of the studies that they considered were based on ROIs analyses, there are further analytical differences to prevent a formal comparison. First, Wilson et al. (2004) used a nominal analysis of the activation patterns as broad as the aforementioned terms (dlPFC; OFC); we used a coordinate-based meta-analysis with 5 mm spatial resolution and an ALE correction for spatial extent; we made a statistical assessment of the relevance of the clusters identified. In addition, Wilson et al. (2004) did not make a statistical evaluation of their findings. In retrospect, a chi-squared analysis based on their Table 1 would be significant for the dlPFC but not for the OFC. Further, Wilson's et al (2004) is based on nineteen studies while we considered sixty-four studies. All these differences may have contributed to the inability to replicate Wilson's et. al (2004) claim.

3.4.5. Strengths and limitations

Along with its limitations, this study has also several strengths. First, I explored for the first time the interaction effects between the class of substances and treatment status (Wilson et al., 2004, Jasinska et al., 2014), which represents a step forward in the understanding of the

neurobiology of drug craving. Second, I selected a highly homogeneous set of imaging studies on the cue-reactivity paradigm (in either visual or imagery modality) while preserving a moderate sample size (64 studies included), which constitutes another strength of the study. Third, I combined the ALE method (Eickhoff et al., 2009), which reveals the brain regions with most convergent activation across the whole dataset, with hierarchical clustering and post-hoc statistical characterization of the clusters concerning the factors of interest (Berlingeri et al., 2019): this approach has been validated in other domains of cognitive neuroscience, such as in the domain of food perception and obesity (Devoto et al., 2018), human volition (Zapparoli et al., 2017), reading dyslexia (Paulesu et al., 2014), single-word reading (Cattinelli et al., 2013a), and noun and verb processing (Crepaldi et al., 2013).

However, I acknowledge that the present meta-analysis has some limitations too. A first obvious limitation concerns the differences in demographic characteristics (e.g., sex distribution, co-occurring disorders, socio-economic status) of the samples across class of substances and treatment status; yet, I acknowledge that this becomes an issue if there is a systematic association of these nuisance variable with one level of our factorial design. If not, one has to assume that the emerging random noise would cancel out. Another limitation concerns the cross-sectional nature of the studies included, which means that we cannot exclude that some of our results reflect brain activation patterns pre-existent to the SUD. Also, I cannot exclude that some of the effects observed in my meta-analysis are due to abstinence-related effects, since abstinence has can potentiate the reward responses to drug cues (McClernon et al., 2008, Li et al., 2012, Lou et al., 2012, Wei et al., 2019); due to the intrinsic difference in average abstinence across substances, it was not possible to include this factor in our analysis. Similarly, the length of drug use has been shown to exert a modulatory effect on the neural response to drug cues (Jasinska et al., 2014), but I could not take this factor into account due to the high number of studies that did not report this information. Nonetheless, as studies with TS individuals have on average a shorter history of abuse compared to studies with NST individuals, I cannot assess the degree to which the observed effects of treatment status are mediated by the history of drug use. Another source of confound may concern the pharmacological effects of methadone-assisted heroin-addicted individuals, as in some of the included studies on heroin addiction, subjects were undergoing methadone-assisted detoxification or were under methadone treatment (Tabatabaei-Jafari et al., 2014, Wang et al., 2014, Li et al., 2015, De Pirro et al., 2018, Wei et al., 2019). In a similar fashion, it is hard or even impossible to isolate treatment type (inpatient vs outpatient, voluntary vs forced) from the effect of class of substances (legal vs illegal), as illegal drugs abusers, due to the illegal nature

of the substance, are more likely to be enrolled in forced and in-patient treatments compared to legal drug abusers (e.g., no forced in-patient treatments are expected for nicotine-dependent individuals). This, in turn, is expected to influence the perceived drug availability and the associated expectation of drug consumption. However, I acknowledge that these limitations reflect the clinical complexity of the matter at stake when considering studies on human subjects, and that the influence of these nuisance variables becomes an issue only when there is a strong and systematic association with one level of our factorial design. If not, one has to assume that the emerging random noise would cancel out.

Consistent with the real-world clinical complexity of the human SUD, in our pool of selected studies, some participants were poly-substance abusers, and most of them had coexisting nicotine addiction, thus raising the possibility that poly-substance use may have affected our results. Also, based on the fact that the potency of a reinforcer can be estimated from its main route of administration (Volkow and Wise, 2005), I cannot exclude that inter-study differences in the route of administration within and between-substance may have affected my results: again, this was impossible to account for, given the multiple ways in which a single substance can be administered, and because many studies did not report this information.

The latter issue is indeed crucial, as the effect of the route of administration on the neural responses to drug cues (in individuals addicted to the same substance) would point to a new relevant factor worth of investigation.

3.4.6. Conclusions and implications for clinical sciences

Taken together, these findings may suggest some initial practical considerations: drug-cue brain reactivity, an index of craving intensity and, possibly, of the risk of relapse into addiction, is not only influenced by the potential harm of a given substance, rather it also depends on internal and contextual determinants. As treatment-seeking patients are characterized by the engagement of specific brain reactions to drug cues depending on the substance of abuse, rehabilitation, particularly when cue-extinction strategies are employed (Conklin and Tiffany, 2002), may thus benefit from tailor-made interventions that consider the influence of internal and environmental contingencies when subjects are likely to be exposed to drug cues.

<u>Summary of Chapter 3</u>

In this Chapter, I combined the CluB method with the GingerALE algorithm to perform a meta-analysis of 64 neuroimaging studies on visual-anticipatory drug cue-reactivity in SUD. In particular, I explored the simple and interactive effect of two factors that modulate the neural

reactivity to drug cues: addiction severity and treatment status. These effects were taken as benchmarks to discuss the validity of Wilson's "expectation hypothesis" (Wilson et al., 2004) on the influence of treatment status on the neural responses to drug cues.

The results show that exposure to visual-anticipatory drug cues, across substances that induce a moderate (legal substances: alcohol, nicotine) to severe (illegal substances: cocaine, heroin) degree of dependence, is associated with an up-regulated activity of discrete portions within the cue-reactivity network (occipital cortices), linked to a share attentional bias toward the substance, and within the cue-regulation (ACC) network, linked to higher-order attentional and top-down processes. Conversely, individuals addicted to illegal substances showed more frequent activity within the cue-reactivity network (VTA, NAc, amygdala/hippocampus), presumably due to the deeper neural sensitization and to the enhanced incentive salience attribution, SUD patients addicted to legal substances are characterized by more frequent activity of the cue-regulation network (dACC), possibly linked to emotion (craving) regulation. Only in partial fulfillment with Wilson's et al. hypothesis (Wilson et al., 2004), I observed an interaction effect within the cue-regulation network (pgACC, mOFC), more frequently engaged by TS patients addicted to legal substances and by NST patients addicted to illegal substances, possibly reflecting the integration between different internal and contextual contingencies aimed at forming an expectation about future drug consumption.

To summarize, in the previous two Chapters I identified the brain networks underlying the reactivity to food and to drug cues, showing that: (i) obesity and SUD are characterized by common (e.g., ventral striatum/NAc) and distinct (e.g., insular cortex) neural correlates of craving; (ii) several internal (e.g., disease severity, satiety state) and external factors (e.g., sensory modality of cue-presentation, treatment status/drug availability) modulate such neural reactivity, in discrete portions of the cue-reactivity and cue-regulation networks.

The question of whether, and how, neurostimulation techniques applied to reduce craving act on the same neural circuits is addressed in the next empirical Chapter.

Chapter 4 – Repetitive Deep TMS for the Reduction of Body Weight: Preliminary Evidence for a Bimodal Effect on the Functional Brain Connectivity in Obese Individuals

4.1. Introduction

Obesity and drug addiction can be both considered as chronic relapsing disorders. Some estimates suggest that only 40-60% of all treatment-seeking SUD patients remain abstinent at 1 year follow-up (McLellan et al., 2000), with relapse rates for tobacco dependence being estimated at about 78% and 85%, respectively for counselling therapy in combination with medication and counselling therapy alone (Fiore, 2000). Similarly, obese patients struggle to maintain the weight they have lost, with 33-66% of the patients regaining it back, or gaining even more weight (Mann et al., 2007). Indeed, several treatments have been proposed for this condition, from life-style and diet interventions to bariatric surgery (Colquitt et al., 2009, Colquitt et al., 2014), but they are often associated with a transient weight-loss (Jeffery et al., 2000, Meany et al., 2014).

As already mentioned in Chapter 1, neuromodulation and neurostimulation techniques, such as transcranial Direct Current Stimulation (tDCS) and Transcranial Magnetic Stimulation (TMS), have been recently considered a promising tool for the treatment of obesity and eating disorders (Val-Laillet et al., 2015). This growing interest into brain-centered treatments for obesity is motivated by two main reasons: first, by the costs and the peri-operative risks associated with bariatric surgery (Colquitt et al., 2009); second, by the large corpus of functional activation neuroimaging studies, and meta-analyses, demonstrating that obese individuals are characterized by (i) perturbed neural activity in response to food cues in key structures involved in sensory, hedonic, and motivational processes, and (ii) in areas supporting higher-order processes such as attention, decision-making, and cognitive control ((Killgore et al., 2003, Rothemund et al., 2007, Dimitropoulos et al., 2012, Brooks et al., 2013, Jastreboff et al., 2013, Kennedy and Dimitropoulos, 2014, Murray et al., 2014, Pursey et al., 2014) and Chapter 2). Crucially, the aberrant activity within, and between, these neural circuits is expressed also in absence of (endogenous or exogenous) stimulation, as revealed by resting-state functional connectivity (rsFC) studies examining the brain's intrinsic activity (Kullmann et al., 2012, Kullmann et al., 2013, Contreras-Rodríguez et al., 2017).

Of course, non-invasive brain stimulation treatments are meant to affect the functioning of those same brain circuits - presumably by up-regulating the cue-regulation network and/or by down-regulating the cue-reactivity network -, hence leading to empowered self-control over eating;

yet, the precise neurobiological mechanisms beyond non-invasive brain stimulation techniques applied to obesity are largely unknown. This is what will be addressed in the current Chapter.

4.1.1. Disruption of large-scale resting-state brain networks and network topology in obesity

Resting-state fMRI aims at identifying the brain's intrinsic functional systems that emerge by the coherent pattern of spontaneous low-frequency BOLD fluctuations, and that are typically involved in cognitive functioning (Biswal et al., 1995, Greicius et al., 2003, Fox and Raichle, 2007). In particular, graph-theoretical approaches (Rubinov and Sporns, 2010) - which consider the brain as a network made of discrete *nodes* (i.e., a set of brain regions according with a particular parcellation scheme) connected by *links* (i.e., functional or structural connections between the nodes) - have been employed to describe the topological organization of the brain network in a variety of psychiatric and neuropsychiatric disorders, such as substance addiction (Jiang et al., 2013, Wang et al., 2015b), obsessive compulsive disorder (Armstrong et al., 2016, Tian et al., 2016), Alzheimer's disease (Sanz-Arigita et al., 2010, Zhao et al., 2012), and depression (Zhang et al., 2011, Ye et al., 2015). Yet, this approach was employed in only few studies investigating the brain functional organization in obese participants (Raschpichler et al., 2013, García-García et al., 2015, Baek et al., 2017, Zhang et al., 2019).

A recent study documented a disruption of brain network properties in a sample of obese individuals, half of which with binge-eating disorder (Baek et al., 2017). The authors observed a reduction in global (e.g., global efficiency, local efficiency, modularity) and local network metrics (e.g., nodal degree centrality, nodal efficiency, nodal betweenness centrality). With respect to regional metrics, obese individuals showed decreased nodal degree centrality (indexing the number of connections between a given brain region, the node, and all the other regions/nodes of the brain) in the pallidum, putamen, and thalamus, together with increased nodal degree centrality in the occipital cortex, indicating a disruption of the functional integration properties of key nodes within the cue-reactivity network (Baek et al., 2017). Another study on obese female patients confirmed and extended previous results, showing that obesity is linked not only to increased nodal centrality within the cue-reactivity network (ventral striatum, caudate), but also to decreased nodal centrality in the orbitofrontal cortex (Zhang et al., 2019), demonstrating that disrupted functional integration properties extend to regions involved in higher-order cognitive processes within the cue-regulation network.

Converging evidence for disrupted functional organization properties in obesity comes from studies using independent component analysis of resting-state fMRI data. Dovetailing with

heightened incentive salience processing of food stimuli in obesity and overeating (Berridge et al., 2010), obese compared to lean participants exhibit increased FC within the salience network (putamen) (García-García et al., 2013). In another study, obese participants displayed enhanced FC strength in the bilateral precuneus, and diminished FC strength in the anterior cingulate cortex and in the insula (Kullmann et al., 2012). These regions, together with the medial prefrontal and the lateral parietal cortices, constitute the default mode network (DMN) (Greicius et al., 2003, Raichle, 2015), a set of functionally connected brain areas that is engaged during rest and disengaged when the subject is performing a task (Fox et al., 2005), and whose activity is associated with the recollection of previous experiences, emotional processing, and with self-referential mental activity (Raichle, 2015).

The overall evidence suggests that obesity is associated with disrupted network properties and altered rsFC patterns within and between key nodes of the cue-reactivity and cue-regulation network implicated in food craving. Crucially, activity in the same brain networks can be successfully modulated by weight-loss interventions, bariatric surgery, and non-invasive brain stimulation.

4.1.2. Changes in rsFC induced by weight-loss

Even if no known study investigated the changes in brain network properties induced by weight-loss, some clues can be obtained by rsFC studies. A six-month exercise intervention in overweight and obese participants was effective in decreasing the activity of the precuneus in the DMN (McFadden et al., 2013), and this change was correlated with weight-loss. Sleeve gastrectomy, a surgical intervention that consists in the reduction of the size of the stomach, is also effective in recovering altered FC patterns in obese individuals. In particular, weight-loss after sleeve gastrectomy was associated with a recovery in the rsFC between several nodes of the cue-reactivity and cue-regulation networks (Li et al., 2018, Cerit et al., 2019), in areas that show aberrant activity at rest and during food cue-reactivity in obese individuals (Kullmann et al., 2012, Kullmann et al., 2013).

As already pointed out in Chapter 1 (section 1.6), non-invasive brain stimulation is also effective in decreasing self-reported food craving and in reducing food consumption in experimental settings (see (Song et al., 2019) for a recent meta-analysis). Yet, fewer studies documented the effect of neurostimulation interventions on weight-loss (Kim et al., 2018, Ferrulli et al., 2019a).

One study showed that a 2-week high-frequency repetitive TMS (rTMS) intervention targeting the left dlPFC was effective in reducing body weight in obese participants (Kim et al., 2018).

Further, compared to the sham stimulation group, the experimental group showed greater decreases in BMI, hunger, and desire for food at 4-week follow-up (Kim et al., 2018). In another rTMS study on individuals with obesity (Ferrulli et al., 2019a), the authors employed an H-coil (Zangen et al., 2005) specifically designed to reach deeper cortical structures like the insular cortex. As sown in Chapter 2, obese patients exhibit more frequent activity of the anterior insular cortex and overlying frontal operculum, particularly during the visual-anticipatory stimulation, suggesting that the insular cortex could be a promising target for neurostimulation applied to obesity (Val-Laillet et al., 2015). The 5-week intervention showed that the high-frequency (18 Hz) stimulation over the bilateral prefrontal and insular cortices was more effective than low-frequency (1 Hz) and sham stimulation in inducing weight-loss up to 1-year follow-up (Ferrulli et al., 2019a).

Yet, to the best of my knowledge, no study to date examined the anatomofunctional mechanism beyond the efficacy of non-invasive brain stimulation applied to obesity. The present preliminary study represents the first attempt to fill this gap in the literature.

4.1.3. Aims of the study

This is the first fMRI study investigating the neurofunctional changes associated with a deep rTMS treatment over the insular and frontal cortices that proved successful in reducing food-craving and improving weight-loss (Ferrulli et al., 2019). In particular, I employed resting-state fMRI and a graph-theoretical approach to identify local changes in the brain functional organization induced by the 5-week high-frequency versus sham deep rTMS treatment.

The current preliminary study was designed to address three main questions: (i) is the bilateral stimulation of the insular and prefrontal cortices capable of inducing neurofunctional changes at the system-level? (ii) Which are the brain circuits most affected by the neurostimulation treatment? (iii) To which cognitive domain(s) are they associated?

In line with previous reports on neural food cue-reactivity in obesity, and consistent with studies on the anatomofunctional changes induced by weight loss, I expected that the deep rTMS treatment would affect the functional integration properties of localized brain regions implied in food craving, particularly in the cue-regulation network (PFC), target of the neurostimulation.

4.2. Materials and methods

4.2.1. Study design

The present study is part of a larger randomized, double-blinded, placebo-controlled clinical trial designed to study the effects of a dTMS treatment aimed at reducing body weight and food craving (Ferrulli et al., 2019a, Ferrulli et al., 2019b). In brief, patients fulfilling all inclusion criteria (see below) were randomized to one of two groups: 18 Hz dTMS (real stimulation group, real) or placebo treatment (sham stimulation group, sham). Participants were randomized in a 1:1 allocation ratio, and the randomization was performed according to a randomization sequence generated by a computer program. The randomization and masking procedure is reported in the Supplementary File 3 (section 1.1).

Participants also underwent two resting-state fMRI scans: before the first dTMS session (T0) and after the 5-weeks intervention (T1, up to maximum two days from the last dTMS session). Participants were scanned at the same time at both T0 and T1, and they were required to fast for at least 3/4 hours before the fMRI session.

The study was conducted in accordance with the 1964 Helsinki declaration, and it received approval from the local institutional review boards (Ethics Committee of San Raffaele Hospital, Milan, Italy) in the amended version (Version Nr.3) dated 06/10/2016 (protocol number: 27778, file # 137498928 #). All participants provided written informed consent before participating in any of the study procedures.

4.2.2. Study participants

Twenty-four adult, obese, treatment-seeking participants (18 females; mean age = 51 ± 9 years; mean educational level = 14 years; mean BMI = 35.8 ± 3.6 Kg/m^2) were involved in the study. Participants had no history of neurological or psychiatric illness. None of the participants was characterized by cognitive impairment as assessed using the Mini Mental State Examination (corrected score > 23.8). Participants referred to the Endocrinology and Metabolic Diseases outpatient clinic, at Policlinico San Donato, for overweight/obesity treatment from January 2017 to November 2019, and were screened by a short interview to determine eligibility. The only recruitment strategy involved direct interviews (no paper or web advertisements were used). Inclusion and exclusion criteria are reported in Table 4.1. Four of the 24 participants enrolled in the study were also part of the sample in Ferrulli et al. (2019).

4.2.3. Intervention overview

Participants enrolled in the study received 15 treatments in total, three times per week over 5 weeks. Patients were not taking any medication during the study period (2 months). Participants could discontinue the treatment for a maximum of three non-consecutive times. The follow-up visit was planned at 1 month (FU1) after the end of the treatment.

Table 4.1. Inclusion and exclusion criteria of participants | List of the inclusion and exclusion criteria for the present study. BMI, body-mass index; fMRI, functional magnetic resonance imaging.

Inclusion criteria	Exclusion criteria
Age 22-65 years	Personal or a family history of seizures
BMI 30-45 Kg/m^2	Psychotic and/or organic brain disorders
Willingness to reduce body weight	Implanted metal devices
	Fasting blood glucose level > 8.33 mmol/L
	Abuse of substances other than nicotine
	Weight variation (>3%) < 3 months prior the screening visit
	Current or recent (<6 months prior the screening visit) treatment with anti-obesity medications or other medications for weight reduction
	Medications associated with lowered seizure threshold
	Type 1 diabetes or insulin-treated type 2 diabetes
	Contraindication to perform fMRI (cardiac implantable electronic device, metallic intraocular foreign bodies, implantable neurostimulation systems, cochlear implants/ear implant, drug infusion pump, catheters with metallic components, metallic fragments, cerebral artery aneurysm clips, magnetic dental implants, tissue expander, artificial limb, hearing aid, piercing, claustrophobia)

4.2.4. Repetitive dTMS

Repetitive dTMS was performed by a trained physician using a Magstim Rapid[2]TMS stimulator (Magstim Co. Ltd, Whitland, UK) equipped with an H-shaped coil (H-ADD), specifically designed to bilaterally stimulate the PFC and the insula (Zangen et al., 2005). The H-coil allows

direct stimulation of deeper brain regions such as the insula (3 cm vs. 1.5 cm from the skull). Details of the stimulation procedure are given below.

Before each dTMS session, the Resting Motor Threshold (RMT) was determined over the left primary motor cortex. The optimal spot on the scalp was localized to stimulate the right abductor pollicis brevis muscle, and the RMT was defined by delivering single stimulations, applying one pulse every 5 seconds to the motor cortex, and gradually decreasing intensity. The RMT was defined as the stimulation with the lowest required intensity to cause the right thumb to move. Once the RMT was defined, the coil was positioned 6 cm anteriorly to the motor spot and aligned symmetrically over the prefrontal cortex.

High-frequency sessions consisted of 80 trains of 18 Hz, each lasting 2 seconds, with an intertrain interval of 20 seconds. The HF treatment duration was 29.3 minutes with 2880 pulses in total. The Sham treatment was performed by a sham coil located in the same case of the real coil, producing similar acoustic artefacts and scalp sensations, inducing only negligible electric fields in the brain. In the group receiving the real treatment, the stimulation was performed with an intensity of 120% of the RMT.

4.2.5. Diet and lifestyle recommendations

During the entire study, all subjects were prescribed a hypocaloric diet. The details of the hypocaloric diet prescribed to the subjects are provided in the Supplementary File 3 (section 1.2).

4.2.6. Clinical and behavioral assessment

Anthropometric measurements were obtained at three time points: at baseline (T0), after 5 weeks of treatment (T1), and after 1 month (FU1). These included body weight and height, in order to calculate BMI (kg/m^2). Body weight was measured without shoes, wearing light underwear or naked, on a standing scale calibrated to the nearest 0.1 kg. Body height was measured without shoes using a stadiometer calibrated to the nearest 0.1 cm.

Food craving was assessed by means of the *Food Craving Questionnaire-Trait* (FCQ-T) (Innamorati et al., 2014), a self-report inventory comprising 39 items that investigate multiple dimensions of food craving. Assessment of food craving was conducted the day of the fMRI scan at both time points (T0 and T1) and at the follow-up visit (FU1).

4.2.7. Analytical strategy of clinical and behavioral data

To assess the effect of intervention on body weight, BMI, and food craving, data were analyzed by means of Linear Mixed Models (LMM) or Generalized Linear Mixed Models (GLMM) on the basis of the data distribution, with group (real vs sham stimulation), time (T0 vs T1 vs FU1), and their interaction as independent variables. Mixed modelling is a useful tool for repeated measures designs, and one of its main advantages is the ability to retain missing data points.

The Shapiro-Wilk test was accompanied by the visual inspection of data distribution to check if the samples were normally distributed. When data did not meet normality assumption, they fitted a gamma distribution and Generalized Linear Mixed Models (GLMM) were employed accordingly. Bonferroni-corrected post-hoc comparisons were conducted to qualify eventual significant interaction effects. A two-sided p-value ≤ 0.05 was deemed to be statistically significant.

Analyses were performed with the software R (version 1.2.5033; https://www.r-project.org/) by means of the lmer and glmer functions (lme4 package; http://cran.r-project.org/web/packages/lme4/index.html).

4.2.8. fMRI data acquisition

MRI scans were performed using a 1.5 Siemens Avanto scanner, endowed with echo-planar hardware for imaging. Whole-brain functional images were obtained with a T2*-weighted gradient-echo, EPI pulse sequence, using BOLD contrast (flip angle = 90°, TE = 60 ms, TR = 2000 ms, FOV = 250 mm and matrix = 64 x 64, slice thickness was 4 mm). We acquired one functional run comprising 350 scans (duration: $\simeq$ 12 minutes). Fifteen initial "dummy" scans were acquired but discarded before fMRI analysis. All of the subjects were also scanned with an MPRAGE high-resolution T1-weighted volumetric scan for further visualization of the results (flip angle = 35°, TE = 5 ms, TR = 21 ms, FOV = 250 mm, matrix = 256 x 256, TI = 768, for a total of 160 slices with 1 x 1 x 1 mm voxels).

4.2.9. Analytical strategy of fMRI data

My analytical strategy involved three sequential stages: first, I identified clusters that showed a significant change (increase or decrease) of Intrinsic Connectivity Contrast (ICC) (Martuzzi et al., 2011) after treatment in the real vs. sham stimulation group. Second, I employed those clusters as regions-of-interest (ROIs) for a seed-based resting-state functional connectivity (rsFC) analysis, in order to map the functional networks of those regions showing an effect of

stimulation. Finally, I performed a cognitive decoding of the obtained rsFC maps by means of the "Decoder" function available on Neurosynth (http://neurosynth.org/decode/). This allowed to obtain a set of key-words associated with the input image based on the NeuroVault repository (https://neurovault.org).

The details of the analyses performed at each stage are described below.

4.2.9.1. Preprocessing

Preprocessing and subsequent analysis of fMRI data were performed with the SPM-based software Conn functional connectivity toolbox (version 18b) (Whitfield-Gabrieli and Nieto-Castanon, 2012) and run on MATLAB (version 2016b; The MathWorks, Inc., Natick, Massachusetts, United States). In particular, I run the "standard" preprocessing pipeline available in Conn, which includes slice-time correction, realignment of the functional images to the first image of the series, T1-weighted image segmentation, co-registration of the mean functional image to the structural image, spatial normalization to the Montreal Neurological Institute (MNI) template and spatial smoothing. The slice-time corrected, realigned, co-registered and normalized images were smoothed with a 10 x 10 x 10 mm full-width half-maximum (FWHM) isotropic Gaussian kernel. This level of smoothing is recommended for the use of Gaussian random fields theory to perform cluster level correction for multiple comparisons (Flandin and Friston, 2019). Scan outliers based on inter-scan global signal changes and movement were detected with the Artifact Detection Tools (ART, http://www.nitrc.org/projects/artifact_detect). Scans were considered as outlier when the scan-to-scan global signal difference exceeded 2 standard deviations of the mean, and when the compounded measure of movement parameters exceeded 2 mm scan-to-scan movement (mean scan outliers: $Real_{T0} = 5.7\%$, $Sham_{T0} = 4.5\%$, $Real_{T1} = 4.2\%$, $Sham_{T1} = 0\%$).

Then, functional images were band-pass filtered to 0.008 Hz ~ 0.09 Hz (the frequency range of spontaneous BOLD signal fluctuations) and motion regressed (six motion parameters included as a first-level covariate) to reduce the influence of noise. To regress-out the BOLD signal associated with the individual white matter (WM) and cerebrospinal fluid (CSF), the WM and CSF masks were entered as confound, following the CompCor strategy implemented in Conn (Behzadi et al., 2007).

4.2.9.2. Intrinsic Connectivity Contrast

At the first level, I computed the Intrinsic Connectivity Contrast (ICC), a voxel-wise measure of degree centrality (Martuzzi et al., 2011). This data-driven approach ensures two main advantages: it does not require the definition of one or more *a priori* ROI(s), and it can be calculated without applying a correlation threshold, thus not requiring any *a priori* knowledge or assumption. For each subject, the ICC index produces voxel-based maps representing the magnitude of the correlation of each voxel with the rest of the brain, regardless of the direction of the correlation. Raw ICC values were then normalized to fit a Gaussian distribution (zICC), such that zICC values reflect the average connectivity across all other voxels, for each participant. The zICC maps were then entered into a second-level ANOVA, conforming to random-effect analysis, with the following factors: *group* (real vs sham) and *time* (T0 vs T1). To examine the directionality of the effects, post-hoc analyses were performed by using linear contrasts and t-statistics.

4.2.9.3. Seed-based resting-state functional connectivity

Significant clusters of increased or decreased ICC in the real vs. sham group after treatment were used as ROIs for a seed-based resting-state functional connectivity (rsFC) analysis in the whole sample at baseline, before treatment (T0). At the first level, Conn computes, for each ROI, a bivariate correlation between the average BOLD signal within the ROI (from unsmoothed volumes) and every other voxel in the brain. The result is a rsFC map for each ROI and for each subject: these were entered into a second-level random-effect analysis (independent sample t-test). I extract the average rsFC patterns regardless of the direction of the correlation (F-contrast) in any of the two groups (real and sham). All the reported results (ICC, rsFC) survive a correction for multiple comparisons: I used the nested-taxonomy strategy recommended by Friston and colleagues (Friston et al., 1996), including regional effects meeting either a clusterwise or voxelwise FWER correction. The voxelwise threshold applied to the statistical maps before the clusterwise correction was $p < 0.001$ uncorrected, as recommended by Flandin and Friston (Flandin and Friston, 2019). For clusters significant at the $p < 0.05$ FWER-corrected level, I also report the other peaks at $p < 0.001$.

4.2.9.4. Cognitive decoding

In order to perform a cognitive decoding of the rsFC results, the rsFC maps obtained from the former analysis were exported in NIfTi (.nii) format and subsequently loaded in the "Decoder"

function available on Neurosynth (http://neurosynth.org/decode/). The Decoder function of Neurosynth allows to retrieve the Pearson correlation of the key-words that are most associated with the input image (in .nii format) based on the NeuroVault repository (https://neurovault.org). In other words, the r-value associated with each key-word reflects the correlation across all voxels between the input map and the map associated with a particular key-word in NeuroVault.

I considered the first 50 entries returned for each rsFC map, and we excluded all the terms associated with an anatomical reference (e.g., orbitofrontal, ventromedial, medial, lateral). The first 25 of the remaining terms and their associated r-values were then plotted by means of the *wordcloud* function implemented in the *wordcloud* package (Ian Fellows (2018). wordcloud: Word Clouds. R package version 2.6) and run in R (R Core Team (2017). R: A language and environment for statistical computing. R Foundation for Statistical Computing, Vienna, Austria).

4.3. Results

4.3.1. Study participants

Out of the 24 participants initially enrolled in the study, 7 dropped out from the study, resulting in 17 participants who completed the study as per protocol. Of these, 9 were allocated to the *real*TMS group and 8 to the *sham*TMS group. Out of the 9 participants allocated to the *real*TMS group, 7 underwent FU1; all of the participants allocated to the *sham*TMS group, underwent FU1 (Figure 4.1). Data from 5 participants at FU1 (3 from the real stimulation group and 2 from the sham stimulation group) were not available for the FCQ-T scores. Details about drop-out patients have been reported in the Supplementary File 3 (section 2.1).

Baseline characteristics of the two groups are reported in Table 4.2. The two groups did not differ significantly in any baseline characteristic.
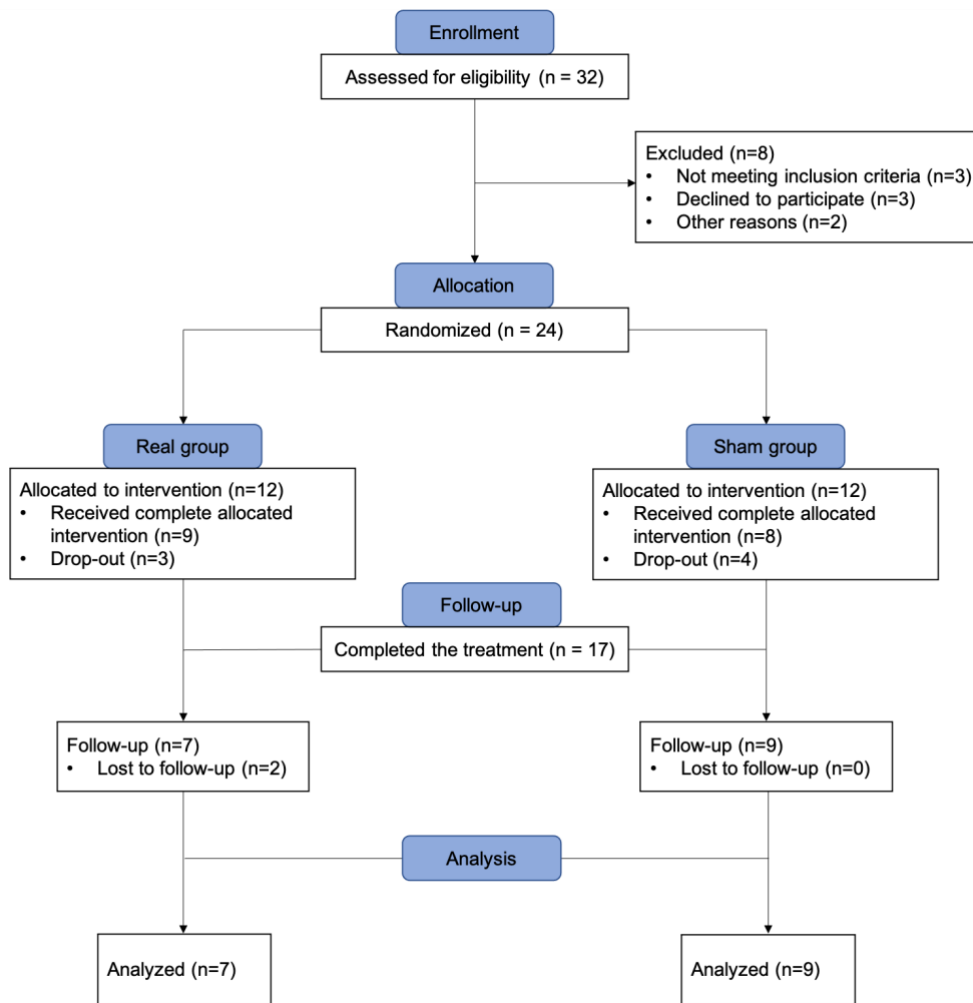
Figure 4.1. CONSORT diagram | CONSORT diagram displaying the number of participants that were enrolled in the study, allocated to the real or sham intervention group, completed the follow-up, and finally included in the analyses.

Table 4.2. Sample characteristics | Baseline characteristics of participants according to the study group. BMI, body-mass index; FCQ-T, Food Craving Questionnaire-Trait.

	realTMS group	shamTMS group	
Female/Male, n	7/2	6/2	$\chi2 = 0.02$, $p = 0.89$
Age, years	50.3 ± 9.2	51.6 ± 10.5	$U = 26$, $p = 0.36$
Body weight, kg	93 ± 14	99.4 ± 12.1	$t(15) = -1$, $p = 0.33$
BMI, kg/m^2	35 ± 3.2	37.5 ± 3.9	$t(15) = -1.47$, $p = 0.16$
FCQ-T score	123.4 ± 41.4	119.6 ± 25.8	$t(15) = 0.22$, $p = 0.83$

4.3.2. Clinical and behavioral results

4.3.2.1. Body weight and BMI

The GLMM on body weight showed a significant *main effect of time* ($\chi^2 = 32.3$, p < .001) that was further qualified by a significant *group-by-time interaction* ($\chi^2 = 6.2$, p = .04) (Figure 4.2A). The *main effect of group* was not significant ($\chi^2 = 1.6$, p = .21). Bonferroni corrected post-hoc comparisons showed that participants in the Real stimulation group exhibited a significant decrease of body weight from T0 (adjusted mean = 87.7 kg, se = 4.7 kg) to T1 (adjusted mean = 85.5 kg, se = 4.1 kg, $\chi^2 = 15.7$, p < .001, Cohen's d = .70), and from T0 to FU1 (adjusted mean = 84.5 kg, se = 4.4 kg, $\chi^2 = 29.9$, p < .001, Cohen's d = .72). After Bonferroni adjustment, decrease in body weight of participants in the Sham stimulation group from T0 (adjusted mean: 95.2 kg, se = 4.3 kg) to T1 (adjusted mean = 93.5 kg, se = 4.4 kg, $\chi^2 = 5.6$, p = .11, Cohen's d = .69) and from T0 to FU1 (adjusted mean = 93.7 kg, se = 5 kg, $\chi^2 = 4.2$, p = .25, Cohen's d = .36). Neither the Real nor the Sham stimulation group showed a significant decrease of body weight from T1 to FU1 (Real: $\chi^2 = 2.5$, p = .67, Cohen's d = .55; Sham: $\chi^2 = 0.1$, p = 1, Cohen's d = .08).

The GLMM on BMI showed a significant *main effect of time* ($\chi^2 = 34.5$, p < .001) and a significant *group-by-time interaction* ($\chi^2 = 5.9$, p = .05) (Figure 4.2B). The *main effect of group* was not significant ($\chi^2 = 1.6$, p = .21). Bonferroni corrected post-hoc comparisons showed that participants in the Real stimulation group exhibited a significant decrease of BMI from T0 (adjusted mean = 34.3 kg/m^2, se = 1.1 kg/m^2) to T1 (adjusted mean = 33.4 kg/m^2, se = 0.8 kg/m^2, $\chi^2 = 15.2$, p < .001, Cohen's d = .79) and from T0 to FU1 (adjusted mean = 32.9 kg/m^2, se = 0.9 kg/m^2, $\chi^2 = 29.5$, p < .001, Cohen's d = 1.05). After Bonferroni adjustment, participants in the Sham stimulation group exhibited a significant decrease of BMI from T0 (adjusted mean: 36.5 kg/m^2, se = 1.4 kg/m^2) to T1 (adjusted mean = 35.8 kg/m^2, se = 1.4 kg/m^2, $\chi^2 = 6.9$, p = .05, Cohen's d = .71), whereas BMI decrease from T0 to FU1 was not significant (adjusted mean = 35.8 kg/m^2, se = 1.6 kg/m^2, $\chi^2 = 5.7$, p = .10, Cohen's d = .45). Neither the Real nor the Sham stimulation group showed a significant decrease of BMI from T1 to FU1 (Real: $\chi^2 = 3.3$, p = .43, Cohen's d = 1.04; *sham*: $\chi^2 = 0.6$, p = 1, Cohen's d = 0).

4.3.2.2. Food craving

The LMM on FCQ-T scores showed a significant *main effect of time* ($\chi^2 = 27$, p < .001), both groups exhibiting a significant decrease of FCQ-T scores over time (Figure 4.2C). The *main effect of group* ($\chi^2 = 1.1$, p = .29) and the *group-by-time interaction* were not significant ($\chi^2 =$

1.8, p = .4). Bonferroni corrected post-hoc comparisons showed that both groups exhibited a significant decrease of FCQ-T scores from T0 (adjusted mean = 112.8, se = 6.5) to T1 (adjusted mean = 86.7, se = 6.5, χ^2 = 16.2, p < .001, Cohen's d = 1.01) and from T0 to FU1 (adjusted mean = 78.2, se = 7.3, χ^2 = 22.2, p < .001, Cohen's d = 1.09). Changes in FCQ-T scores from T1 to FU1 were not significant (χ^2 = 1.3, p = .75, Cohen's d = .51).
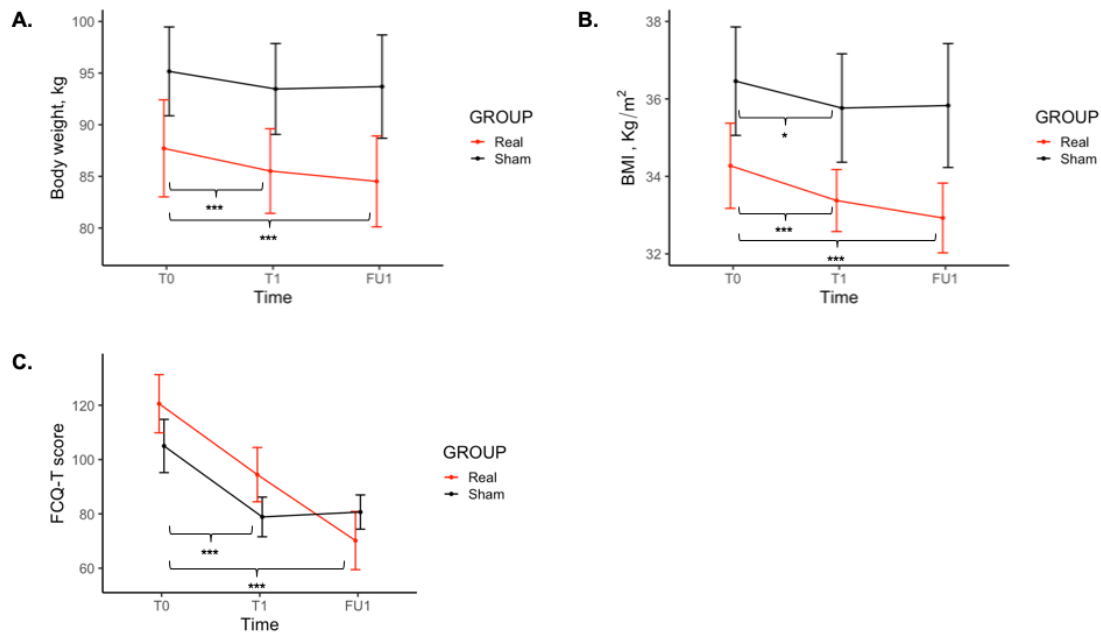
Figure 4.2. Effect of treatment on clinical and behavioral data | Results of the GLMM and LMM analyses on **(A)** body weight, **(B)** BMI, and **(C)** FCQ-T scores. FCQ-T, Food Craving Questionnaire-Trait; GLMM, generalized linear mixed models; LMM, linear mixed models; T0, baseline; T1, post 5-weeks intervention; FU1, 1-month follow-up. *, p < .05; ***, p < .001.

4.3.3. Neuroimaging results

4.3.3.1. Intrinsic Connectivity Contrast

I observed a significant main effect of time in the bilateral superior (STG) and middle temporal gyri (MTG), showing increased ICC after treatment across groups (Table 4.3A). No cluster showed a significant *main effect of group*. We also observed a *group-by-time interaction* in the left gyrus rectus (medial orbitofrontal cortex, mOFC) and in the occipital pole, comprising the left superior and inferior occipital gyrus, the right lingual gyrus and the left calcarine fissure (Table 4.3B and Figure 4.3). Post-hoc analyses revealed that the mOFC showed a significant increase of ICC in the real-TMS compared to the sham-TMS stimulation group after treatment,

whereas the occipital pole showed a significant decrease of ICC in the real-TMS compared to the sham-TMS stimulation group after treatment.

Table 4.3. Results of the ICC analysis | Brain regions displaying a significant **(A)** main effect of time and **(B)** group-by-time interaction. BA, Brodmann Area.

Brain regions (BA)	MNI coordinates							
	Left hemisphere				Left hemisphere			
	X	Y	Z	Z-score	X	Y	Z	Z-score
A) Main effect of Time								
Sup. temporal gyrus (22)	-60	-46	14	3.29				
Sup. temporal gyrus (21)					52	-24	-2	3.97
Sup. temporal gyrus					52	-14	-2	4.16
Mid. temporal gyrus (37)					42	-58	12	4.21
Mid. temporal gyrus (22)	-56	-42	8	3.85				
	-52	-36	4	4.62				
					52	-28	0	3.90
Mid. temporal gyrus (21)					46	-48	10	3.65
					50	-32	2	3.68
					54	-34	2	3.65
					48	-38	2	3.64
B) Group-by-Time interaction								
Gyrus rectus (11)	-8	32	-14	4.93				
	-14	26	-14	3.50				
	-8	30	-22	4.31				
Sup. occipital gyrus (17)	-12	-92	4	3.61				
Calcarine fissure (17)					0	-86	10	3.45
	-2	-86	4	3.71				
	-8	-90	4	3.67				
	-12	-88	2	3.48				
	-4	-90	-2	3.50				
	-2	-80	-6	3.60				
	-2	-92	-12	4.36				
Calcarine fissure (18)	-6	-90	-8	3.54				
	-4	-94	-8	4.09				
Lingual gyrus (18)					14	-88	-2	3.49
Lingual gyrus (17)					16	-100	-8	3.37
					18	-104	-8	3.51
	-4	-90	-16	4.14				
Inf. occipital gyrus (17)	-12	-100	-6	3.99				
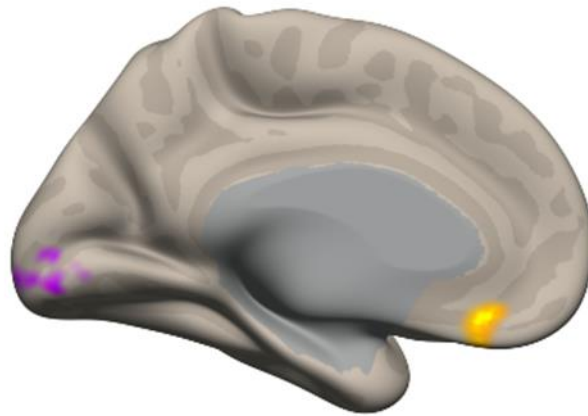
Figure 4.3. Results of the ICC analysis | Results of the significant group-by-time interaction effects in the ICC analysis overlaid on the left medial surface of the brain. Decreases in ICC values in the realTMS vs. shamTMS after treatment are represented in violet, whereas increases in ICC values are represented in yellow.

4.3.3.2. Resting-state functional connectivity results

The mOFC was significantly functionally connected with a cortical fronto-temporal-parietal network comprising the pars orbitalis of the inferior, medial, middle, and superior frontal gyrus, the anterior cingulate cortex and corona radiata, the superior, middle, and inferior temporal gyrus, the middle and superior temporal pole, the precuneus, the insular cortex, the thalamus, the ventral and dorsal (putamen, caudate) striatum (Table 4.4A and Figure 4.4A).

The occipital pole was significantly functionally connected with the inferior parietal lobule, the supramarginal gyrus, the cuneus, the lingual gyrus, the calcarine fissure, and the cerebellum, extending to the midbrain (Table 4.4B and Figure 4.4B).

Table 4.4. Results of the seed-based rsFC analysis. Brain regions displaying a significant functional connectivity with the **(A)** medial orbitofrontal cortex and **(B)** occipital pole. BA, Brodmann Area; *, peak survives FWE-correction; #, peak survives FDR-correction.

Brain regions (BA)	MNI coordinates							
	Left hemisphere				Left hemisphere			
	X	Y	Z	Z-score	X	Y	Z	Z-score
A) Medial orbitofrontal cortex (mOFC)								
Sup. frontal gyrus, pars orbitalis (11)					18	24	-24	4.14
Sup. medial frontal gyrus (10)	-2	62	20	3.93				
					0	58	20	3.71
	-2	56	24	3.78				

Region	x	y	z	value	x	y	z	value
	-6	54	22	3.76				
Sup. medial frontal gyrus (9)					6	50	36	4.26
Med. frontal gyrus, pars orbitalis (11)					16	46	-2	3.50
Med. frontal gyrus, pars orbitalis					0	20	-12	4.97
Mid. frontal gyrus	-28	40	14	4.30				
	-28	36	16	4.46				
Inf. frontal gyrus, pars triangularis (47)	-26	38	10	4.22				
Inf. frontal gyrus, pars orbitalis (47)					36	34	-16	4.31
Inf. frontal gyrus, pars orbitalis (11)					28	36	-18	3.68
	-20	16	-24	4.23				
Inf. frontal gyrus, pars orbitalis (38)	-32	22	-24	3.84				
Insula (47)	-32	28	0	3.68				
	-28	26	6	3.38				
	-30	24	2	3.61				
Insula	-28	30	20	4.61				
	-32	18	6	3.58				
	-30	16	10	3.61				
	-34	14	8	3.67				
	-36	10	6	3.46				
	-40	4	8	3.56				
	-36	4	6	3.56				
	-42	-2	6	3.66				
Ant. cingulum (32)					8	46	30	4.02
Ant. cingulum (11)					8	38	-6	5.04
Ant. cingulum (24)	-6	32	-20	7.14*#				
Ant. corona radiata (white matter)	-20	34	18	3.86				
	-16	30	20	3.51				
Sup. temporal pole (38)	-34	18	-30	4.14				
					42	16	-26	4.67
Mid. temporal pole (38)					44	16	-34	4.08
Mid. temporal pole (36)	-30	8	-34	3.85				
Mid. temporal gyrus (21)					52	4	-28	3.86
					54	-2	-20	4.31
					50	-4	-24	3.95
Inf. temporal gyrus (20)					54	6	-34	4.04
					56	-2	-38	3.68
Inf. temporal gyrus (21)					54	2	-32	4.41
					56	-4	-28	3.64
Precuneus (23)					10	-52	24	3.18
					8	-56	28	3.24
Precuneus					2	-66	26	3.54
					2	-68	30	3.52
Ventral striatum					6	8	-16	5.36*
Ventral striatum (25)	-6	16	-14	4.87				

Region								
	-10	14	-16	5.04				
	-4	12	-16	4.95				
Parahippocampal gyrus (36)	-28	0	-34	3.89				
Putamen	-28	14	6	3.95				
	-26	8	4	3.41				
					24	6	18	3.72
					24	-6	14	4.36
Pallidum	-12	0	4	4.32				
Caudate					24	14	22	4.28
	-10	2	12	4.08				
Thalamus					6	-2	8	3.78
	-14	-4	12	3.98				
	-12	-8	16	3.71				
	-16	-8	14	3.91				
	-20	-16	14	3.97				
	-22	-26	16	4.24				
					16	-16	0	3.99
					20	-16	4	3.87
					20	-20	2	3.91
					20	-24	4	3.83
					26	-28	10	3.73

B) Occipital pole

Region								
Supramarginal gyrus					60	-22	36	3.90
					54	-24	28	3.25
					50	-24	26	3.38
					58	-42	36	3.18
Supramarginal gyrus (40)					54	-36	44	4.22
					60	-42	44	3.34
Inf. parietal lobule (40)					42	-42	36	3.82
Cuneus (18)	-8	-92	26	4.74				
Cuneus	-4	-92	36	4.95#				
					4	-96	18	5.21*#
Lingual gyrus (18)					12	-74	2	5.77*#
					14	-78	0	5.73*#
	-14	-80	0	6.12*#				
Lingual gyrus (17)	-12	-84	0	6.19*#				
					8	-88	-2	6.06*#
Calcarine fissure (17)					4	-80	2	5.97*#
					0	-84	2	5.91*#
					0	-90	-10	6.89*#
	-8	-96	-6	6.37*#				
					10	-96	6	5.31*#

Calcarine fissure (18)	-2	-94	12	6.64*#					
					18	-94	-4	5.88*#	
Cerebellum VI	-2	-78	-12	6.02*#					
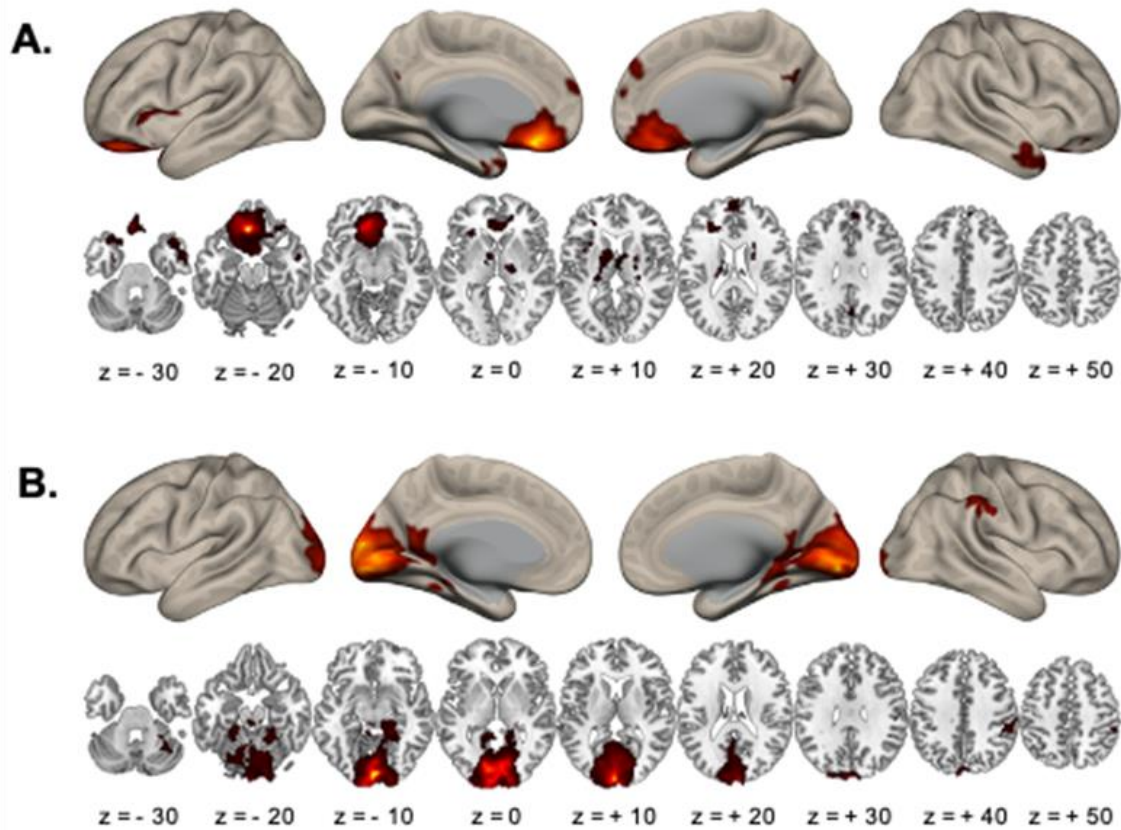
Figure 4.4. Results of the seed-based rsFC analysis | Results of the seed-based rsFC analysis for the seed in the (**A**) medial orbitofrontal cortex and (**B**) occipital pole. Coordinates are reported in MNI stereotaxic space.

4.3.3.3. Correlation between mOFC connectivity at baseline and BMI change after 1 month

I performed an exploratory correlational analysis between the rsFC patterns identified in the previous analysis and BMI change after 1 month from the end of the treatment ($BMI_{FU1}-BMI_{T0}$). In particular, I observed a significant negative correlation between mOFC-insula rsFC strength and BMI change at follow-up (Spearman's ϱ = - .54, p = .04, n = 15): the stronger the negative mOFC-insula rsFC, the lesser the decrease in BMI at 1-month follow-up (Figure 4.5).
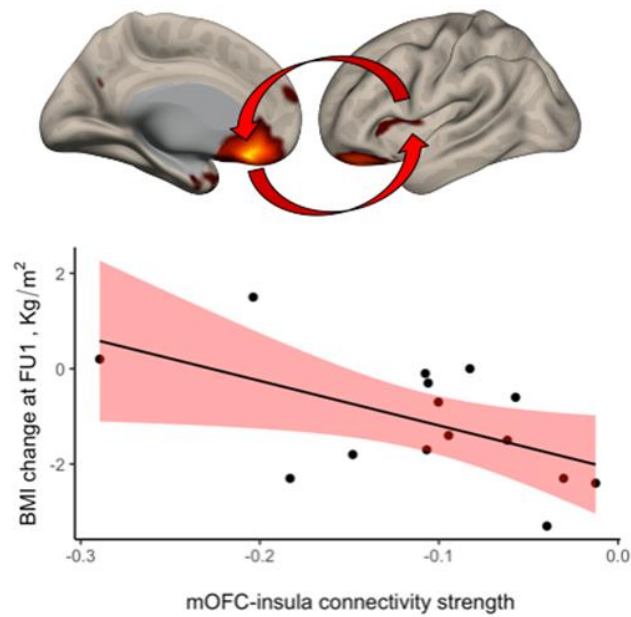
Figure 4.5. Results of the exploratory correlational analysis | Association between mOFC-insula rsFC and BMI change at 1-month follow-up showing that stronger mOFC-insula rsFC is associated with lower BMI change at 1-month follow-up.

4.3.3.4. Cognitive decoding through the Neurosynth.org database

After removal of anatomical terms, the first 25 terms associated with the mOFC rsFC map were mainly related to reward processing (e.g., value, reward, reinforcement, food) (Table 4.5A and Figure 4.6A). Conversely, after removal of anatomical terms the first 25 terms associated with the occipital pole rsFC map were mainly related to visual perception (e.g., early visual, sighted, visual stimuli, mental imagery) (Table 4.5B and Figure 4.6B). The full list of 50 terms returned by Neurosynth for the two rsFC maps is reported in the Supplementary File 3 (Table S4.1).

Table 4.5. Results of the Neurosynth analysis | The first 25 non-anatomical terms returned by Neurosynth for the **(A)** medial orbitofrontal cortex and **(B)** occipital pole rsFC maps are reported, along with their associated Pearson's correlation coefficient.

A) mOFC　　　　　　　　　　　　**B) Occipital pole**

Term	Correlation	Term	Correlation
value	0.199	early visual	0.311
reward	0.180	visual	0.230
reinforcement	0.133	sighted	0.147
social	0.115	mental imagery	0.124
spectrum disorder	0.114	metabolism	0.100
food	0.113	visual stimulus	0.096
valence	0.097	eye movement	0.091
rewards	0.093	vision	0.069
olfactory	0.089	sensory information	0.047
positive negative	0.089	erp	0.044
arousal	0.083	visual field	0.038
autonomic	0.083	negativity	0.037
suffering	0.080	invasive	0.034
mentalizing	0.078	naturalistic	0.034
decision	0.077	category	0.033
affective	0.077	agent	0.031
implicit	0.076	navigation	0.029
pleasant	0.073	low level	0.028
computation	0.071	integrative	0.027
choices	0.070	eye movements	0.026
conductance	0.068	pair	0.026
skin conductance	0.068	categorization	0.025
taste	0.065	imagery	0.025
emotional	0.065	add	0.024
subjective	0.064	competition	0.024
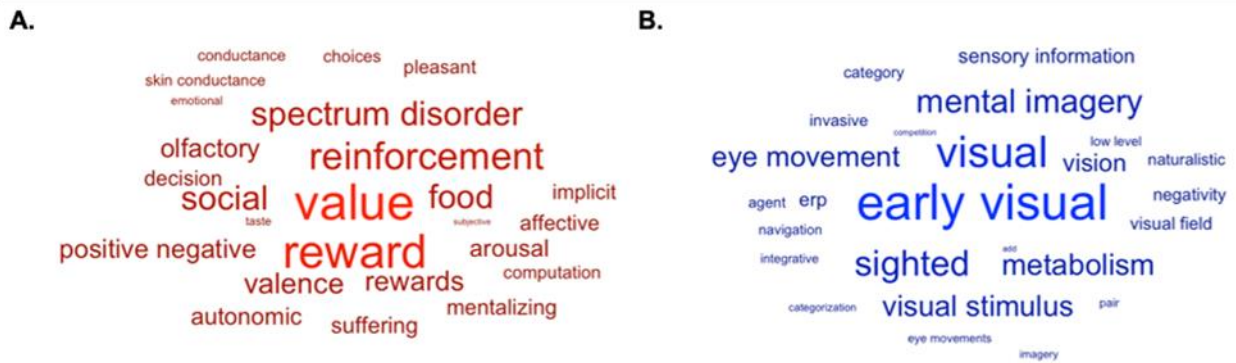
Figure 4.6. Results of the Neurosynth analysis | The first 25 non-anatomical terms returned by Neurosynth for the **(A)** mOFC rsFC map and for the **(B)** occipital pole rsFC map were plotted such that the bigger the font size, the greater the association with a given term. mOFC, medial orbitofrontal cortex; rsFC, resting-state functional connectivity.

4.4. Discussion

In this placebo-controlled longitudinal study, for the first time, the intrinsic connectivity contrast (ICC) - a data-driven, voxel-wise measure of degree centrality obtained from resting-state fMRI data - was used to capture local changes in functional integration properties induced by 5-weeks of deep rTMS treatment in individuals with obesity. Further, a seed-based rsFC analysis was performed, considering as regions of interest the "hubs" significantly affected by the rTMS to reveal their FC patterns. Finally, the functional meaning of the resulting FC maps was corroborated by a quantitative association analysis through the Neurosynth.org repository. Concerning the effects of deep rTMS on anthropometric measures (body weight and BMI), I found a significant group-by-time interaction, with a significant decrease in body weight and BMI in the *real*TMS group, up to 1-month follow-up. Conversely, food craving as assessed by the Food Craving Questionnaire-Trait (Innamorati et al., 2014) exhibited a significant reduction over time, without significant differences between the groups. These findings confirmed the results of Ferrulli and colleagues, showing that high frequency (18 Hz) deep rTMS over the bilateral prefrontal and insular cortices was more effective than sham stimulations in inducing weight-loss in individuals with obesity (Ferrulli et al., 2019b), a result that has been recently replicated by another randomized controlled trial (Kim et al., 2019a).

Also, in the study by Ferrulli and colleagues (2019b), a decreasing trend (p = .073) in food craving in the high-frequency vs. low-frequency and sham stimulation group was observed (Ferrulli et al., 2019b), the interaction driven mainly by between-group differences in food craving occurring *after* T1. There are, at least, two alternative explanations for the dissociation between the effect of realTMS on body weight and BMI, and the lack of such effect in self-

reported food craving. First, as all explicit meta-cognitive evaluations, self-reported craving may be prone to a number of limitations: it can be influenced by self-presentation strategies or social desirability bias (Fisher, 1993b), that is the tendency to give desirable responses instead of responses that reflect true feelings, or by a limited introspective capability of the subject (Greenwald et al., 2002). In other words, subjects might tend to give responses that reflect their adherence to the treatment scheme, especially during their active involvement in the trial (i.e., at the baseline and at the end of the 5-weeks treatment). Second, a reduction in food craving *per se* might not be the only mechanism beyond the efficacy of deep rTMS. As only the realTMS group showed a significant decrease in body weight and BMI up to 1-month follow-up, it is plausible that the high-frequency deep rTMS does not result in a greater reduction in the quantity and quality of food cravings, but in the capability of resisting them for a longer period of time.

As discussed below, this might be due to the fact that deep rTMS induced plastic changes in regions of the brain involved not only in cue-reactivity, but also in brain regions involved in higher-order regulatory processes.

4.4.1. Deep rTMS over the bilateral insular and prefrontal cortices induces changes in the functional brain organization

In this study, I used a novel data-driven connectivity measure (the ICC) (Martuzzi et al., 2011), that quantifies the degree of brain functional integration at the voxel-level. In particular, I observed that only the real TMS induced a significant increase of ICC in the mOFC, and a significant decrease of ICC in the occipital pole, after treatment.

The OFC is a prefrontal cortex (PFC) region involved in sensory integration, in representing the affective value of the reinforcers, in decision-making, and expectation (Kringelbach, 2005). Specifically, the OFC integrates sensory modalities such as taste, smell, and vision, and, through its dense reciprocal projections into thalamic, midbrain, and striatal regions, it is a critical *hub* for decision-making on highly motivating stimuli (Rolls, 2015). There is much evidence that point to disrupted anatomofunctional and structural alterations of the OFC in obesity. For example, it has been reported that obese individuals display lower gray and associated with matter volumes in the OFC, as well as of the insula and striatum (Shott et al., 2015). A recent meta-analysis of 25 voxel-based morphometry studies showed that greater BMI is associated with lower grey matter volume in the medial OFC, encompassing Brodmann areas 10 and 11 (Chen et al., 2020). There is also evidence that obesity is associated with altered mOFC functional connectivity. Adolescents with obesity, compared to healthy weight controls,

show stronger rsFC between the mOFC and key structures involved in sensory and reward processing, such as the olfactory tubercle and the pallidum, and reduced rsFC between the mOFC and the ventrolateral PFC, a core region of the cue-regulation network involved in cognitive control (Borowitz et al., 2020). Further, a recent study documented decreased degree centrality of the OFC, together with increased degree centrality of the ventral striatum, in obese compared to healthy weight subjects (Zhang et al., 2019).

Consistent with the role of the OFC in integrating different aspects of reward-related processing, the seed-based rsFC analysis shows that the mOFC is functionally connected with regions associated with sensory and motivational processing (thalamus, parahippocampus, dorsal and ventral striatum, anterior insula, precuneus), as well as with brain regions involved in the regulation of behavior (vlPFC, superior medial PFC, subgenual anterior cingulate cortex). The results of the decoding analysis performed through Neurosynth (e.g., value, reward, food, decision, choices) are also consistent with the hypothesis that one of the mechanisms underlying the augmented control over eating is the enhancement of the OFC capacity of integrating information from the rest of the brain, thus favoring food-related decision-making.

Perhaps surprisingly, a decreased ICC in the occipital pole has been reported in the realTMS group only, after the 5-weeks treatment. The occipital lobe it is mainly involved in visuospatial processing, and it is part of the part of the visual network, a set of brain regions that show a coherent pattern of functional connection at rest, in absence of external visual stimulation (Damoiseaux et al., 2006). In our sample, the occipital pole was mainly functionally connected within the occipital cortex (calcarine scissure, lingual gyrus (BA17 and BA18), cuneus), extending to the precuneus and the right parietal cortex (supramarginal gyrus, inferior parietal lobule), consistent with an occipito-parietal network involved in visual processing and visuo-spatial attention (Lauritzen et al., 2009). Further, the occipital cortex is highly connected with several cortical and subcortical structures, sch as the middle temporal lobe, the thalamus, and the PFC through long-range projections (Haxby et al., 1994). An early study employing graph-theoretical analysis on rsFC data documented increased nodal degree in the occipital cortex, indexing increased functional connections of the occipital lobe with the rest of the brain (Baek et al., 2017). The current results may suggest that high-frequency deep rTMS over bilateral insula and PFC modulates the global connectivity profile of brain areas functionally connected with the occipital lobe, thus leading to reduced functional connections with the occipital pole. The results of the decoding performed through Neurosynth (e.g., early visual, mental imagery, visual stimulus, sighted, sensory information) are also consistent with the idea that a diminished ICC in the occipital pole might lead to a reduced reactivity to bottom-up visual-sensory

processes, as previously observed in alcohol-dependent patients (Herremans et al., 2015). Specifically, in the last study, 15 sessions of high frequency rTMS applied to the right DLPFC in recently detoxified alcohol-dependent patients had more influence on the attentional network rather than on the craving neurocircuit, during an alcohol-related cue-exposure (Herremans et al., 2015).

The present results are somehow different from the ones obtained recently in a similar study conducted by Kim and colleagues (Kim et al., 2019b). In that study, the authors explored the changes in brain connectivity after an rTMS treatment over the DLPFC in adults with obesity: they found that real rTMS induced an increase in functional integration properties within the right frontoparietal network, including the right dorsolateral and ventrolateral PFC, and the right parietal cortex (Kim et al., 2019b).

With this regard, I argue that several factors may explain the differences with the present results: 1. A different stimulatory protocol (8-shaped coil vs H-coil; 10 Hz vs 18 Hz; total number of sessions); 2. Different stimulated brain areas (only left DLPFC); 3. Different graph-theoretical measures (betweenness centrality vs ICC); 4. Different dietary regimen; 5. Different satiety states of the participants at the time of scanning. In particular, the use of the H-coil allowed us to stimulate deeper cortical structures, such as the insula (Zangen et al., 2005).

4.4.2. Neurofunctional markers of weight loss

In this study, I also investigated the association between rsFC and weight-loss at 1-month follow-up (FU1). Exploratory correlational analysis highlighted a significant inverse correlation between the mOFC-insula connectivity strength and BMI change at a 1-month follow-up, whereby stronger negative mOFC-insula rsFC is associated with lower weight-loss. As mentioned above, the OFC is involved in the integration process of food-related inputs (taste, olfaction, touch, hearing, and vision), leading to decision making, goal-directed behavior, and prediction of the anticipated reward value of specific actions (Rolls, 2015). The insula, which represents another target of neurostimulation together with PFC, plays a role in the recognition of taste and, particularly the anterior part, is involved in salience processing (Cauda et al., 2011). Several rsFC studies showed that individuals with obesity exhibit altered FC between regions involved in metabolic sensing and interoception (i.e., hypothalamus, posterior insula) and regions involved in reward and salience processing (i.e., striatum, OFC, anterior insula) (Kullmann et al., 2014, Wijngaarden et al., 2015, Contreras-Rodríguez et al., 2017).

In this study I highlighted that individuals with obesity who present a stronger mOFC-insula rsFC are less likely to lose weight, probably due to enhanced saliency value of food and its cues, along with an enhanced awareness of a desire to consume them. Conversely, a weakening of rsFC between OFC and insula could represent a predictive factor for a greater weight loss, as well as a possible specific target for the treatment with rTMS in obesity. Of note, a reduced rsFC between the insula and medial PFC has been already observed in healthy subjects after rTMS compared to sham, regardless of the low (1 Hz) or high-frequency (10 Hz) stimulation (Lee et al., 2020).

To summarize, in this study I applied graph-theoretical analysis to resting-state functional connectivity data to investigate the neurofunctional changes associated with a deep rTMS treatment over the insular and prefrontal cortices that reduces food-craving while achieving a weight-loss superior to a simple diet. In the *real*TMS group, compared with the shamTMS group, I found a significant increase of functional integration properties in the mOFC and a significant decrease in the occipital pole: this suggests a diminished reactivity to bottom-up visual-sensory processes in favor of an increased reliance on top-down decision-making processes. These findings lay the groundwork for a better understanding and knowledge of the mechanisms by which rTMS may represent a promising complementary treatment for obesity.

4.4.3. Strengths and limitations

A major strength of this placebo-controlled longitudinal study consists in the fact that it represents the first attempt to investigate the neurofunctional changes associated with a deep rTMS treatment applied to obesity. The graph-theoretical approach employed in the current study, the Intrinsic Connectivity Contrast (ICC) measure (Martuzzi et al., 2011), is another strength of this work. In particular, the ICC is a voxel-wise data-driven approach that does not require *a priori* knowledge about: (i) the regions of interests to include in the analyses, and (ii) the statistical threshold to apply to determine the functional connections between the voxels (Martuzzi et al., 2011). The first point is particularly relevant when the brain region under investigation is highly heterogeneous, such as the insula and the PFC. For example, the anatomical brain templates commonly employed in graph-theoretical analyses of resting-state fMRI data, the AAL and Harvard-Oxford cortical probability maps implemented in the MRIcron software (Rorden and Brett, 2000), rely on gross anatomical subdivisions and consider the insular cortex as a single discrete brain region. However, there is compelling evidence that insular cortex activity and connectivity reflects a rostro-caudal gradient (Cauda

et al., 2011, Cauda et al., 2012), with anterior insula activity and connectivity being more tightly related with attentional processing, and posterior insula activity and connectivity to sensorimotor processing. As a consequence, by considering a single region of interest for the insular cortex, such a gradient cannot be appreciated. Conversely, the approach employed here allows to take into account the connectivity of every single voxel in the brain, without constraining the analysis to a particular region of interest but focusing on the changes in the global pattern of functional connectivity that occur in localized brain regions.

However, the present study has also some obvious limitations. First of all, the limited sample size makes it difficult to generalize current findings to the general population. Similarly, the mean age of the sample size (50 years) does not allow to extend the present findings to younger individuals, which may benefit of the rTMS treatment to a different extent. Finally, the limited sample size, together to the uneven distribution of the cue conditions in the sample, did not allow a proper statistical investigation of the effect of cue-exposure prior to rTMS. However, since the previous study did not report any significant difference between the cue and no-cue condition with respect to weight loss and food craving, it is unlikely that the current results are influenced by this factor.

Summary of Chapter 4

In this randomized, double-blind, placebo-controlled study I investigated the effects of deep rTMS on (i) body weight and BMI, (ii) food craving, and (iii) the functional brain organization. To this aim, seventeen obese participants were randomized and completed the 5-week neurostimulation intervention: nine were treated with the high-frequency stimulation (*real*TMS group), and eight were sham-treated (*sham*TMS group). Seven participants from the real group and eight from the sham group completed the follow-up visit at 1 month (FU1). Resting-state fMRI scans were acquired at baseline (T0) and after the 5-weeks intervention (T1). Body weight and food craving were measured at three time points (T0, T1, FU1).

A mixed-model analysis showed a significant group-by-time interaction for body weight (p=.04) and for BMI (p=.05), with a significant decrease of body weight (p<.001) and BMI (p<.001) in the realTMS stimulation group only up to FU1. Food craving showed a significant decrease over time (p<.001) in both groups. The resting-state functional connectivity (rsFC) fMRI data revealed a significant increase of degree centrality (index of whole-brain functional integration) for the realTMS group in the medial orbitofrontal cortex (mOFC), and a significant decrease in the occipital pole. Baseline rsFC between mOFC and the left insula was

significantly and negatively correlated with BMI changes at FU1 (Spearman's ϱ = - .54, p = .04, n = 15).

I propose that the decrease of whole-brain functional connections with the occipital pole, in the cue-reactivity network, together with an increase of whole-brain functional connections with the mOFC, in the cue-regulation network, may reflect a brain mechanism behind weight-loss through a diminished reactivity to bottom-up visual-sensory processes in favor of an increased reliance on top-down decision-making processes.

Chapter 5 – General Discussion

The drive for pleasure is "hard-wired" in our (neuro)biology. From the pleasure derived from food, water, sex and social interaction, that granted the survival of our species, to the enjoyment of beauty and discovery, which led to the realization of remarkable endeavors in arts and sciences, the relentless search for gratification *motivated* our evolution. Yet, there are situations in which these adaptive motivational processes have gone awry.

Obesity and Substance Use Disorder (SUD) can be considered as an example of this scenario, whereby highly reinforcing stimuli disrupt motivational processes, leading to maladaptive compulsive-like patterns of behavior. Paradoxically, greatly pleasurable stimuli such as high-calories palatable food, and drugs of abuse, can "hijack" the same neurocognitive machinery that evolved to grant our survival.

As I pointed out in Chapter 1, there are two main neural circuits that are involved in the processing food and drug-related cues: one underlies the sensory, hedonic, and motivational reactions to cues (cue-reactivity), while the other supports the regulation and valuation of such cues (cue-regulation) through higher-order attentional, decision-making, and inhibitory control processes (Figure 1.3). Dovetailing with Jasinska et al. (2014), I argued that activity within these networks can be modulated by several internal and external factors, and that these can interact meaningfully, giving rise to specific brain activation patterns. I also assumed that non-invasive brain stimulation techniques applied to obesity, with particular reference to high-frequency deep rTMS over the bilateral insular and prefrontal cortices, would be associated with plastic changes in key areas of the cue-reactivity and cue-regulation circuits.

In what follows, I will first incorporate my meta-analytical findings on food and drug cue-reactivity into the unitary model represented in Figure 1.4 (Chapter 1). Stemming from the simple and interactive effects observed in the meta-analytical clusters (Chapters 2 and 3), I will attempt to assign a "neurocognitive meaning" to different portions of the cue-reactivity and cue-regulation networks. Then, I will discuss the findings on the effect of deep rTMS (Chapter 4) in light of the main and interactive effects identified within the main circuits involved in food and drug cue-reactivity.

Finally, the implications of current findings for basic research and clinical practice, as well as a brief discussion of the outstanding issues on the matter, will be given.

5.1. A provisional unitary neurocognitive model of craving

As a first step for the discussion of a unitary framework for the factors that modulate the neural reactivity to cues, I summarized the findings of the meta-analyses on cue-reactivity in obesity

(Chapter 2) and in SUD (Chapter 3) in a single picture (Figure 5.1, please refer to the caption to interpret the figure).
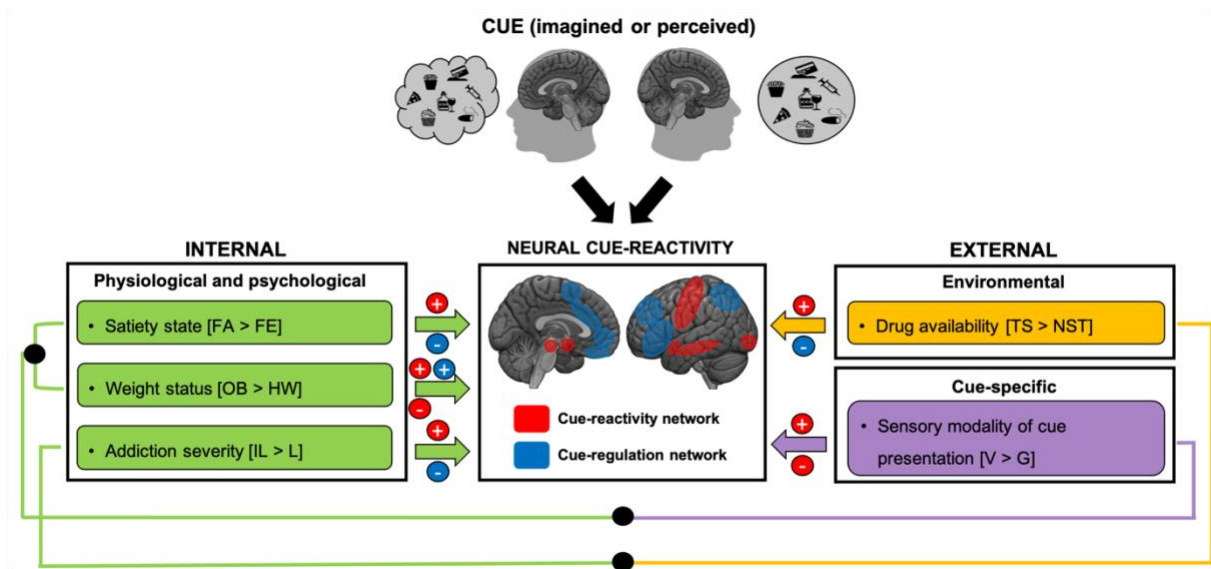
Figure 5.1. Summary of the meta-analytical results in light of a unitary model | Graphical representation of the effects of internal (satiety state, weight status, addiction severity) and external factors (drug availability, sensory modality of cue presentation) on the neural responses to drug cues in the cue-reactivity and cue-regulation network. The contrast observed in the meta-analysis (main effect) is reported within square brackets: "+" and "-" refer to the direction of the effect (e.g., "+" = FA > FE; "-", FE > FA) on the cue-reactivity (red circles) and cue-regulation (blue circles) network. Interacting factors are represented by colored lines linked by black circles. FA, fasting; FE, fed; G, gustatory; HW, healthy weight; IL, illegal; L, legal; NST, not-seeking treatment; OB, obese; TS, treatment-seeking; V, visual.

At the network level, I found that all the factors under examination, except for the sensory modality of cue presentation, can modulate the neural responses to cues in the cue-reactivity and cue-regulation network; more importantly, I observed significant interactions between internal and external factors in key nodes of the cue-reactivity (ventral and dorsal striatum, thalamus) and cue-regulation circuits (mOFC, ACC).

Taken together, the present findings suggest two main general conclusions. First, in agreement with previous reviews (Dagher, 2012, Garrison and Potenza, 2014, Giuliani et al., 2018) and meta-analyses (Chase et al., 2011, Kühn and Gallinat, 2011, van der Laan et al., 2011, Engelmann et al., 2012, Brooks et al., 2013, Schacht et al., 2013, Huerta et al., 2014, Kennedy and Dimitropoulos, 2014, Pursey et al., 2014, van Meer et al., 2015), the present findings confirm the existence of a distributed network of brain regions involved in the sensory, hedonic, and motivational reactions to cues, as well as in higher-order attentional, decision-making, and inhibitory control processes, involved in cue-reactivity. Second, they confirm and expand

Jasinska's claim that "[…] these factors are likely to have both main and interactive effects" (Jasinska et al., 2014, p. 18), suggesting that is also the case for food cue-reactivity in obesity. The evidence that internal and external factors can interact and modulate the neural response to reward-related cues is not only relevant from a purely theoretical perspective, but it can also tell us something about the functional role of specific brain areas in the experience of craving. The key points for the cue-reactivity and cue-regulation networks are summarized below.

5.1.1. Modulations within the cue-reactivity network

5.1.1.1. VTA, ventral striatum, amygdala

The VTA, the NAc and the amygdala are crucial structures for the expression of cue-elicited reward-seeking behaviors and of incentive motivational processes (Everitt et al., 1999, Warlow et al., 2017). In humans, activity of these regions in response to food and drug cues is associated with the BMI (Rothemund et al., 2007, Martens et al., 2013), with measures of addiction severity (McClernon et al., 2008, Claus et al., 2011), and with clinical outcomes (Grüsser et al., 2004, Murdaugh et al., 2012, Yokum et al., 2014), suggesting that neural cue-reactivity within these regions may be reliable a biomarker of the severity of the condition.

I provided evidence that obesity and SUD are both characterized by enhanced neural responses to cues in key areas of the cue-reactivity network, including the VTA, ventral striatum, and amygdala, involved in incentive motivational processes, with some key differences.

First, compared to obesity, SUD patients addicted to illegal substances show a wider recruitment of the mesocorticolimbic pathway, including the midbrain (VTA/SN), the amygdala and the hippocampus, in addition to the ventral striatum, in response to cues. The greater involvement of brain areas involved in key aspects of reward and motivation in illegal substance abusers may prove in favor of the notion that severe conditions are associated with a deeper sensitization of the mesocorticolimbic circuitry, in line with the incentive sensitization theory of addiction (Robinson and Berridge, 1993, Berridge et al., 2010). If one accepts this, the arguments in favor of obesity as a very case of "addiction to food" (Davis et al., 2004, Ziauddeen et al., 2012, Ziauddeen and Fletcher, 2013, Fletcher and Kenny, 2018) provided by the available neuroimaging evidence are very weak.

Second, whereas obesity seems to be associated with a *down-regulation* of the activity of the dopaminergic nuclei of the midbrain (VTA/SN), consistent with a reward deficit hypothesis (Wang et al., 2001, Wang et al., 2002), severe addiction to substances of abuse is linked to *up-regulated* activity of the VTA/SN, which results in heightened cue-induced activity. This

evidence echoes the results of previous animal studies showing that exposure to cafeteria diet food induces a down-regulation of ventral tegmental activity, particularly in specific DA and GABAergic populations of neurons (Koyama et al., 2013, Cook et al., 2017), and that different drugs of abuse induce neuroadaptations at the level of excitatory inputs to the VTA, reflected by an up-regulation of glutamate receptors (Self, 2004), suggesting that the different neurochemical adaptations at the level of the VTA may occur in obesity and SUD.

Third, in obesity the sensory modality of cue presentation and the satiety state interact with the weight status, suggesting two potential neurocognitive mechanisms behind overeating: increased reward system activity in response to gustatory taste cues (ventral striatum), and persistent reward system activity in response to anticipatory visual food cues (NAc), confirming and expanding the results of previous meta-analyses on the topic (Brooks et al., 2013, Pursey et al., 2014).

5.1.1.2. Insula

In contrast with prior evidence for the involvement of the insula in drug craving (Naqvi et al., 2007, Naqvi and Bechara, 2009), no convergent activity in this region was found in the meta-analysis on drug cue-reactivity. Admittedly, the lack of convergent brain activity in response to drug cues may be a by-product of the fact that I considered different legal (nicotine, alcohol) and illegal (cocaine, heroin) substances together, making it difficult to detect insular responses that are specific for a given population of SUD patients. Accordingly, convergent activity of the insular cortex in response to drug cues was reported only in meta-analysis that considered a single population of SUD patients (Kühn and Gallinat, 2011, Engelmann et al., 2012, Schacht et al., 2013), whereas no such finding was observed when different populations of SUD patients are considered together (Chase et al., 2011, Kühn and Gallinat, 2011). As argued by Chase and colleagues, the size and heterogeneity of the insular cortex, together with a specialization of function in different portions of the insula, might reduce the possibility of reporting a localized statistical convergence (Chase et al., 2011)

Partially in line with this observation, I found that discrete portions of the insular cortex are associated with different processes in obesity. In particular, I found that the ventral anterior portion of the insula is specific for the visual-anticipatory stimulation (and with obese participants), probably linked to enhanced salience processing, whereas the mid-posterior portion of the insula is associated with the physiological state of hunger, regardless of weight-status and sensory modality of cue presentation. This pattern of results is consistent with recent neurocognitive models of the functions of the insular cortex suggesting a rostral-caudal

functional gradient: the most anterior part would be involved in salience detection and attentional control, and the most posterior part would be associated with the integration of cognitive, homeostatic, and interoceptive processing (Cauda et al., 2011, Cauda et al., 2012).

In sum, the overall findings on the key nodes of the cue-reactivity circuit suggest that: (i) the VTA, ventral striatum, and amygdala are the core structures underlying aberrant incentive motivational processing in obesity and SUD; (ii) the anterior insula is involved in visual salience processing of food cues only; (iii) the posterior insula is involved in sensory-interoceptive processing.

5.1.2. Modulations within the cue-regulation network

5.1.2.1. Dorsomedial and lateral PFC

I found a widespread involvement of the dorsomedial (medial SFG) and lateral subdivisions (lateral SFG, lateral OFC) of the PFC during the state of satiety in the meta-analysis on food cue-reactivity, consistent with the role of the PFC in meal termination and, ultimately, cognitive control (Tataranni et al., 1999, Del Parigi et al., 2002). As already pointed out in the discussion of Chapter 2, I could not find evidence of reduced PFC activity in response to food cues in obese individuals: conversely, I found that a satiety-specific cluster localized in the right SFG that was also associated with obese individuals, consistent with the hypothesis that obese individuals, in the attempt to suppress striatal and limbic hyperactivations, recruit greater cognitive control processes (Gautier et al., 2000, Gautier et al., 2001). Admittedly, the lack of support for an Inhibitory Control Deficit Theory of obesity may be due to the fact that mere exposure to anticipatory food cues might not be sufficient to detect a deficient activity in inhibitory control regions: these are more likely to be engaged during active cognitive control paradigm, or during the active suppression of craving (e.g., during explicit cognitive regulation).

In the drug cue-reactivity meta-analysis, I found that a dorsomedial portion of the ACC (dACC) is more frequently activated by individuals addicted to legal substances *and* by not-seeking treatment individuals. The ACC and medial PFC, particularly their dorsal subdivisions, have been implicated in attentional control (Liu et al., 2004), cognitive reappraisal and cognitive modulation of emotions (Ochsner et al., 2004, Kalisch et al., 2006). Interestingly, the coordinates of the dACC cluster (MNI coordinates: X = 0 ± 2.3, Y = 29 ± 4.2, Z = 22 ± 6.1) observed in Chapter 3 match very closely those of a dACC cluster reported in a meta-analysis

of neuroimaging studies on craving-related nicotine cue-reactivity (MNI coordinates: X = -2, Y = 28, Z = 23) (Kühn and Gallinat, 2011). The authors proposed that dACC activity in response to cigarette cues may underlie the process of directing the attention away from the stimulus, in an effort to revert the automatic pattern of attention towards drug-related cues; further, they suggested dACC activity is associated with self-reported nicotine craving because it reflects an attempt to suppress the urge to consume a drug that it is clearly impossible to consume in the scanner environment (Kühn and Gallinat, 2011). My results are partially in line with this interpretation, as the dACC was specific for not-seeking treatment individuals, who expect to smoke soon and, as such, their urge to smoke during cue-reactivity should be higher compared to those who do not expect to smoke soon (Carter and Tiffany, 2001). Conversely, patients addicted to illegal substances, that induce a more severe dependence and neural sensitization, may lack this capability: as a consequence, their dACC may fail to down-regulate mesolimbic reactivity to drug cues.

5.1.2.2. Ventromedial PFC

Whereas the abovementioned results support the view that more superior and lateral subdivisions of the cue-regulation network are involved in "top-down" attentional and cognitive control processes, the interaction effects observed in the drug cue-reactivity meta-analysis suggest that the ventromedial portion of the PFC, comprising the perigenual ACC (pgACC) and the medial OFC (or ventromedial PFC, vmPFC) is implicated in decision-making and reward-evaluation processes. In line with the role of the vmPFC in delay-discounting and decision-making (Bechara et al., 2000, Carter et al., 2010, Rolls et al., 2010, Wesley and Bickel, 2014), I suggested that this region plays a crucial role in forming an expectation about the delay of reward consumption, particularly when internal (motivation to quit) and external factors (drug availability) conflict.

In SUD, this is the case of treatment-seeking individuals addicted to legal substances (they are motivated to quit, yet the substance is widely available) and not-seeking treatment individuals addicted to illegal substances (they are not motivated to quit, but the substance is costly and less widely available). A similar situation of conflict can be modeled in a food cue-reactivity paradigm, by adopting a 2 (food vs. control cue)-by-2 (treatment-seeking vs not-seeking treatment)-by-2 (food available vs. not available after the experiment) factorial design: in such a scenario (i) obese patients who try to stick on a diet and that will have access to palatable food after the experiment, and (ii) those who are unwilling to lose weight but will have no access to the food after cue-exposure, should display greater vmPFC – and pgACC – activity compared

to the other two conditions. Interestingly, preliminary results in healthy weight participants suggest that the mOFC – together with a wider network of striatal, prefrontal, and occipito-temporal regions – is more active when the foods observed during cue-reactivity are available, indicating that the mOFC mediates at least some aspects of availability and expectancy for primary rewards such as food (Blechert et al., 2016).

To summarize, the overall results on the cue-regulation network suggest that: (i) the dorsomedial and lateral subdivisions of the PFC, including the medial SFG, the lateral SFG and OFC, are implicated in satiety-related cognitive control processes; (ii) the dACC is associated with attentional control, particularly in not-seeking treatment individuals addicted to legal substances; (iii) the vmPFC, comprising the pgACC, is implicated in higher-order decision-making and reward-evaluation processes, particularly when internal and external contingencies make it difficult to form an expectation about the potential delay of reward consumption.

5.2. Neurofunctional overlap between brain regions involved in food and drug cue-reactivity and neural circuits influenced by rTMS

To complement the discussion of the main circuits involved in food and drug cue-reactivity, I searched for the neurofunctional maps between the rsFC maps identified in Chapter 4 and the clusters discussed above, identified in Chapters 2 and 3 (Figure 5.2.)
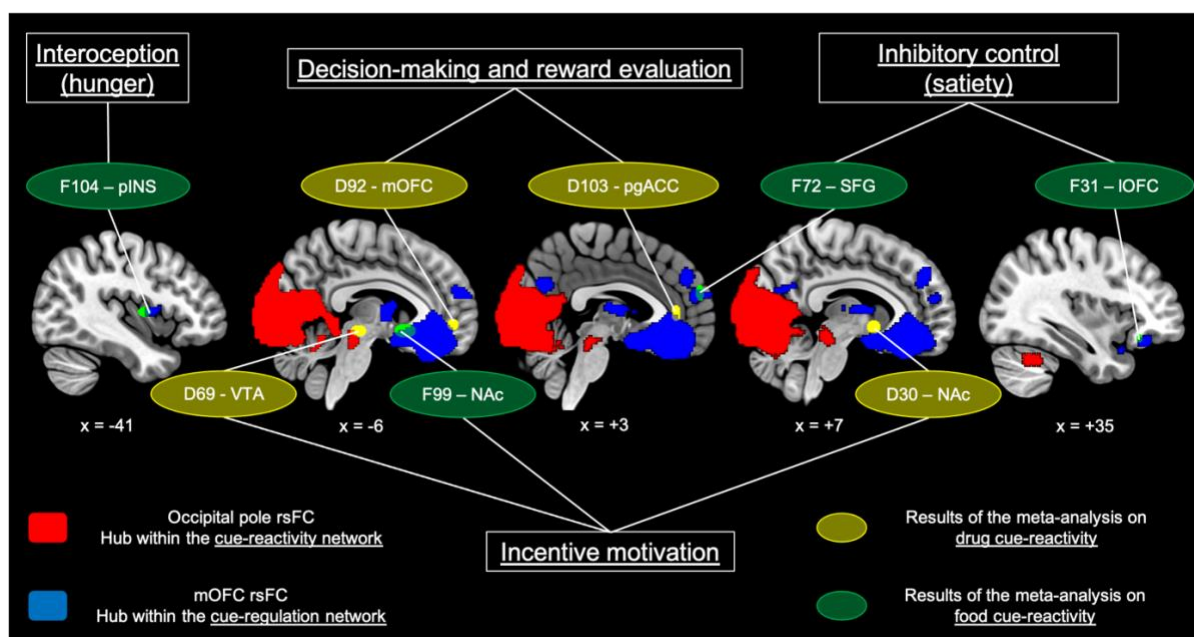
Figure 5.2. Neuroanatomical overlap between rsFC maps and the results of the meta-analyses | The ID of the clusters is preceded by an F (food cue-reactivity) or D (drug cue-reactivity). Brain slices reported in MNI stereotaxic space.

Whereas the resting-state FC map of the occipital pole overlapped only with the VTA cluster identified in the meta-analysis on substance use disorder, the rsFC map of the mOFC overlapped with a number of clusters involved in incentive motivation (NAc), interoception and hunger (posterior insula), inhibitory control and satiety (SFG, lOFC), decision-making and reward evaluation (mOFC, pgACC). This pattern of overlap dovetails with the notion that the medial orbitofrontal cortex integrates different types of information, from interoceptive and motivational signals to higher-order cognitive control processes, to produce coherent goal-directed behaviors (Rolls, 2008, Rolls, 2015).

In particular, the rsFC map of the mOFC overlaps with discrete portions of the insula and of the PFC involved in hunger and satiety, respectively[19]; further, it is functional connected with the ventral striatum, including the NAc, which also showed an influence of satiety in the meta-analysis of food cue-reactivity (Chapter 2). As a consequence, it is reasonable to hypothesize that the mOFC circuit participates in appetitive behavior by integrating satiety-related and reward-value information to produce the behavior accordingly. There is evidence that the functional connectivity of the OFC is modulated by peripheral signals of satiety, such as insulin (Kullmann et al., 2012), that can pass through the blood brain barrier and whose receptors are expressed throughout the brain (Unger et al., 1991). It is therefore possible that another way through which the mOFC circuit participates in appetitive behavior is the integration of hormonal signals that provide and updated information about the homeostatic state of the organism.

If anything, this supplemental analysis corroborates and expands the results of the semantic association performed with Neurosynth for the rsFC map, revealing a brain circuit involved in different sensory, affective, and cognitive processes that are relevant to food reward-processing.

5.3. Implications for basic research and translational medicine

An overarching goal of the present thesis was to provide a unitary neurocognitive framework for the study of craving, and of the pathological motivation in general. I have shown that the model proposed by Jasinska and colleagues (2014) for the study of drug cue-reactivity in SUD can be translated to the domain of food cue-reactivity in obesity. Further, I have demonstrated

---

[19] It is worthy to note that CluB, compared to other meta-analytic techniques like GingerALE, returns discrete ellipsoidal clusters based on a predefined user's criterion (5 mm-radius clusters in Chapters 2 and 3). With this approach, I obtained relatively small clusters that can better accommodate the functional specialization that occurs within a single brain region (see clusters F31, F72, F104 in Figure 5.2).

that different internal and external factors modulate the neural reactivity to food and drug cues, both in isolation and in interaction, in specific portions within two main circuits involved in cue-reactivity: the cue-reactivity and the cue-regulation network. By means of a new method for coordinate-based meta-analyses, CluB (Berlingeri et al., 2019, Appendix A), I was able to identify discrete portions of the brain that are sensitive to specific internal or/and external contingencies, providing new insights into the neurocognitive processes underlying food and drug-cue reactivity. Finally, I have provided preliminary evidence that high-frequency deep rTMS over the bilateral insula and PFC, when accompanied by a hypocaloric diet, may be a promising treatment option for obesity, probably due to the changes in the functional integration properties induced to brain regions that participate in cue-reactivity.

I believe that the present findings have several implications for basic research and translational medicine. The main points, and the associated outstanding issues, are described below:

–　　Given the evidence that several internal and external factors have on the neural responses to cues, future cue-reactivity studies should acknowledge these effects either by controlling for unwanted variables, or by modelling the experiment according to a factorial design that can account for such main and interactive effects;

–　　The CluB toolbox is a freely available software can be used to test this kind of factorial designs at the meta-analytical scale;

–　　Future studies will also contribute to identify other internal and external factors that contribute to the modulation of the neural cue-reactivity, and that can be easily incorporated in the model; for example, it may be interesting to study how the level of food transformation modulates the neural responses to food cues in lean versus obese individuals;

–　　The neurocognitive framework introduced in the present thesis can be also employed to generate new hypotheses about the main and interactive effects of a given factor, in different populations; for example, it may be interesting to investigate to what extent food availability modulates the neural response to food cues in obesity, and whether shared or different neural substrates underlie reward expectancy for primary versus secondary rewards;

–　　This model can be expanded by including different disorders of the motivation, such as gambling disorder, internet gaming disorder, and internet pornography addiction; for instance, it would be interesting to investigate how abstinence modulates the neural response to cues in gambling disorders versus addiction, to identify common and distinct neurocognitive processes;

– Similarly, brain reactions to food cues occurring in other clinical populations, such as anorexia nervosa, bulimia nervosa, and Prader-Willi's syndrome can also be interpreted in light of this unitary model; for example, brain reactions to food cues in obesity and anorexia nervosa may be characterized by population-specific effects that emerge only when one or more internal and external factors (e.g., satiety state, sensory-modality of cue-presentation) are taken into account;

– Some of the effects observed here, particularly those pertaining the interactions, point to complex neurocognitive mechanisms underlying obesity (e.g., persistent motivational responses to food cues while satiated) and substance use disorder (e.g., interaction between treatment status and type of substance) that are worth of further investigation; in particular, future studies should qualify these effects with respect to their association with clinical variables and treatment outcomes;

– The evidence that severe cases of addiction are characterized by increased activity of the mesolimbic system in response to drug cues corroborates the notion that mesolimbic responses to drug cues may be a reliable neurofunctional marker of addiction severity;

– My results provide also a pool of brain regions that may be used during real-time neurofeedback, to train the patient to regulate the brain activity of a given region of interest; for example, it may be possible to train obese patients to down-regulate ventral striatal activity in response to food cues when satiated;

– The design of cognitive-behavioral interventions may also benefit from the present findings, particularly if the intervention includes the empowerment of cognitive and emotional regulation in response to cues; for instance, a cognitive-behavioral treatment aimed at reducing food cravings through cognitive reappraisal strategies may be performed under specific circumstances (e.g., in a fasting state) and with a particular cue (e.g., a gustatory cue, a sip of a sweetened drink);

– High-frequency deep rTMS over the bilateral insula and PFC is a promising intervention tool for obesity, and it is associated with changes in the brain functional organization of the mOFC and of the occipital pole; though preliminary, these findings may be sufficient to motivate the replication of the study with larger samples, and with different population of patients (e.g., in gambling disorder).

The present findings have also some societal implications.

Trivially, the evidence that obesity and SUD share some neural vulnerabilities, like the heightened mesolimbic activity in response to reward-associated cues, is a cogent argument in favor the recognition of some phenotypes of obesity as mental disorders (Volkow and O'Brien, 2007); this, in turn, is likely to prompt a change not only in the societal representations of obesity, but also in the way the healthcare system takes charge of obese patients. Again, I am not arguing for viewing obesity as a case of addiction to high-calories, palatable food; yet, I am suggesting that the two conditions share some intriguing similarities that are worth of further investigation.

Lastly, the fact that the perceived availability of a given reward can affect our neural reactions to reward-related stimuli, influencing our behavior, should motivate a discussion on how the exposure to such stimuli might be regulated. This issue is particularly relevant for the "substances" - including highly palatable caloric-dense food and alcohol - that are widely available in our modern environment and that, at least in Western countries, are heavily advertised through the media. As far as I was able to document, "non-core" food products (high in undesirable nutrients or energy, often with a high level of food transformation) account for the 53% to 87% of the total food TV advertisements in Western countries, particularly during children's peak viewing times (Kelly et al., 2010).

Something that clashes with the overall evidence discussed in the present work.

Appendix A – Clustering the Brain With "CluB": A New Toolbox for Quantitative Meta-Analysis of Neuroimaging Data

A1. Introduction

As the number of neuroimaging studies published spreads, the development of reliable methods that allow to identify the most convergent results across a given literature becomes increasingly vital.

A simple approach to summarize the results of a group of independent neuroimaging studies implies reporting the significant peaks of activation in a single table (e.g., (Wilson et al., 2004)), or in a summary picture (e.g., (Demonet et al., 1996)). Typically, neuroimaging papers report the significant peaks of activation, expressed as triplets of x, y, and z coordinates, in a stereotaxic space (Montreal Neurological Institute or MNI, or Talairach); these peaks, or foci, are the result of one or more statistical contrasts between different conditions (e.g., exposure to food pictures vs. cars pictures), and/or between different groups of subjects (e.g., healthy weight vs. obese individuals). Merging these activation foci in a single table would allow one to evaluate the between-study concordance, by exploring the spatial proximity between the reported coordinates and/or anatomical brain labels with respect to a given task or population of patients; however, this procedure is completely subjective, as it is the scientist that decides whether a group of activation foci are close enough to each other to be deemed as convergent, or not. Since studies employing this approach do not use any data-driven statistical method, they are usually considered as "narrative" or "illustrative reviews".

By contrast, proper meta-analyses are characterized by the use of objective statistical methods to combine the results of different independent studies, and thus permit to generate data-driven inferences about the convergence of a set of studies. Quantitative meta-analytical approaches can be categorized into two broad categories: image-based meta-analyses (IBMA), or coordinate-based meta-analyses (CBMA). IBMA rely on the original neuroimaging datasets to combine the whole-brain statistical volumes across several studies; however, since sharing databases of raw neuroimaging data is far from being the norm, the authors rarely have the original data available to them. Conversely, CBMA rely on a summary of the whole-brain statistical volumes typically originated by a neuroimaging experiment: a list of triplets of coordinates indicating the local maxima of activation (see (Salimi-Khorshidi et al., 2009) for a formal comparison between the two approaches). As already pointed out in Chapter 1, several methods for CBMA exist, including hierarchical clustering (Jobard et al., 2003), kernel density analysis (Wager & Smith, 2003), and signed differential mapping (Radua & Mataix-Cols,

2009); however, the Activation Likelihood Estimation (ALE) method is probably the most widely popular approach (Eickhoff et al., 2012; Eickhoff et al., 2009; Turkeltaub et al., 2012), even if it can only handle simple designs (e.g., two-level factors, experimental group vs. control group). Another computerized method that has been adopted to pool together the fMRI data available in the literature is hierarchical clustering (Goutte et al., 2001): even though it is less widely used compared to other methods (see below) it has been the basis of some with well-cited papers (e.g., (Jobard et al., 2003, Salvador et al., 2005, Shehzad et al., 2009, Liakakis et al., 2011)

Recently, our group proposed a revival of the hierarchical clustering approach to neuroimaging data, developing a software for CBMA (Clustering the Brain, CluB; (Berlingeri et al., 2019)), based on a novel hierarchical clustering algorithm (Cattinelli et al., 2013b), which can also handle complex factorial designs (e.g., three-level factors, two-by-two, and two-by-two factorial designs). An in-depth description of the software, and of the computational details, can be found in the original publications (Cattinelli et al., 2013b, Berlingeri et al., 2019).

Indeed, the scope of this Appendix is to give an overview of the method that I have employed for the studies described in Chapters 2 and 3, and that represents an established method for our group (Cattinelli et al., 2013a, Crepaldi et al., 2013, Paulesu et al., 2014, Zapparoli et al., 2017, Devoto et al., 2018, Seghezzi et al., 2019a, Seghezzi et al., 2019b; Devoto et al., *under second review*[4]; Devoto et al., *under review*[20]). In what follows, I will provide a brief description of the key "modules" of CluB: the Hierarchical Clustering Analysis (HCA) and Cluster Composition Analysis (CCA) module[21]; then, I will provide the rationale for two validation studies aimed at assessing the realibility of the HC and CCA procedures, by comparing their performance with the GingerALE approach.

A1.1. Hierarchical Clustering Analysis

The basic notion underlying the application of hierarchical clustering to neuroimaging datasets is that several elements (e.g., local maxima of activation from different studies) can be grouped

---

[20] Devoto F., Carioti D., Danelli L., and Berlingeri M. "A meta-analysis of functional neuroimaging studies on developmental dyslexia across European orthographies: the ADC model".

[21] CluB is also equipped with two additional modules: the Spatial Transformation module, which allows to transform coordinated from one stereotaxic system of coordinated to the other (MNI-Talairach and Talairach-MNI transformations), and the Peaks Segregation tool, which allows to perform meta-analyses according with a region-of-interest approach, by selecting a user-defined group of brain regions of the Automatic Anatomical Labelling template labels (**Rorden C and Brett M** (2000) Stereotaxic display of brain lesions. *Behav Neurol,* **12,** 191-200.).

into clusters, according to a given dissimilarity measure (e.g., Euclidean distance). At the begininning of the procedure, each single element represents one cluster; then, according to a dissimilarity measure, two clusters are merged, and the procedure is iterated until a single cluster that contains all the initial elements is obtained. The hierarchy of nested solutions that is obtained through this procedure can be represented by a dendrogram. The final pool of clusters, the clustering solution, is obtained by "cutting" the dendrogram at a certain level according to what has been called "the user's spatial criterion": in other words, the user decides the amount of global variability that is acceptable for the specific scientific issue of interest. Crucially, this procedure is often associated with a serious bias: the final clustering solution may depend on the order of the input data (van der Kloot et al., 2005), particularly when the data to be clustered are represented by integer values, as in the case of stereotactic coordinates used in neuroimaging (the problem of "non-uniqueness" of the clustering solution).

The Hierarchical Clustering Analysis (HCA) module implements a novel unique-solution clustering algorithm (Cattinelli et al., 2013b): in brief, after the Euclidean distance between each pair of the input foci is computed, activation peaks with the minimal distance are recursively merged into clusters by using Ward's criterion (Ward, 1963), which minimises the total intra-cluster variance after each merging step. This procedure leads to a tree-like structure called dendrogram: in a "bottom-up" clustering algorithm as the one by Cattinelli et al. (2013), the leaves of the dendrogram represent clusters composed of a single activation peak, while the top represents one large cluster made up of all the activation foci submitted to the procedure (Figure A1.1): the dendrogram is then "cut" according to the user's spatial criterion, that is the average standard deviation of the distance in the x, y and z directions from the centroid of each cluster, expressed as millimeters (red dotted line in Figure A1.1).
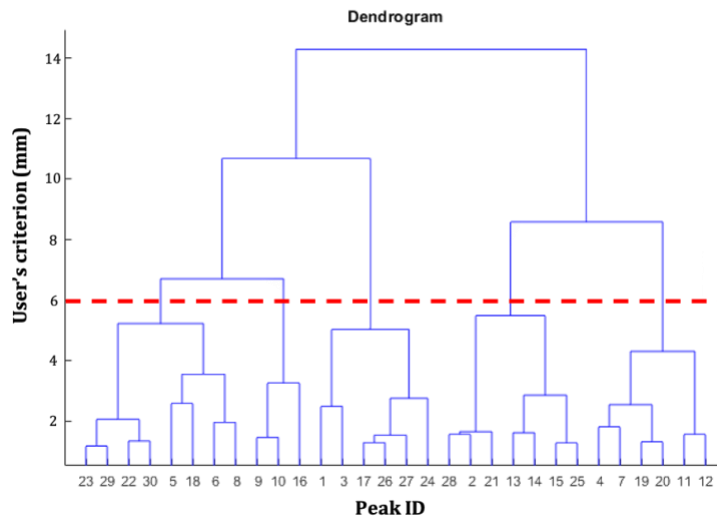
Figure A1.1 | Example of a hierarchical clustering dendrogram. The initial dataset of peaks is represented on the x-axis. On the y-axis are represented the spatial thresholds that can be selected by the users to let the clustering solution emerge. For example, the red dotted line shows the clustering solution for a user's spatial criterion = 6 mm. Adapted from: Berlingeri et al., 2019.

The HCA module produces two maps of clusters and two spreadsheet files. In particular, the "cardinality map" includes all the clusters returned by the HC procedure and contains, for each cluster, the information about its numerosity (i.e., number of ariginal peks of activation that it contains) (Figure A1.2A); conversely, the "density map" represents the spatial density of each cluster returned by the HCA (Figure A1.2B). The images in the ANALYZE formats are accompanied by two spreadsheet files: the "cluster-mapping" file, which includes the x, y, z of the centroid, the standard deviation along the three axes, the cardinality, and the anatomical label of each cluster (Figure A1.2C); the "peaks-clustering" file, including all the activation peaks reported in the input file, the cluster ID of each peak, and the factors that characterize each activation peak (please refer to the methods section for further details about foci classification) (Figure A1.2D).

The information produced by the HCA procedure above is then fed into the CCA module, which allows to give a "functional meaning" to each cluster by performing statistical tests on their peak composition.
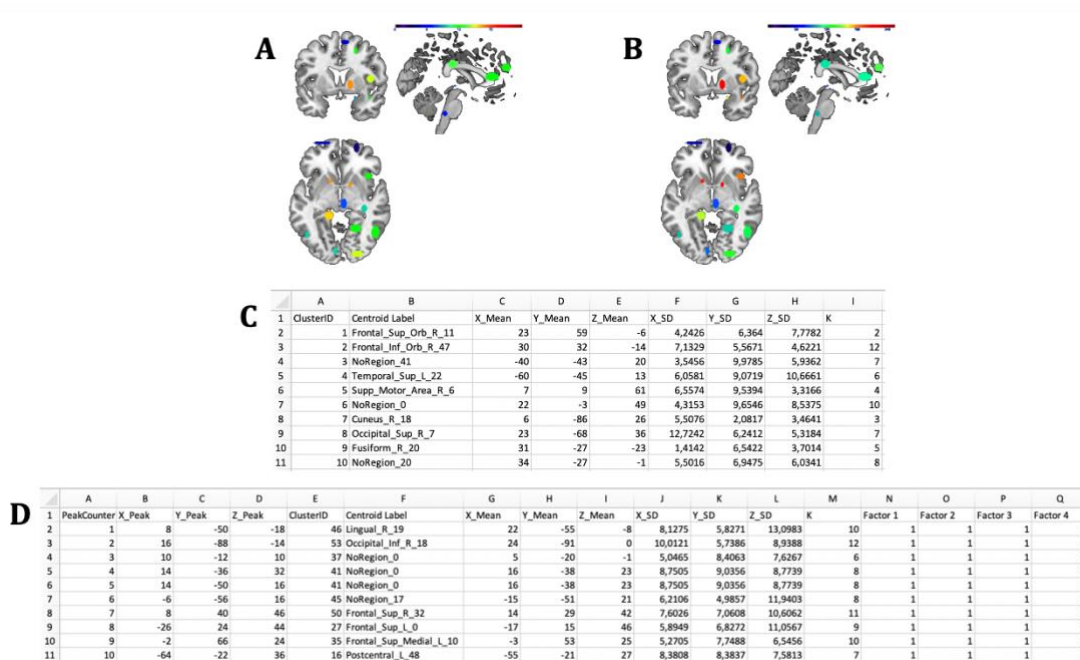
Figure A1.2 | Output files of the HCA module. A. "Cardinality" map representing the number of peaks included in each cluster. **B.** "Density" map representing the ratio of the cardinality and the spatial extent of the cluster. **C.** "Cluster-mapping" spreadsheet file in which the anatomical and spatial information about the clusters is stored. **D.** "Peaks-clustering" spreadsheet file in which each peak is associated with its cluster. Adapted from: Berlingeri et al., 2019.

A1.2. Cluster Composition Analysis (CCA)

The Cluster Composition Analysis (CCA) module is the most innovative feature of CluB: it allows to perform both asymptotic and exact tests on the composition of the clusters, in order to give them a "functional meaning". With CluB it is possible to perform categorical data analysis on the composition of each cluster, allowing the implementation of different designs involving one or more factors. In particular, CluB allows to perform a series of statistical tests that accommodate a diverse range of factorial designs. An important aspect left to the user's choice is the setting of the Prior-Likelihood (PL) to perform categorical analyses in a bayesian context. A brief description of the statistical tests implemented in the CluB toolbox is given below.

The binomial test would be the test of choice when one wants to evaluate the association of a cluster with one level of a two-levels factor: for example, the comparison of lean and obese individuals. The software computes a binomial test within each cluster, returning a matrix with as many rows as the number of clusters. For each cluster the cluster ID, the factor of interest, the category of the successful events (i.e., the level of the factor of interest), the number of

observed successes, the cardinality, and the p-value of the binomial test are displayed. The chosen null and alternative hypotheses are also printed (Figure A1.3A). To make a practical example, let's consider a dataset of 650 activation foci, 377 of which belong to lean individuals, and the remaining 273 to obese individuals (one factor = group). The HCA returns a cluster X with a cardinality of N = 20, which includes 15 foci associated with the level "lean" of the factor "group". CluB computes the within-cluster proportion 15/20 (i.e., 0.75), and compares it with one of two different proportions (p) according to the user's choice: (i) p = .50, or (ii) p = PL, that is the proportion of the theoretical distribution computed over the entire dataset (e.g., PLlean = 377/650 = .58). The PL represents the probability of success under the null hypothesis that the distribution of lean-related peaks within a given cluster reflects the overall distribution of lean-related peaks across the entire dataset; hence, a significant (p < .05) binomial test indicates that the proportion of activation peak included in that specific part of the brain is higher than the proportion computed all over the brain. A similar principle is applied to the statistical tests described below.

Conversely, the multinomial test would be the test of choice when one wants to test the association of a cluster with one level of a multi-level factor, for example, the comparison of three tasks within the same group, or the comparison of three groups. CluB returns a matrix with as many rows as the number of clusters. For each cluster, the software gives back the cluster ID, the factor of interest, the distribution of the observed frequencies (i.e., the number of peaks within level 1, level 2, and so on), the cardinality, the p-value. In the last n columns (depending on the number of levels of the factor), the PL of each level is reported, as well as the observed probability for each cluster (i.e., the proportion of foci for each level with respect to the cardinality of the cluster) (Figure A1.3B). This information is needed to infer which of the n levels significantly exceeds the PL. On the top row, the selected H0 (e.g., p = total input foci / number or levels or p = PL) and the selected type of multinomial test are reported.
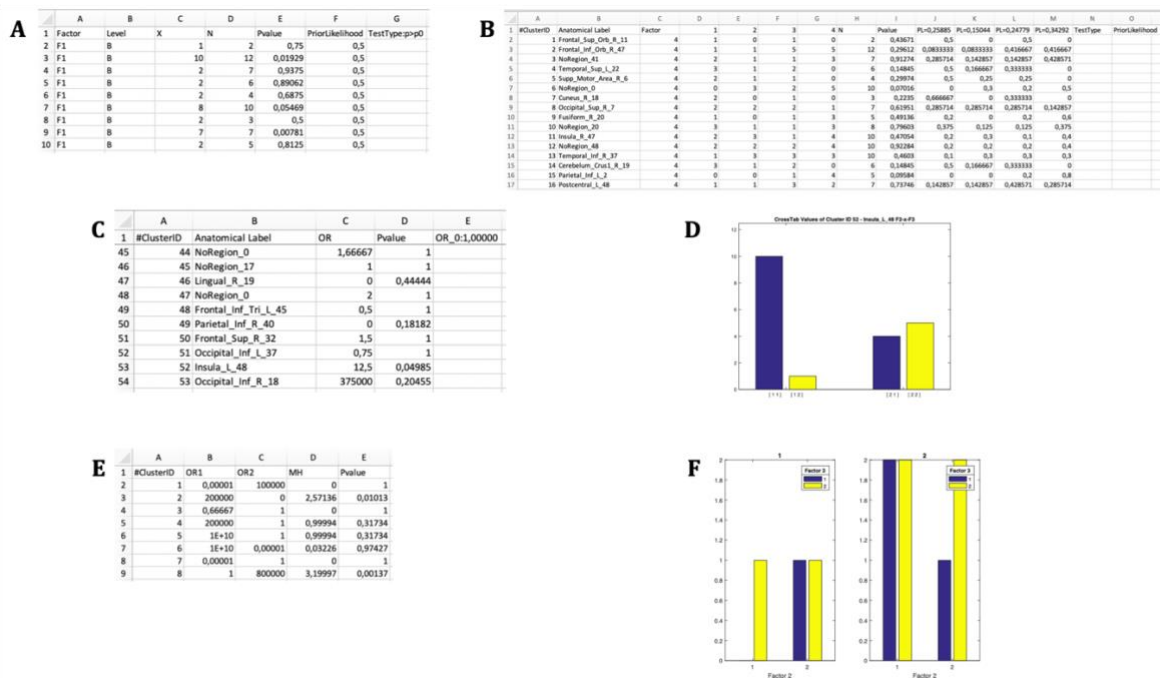
Figure A1.**3 | Output files of the CCA module. A.** Output file for a "binomial test" on the Level B of Factor F1. **B.** Output .xls file for a "multinomial test" on Factor F4. **C.** Output . file for a "Fisher's test" for 2 x 2 interactions between two factors: Factor F2 and F3. **D.** Bar plot generated by the "Fisher's test". **E.** Output file for a "Mantel-Haenszel test" for 2 x 2 x 2 interactions across three factors: Factor F1, F2 and F3. **F.** Bar plot generated by the "Mantel-Haenszel test".

CluB also allows to test more complex factorial designs, such as 2-by-2 and, recently, 2-by-2-by-2 designs, thus permitting a stastical evaluation of two and three-way interaction effects. In particular, the Fisher's exact test (Fisher, 1970) would be the test of choice, for example, when one wants to test the hypothesis that two groups of subjects (lean vs. obese) differ in a given cluster specifically for one of two tasks (visual food cues vs. taste food cues), according to a 2-by-2 factorial design. Again, different types of null hypothesis are considered: (1) the hypothesis of independence is H0: OR = 1; (2) the PL hypothesis is H0: OR = OR$_{dataset}$ (i.e., the OR computed in the whole dataset before clustering the data). The alternative hypothesis is H1 : OR ≠ OR$_0$. CluB returns a matrix with as many rows as the number of clusters. For each cluster, the software returns the cluster ID, the observed odds ratio and the p-value. The selected null hypothesis is also printed (Figure A1.3C). A bar-plot representing the observed distribution of each cluster is also printed (Figure A1.3D).

Finally, the Mantel-Haenszel test (MANTEL and HAENSZEL, 1959) can be applied to explore $2 \times 2 \times 2$ interactions by identifying the factor that, according to the specific users' hypotheses, can be considered the moderator. This test would allow one, for example, to the hypothesis that anatomofunctional convergence between two groups (e.g., lean vs. obese subjects) differ across

two different sensory modalities of cue-presentation (e.g., visual vs. taste), providing that cues are delivered during one of two physiological states (e.g., hungry vs. satiated). Similarly to the previous tests, the program computes a Mantel-Haenszel test for each cluster, returning the ID of the cluster, the OR for each of the two levels of the moderator, the statistic, and the p-value (Figure A1.3E). A bar-plot representing the observed distribution of each cluster is also printed: the joint bar-plot is split according with the factor chosen to stratify the analysis (Figure A1.3F).

To summarize, the HCA and CCA are the core modules of CluB. The HCA performs a hierarchical clustering on the input data, by means of a novel clustering algorithm that overcomes the problem of non-uniqueness of the clustering solution (Cattinelli et al., 2013b), returning a set of clusters according to a specific user's criterion (i.e., average standard deviation of the distance in the x, y and z directions from the centroid of the clusters, expressed as millimeters). The CCA involved a series of statistical tests, which can be performed within a bayesian context, that allow to assign a "functional meaning" to the clusters obtained in the HCA, hence tolerating the implementation of a diverse range of factorial designs.

In what follows, I will describe two validation studies that assess the reliability of the HCA and CCA methods. In particular, I will compare the performance of CluB with one of the most widely used approaches for CBMA: the ALE method (Eickhoff et al., 2009, Eickhoff et al., 2012, Turkeltaub et al., 2012).

A1.3. Aims of the study

The aim of the current study is to perform a validation of the two core modules of CluB: the HCA and the CCA. In particular, with respect to the HCA, we adhered to the following logic: if a CBMA algorithm performs well, than it should be capable of reproducing the effects obtained by pooling together the data in standard random effect group analysis, an approach similar to the one adopted by Salimi-Khorshidi et al. (2009) and that has been further tested and validated in a more recent methodological paper (Maumet and Nichols, 2016). To this aim, we selected the fMRI data from normal controls involved in words and pseudo-words reading (Danelli et al., 2017). We run standard random effects second level analysis to obtain the pattern of activations associated with words and pseudo-words reading: these group-level results were considered our "Gold Standard" reference. In a second step, the subject-specific reading effects were extracted, and the activation peaks were used to create a database of coordinates; accordingly, each single participant was treated as an independent fMRI study on reading. The same database of coordinates was used to run a meta-analysis using the CluB software and the

GingerALE algorithm (Eickhoff et al., 2009). The two meta-analytic results were compared against the Gold Standard to compute performance measures, i.e., sensitivity, specificity and accuracy. The CluB toolbox is compared with the GingerALE approach for two main reasons: (i) GingerALE is the most commonly used software for CBMA; (ii) GingerALE and CluB are based on completely different assumptions. In fact, whereas GingerALE relies on the assumption each peak of activation is better represented by a probability distribution and is modeled accordingly, in CluB each activation peak is considered as a single data-point and it is not weighted or modeled any further. This, in turn, provides a measure of concurrent validity for the CluB toolbox.

For the validation study of the CCA, I will use CluB and GingerALE to assess task-specific convergence across a set of studies conforming to a factorial design, and involving one three-level factor (i.e., TASK = face processing vs. reading vs. object processing). In particular, the task-specific brain maps returned by the two methods will be analyzed by means of the "decoder" function of Neurosynth (http://neurosynth.org/decode/), which allows to retrieve the Pearson correlation of the key-words that are most associated with the input image, based on the NeuroVault repository. The r-value associated with each key-word reflects the correlation across all voxels between the input map and the map associated with a particular key-word in NeuroVault. This design was chosen over more complex designs (e.g., multi-factorial deigns) because (i) a large body of neuroimaging evidence about the neural correlates of face, reading, and object processing exists, and because (ii) GingerALE can still produce task-specific maps in such a design, by performing a contrast study between one set of studies (e.g., face processing) and the other two merged together (e.g., face processing vs. reading and object processing). The overall purpose of this validation study is to provide a proof-of-concept that CluB, compared to GingerALE, is better suited for handling more complex designs.

A2. Materials and methods

Since the two validation studies employ different methodological approaches, and the methods of the first validation study have been already published in a peer-reviewed journal (Berlingeri et al., 2019), the details of each study will be reported separately. In particular, the validation study for the CCA will be originally described in the present thesis[22].

---

[22] The validation study of the CCA was initially performed as a part of a formal response to an anonymous reviewer. She/he particularly appreciated this approach, as it helped her/him to fully

A2.1. Validation study for the HCA

This validation implied the following steps:

1. The analysis of the fMRI data of 24 subjects during a reading experiment (block-design) and the identification of a reference reading map with a standard second–level random effect analysis;

2. The extraction of individual activation peaks for the reading task from individual fixed-effects analysis;

3. The meta-analysis of the individual data collected at step 2 with both CluB and GingerALE;

4. The comparison of the meta-analyses with the reference reading map and estimates of sensitivity, specificity and accuracy for both the CluB and GingerALE analyses.

It is worthy to note that, by following this approach, each single subject was treated as a single experiment in which within-study variability can be assumed to be roughly constant (as a result of the experimental task constraints), while taking mostly into account between-studies variability. The details about methods of fMRI scanning are fully described in another paper (Danelli et al., 2017). The fMRI task involved 120 fMRI entire brain volumes collected in alternating blocks of 10 scans of the baseline condition and 10 scans of the experimental task (TR = 3"), thus resultinng in six blocks of baseline and six blocks of experimental stimuli. The participants were asked to silently read words and pseudowords. A total of 45 words and 45 pseudowords were presented in the six experimental blocks (15 for each block).

For all participants, the sampled anatomical space included the entire cerebral hemispheres and the cerebellum. For each participant, a standard pre-processing and a Hemodynamic Response Function (HRF) convolution were applied using SPM12; once obtained the smoothed-normalized-realigned-coregistered images, the two experimental conditions (baseline and reading conditions) were modeled in a first level-analysis conforming to a standard block-design. This allowed us to estimate, according to the general linear model implemented in SPM12, the subject-specific effect of interest: the contrast image (con-image) "reading > baseline" extracted at p < 0.001 uncorrected. The significant activation peaks were saved in an excel file to create a database for the meta-analytic procedures. As a consequence, each single subject was considered as an independent study. In particular, a total of 579 activation peaks

---

understand in which situations CluB is more suitable compared to the GingerALE approach. I hope that this additional section would also help the reader to fully understand the approach that I have adopted to perform the studies described in Chapter 2 and 3.

were extracted from the 24 subject-specific reading > baseline comparison. Thus, for the 24 participants we extracted a mean of 24.2 activation peaks (min =3; MAX =77). The raw dataset was then passed to the GingerALE 2.3.6 software in order to exclude, from the pool of 579 activation peaks, coordinates laying outside the less conservative brain mask available within the software (this was done in order to maintain only the stereotactic coordinates located in gray matter). The removal of out-of-mask activation peaks led to a pool of 520 activation peaks (the 10.19% of the original dataset was eliminated). The 520 activation peaks constituted the pool of data that we used to run the two meta-analyses: one with the GingerALE method and the other with the CluB method.

The analysis with Ginger-ALE was run by setting the following parameters: (1) brain mask: less conservative; (2) uncorrected threshold $p < 0.001$; (3) no minimum cluster volume.

For the meta-analysis run with CluB the following parameters were set: (1) Users' spatial criterion: mean standard deviation along the three axes <6 mm. This was done in order to conform the spatial resolution of the CluB method to the spatial resolution applied in GingerALE 2.3.6 (the standard deviation of the Gaussian Probability Distribution used to compute the ALE maps is set to 6 mm).

Finally, the 24 con-images representing the single-subject voxel-by-voxel difference between reading and baseline were entered in a random effect second level analysis to obtain our gold-standard reference activation map. The General Linear Model (GLM) was designed to model a one-sample t-test and to extract the mean neural network associated with single word silent reading (once the effect of the early visual processes was eliminated). The results were extracted at $p < 0.001$, no spatial extent threshold has been adopted here.

As described at point 4, we compared the results of the two meta-analytic procedures with the results of the standard random effect analysis according to the following steps:

1. Extraction the t-map corresponding to the reference reading map (our gold-standard) from the SPM12 analyses;
2. Conversion of the results of our meta-analyses from .nii to .voi;
3. Overlap of the .nii and the .voi files on to the "ch2bet" template available in MRIcron (Rorden and Brett, 2000) to identify, for each single meta-analytic map, the brain regions shared with the reference-reading map,
4. Saving the shared regions in dedicated .voi files called GingerALE-intersection and CluB-intersection, respectively.

The intersections were overlaid to the "ch2bet" template and explored using the "descriptive" function available in MRIcron.

As a result we obtained the anatomical distribution of the overlays and the associated voxel-count and volumetry. This result represents, for each single meta-analytic procedure, the so called true positives (TP), i.e., the voxels that are actually activated by our subjects, and that resulted to be active according to the specific pooling method of each meta-analytic algorithm (Figure A1.4).
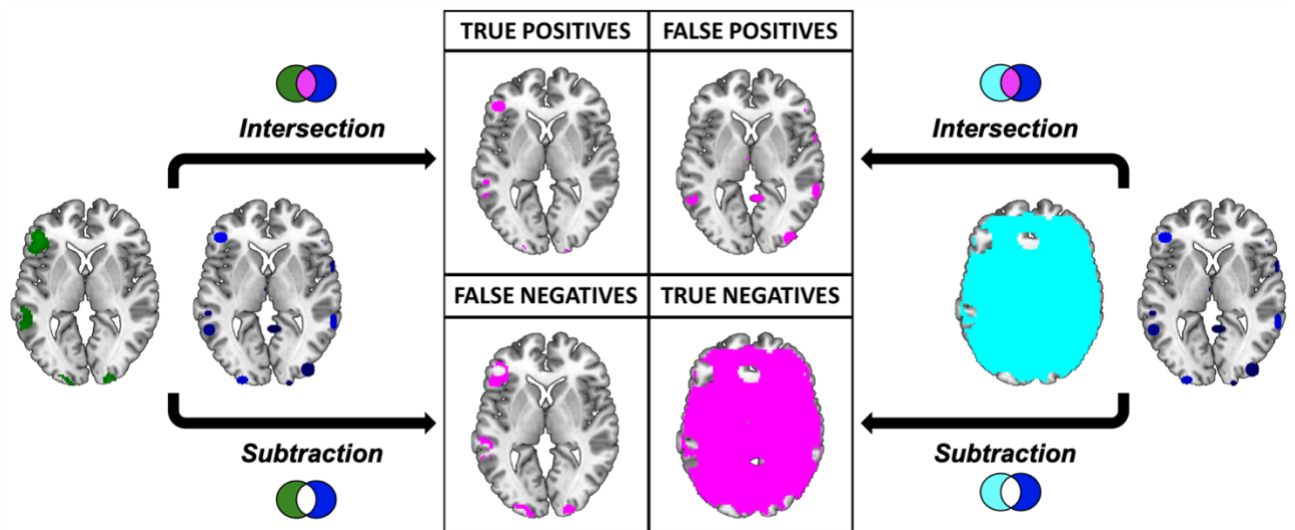
Figure A1**.4 | Graphical representation of the procedure implied in the calculation of the performance measures.** Graphical representation of the comparison between the results of the "Gold Standard" (green) and the meta-analytic map (CluB, in blue). Inactive voxels (i.e., voxels not displaying a significant effect in the second-level SPM fMRI results – the "Gold Standard") are represented in cyan. The output of the comparison (i.e., intersection or subtraction) between the maps is represented in purple. The same procedure was applied to compare the meta-analytic map generated by the GingerALE software with the "Gold Standard". Taken from: Berlingeri et al. 2019.

To identify the true negatives (TN), i.e., the brain regions that were not active in our sample and that did not result activated in the meta-analytic procedures, we selected the mask file of the SPM 12 one sample t-test (i.e., the neurofunctional space mapped by our experiment) and we subtracted the reference reading map to obtain the so-called "inactive map". Secondly, we overlapped the inactive map with each single meta-analytic map and we applied the masking procedure (i.e., a subtraction) to obtain the distribution of the TN voxels (Figure A1.4). The false positives (FP, i.e., the voxels that resulted to be activated in the meta-analytic map, but that were not active in our gold-standard result) were identified by overlapping the inactive map with the results of each single meta-analysis (Figure A1.4). Finally, the false negatives (FN, i.e., the voxels that were significantly activated in the gold-standard map, but not detected by the meta-analysis) were obtained by subtracting the results of the meta-analysis from the

reference reading map (Figure A1.4). These measures were used to compute performance measures for the two meta-analytic procedures: *sensitivity*, *specificity* and overall *accuracy*.

In particular, *sensitivity* expresses the proportion of actual positives findings that are correctly identified. Thus, it represents the true positive rate [TP/(TP + FN)]. *Specificity* corresponds to the proportion of negatives that are correctly identified. Thus, specificity expresses the proportion of "real" negative findings [TN/(TN + FP)]. Finally, *accuracy* is calculated as the proportion of correct assessments (both positive and negative) over the entire sample [(TN + TP)/(TN + TP + FN + FP)].

The performance measures described above, and the corresponding confidence intervals (95%) were computed using the "epi.tests" function available in the "epiR" library of R (version 0.9-48, (Stevenson et al., 2013)).

Finally, to conclude this empirical evaluation, the concordance between the two meta-analytic methods was assessed. The two meta-analytic methods were treated as "two independent classifiers". Thus, in order to obtain a global measure of concordance between the two meta-analytic methods, a 2×2 contingency table was created and, as a consequence, four classes of events were considered:

1. Active voxels both in the GingerALE and in the CluB maps, that were calculated as an intersection between the two neurofunctional maps;
2. Active voxels in the CluB map only, i.e., the result of the subtraction between the CluB map and the GingerALE map;
3. Active voxels in the GingerALE map only, i.e., the result of the subtraction between the GingerALE map and the CluB map;
4. Inactive voxels both in the GingerALE and in the CluB maps, that were calculated as a difference between the total number of voxels investigated and the number of voxels classified according to the previous classes of events.

This classification was performed by computing nine clustering maps varying the user's spatial criterion from 6 to 14 mm[23] (with steps of 1 mm). In order to overcome some of the methodological limitations encountered with the classical Cohen's Kappa measure (it has been demonstrated that the Cohen's kappa is sensitive to trait prevalence and marginal probabilities), the AC^1 measure proposed by Gwet (2002) was adopted here. With respect to table, the AC^1 is calculated as follows:

---

[23] Detailed information about the clustering solutions computed for the different user's criteria is reported in Tables SA1.1–SA1.8 in the Supplementary File 4.

$$AC_1 = \frac{P_\alpha - P_e(\gamma)}{1 - P_e(\gamma)} \qquad [1]$$

$$P_\alpha = \frac{a+d}{n} \qquad [2]$$

$$P_e(\gamma) = 2\,P_+\,(1 - P_+) \qquad [3]$$

$$P_+ = \left(\frac{A_+ + B_+}{2}\right)/n \qquad [4]$$

Where P_α represents the observed concordance [see Equation (2)], $P_e(\gamma)$, represents the modified chance correction [see Equation (3)]; while A+ and B+ represent the marginal frequency.

A2.2. Validation study for the CCA

The validation study for the CCA implied the following steps:

1. Study selection;
2. Foci classification and filtering;
3. GingerALE meta-analysis: single and contrast datasets;
4. CluB meta-annalysis: HCA and CCA;
5. Neurosynth comparison between CluB and GingerALE.

For the study selection step, we used the software Sleuth (http://www.brainmap.org/sleuth/, version 3.0.3) to obtain a reasonable pool of neuroimaging articles; in particular, we were interested in creating a factor "TASK" with three levels, one for each paradigm class: face monitor/discrimination, reading (overt and covert) and visual object identification. To this aim, we employed Sleuth to perform three separate searches in the functional brainmap database, with the following parameters:

1. Experiments – Paradigm Class – IS - Face Monitor/Discrimination
    a. Experiments – Activation – IS – Activations only OR Deactivations only
    b. Subjects – Handedness – IS – Right OR Not Right
2. Experiments – Paradigm Class – IS - Reading (overt) OR Reading (covert)
    a. Experiments – Activation – IS – Activations only OR Deactivations only
    b. Subjects – Handedness – IS – Right OR Not Right
3. Experiments – Paradigm Class – IS - Visual Object Identification
    a. Experiments – Activation – IS – Activations only OR Deactivations only
    b. Subjects – Handedness – IS – Right OR Not Right

In total, these queries to the brainmap functional database returned 2431 experiments (20031 activation foci): 1477 (10154 activation foci) belonging to Face Monitor/Discrimination (or face hereafter), 802 (8524 activation foci) belonging to Reading (overt and covert) (or reading hereafter), and 152 (1353 activation foci) belonging to Visual Object Identification (or object hereafter). Activation peaks were exported in MNI stereotaxic space.

In the foci classification and filtering step, each activation focus was labeled according with the Automatic Anatomical Label (AAL) template, by means of the label4mri function in R (freely available on github: https://github.com/yunshiuan/label4MRI). The function returns 4 variables: (i) aal.distance, the minimum distance (in mm) necessary to reach the first aal region if the peak falls within the white matter or outside of the bounding box; (ii) aal.label, the brain region according with the AAL template; (iii) ba.distance, the minimum distance (in mm) necessary to reach the first Broadmann Area if the peak falls within the white matter or outside of the bounding box; (iv) ba.label, the brain region according with the Broadmann Area. Only the activation foci falling within the following brain regions, according with the AAL template (aal.distance = 0), were selected: the fusiform, inferior temporal and lingual gyri bilaterally. The final dataset included 262 experiments (1607 activation foci): 147 (926 activation foci) belonging to Face Monitor/Discrimination, 62 (557 activation foci) belonging to Reading (overt and covert) and 53 (124 activation foci) belonging to Visual Object Identification. Each activation focus was then classified as a function of the experimental task that generated it, by assigning to it a dummy code (e.g., face = 1; reading = 2; object = 3). The selected pool of coordinates was employed to run three ALE meta-analyses with the GingerALE software (version 2.3.6), one for each group of task-specific coordinates, with the following parameters: (1) brain mask: less conservative; (2) uncorrected threshold p < 0.001; (3) no minimum cluster volume.with an uncorrected threshold of p < .001, no minimum volume threshold. Then, to extract task-specific ALE maps (i.e., the brain areas where convergence across studies is higher in for a task compared to the others), three different contrast meta-analyses were run (parameters: (1) brain mask: less conservative; (2) uncorrected threshold p < 0.001; (3) no minimum cluster volume; permutations: 10000):

1. Face > [Reading + Object];
2. Reading > [Face + Object];
3. Object > [Face + Reading].

Then, the three datasets employed for the ALE annalyses were merged into a single dataset to perform a CBMA with CluB. For the HCA performed with CluB, the user's criterion was set

at 6 mm. Then, a CCA was run by performing a series of multinomial tests (weighted by the Prior Likelihood) on the clusters returned by the HCA, in order to identify those clusters where the proportion of activation peaks associated with a given task is significantly ($p < .05$) different to that expected considering the overall dataset (H0: $p = PL$). Task-specific clustering maps were then obtained by inspecting the composition of each significant cluster.

Finally, as a last proof-of-concept in favor of the validity and reliability of the CluB approach, the results of the the task specific maps obtained from CluB and GingerALE were analyzed by means of the "decoder" function available on Neurosynth (http://neurosynth.org/decode/). This function allows to retrieve the Pearson correlation with the key-words that are most associated with the input image (in .nii format) based on the NeuroVault repository (https://neurovault.org). As the function is influenced by the threshold of the image, and the maps generated by CluB and GingerALE are different (e.g., the ALE maps are thresholded, whereas the CluB maps are not), all the images were binarized with the ImCalc extension available in SPM12. The first 25 key-terms returned by Neurosynth for the CluB and GinngerALE task-specific maps were then plotted as a function of their Pearson's coefficient value.

A3. Results

A3.1. Validation study for the HCA

A3.1.1. GingerALE meta-analysis

The GingerALE method identified 10 clusters, with an average extended volume 8154 mm^3. The centroids of these clusters were mainly located in the left hemisphere, and included frontal (inferior frontal gyrus, pars triangularis, opercularis, and orbitalis, precentral gyrus), temporal (middle temporal gyrus, fusiform gyrus), parietal (supramarginal gyrus, inferior parietal lobule), occipital (inferior and middle occipital gyri), and cerebellar regions. The detailed description of the brain regions underlying reading, according to GingerALE, is reported in Table A1.1 and in Figure A1.5A.

Table A1.1 | Results of the ALE analysis with a cluster forming threshold of p < .001, uncorrected.
For each cluster, the volume, the coordinates in MNI stereotaxic space of the local maxima and the maximum ALEscore observed are reported. Taken from: Berlingeri et al. 2019.

Cluster ID	Anatomical Label	Volume (mm³)	Left Hemisphere			Right Hemisphere			Max. ALE score
			x	y	z	x	y	z	
1	Inferior Frontal Gyrus. pars Triangularis (47)	35280	-42	34	0				0.0056
	Inferior Frontal Gyrus. pars Opercularis		-48	14	10				0.0069
	Middle Temporal Gyrus (22)		-60	-4	-12				0.0050
			-60	-38	2				0.0066
			-62	-24	-4				0.0052
2	Inferior Occipital Gyrus (18)	17520	-24	-100	-10				0.0110
3	Inferior Occipital Gyrus (17)	15752				24	-102	0	0.0092
	Cerebellum					34	-80	-26	0.0045
4	Middle Temporal Gyrus (21)	6272				58	-28	-8	0.0049
						62	-32	-4	0.0050
						64	-40	-2	0.0050
						64	-40	-6	0.0050
5	Precentral Gyrus (6)	3912	-48	0	54				0.0055
6	Inferior Frontal Gyrus. pars Orbitalis (47)	1968				46	36	-12	0.0047
7	Fusiform Gyrus (37)	528	-42	-60	-20				0.0039
			-44	-48	-22				0.0040
8	Supramarginal Gyrus	224	-54	-42	26				0.0039
9	Inferior Parietal Lobule (40)	48	-50	-46	54				0.0038
10	Middle Occipital Gyrus (19)	40	-28	-70	36				0.0037
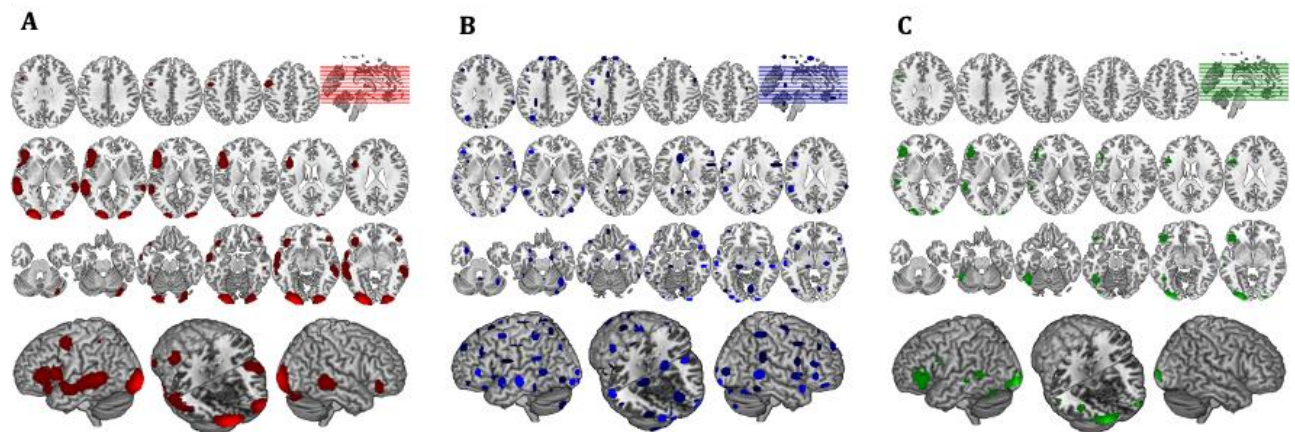
Figure A1.5 | Comparison of GingerALE and CluB solutions with reference to a data set of 24 subjects involved in a reading task. Axial view (top) and 3D rendering (bottom) of the results generated by **(A)** the GingerALE software; **(B)** the optimized hierarchical clustering algorithm implemented in CluB; **(C)** the second-level SPM random-effects analysis (i.e., the "Gold Standard"). Taken from: Berlingeri et al. 2019.

A3.1.2. CluB meta-analysis

The HCA identified a total of 75 clusters scattered all over the brain, with 3–15 individual activation peaks each (median value = 6). The mean standard deviation along the three axes was 5.60 mm (x axis), 5.94 mm (y axis), and 5.78 mm (z axis). A complete list of these clusters is provided in Table A1.2, and the spatial distribution of the clusters (according to the cardinality map)[24] is represented in Figure A1.5B.

A3.1.3. Random-effect second-level analysis ("gold standard")

The results of the second-level SPM analysis, extracted at p < .001, uncorrected (with no spatial threshold) are much in line with the literature on word reading (Turkeltaub et al., 2002). A complete list of these clusters is provided in Table A1.3, whereas the spatial distribution of the clusters is represented in Figure A1.5C.

---

[24] In order to maximize the chance of overlap between the HC solution and the uncorrected GingerALE map (p < .001 uncorrected), no threshold of minimum # of peaks per cluster was imposed in our validation analyses. However, in daily practice one should avoid considering clusters with limited cardinality (e.g., clusters whose cardinality falls below the 25th percentile of the cardinality distribution of all the clusters).

Table A1.2 | Results of CluB with user's spatial criterion set to 6 mm. For each cluster, the mean centroid coordinates in MNI stereotaxic space (standard deviation along the three axes), and the cardinality (N) are reported. Taken from: Berlingeri et al. 2019.

Anatomical Label	Left Hemisphere				Right Hemisphere			
	μx (SD)	μy (SD)	μz (SD)	N	μx (SD)	μy (SD)	μz (SD)	N
Middle Frontal Gyrus					39 (3)	39 (3)	40 (7)	3
Middle Frontal Gyrus, pars Orbitalis	-36 (5)	51 (4)	-7 (9)	5	37 (9)	45 (8)	-15 (4)	10
Superior Frontal Gyrus	-16 (6)	19 (5)	63 (7)	3				
	-14 (6)	57 (6)	38 (8)	5				
Superior Medial Frontal Gyrus					10 (10)	58 (5)	36 (7)	8
					7 (8)	38 (2)	58 (4)	4
Inferior Frontal Gyrus, pars Orbitalis					52 (5)	34 (5)	-2 (5)	10
Inferior Frontal Gyrus, pars Triangularis	-46 (7)	37 (5)	3 (7)	14	57 (3)	34 (7)	16 (5)	7
	-42 (4)	32 (4)	29 (11)	6				
Inferior Frontal Gyrus, pars Opercularis	-49 (3)	14 (4)	10 (2)	8	54 (13)	9 (5)	19 (7)	4
	-45 (5)	11 (6)	24 (6)	11				
Gyrus Rectus	-3 (4)	50 (7)	-19 (4)	3				
Precentral Gyrus	-45 (6)	4 (7)	55 (4)	10	49 (5)	10 (9)	43 (3)	5
	-39 (5)	5 (8)	38 (3)	11	36 (3)	-10 (8)	58 (11)	5
	-27 (8)	-25 (8)	73 (1)	3				
Supplementary Motor Area	-4 (7)	2 (8)	68 (6)	9				
Middle Cingulum	-6 (4)	22 (8)	39 (6)	4				
Postcentral Gyrus	-61 (3)	-3 (9)	21 (3)	3				
	-59 (1)	-16 (8)	43 (2)	4				
Paracentral Lobule	5 (8)	-27 (4)	60 (6)	4				
Insula	-37 (6)	16 (7)	-4 (5)	5				
Superior Parietal Lobule	-31 (3)	-63 (4)	60 (6)	5				

Region								
Inferior Parietal Lobule	-50 (4)	-42 (6)	57 (7)	9	48 (8)	-42 (10)	56 (5)	6
Supramarginal Gyrus	65 (5)	-39 (6)	26 (8)	4				
Superior Temporal Pole	-41 (4)	28 (4)	-19 (4)	7	62 (2)	9 (10)	-1 (5)	8
	-28 (5)	8 (8)	-29 (5)	9	48 (7)	15 (5)	-19 (8)	12
Superior Temporal Gyrus	-58 (3)	4 (6)	-10 (8)	10				
	-53 (7)	-44 (8)	24 (6)	10				
Middle Temporal Gyrus	-62 (5)	-20 (7)	-7 (9)	15	63 (4)	-44 (8)	1 (6)	12
	-58 (4)	-36 (3)	2 (3)	7	55 (7)	-26 (4)	-12 (7)	14
	-57 (6)	-52 (6)	5 (5)	8				
Inferior Temporal Gyrus	-62 (5)	-41 (3)	-15 (8)	6	61 (3)	-47 (6)	-19 (4)	4
Parahippocampal Gyrus	-26 (5)	-12 (5)	-24 (5)	8	18 (6)	-7 (8)	-22 (5)	7
	-14 (9)	-27 (6)	-10 (7)	5				
Hippocampus	-27 (3)	-49 (7)	14 (5)	4	25 (7)	-20 (5)	-7 (9)	9
Fusiform Gyrus	-43 (4)	-63 (4)	-18 (6)	6				
	-42 (2)	-47 (5)	-24 (7)	8				
Precuneus	-10 (11)	-53 (7)	71 (8)	5	6 (9)	-51 (5)	9 (9)	5
Cuneus	7 (5)	-92 (5)	24 (8)	4				
Lingual Gyrus					25 (7)	-98 (4)	-13 (6)	15
					10 (7)	-76 (10)	-10 (6)	6
Superior Occipital Gyrus					27 (1)	-63 (3)	37 (4)	3
					20 (4)	-103 (3)	5 (5)	6
Middle Occipital Gyrus	-32 (6)	-73 (7)	34 (10)	10	38 (7)	-90 (7)	3 (6)	6
	-25 (6)	-100 (4)	2 (4)	12				
Inferior Occipital Gyrus	-43 (8)	-79 (5)	-7 (4)	4				
	-30 (6)	-93 (5)	-11 (5)	14				
	-18 (5)	-102 (3)	-11 (4)	12				
Cerebellum	-32 (8)	-80 (6)	-44 (7)	5	38 (7)	-60 (10)	-26 (6)	10
	-13 (6)	-82 (5)	-41 (3)	4	30 (10)	-76 (5)	-45 (4)	8

						29 (5)	-83 (4)	-25 (4)	7	
						8 (5)	-68 (1)	-45 (6)	4	
						2 (6)	-54 (3)	-31 (8)	4	
Thalamus	-3 (2)	-13 (4)	8 (6)	4						
Putamen						30 (11)	5 (1)	-6 (5)	3	
Pallidum	-12 (2)	3 (8)	-7 (4)	3						
No Region	-25 (4)	-39 (12)	38 (5)	3						
	-11 (9)	23 (13)	16 (2)	6						

Table A1.3 | Results of the random-effects second-level SPM analysis with a significance threshold set to p < .001, uncorrected. For each local maxima the coordinates in MNI stereotaxic space, the cluster extent (k, number of voxels) and the Z-score are reported. Taken from: Berlingeri et al. 2019.

Anatomical Label (BA)	Left Hemisphere					Right Hemisphere				
	x	y	z	k	Z-score	x	y	z	k	Z-score
Inferior Frontal Gyrus, pars Triangularis (47)	-44	34	0	1198	4.19					
	-50	34	-8		3.89					
	-42	34	-10		3.89					
Precentral Gyrus (6)	-44	2	34	37	3.41					
Middle Temporal Gyrus (21)	-62	-50	6	279	3.83					
	-62	-30	0		3.79					
	-56	-44	8		3.63					
Fusiform Gyrus (37)	-44	-56	-20	585	4.87					
	-44	-46	-26		4.16					
Inferior Occipital Gyrus (18)	-26	-98	-10	533	5.75	24	-100	-4	159	4.75

A3.1.4. Performance measures (sensitivity, specificity, accuracy)

The procedure illustrated in Figure A1.4 led to the identification of two 2-by-2 contingency tables, from which the performance measures were calculated: one for the comparison between GingerALE and the "gold standard" (Table A1.4), and one for the comparison between CluB and the "gold standard" (Table A1.5). The GingerALE method obtained the following performance scores: (1) *Sensitivity* = 0.728 [0.722–0.734]; (2) *Specificity* = 0.971 [0.97–0.971]; (3) *Accuracy* = 0.967 [0.966–0.967]. The CluB method obtained (1) *Sensitivity* = 0.139 [0.134–0.143], (2) *Specificity* = 0.969 [0.969–0.97], (3) *Accuracy* = 0.956 [0.955–0.956].

Table A1.4 | Contingency table of the second-level SPM results (i.e., the Gold-Standard) and the GingerALE map. Taken from: Berlingeri et al. 2019.

GingerALE	Gold Standard		
	Active	**Inactive**	*Total*
Active	16136	39550	55686
	1.16%	*2.84%*	*4.01%*
Inactive	6087	1328491	1334578
	0.44%	*95.56%*	*95.99%*
Total	22223	1368041	1390264
	1.60%	*98.40%*	*100%*

Table A1.5 | Contingency table of the second-level SPM results (i.e., the Gold-Standard) and the CluB map. Taken from: Berlingeri et al. 2019.

CluB	Gold Standard		
	Active	**Inactive**	*Total*
Active	3083	41872	44955
	0.22%	*3.01%*	*3.23%*
Inactive	19140	1326169	1345309
	1.38%	*95.39%*	*96.77%*
Total	22223	1368041	1390264
	1.60%	*98.40%*	*100%*

A3.1.5. Between-methods concordance (AC[1])

To calculate the between-methods concordance by means of equation (1), a 2-by-2 contingency table was created (Table A1.6). The between-methods concordance when the user's spatial criterion was set to 6mm is AC1 = 0.933. The neuroanatomical distribution of the overlap between the GingerALE and the CluB maps is reported in Figure A1.6; among the 75 clusters identified by the CluB method, 47 (i.e., the 62.67%) fell outside the GingerALE map. The details about the concordance measures computed for the remaining clustering solutions are reported in Table A1.7.

Table A1.6 | Contingency table of the GingerALE and the CluB maps. Taken from: Berlingeri et al. 2019.

CluB	Ginger ALE		Total
	Active	Inactive	
Active	7255	37700	44955
	0.52%	*2.71%*	*3.23%*
Inactive	48431	1296878	1345309
	3.48%	*93.28%*	*96.77%*
Total	55686	1334578	1390264
	4.01%	*95.99%*	*100%*
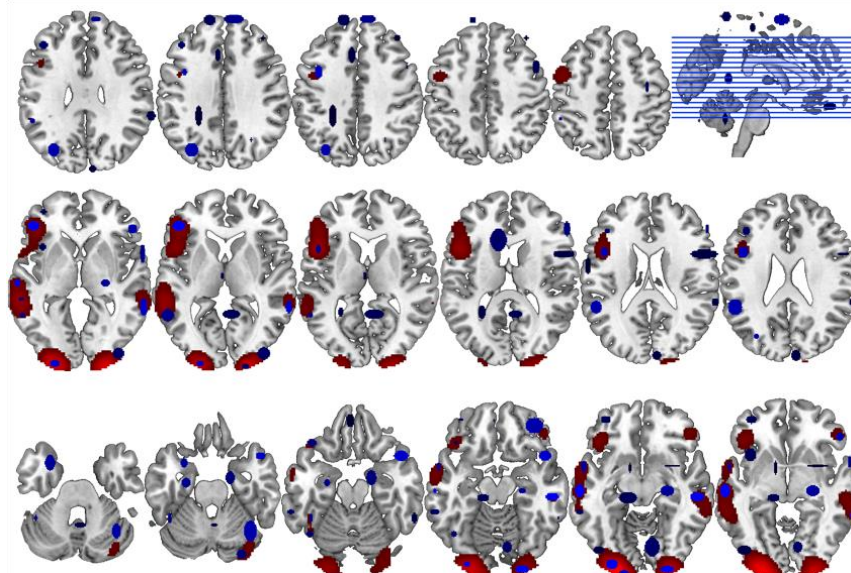
Figure A1.6 | Comparison between CluB and GingerALE. Axial view of the neuroanatomical distribution of the overlap between the CluB map (in blue) and the GingerALE map (in red). These overlaps were used to compute the concordance measures between the two meta-analytic methods, as described in the main text. Taken from: Berlingeri et al. 2019.

Table A1.7 | Between-methods concordance. Concordance measures (AC[1]) between the GingerALE map and the results of CluB with the User's Spatial Criterion set from 7 to 14 mm. Taken from: Berlingeri et al. 2019.

User's spatial criterion	6 mm	7 mm	8 mm	9 mm	10 mm	11 mm	12 mm	13 mm	14 mm
AC[1]	0.933	0.928	0.958	0.942	0.905	0.904	0.892	0.897	0.893

A3.2. Validation study for the CCA

A3.2.1. GingerALE meta-analyses: single and contrast datasets

For the single-dataset meta-analyses, the GingerALE method identified 5 clusters for the face monitor/discrimination dataset, 12 clusters for the reading (overt and covert) dataset, and 7 clusters for the visual object identification dataset (Table A1.8A-C, Figure A1.7A-C). For the contrast-dataset meta-analysis, the GingerALE method identified 3 clusters for the face > reading + object contrast, and 7 clusters for the reading > face + object contrast (Table A1.9A-B, Figure A1.8A-B); no cluster survived the uncorrected p < .001 threshold in the object > face + reading contrast.
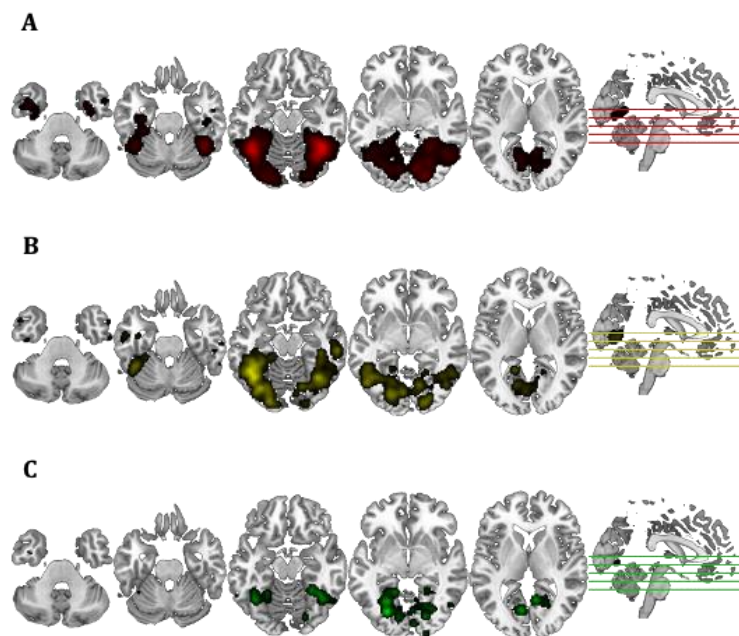
Figure A1.7 | Results of the single-dataset meta-analyses. Axial view of the neuroanatomical distribution of the ALE maps for the **(A)** face dataset, **(B)** reading dataset, and **(C)** object dataset.

Table A1.8 | Results for the ALE meta-analyses on the single-dataset. The cluster ID, the anatomical label (and the Brodmann Area, BA), the volume, the coordinates in MNI stereotaxic space of the local maxima and the maximum ALEscore observed are reported for the (A) face dataset, (B) reading dataset, (C) objects dataset.

Dataset	Cluster ID	Anatomical Label (BA)	Volume (mm³)	Left Hemisphere			Right Hemisphere			Max. ALE score
				x	y	z	x	y	z	
A. Face monitor/discrimination	1	Fusiform Gyrus (37)	112560				42	-52	-20	0.177
		Fusiform Gyrus (37)		-42	-54	-18				0.1453
		Lingual Gyrus (18)					20	-86	-10	0.0855
		Lingual Gyrus (18)					10	-76	-4	0.0737
		Fusiform Gyrus (19)					24	-72	-4	0.0633
		Fusiform Gyrus (37)		-28	-52	-12				0.0628
		Fusiform Gyrus (37)		-32	-32	-22				0.0606
		Lingual Gyrus (18)		-20	-82	-12				0.0587
		Lingual Gyrus (18)		-14	-88	-12				0.0585
		Lingual Gyrus (18)		-30	-86	-16				0.0543
		Lingual Gyrus (18)		-12	-78	-6				0.0518
		Lingual Gyrus (18)		-10	-68	2				0.0469
		Lingual Gyrus (18)					10	-58	2	0.044
		Fusiform Gyrus (36)		-34	-16	-30				0.0416
		Fusiform Gyrus (36)		-34	-18	-24				0.0386
		Fusiform Gyrus (20)		-36	-2	-38				0.0386
		Fusiform Gyrus (20)					46	-20	-28	0.0292
		Fusiform Gyrus (20)					42	-22	-22	0.0291
		Lingual Gyrus (36)		-14	-36	-4				0.0259
		Lingual Gyrus (36)					10	-38	-4	0.0222
	2	Fusiform Gyrus (36)	2096				32	-2	-36	0.0342

152

#	Region	Size	x	y	z	x	y	z	Value
3	Inferior Temporal Gyrus (20)	816				48	4	-40	0.0225
4	Inferior Temporal Gyrus (21)	240				52	-6	-28	0.0222
5	Inferior Temporal Gyrus (21)	16	-60	-12	-26				0.0171
B. Reading (overt and covert) 1	Fusiform Gyrus (37)	83648	-40	-60	-12				0.0763
	Fusiform Gyrus (37)		-42	-48	-20				0.0701
	Fusiform Gyrus (37)		-44	-52	-16				0.0654
	Fusiform Gyrus (18)		-22	-78	-10				0.0528
	Fusiform Gyrus (19)		-32	-72	-14				0.0517
	Fusiform Gyrus (37)					36	-60	-16	0.0515
	Lingual Gyrus (18)		-22	-86	-12				0.0512
	Lingual Gyrus (18)					18	-70	-12	0.0509
	Inferior Temporal Gyrus (37)		-50	-66	-6				0.0406
	Lingual Gyrus (18)		-18	-50	0				0.0395
	Lingual Gyrus (18)					18	-92	-8	0.039
	Fusiform Gyrus (37)					28	-70	-12	0.0387
	Lingual Gyrus (18)		-6	-78	-4				0.0382
	Inferior Temporal Gyrus (21)					58	-28	-16	0.0373
	Inferior Temporal Gyrus (37)					46	-68	-10	0.0353
	Lingual Gyrus (18)					10	-78	-12	0.0332
	Fusiform Gyrus (36)					40	-30	-16	0.0314
	Lingual Gyrus (18)		-14	-68	2				0.0304
	Lingual Gyrus (19)		-20	-64	-8				0.0304
	Fusiform Gyrus (37)					38	-40	-14	0.0288

No.	Region	Size	x	y	z	x	y	z	Value
	Inferior Temporal Gyrus (37)					50	-54	-10	0.0284
	Fusiform Gyrus (37)					38	-46	-20	0.0254
	Fusiform Gyrus (37)		-18	-36	-14				0.024
	Inferior Temporal Gyrus (21)					56	-18	-20	0.023
	Lingual Gyrus (19)					22	-54	-4	0.0201
	Lingual Gyrus (18)					10	-60	0	0.0194
	Inferior Temporal Gyrus (37)					60	-44	-22	0.0168
	Lingual Gyrus (18)					18	-52	4	0.0147
2	Inferior Temporal Gyrus (20)	1288	-40	-12	-32				0.0242
3	Inferior Temporal Gyrus (21)	856	-54	-8	-26				0.0175
	Inferior Temporal Gyrus (20)		-56	-16	-24				0.0163
4	Inferior Temporal Gyrus (20)	400				58	-10	-34	0.0169
	Inferior Temporal Gyrus (20)					56	-8	-30	0.0152
5	Inferior Temporal Gyrus (38)	280				56	8	-34	0.0178
6	Inferior Temporal Gyrus (38)	240	-48	10	-36				0.015
7	Inferior Temporal Gyrus (20)	96				42	-6	-32	0.0132
8	Inferior Temporal Gyrus (21)	40	-62	-16	-22				0.0128
9	Lingual Gyrus (36)	16				14	-34	-10	0.0123
10	Lingual Gyrus (18)	16				10	-46	4	0.0125

	#	Region	Size	x	y	z	x	y	z	p
	11	Lingual Gyrus (36)	8				14	-28	-8	0.0122
	12	Lingual Gyrus (18)	8				8	-44	4	0.0122
C. Visual object identification	1	Fusiform Gyrus (19)	35496	-26	-72	-8				0.0456
		Lingual Gyrus (18)					20	-78	-10	0.0383
		Lingual Gyrus (19)		-24	-60	-10				0.0347
		Lingual Gyrus (18)					8	-58	2	0.0336
		Lingual Gyrus (18)		-8	-70	4				0.0289
		Fusiform Gyrus (37)		-38	-58	-16				0.0264
		Fusiform Gyrus (37)					42	-56	-16	0.0261
		Fusiform Gyrus (19)					30	-70	-2	0.0252
		Fusiform Gyrus (37)					38	-50	-18	0.0248
		Fusiform Gyrus (37)					30	-46	-16	0.0244
		Lingual Gyrus (17)					6	-86	-2	0.0244
		Lingual Gyrus (19)		-14	-50	-8				0.0231
		Fusiform Gyrus (37)		-38	-50	-20				0.0211
		Lingual Gyrus (18)		-12	-80	-8				0.0204
		Lingual Gyrus (19)					18	-64	0	0.018
		Lingual Gyrus (19)					22	-66	-8	0.0175
		Lingual Gyrus (18)					6	-70	-4	0.0175
		Fusiform Gyrus (19)					24	-48	-10	0.0161
		Inferior Temporal Gyrus (37)					52	-66	-10	0.0131
		Inferior Temporal Gyrus (37)					54	-58	-16	0.012
	2	Calcarine Scissure (18)	400				20	-98	-6	0.0156
	3	Inferior Temporal Gyrus (37)	344	-62	-52	-12				0.0134

#	Region	Volume	x	y	z	x	y	z	ALE
4	Inferior Temporal Gyrus (21)	152				54	-16	-20	0.0106
5	Inferior Temporal Gyrus (20)	88	-40	0	-36				0.0095
6	Lingual Gyrus (36)	8				12	-36	-8	0.009
7	Lingual Gyrus (36)	8				10	-38	-2	0.009
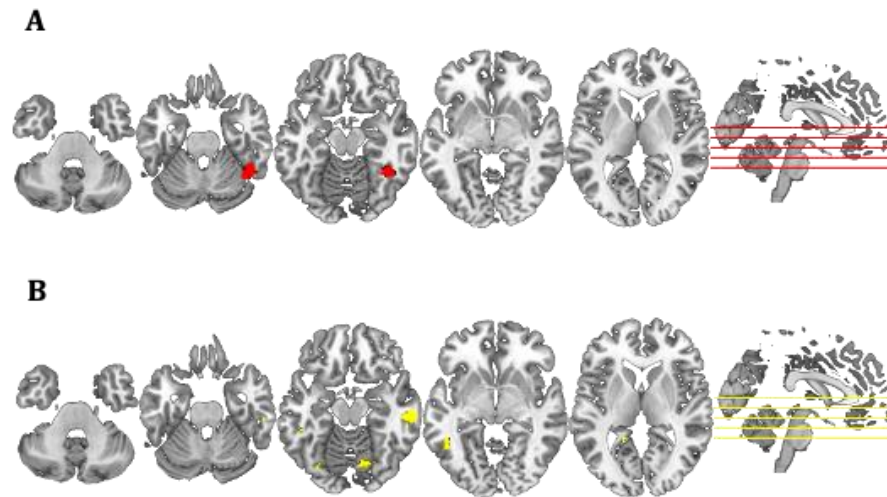
Figure A1.8 | Results of the contrast-dataset meta-analyses. Axial view of the neuroanatomical distribution of the ALE maps for the contrast **(A)** face > reading + object, and **(B)** reading > face + object.

Table A1.9 | Results for the ALE meta-analyses on the contrast-dataset. The cluster ID, the anatomical label (and the Brodmann Area, BA), the volume, the coordinates in MNI stereotaxic space of the local maxima and the maximum ALEscore observed are reported for the (A) face > reading + object contrast, and the (B) reading > face + object contrast.

Dataset	Cluster ID	Anatomical Label (BA)	Volume (mm³)	Left Hemisphere			Right Hemisphere			Max. ALE score
				x	y	z	x	y	z	
A. Face > Reading + Object	1	Fusiform Gyrus (37)	4512				44	-50	-23	3.8906
		Fusiform Gyrus (37)					29	-52	-11	3.7190
	2	Lingual Gyrus (17)	368				19	-76	1	3.8906
		Lingual Gyrus (18)					12	-80	-2	3.4316
	3	Parahippocamal Gyrus (36)	128	-32	-22	-25				3.4316
B. Reading > Face + Object	1	Inferior Temporal Gyrus (21)	2336				60	-25	-18	3.8906
	2	Inferior Temporal Gyrus (37)	1872	-48	-49	-9				3.8906
	3	Cerebellum	904				14	-72	-16	3.8906
	4	Inferior Occipital Gyrus (18)	464	-23	-90	-9				3.8906
	5	Cerebellum	440	-31	-73	-18				3.8906
	6	Hippocampus (54)	376				41	-33	-11	3.8906
	7	Precuneus (30)	344	-16	-47	3				3.8906
	8	Middle Occipital Gyrus (19)	328	-47	-67	0				3.7190
		Inferior Occipital Gyrus (19)		-50	-72	-4				3.5401
	9	Fusiform Gyrus (37)	64	-37	-42	-25				3.1947

10	Cerebellum	64	-30	-42	-26				3.2389
11	Inferior Occipital Gyrus (19)	48				46	-72	-14	3.2905
12	Inferior Occipital Gyrus (18)	16	-32	-82	-8				3.4316
13	Inferior Occipital Gyrus (18)	8	-30	-84	-6				3.5401

A3.2.2. CluB meta-analysis: HCA and CCA

In the HCA, the CluB method identified 22 clusters with 23–192 individual activation peaks each (median value = 65.5). The mean standard deviation along the three axes was 5.83 mm (x axis), 5.71 mm (y axis), and 4.30 mm (z axis). A complete list of these clusters is provided in Table A1.10, and the spatial distribution of the clusters (according to the cardinality map) is represented in Figure A1.9.

In the CCA, 12 clusters displayed a significant (p < .05) multinomial test: inspection of the composition of the cluster revealed that 6 were specific for the face studies, 4 for the reading studies, and 2 for the object studies (Table A1.11A-C). The CCA maps for each task-specificity are reported in Figure A1.10A-C.
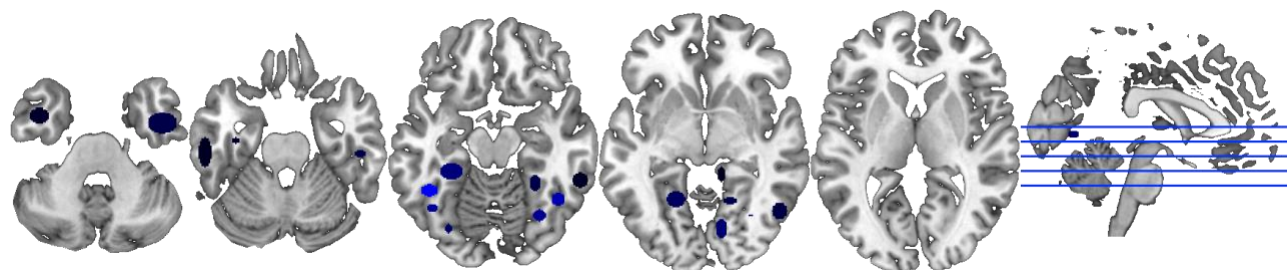
Figure A1.9 | Results of the HCA. Axial view of the neuroanatomical distribution of the cardinality map returned by the HCA.
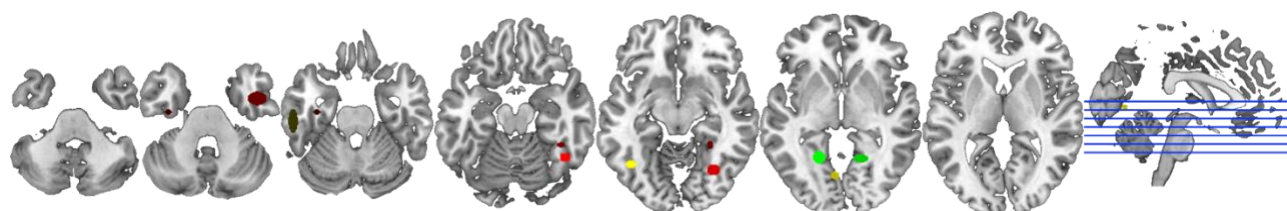
Figure A1.10 | Results of the CCA. Axial view of the neuroanatomical distribution of the CA map dislpaying the clusters that resulted significant at the multinomial test, and that were specific for the face dataset (red), reading dataset (yellow), and object dataset (green).

Table A1.10 | Results of the HCA. For each cluster, the cluster ID, the anatomical label (Brodmann Area), the mean centroid coordinates in MNI stereotaxic space (standard deviation along the three axes), and the cardinality (N) are reported.

Cluster ID	Anatomical label (BA)	Left Hemisphere			Right Hemisphere			N
		µx (SD)	µy (SD)	µz (SD)	µx (SD)	µy (SD)	µz (SD)	
1	Fusiform Gyrus (37)				40 (5)	-44 (3)	-19 (3)	61
2	Fusiform Gyrus (37)				28 (4)	-44 (6)	-13 (4)	56
3	Lingual Gyrus (27)				11 (3)	-38 (6)	-3 (5)	23
4	Lingual Gyrus (18)				17 (7)	-56 (4)	-1 (5)	56
5	Fusiform Gyrus (20)	-35 (5)	-15 (4)	-29 (5)				32
6	Inferior Temporal Gyrus (20)	-40 (7)	2 (5)	-36 (4)				33
7	Inferior Temporal Gyrus (37)				51 (5)	-63 (6)	-6 (3)	50
8	Fusiform Gyrus (37)				44 (5)	-55 (4)	-16 (5)	131
9	Inferior Temporal Gyrus (20)				59 (5)	-42 (5)	-16 (4)	29
10	Inferior Temporal Gyrus (20)				50 (9)	-24 (6)	-21 (4)	56
11	Lingual Gyrus (18)	-18 (5)	-84 (6)	-10 (5)				102
12	Fusiform Gyrus (19)	-31 (5)	-75 (7)	-12 (3)				76
13	Fusiform Gyrus (37)	-42 (5)	-61 (4)	-12 (4)				114
14	Inferior Temporal Gyrus (20)	-44 (7)	-49 (5)	-17 (4)				192
15	Lingual Gyrus (18)				23 (5)	-87 (6)	-10 (4)	80
16	Lingual Gyrus (18)				11 (4)	-75 (7)	-6 (4)	83
17	Inferior Temporal Gyrus (20)	-56 (5)	-23 (12)	-23 (4)				26
18	Lingual Gyrus (18)	-6 (6)	-71 (5)	0 (4)				84
19	Lingual Gyrus (19)	-20 (6)	-55 (6)	-5 (5)				70
20	Fusiform Gyrus (37)				31 (6)	-66 (5)	-11 (6)	108
21	Fusiform Gyrus (37)	-29 (8)	-36 (6)	-17 (5)				91
22	Inferior Temporal Gyrus (20)				44 (10)	-3 (7)	-35 (4)	54

Table A1.11 | Results of the CCA. For each cluster, the cluster ID, the anatomical label (Brodmann Area), the mean centroid coordinates in MNI stereotaxic space (standard deviation along the three axes, the cardinality (N), and the p-value associated with the multinomial test are reported. F = face-specific, R = reading-specific, O = object-specific.

Cluster ID	Anatomical label (BA)	Left Hemisphere			Right Hemisphere			N	p-value
		μx (SD)	μy (SD)	μz (SD)	μx (SD)	μy (SD)	μz (SD)		
1	Fusiform Gyrus (37)				40 (5)	-44 (3)	-19 (3)	61	< .001 [F]
2	Fusiform Gyrus (37)				28 (4)	-44 (6)	-13 (4)	56	< .001 [F]
4	Lingual Gyrus (18)				17 (7)	-56 (4)	-1 (5)	56	< .05 [O]
5	Fusiform Gyrus (20)	-35 (5)	-15 (4)	-29 (5)				32	< .05 [F]
8	Fusiform Gyrus (37)				44 (5)	-55 (4)	-16 (5)	131	< .001 [F]
10	Inferior Temporal Gyrus (20)				50 (9)	-24 (6)	-21 (4)	56	< .001 [R]
13	Fusiform Gyrus (37)	-42 (5)	-61 (4)	-12 (4)				114	< .05 [R]
17	Inferior Temporal Gyrus (20)	-56 (5)	-23 (12)	-23 (4)				26	< .05 [R]
18	Lingual Gyrus (18)	-6 (6)	-71 (5)	0 (4)				84	< .01 [R]
19	Lingual Gyrus (19)	-20 (6)	-55 (6)	-5 (5)				70	< .01 [O]
20	Fusiform Gyrus (37)				31 (6)	-66 (5)	-11 (6)	108	< .05 [F]
22	Inferior Temporal Gyrus (20)				44 (10)	-3 (7)	-35 (4)	54	< .01 [F]

A3.3.3. Neurosynth decoding

For each GingerALE task-specific map, the first 25 words returned by the decoder function of Neurosynth are reported (Table A1.12A-B). A graphical representation is given in Figure A1.11A-B.

For each CluB task-specific map, the first 25 words returned by the decoder function of Neurosynth are reported (Table A1.13A-C). A graphical representation is given in Figure A1.12A-C.

Table A1.12 | Results of the Neurosynth decoding for the GingerALE maps. The first 25 words returned by Neurosynth, and their associated r-value, are reported for the (A) Face > Reading + Object contrast map, and (B) Reading > Face + Object contrast map.

A. Face > Reading + Object		B. Reading > Face + Object	
Word	**r-value**	**Word**	**r-value**
ffa	0.337	lateral occipital	0.11
fusiform face	0.326	fusiform gyrus	0.1
face ffa	0.323	ventral visual	0.099
images	0.304	fusiform	0.098
face	0.292	occipitotemporal	0.09
face recognition	0.274	object	0.089
faces	0.269	object recognition	0.089
fusiform	0.246	extrastriate	0.088
fusiform gyrus	0.237	visual	0.081
category	0.224	occipital	0.08
selective	0.221	objects	0.079
recognition	0.211	visual stream	0.079
categories	0.201	occipito	0.075
recognize	0.198	inferior temporal	0.075
viewing	0.196	occipito temporal	0.075
expression	0.159	inferior occipital	0.074
object recognition	0.141	learning task	0.074
objects	0.139	visual perception	0.072
extrastriate	0.134	orthographic	0.067
facial	0.133	perception	0.061
matching task	0.129	written	0.061
ventral visual	0.125	face	0.059
fusiform gyri	0.12	fusiform face	0.059
inferior occipital	0.119	recognize	0.057
occipito temporal	0.117	occipital cortex	0.054
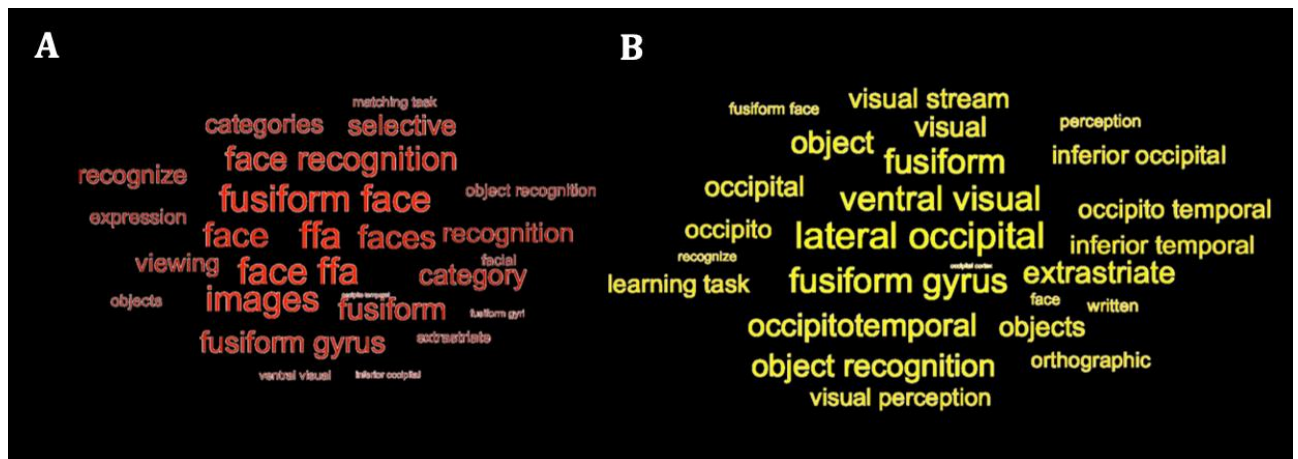
Figure A1.11 | Results of the the Neurosynth decoding for the GingerALE maps. The first 25 words returned by Neurosynth for the (A) Face > Reading + Object contrast map, and (B) Reading > Face + Object contrast map are plotted as a function of their r-value: the greater the r-value, the bigger the font size.

Table A1.13 | Results of the Neurosynth decoding for the CluB CCA maps. The first 25 words returned by Neurosynth, and their associated r-value, are reported for the (A) Face-specific, (B) Reading-specific, and (C) Object-specific CCA maps.

A. Face-specific clusters		B. Reading-specific clusters		C. Object-specific clusters	
Word	**r-value**	**Word**	**r-value**	**Word**	**r-value**
images	0.169	character	0.141	lingual	0.22
fusiform	0.127	chinese	0.137	lingual gyrus	0.111
fusiform gyri	0.125	form	0.131	occipital temporal	0.066
faces	0.113	bilinguals	0.13	nouns	0.057
fusiform gyrus	0.113	characters	0.122	spectrum disorders	0.043
ventral visual	0.112	written	0.121	parahippocampal cortex	0.039
face	0.106	letters	0.111	animals	0.034
fusiform face	0.097	letter	0.111	stream	0.03
recognize	0.096	lexical decision	0.11	eyes	0.027
face ffa	0.094	occipitotemporal cortex	0.109	cuneus	0.024
ffa	0.09	cortex pcc	0.109	parahippocampal	0.023
letters	0.077	visual word	0.109	cross modal	0.02
face recognition	0.073	word form	0.103	salience network	0.02
object	0.071	orthographic	0.099	autism spectrum	0.017
objects	0.07	abuse	0.098	negative feedback	0.016
extrastriate	0.069	decision task	0.097	events	0.012
recognition	0.068	occipitotemporal	0.097	primary visual	0.012
occipital	0.067	occipito temporal	0.096	asd	0.012
viewing	0.066	inferior temporal	0.094	simulation	0.011
visual	0.062	readers	0.091	retrosplenial	0.01

visual stream	0.062	speakers	0.091	fusiform	0.01
category object	0.061	perceptual	0.09	task difficulty	0.01
recognition	0.061	occipito	0.088	recall	0.009
occipito temporal	0.059	word recognition	0.087	occipital	0.007
occipito	0.058	temporal cortex	0.079	frontoparietal	0.005

Figure A1.12 | Results of the the Neurosynth decoding for the CluB CCA maps. The first 25 words returned by Neurosynth for the (A) Face-specific, (B) Reading-specific, and (C) Object-specific CCA maps are plotted as a function of their r-value: the greater the r-value, the bigger the font size.

A4. Discussion

Meta-analyses, by pooling together the results of different independent studies, can overcome, or at least minimize, some typical methodological limitation of neuroimaging studies: (1) the specific influence of the selected experimental paradigm that makes the results of a single study not necessarily bound to gain a general validity (with the well-known problem associated with the subtraction logic; (Logothetis, 2008)); (2) the problem of multiple comparisons and of the balance between false positive and false negative rates (Lieberman and Cunningham, 2009); (3) the typical small sample sizes of neuroimaging studies (Murphy and Garavan, 2004).

In this Chapter, I have described two validation experiments by comparing the performance of a novel toolbox for CBMA based on hierarchical clustering, CluB, with one of the most popular software for CBMA: GingerALE.

A4.1. CluB vs. GingerALE: two sides of the same coin

The first validation study aimed at assessing the *accuracy* (i.e., the proportion of correct assessments, both positive and negative, over the entire sample), s*pecificity* (i.e., the proportion of actual negatives that are correctly identified), and *sensitivity* (i.e., the proportion of actual

positives findings that are correctly identified), of the two methods by comparing the individual meta-analytical maps with the "gold standard" (i.e., second-level SPM map of reading-related activation). In particular, the GingerALE method obtained a high level of accuracy (0.967), associated with a high sensitivity (0.728), and specificity (0.971); similarly, the CluB method obtained a high level of accuracy (0.956) and specificity (0.969), notwithstanding the low-level of sensitivity (0.14). The concordance between the two methods assessed by the AC^1 was 93.3%, showing that the two methods have a high level of agreement.

Whereas both CluB and GingerALE perform well in identifying true negatives, the CluB method is not as sensitive as the GingerALE method in identifying the true positives, as it correctly identified only 3,083 voxels (i.e., the 13.8%). With this regard, it is worthy to note that the GingerALE method is based on the application of a three-dimensional Gaussian filter to each single activation peak collected in the input dataset. This process results in a continuously distributed anatomo-functional map; conversely, the CluB method creates a discrete and spatially sparse map of clusters, as one of the intrinsic aims of the hierarchical clustering procedure is to obtain a map of distinct entities whose spatial extension is limited by the choice of the "user's spatial criterion" (see Figure 2.5 to better appreciate the differences between the different output maps). In other words, whereas GingerALE models the input data to simulate a standard activation map, CluB works on raw data (the stereotactic coordinates reported in the peer-reviewed selected literature), and it returns small and spatially discrete clusters.

From the neuroanatomical point of view, this feature represents one of the strengths of the CluB approach. Indeed, the relative finer-grained and unsmoothed spatial resolution of the clustering maps, together with the maintenance of the original distribution of the data, permits to explore neurofunctional segregation with a robust statistical approach (the one described in the CCA) based on non-parametric, exact tests. This is something that can be hardly done with GingerALE, which, at the most, can identify the commonalities and the differences between two sets of data (see, for example, (Fornara et al., 2017), but no higher order effects like 2×2 interactions in a data-driven manner, starting from meta-analyses containing more than two classes of data (Paulesu et al., 2014).

The above-mentioned considerations are corroborated by the results of the validation study for the CCA. When dealing with one factor (i.e., TASK) with more than two levels (i.e., 1 = Face monitor/discrimination, 2 = Reading (overt and covert), 3 = Visual Object Identification), GingerALE allows to test task-specific convergent activations only by performing three separate contrast studies; conversely, such a multi-level design can be implemented in a single

meta-analysis in CluB, by performing a multinomial test on the distribution of the clusters returned by the HCA.

Two main findings worth mentioning here: (i) GingerALE could not detect any object-specific convergent activity at the uncorrected threshold of p < .001 (see Figure A1.8), whereas the multinomial test performed with CluB identified two clusters localized in the bilateral lingual gyrus (BA 18,19); (ii) the reading-specific GingerALE map was not directly associated with language and reading-related terms (top 5 words unrelated to brain anatomy: object, object recognition, visual, objects, learning task; Figure A1.11B), whereas the reading-specific clusters identified by CluB were associated with a set of words easily attributable to linguistic and reading-related processes (top 5 words unrelated to brain anatomy: character, Chinese, form, bilinguals, characters; Figure A1.12B). This proof-of-concept study suggests that, despite the lower *sensitivity* of CluB, due to the relative finer-grained spatial resolution of the clustering maps, the clusters identified by the HCA and CCA procedure, compared to the ones identified by the GingerALE approach, are better associated with the "cognitive dimension" that generated them.

As a final consideration about the differences between the two approaches, it is worthy to note that the smoothing applied by GingerALE to the input data tends to inflate the spatial distribution of the native data beyond the expected anatomical boundaries (see Figure A1.13 for an illustration). This is even more evident in the case of the dataset generated *ad-hoc* for the validation study for the CCA (see the methods section): in that case, we filtered *a priori* the activation foci that entered the CluB meta-analysis, by selecting only the activation foci localized within the bilateral fusiform, inferior temporal, and lingual gyri. Nonetheless, whereas the centroids of the clusters returned by the HCA are all localized within those anatomical boundaries (see Table A1.10 and Figure A1.9), the clusters returned by the GingerALE approach extend well beyond them, including local maxima localized in the parahippocampus and hippocampus, inferior and middle occipital gyri, precuneus, and cerebellum (see Table A1.9 and Figure A1.8).
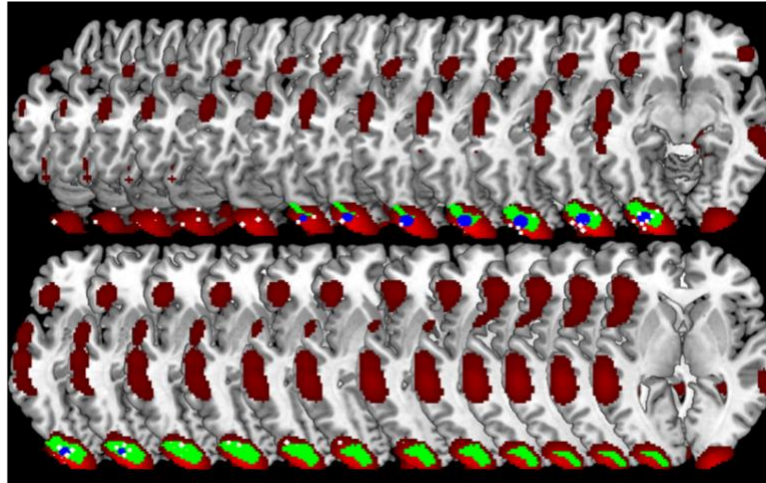
Figure A1.13 | Region of interest oriented comparison of CLuB and GingerALE. The region of interest (in green, the "Gold Standard") was taken from the SPM data analysis on 24 readers. The peaks composing the left inferior occipital cluster (X = −30, Y = −93, Z = −11) in the HC map (user's spatial criterion = 6 mm) are shown as $2 \times 2 \times 2$ mm white cubic voxels. The cluster obtained in the HC map (user's spatial criterion = 6 mm) is depicted in blue. The ALE map obtained by GingerALE is depicted in red. It can be seen that while the clustering solution (in blue) is contained within the SPM "Gold Standard" map, GingerALE somewhat overestimated the activation effect as a consequence of the Gaussianization of the raw data implied. From slice in top left: Z = −20 to Z = +3 in the right bottom corner. Taken from: Berlingeri et al. 2019.

To conclude, it is important to underline that these seemingly contrasting meta-analytic approaches compared here are indeed complementary: one, GingerALE, is based on the idea that each focus of activation is better represented by a probability distribution rather than in terms of a single data-point; CluB tackles the same issue with a different approach, by considering each activation peak as a single data-point that is not weighted nor modeled any further. In other words, these two methods could be thought as "two sides of the same coin", with the GingerALE approach being optimal for neurofunctional mapping of pooled data, and the CluB method being the most suitable choice if one wants to test more specific neurocognitive hypotheses. As a final remark, it is important to note that the congruence between the HC solutions and those of an ALE map, corrected for multiple comparison, may permit to decide on which set of clusters to proceed with further assessments of the data using a CCA (see, for example, Paulesu et al., 2014), with the trust that the cluster considered is "spatially significant".

This combined approach is the one that I adopted to perform the meta-analytical studies reported in Chapter 2 and 3.

A4.2. Future directions

Along with its strengths, the CluB approach comes with its own limitations.

As a first limitation, which is shared with the GingerALE method, concern the fact that effect sizes, usually expressed as t-value or Z-score and associated with each activation peak, do are not taken into account. Thus, it may be desirable to develop new algorithms capable of taking into account also one of these measures (arguably the Z-scores, as they do not depend on the degrees of freedom of the test) to obtain a better fitting of the data to the expected results. Moreover, by introducing the t-value or the Z-score associated with each activation peak, the lack of between-studies uniformity in reporting the coordinates may be reduced, as usually the papers that report the higher number of activation peaks are also those that adopted a less conservative statistic threshold (David et al., 2013). This issue was recently addressed in the GingerALE algorithm by introducing also the study as one of the level in the analysis and hence taking into account also within- study variability. By doing this, the probability that one study with many foci drives a meta-analytic result has been mitigated (Turkeltaub et al., 2012).

At the moment, this issue remains unaddressed by the CluB method. As a form of best practice, one should reduce the amount of data per study, when these are exceedingly redundant, by taking only the local maximum for each region, or by calculating a preliminary high-resolution CluB clustering solution on the redundant study. Admittedly, this approach requires some a-priori decision on what a "redundant style" of data description would be.

Another important issue is related with the problem of inactive areas. Since imaging papers only report positive findings in the form of stereotactic coordinates, the inactive voxels are just represented, both in GingerALE and CluB, by zeros. As a consequence, measurements of non-active areas are lost and this, in turn, makes impossible to evaluate whether the outcome in that particular brain region would have become significant by pooling data from different studies. This means that CBMAs, in general, cannot aggregate power across studies, unless the effect of every single voxel is taken into account (Costafreda, 2009).

The last methodological consideration is about the adoption of hierarchical clustering and of the Ward's method (Ward, 1963). This clustering procedure maximizes the between-cluster difference and minimizes the within cluster variability; this, in turn, creates localized blobs, such as those represented in Figure 2.5B. The result is the emergence of localized sets of activations that, however, do not seem to fully represent the complexity of brain functioning and connection. It may be the case that the adoption of a different clustering procedure, that returns distributed clusters rather than localized blobs, may provide a more adequate model of the neurofunctional effects of interest. A possible candidate may be the adoption of minimum

spanning tree (Jain et al., 1999), a clustering method that is typically used, and had been fully developed, to design networks, such as computer or electrical networks (Graham and Hell, 1985). Recently, this approach has been used to identify the neural network underlying specific cognitive functions in the context of functional connectivity studies (Baumgartner et al., 2001, Firat et al., 2013). The authors relied on the simple assumption that brain regions that show the same type of activation may constitute spatially sparse brain networks (Carpenter and Just, 1999). Therefore, in this case, the similarity measure would not be based on spatial proximity (i.e., Euclidean distance), but rather on temporal co-occurrence of brain activity.

Further studies are needed to better address this issue, in order to develop a software implementation.

Summary of Appendix A

In this Appendix, I have described a novel toolbox for coordinate-based meta-analysis (CBMA): Clustering the Brain, or CluB. Two validation studies, each one designed to test a core module of the toolbox, were performed.

In the first validation study, aimed at assessing the reliability of the HCA module, I compared the performance of CluB with that of GingerALE, one of the most popular toolboxes for CBMA. In particular, I assessed their *accuracy* (i.e., the proportion of correct assessments, both positive and negative, over the entire sample), s*pecificity* (i.e., the proportion of actual negatives that are correctly identified), and *sensitivity* (i.e., the proportion of actual positives findings that are correctly identified), in reproducing a "gold standard" map that was derived empirically from the second-level random-effect analysis of 24 participants involved in a reading task. The results show that both methods have a high accuracy (GingerALE = 0.967, CluB = 0.956) and specificity (GingerALE = 0.728, CluB = 0.969), notwithstanding a lower level of sensitivity of CluB (0.14), due to the lack of prior Gaussian transformation of the data. Nonetheless, the two methods obtained a good-level of between-method concordance, as assessed by the AC^1 measure (0.93).

In the second validation study, aimed at assessing the reliability of the CCA module, I employed the software Sleuth to create a dataset of stereotaxic coordinates extracted from three different experimental paradigms available in the Brainmap.org database: face monitor/discrimination (face), reading (overt and covert) (reading), and visual object identification (object). As GingerALE only allows the comparison of two classes of studies at a time, three contrast studies were performed to obtain the task-specific ALE maps, once the single-study ALE maps were obtained for the three classes of task. Conversely, the HCA module of CluB was used on the

single dataset comprising the three classes of task to obtain the clustering solution, and the CCA module was used to perform the multinomial test on the clusters returned by the HCA, in order to obtain task-specific maps of clusters. The meta-analytic maps generated by the two methods were analyzed with the decoder function of Neurosynth, which allows to assign a set of words to a brain map based on the studies available in the Brainmap.org database. The results show that CluB was able to identify a set of face, reading, and object-specific clusters, whereas GingerALE was not able to identify any object-specific convergent activation. Furthermore, whereas the decoder function of Neurosynth returned a congruent set of words linked to face processing for the face-specific maps obtained by the two methods, the reading-specific map obtained from CluB was more directly associated with reading-related terms compared to the map generated by GingerALE.

In sum, the results show that GingerALE and CluB may be considered the "two sides of the same coin": the first is optimal for neurofunctional mapping of pooled data, whereas the second is the method of choice if one wants to test more specific neurocognitive hypotheses.

Supplementary File 1 - Hungry Brains: A Meta-analytical Review of Brain Activation Imaging Studies On Food Perception and Appetite in Obese Individuals

Supplementary File 1

1. Supplementary Figures

2. Supplementary Tables
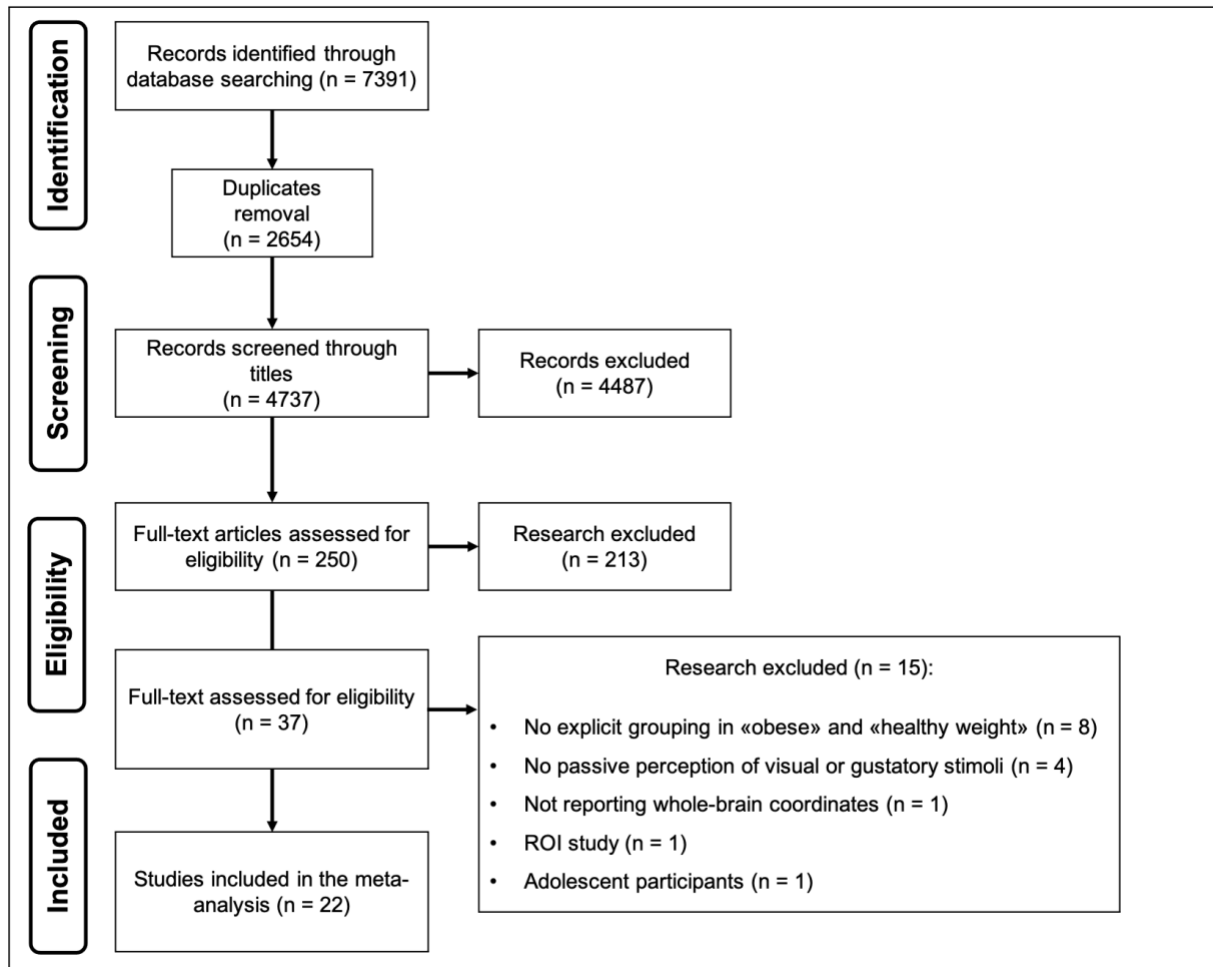
Figure S1.1 | Flowchart of the selection process that led to the identification of the studies included in the meta-analysis. Taken from: Devoto et al. 2019.

Table S1.1 | Neuroimaging studies included in the current meta-analysis. For each study, the following information is reported: the neuroimaging technique employed; the sample size; the classification of the activation foci included for the factor "sensory modality of cue presentation"; the experimental paradigm that entered the meta-analysis; additional information on the subjective ratings of the stimuli (when available); the average time of fasting (in hours); whether the study included a fed condition or not. HW, healthy weight; OB, obese. Adapted from: Devoto et al. 2019.

Authors	Year	Technique	Sample size (HW/OB)	Sensory modality of cue presentation	Experimental paradigm	Subjective ratings	Hours of fasting	Fed condition?
Blechert et al.	2016	fMRI	32/0	Visual – Anticipatory	**Task**: Passive perception of pictures. **Experimental stimuli**: Color pictures taken from a standardized database and belonging to: i) high-calories food and ii) 20 low-calories food. Half of the foods of both categories were available for consumption during as well as after scanning. **Control stimuli**: Fixation cross.	**Quality of the stimuli being assessed**: i) palatability; ii) desire to eat. **Measurement scale**: 7-point Likert scale. **Results**: Analyses on subjective ratings are reported only for palatability. Significantly higher ratings for high-calories compared to low-calories foods and for available compared to non-available foods.	7	No

Cornier et al.	2013	fMRI	25/0	Visual – Anticipatory	**Task**: Passive perception of pictures. **Experimental stimuli**: Color pictures belonging to: i) foods of high hedonic value; ii) foods of neutral hedonic value. **Control stimuli**: Non-food pictures.	Subjective ratings were not collected by the authors.	10	Yes
Cornier et al.	2009	fMRI	22/0	Visual – Anticipatory	**Task**: Passive perception of pictures. **Experimental stimuli**: Color pictures belonging to: i) foods of high hedonic value; ii) foods of neutral hedonic or utilitarian value. **Control stimuli**: Non-food pictures.	Subjective ratings were not collected by the authors.	8	No
Cornier et al.	2012	fMRI	0/12	Visual – Anticipatory	**Task**: Passive perception of pictures. **Experimental stimuli**: Color pictures belonging to: i) foods of high hedonic value; ii) foods of neutral hedonic or utilitarian value. **Control stimuli**: Non-food pictures.	**Quality of the stimuli being assessed**: i) appeal; ii) desire to eat; iii) pleasantness. **Measurement scale**: Visual Analogue Scale (VAS). **Results**: Analyses on the collected subjective ratings are not reported by the authors.	10	No

					Task	Quality		
Dimitropoulos et al.	2012	fMRI	16/22	Visual – Anticipatory	**Task**: Perceptual discrimination task. Subjects are asked to press a button when two simultaneously presented images where the "same" or "different". **Experimental stimuli**: Color pictures belonging to: i) high-calories foods; ii) low-calories foods. **Control stimuli**: Non-food pictures.	**Quality of the stimuli being assessed**: i) liking. **Measurement scale**: 5-point Likert scale. **Results**: Subjective ratings did not differ between and within groups.	6.2	Yes
Gautier et al.	1999	PET	11/0	Gustatory – Consummatory	**Task**: Passive perception of tastes. **Experimental stimuli**: Flavoured liquid-formula meal (2 mL, 1.5 kCal/mL) of different flavours, chosen by the participant: i) chocolate; ii) vanilla; iii) strawberry. **Control stimuli**: Water (2 mL).	**Quality of the stimuli being assessed**: i) pleasantness and palatability. **Measurement scale**: Visual Analogue Scale (VAS) ranging from 0 to 100 mm. **Results**: The average ratings reported by the authors suggest that all participants rated as pleasant (64 ± 18 mm) and palatable (65 ± 16 mm).	36	No

Geliebter et al.	2013	fMRI	0/31	Visual – Anticipatory	**Task**: Passive perception of pictures. **Experimental stimuli**: Color pictures belonging to: i) high-calories foods; ii) low-calories foods. **Control stimuli**: Non-food pictures.	Subjective ratings were collected but not reported.	12	Yes
Haase et al.	2011	fMRI	21/0	Gustatory – Consummatory	**Task**: Passive perception of tastes. **Experimental stimuli**: Tastants dissolved in distilled water and reflecting 4 basic tastes: i) caffeine (0.04 M); ii) citric acid (0.01 M); iii) sucrose (0.64 M); iv) sodium chloride (NaCl, 0.16 M). **Control stimuli**: Water.	- **Quality of the stimuli being assessed**: i) pleasantness. **Measurement scale**: modified version of the labeled Magnitude Scale (gLMS). **Results**: Sucrose was significantly rated more pleasant compared to the other stimuli; both citric acid and NaCl were rated as significantly more pleasant than caffeine.	12	Yes
Jastreboff et al.	2013	fMRI	25/25	Visual – Anticipatory	**Task**: Visual imagery of food guided by aurally-presented personalized scripts. **Experimental stimuli**: Personalized imagery scripts about the favorite high-calories foods of participants. **Control stimuli**: Neutral-relaxing Visual imagery.	Subjective ratings were not collected by the authors, as guided imagery scripts were prepared ad hoc to reflect the participant's favorite preferences about food.	2	No

					Task			
Karra et al.	2017	fMRI	24/0	Visual – Anticipatory	**Task**: Passive perception of pictures. **Experimental stimuli**: Color pictures belonging to: i) high-calories foods; ii) low-calories foods. **Control stimuli**: Non-food pictures.	Subjective ratings (appeal) were collected but not reported by the authors.	12	No
Killgore et al.	2003	fMRI	13/0	Visual – Anticipatory	**Task**: Perception of pictures. Subjects are instructed to try to remember them for a recognition test after imaging. **Experimental stimuli**: Color pictures belonging to: i) high-calories foods; ii) low-calories foods; iii) nonedible food-related utensils. **Control stimuli**: Non-food pictures.	**Quality of the stimuli being assessed**: i) motivational salience ("how much the picture affects your appetite?"). **Measurement scale**: 11-point Likert scale. **Results**: High-calories compared to low-calories foods were rated as more appealing.	4	No
Lundgren et al.	2013	fMRI	0/14	Visual – Anticipatory	**Task**: Passive perception of pictures. **Experimental stimuli**: Color pictures of different foods. **Control stimuli**: Non-food pictures.	Subjective ratings were not collected by the authors.	4	Yes

						Quality of the stimuli being assessed: i) desire to eat sweet and savory foods.		
Luo et al.	2013	fMRI	0/13	Visual – Anticipatory	Task: Passive perception of pictures. Experimental stimuli: Color pictures belonging to: i) high-calories foods; ii) low-calories foods. Control stimuli: Non-food pictures.	Quality of the stimuli being assessed: i) desire to eat sweet and savory foods. Measurement scale: Visual Analogue Scale (VAS), ranging from 1 to 10. Results: The desire for savory and sweet food was significantly greater than for neutral stimuli.	10-12	No
Martin et al.	2010	fMRI	10/10	Visual – Anticipatory	Task: Passive perception of pictures. Experimental stimuli: Color pictures of different foods. Control stimuli: Non-food pictures.	Subjective ratings were not collected by the authors.	4	Yes
Murdaugh et al.	2012	fMRI	25/13	Visual – Anticipatory	Task: Passive perception of pictures. Experimental stimuli: Color pictures of different foods. Control stimuli: Non-food pictures.	Subjective ratings (appetite motivation and emotional valence) were collected but not reported by the authors.	8	No

					Task: Passive perception of pictures. **Experimental stimuli**: Color pictures of chocolate. **Control stimuli**: Grey pictures.	**Quality of the stimuli being assessed**: i) liking and craving chocolate. **Measurement scale**: Chocolate eating questionnaire (Rolls and McCabe, 2007). **Results**: High levels of chocolate liking and craving.		
Murray et al.	2014	fMRI	20/0	Visual – Anticipatory			0	Yes
Nummenmaa et al.	2012	fMRI	15/19	Visual – Anticipatory	**Task**: Perception of pictures. Subjects are instructed to press a button to indicate whether a picture was slightly displaced leftward or rightward in the screen. **Experimental stimuli**: Color pictures belonging to: i) high-calories foods; ii) low-calories foods. **Control stimuli**: Non-food pictures.	**Quality of the stimuli being assessed**: i) valence (pleasantness vs. unpleasantness), after fMRI scanning. **Measurement scale**: Self-Assessment Manikin (SAM) scale, ranging from 1 to 9. **Results**: Appetizing foods were rated as more pleasant than the bland foods and neutral stimuli, but results were similar for both obese and healthy weight participants.	3	No

					Task / Stimuli	Quality / Results		
Puzziferri et al.	2016	fMRI	15/15	Visual – Anticipatory	**Task**: Perception of pictures. Subjects are asked to rate the appeal of the pictures. **Experimental stimuli**: Color pictures belonging to different categories: i) high-calories savory foods; ii) high-calories sweet foods; iii) low-calories foods. **Control stimuli**: Null directional arrow.	**Quality of the stimuli being assessed**: i) appeal. **Measurement scale**: appeal-rating scale, ranging from 1 to 3. **Results**: The appeal ratings were different between the two groups and between fasting and fed conditions. When satiated, obese individuals rated all the stimuli as more appealing than lean participants (the satiety state-by-group interaction showed a trend towards significance with $p = 0.07$).	9	Yes
Rothemund et al.	2007	fMRI	13/13	Visual – Anticipatory	**Task**: Passive perception of pictures. **Experimental stimuli**: Color pictures belonging to different categories: i) high-calories foods; ii) low-calories foods; iii) eating-related utensils. **Control stimuli**: Non-food pictures.	Subjective ratings were not collected by the authors.	1.5	No

					Task			
St-Onge et al.	2014	fMRI	26/0	Visual – Anticipatory	**Task**: Passive perception of pictures. **Experimental stimuli**: Color pictures belonging to: i) healthy foods; ii) unhealthy foods. **Control stimuli**: Non-food pictures.	Subjective ratings were not collected by the authors.	8	No
Szalay et al.	2012	fMRI	12/12	Gustatory – Consummatory	**Task**: Passive perception of tastes. **Experimental stimuli**: Simple tastes and nourishment solution (100 mL): i) sucrose (0.1 M); ii) quinine hydrochloryde (0.03 mM); iii) vanilla flavoured nourishment solution (150 kCal/mL). **Control stimuli**: Distilled water.	**Quality of the stimuli being assessed**: i) pleasantness. **Measurement scale**: Visual Analogue Scale (VAS) . **Results**: Pleasantness scores were significantly higher (for sucrose and vanilla) and lower (for quinine) in obese compared to healthy weight participants.	3.5	No

Van Bloemendaal et al.	2014	fMRI	16/16	Visual – Anticipatory	**Task**: Perception of pictures. Subjects are instructed to try to remember them for a recognition test after imaging. **Experimental stimuli**: Color pictures belonging to: i) high-calories foods; ii) low-calories foods. **Control stimuli**: Non-food pictures.	Subjective ratings (hunger, fullness, appetite, prospective food consumption and desire to eat) were collected (before and after fMRI scanning) but not reported by the authors.	8	No

Table S1.2 | Results of the HCA and CCA for all the clusters overlapping with the Ginger ALE maps. For each cluster the following information is reported: the anatomical label according to the AAL; the cluster ID; the centroid coordinates in the MNI stereotaxic space (standard deviation of the distance from the centroid along the three axes); the number of foci falling within the cluster (N); the p-values associated with the binomial and Fisher's tests. Significant main and interaction effects are shown in bold. FA, fasting state; FE, fed state; G, gustatory modality; GR, group; GRxS, group-by-satiety interaction; GRxSM, group-by-sensory modality interaction; HW, healthy weight; OB, obese; S, satiety; SM, sensory-modality; V, visual modality. Adapted from: Devoto et al. 2018.

Anatomical Label	Cluster ID	Left Hemisphere			Right Hemisphere			N	GR-specific		SM-specific		S-specific		GRxSM	GRxS	SMxS
		X (SD)	Y (SD)	Z (SD)	X (SD)	Y (SD)	Z (SD)		HW	OB	V	G	FA	FE			
Temporal_Sup_R_41	2				53 (3)	-33 (4)	17 (5.1)	5	0.647	0.697	0.792	0.537	0.660	0.741	0.382	1	1
Amygdala_R_34	8				21 (2.8)	1 (4.6)	-18 (5.1)	7	0.975	0.117	0.828	0.427	0.151	1	0.074	1	1
Cingulum_Ant_L_24	10	-1 (3.4)	29 (7)	16 (2.9)				6	0.792	0.497	0.353	0.911	0.565	0.803	1	1	1
Frontal_Sup_L_0	18	-19 (6.3)	20 (2.9)	43 (3.6)				5	0.303	0.934	0.133	1	0.259	1	1	1	1
Frontal_Sup_R_8	23				22 (3.5)	25 (3.8)	51 (6.1)	4	1	**0.031**	0.199	1	0.997	**0.044**	1	1	1
ParaHippocampal_L_36	26	-24 (4)	-13 (5.8)	-24 (4)				8	0.275	0.913	0.743	0.529	0.903	0.289	1	1	0.429
Caudate_R_25	28				9 (4.6)	13 (2.2)	11 (2.6)	4	0.797	0.559	0.199	1	0.956	0.24	1	1	1
Pallidum_R_0	29				14 (4.5)	6 (6.2)	-1 (5)	15	0.737	0.453	0.992	**0.03**	0.098	0.983	0.093	1	1
Frontal_Inf_Orb_R_47	31				34 (6.2)	30 (2.6)	-15 (4.4)	12	0.804	0.389	0.396	0.817	0.989	**0.043**	0.516	0.608	1
Frontal_Inf_Orb_L_47	36	-30 (3)	25 (4.5)	-13 (7.1)				5	0.647	0.697	0.463	0.867	0.259	1	0.164	1	1

Region	#	x1	y1	z1	x2	y2	z2	n	p1	p2	p3	p4	p5	p6	p7	p8	p9
Frontal_Sup_Orb_L_11	37	-24 (4.7)	39 (5.9)	-12 (6.1)				7	0.671	0.623	0.828	0.427	0.478	0.849	1	1	1
Frontal_Inf_Tri_R_48	39				48 (2.4)	18 (6.9)	26 (6.4)	6	0.949	0.208	0.901	0.318	0.565	0.803	0.493	0.488	1
Insula_R_47	41				38 (3.9)	18 (4.9)	-3 (4)	14	0.636	0.575	1	**0.001**	0.779	0.432	0.225	0.244	0.221
Amygdala_L_28	42	-20 (1.9)	2 (4.8)	-22 (2.3)				6	0.792	0.497	0.682	0.647	0.565	0.803	0.493	1	1
Ventral striatum_L_48	43	-19 (4)	5 (5.8)	-9 (3.5)				11	0.999	**0.009**	1	**0.001**	0.051	1	**0.002**	1	1
Midbrain	45	-5 (3.8)	-15 (2.1)	-4 (6.2)				9	**0.007**	1	0.653	0.62	0.088	1	1	1	1
Precuneus_R_7	48				26 (3.7)	-50 (2.3)	1 (3.5)	5	0.897	0.353	0.463	0.867	0.91	0.34	1	0.166	0.211
Temporal_Sup_L_41	52	-43 (3.4)	-34 (2.6)	18 (6.3)				6	0.995	0.051	0.901	0.318	0.565	0.803	1	0.276	1
Frontal_Mid_L_46	63	-30 (4)	37 (2.3)	33 (6.2)				6	0.792	0.497	0.353	0.911	0.565	0.803	0.228	1	0.471
Lingual_R_19	64				40 (3.3)	-78 (5.3)	-16 (0.8)	4	0.797	0.559	0.199	1	0.339	1	1	1	1
Insula_R_48	66				41 (2.1)	-3 (4.1)	-2 (4.2)	7	0.134	0.978	0.955	0.172	0.783	0.522	1	1	1
Insula_R_48	67				43 (3.5)	3 (8.1)	12 (5.6)	10	0.929	0.202	0.981	0.076	0.275	0.933	0.18	1	1
Frontal_Sup_Medial_L_0	72				2 (2.1)	59 (3.8)	21 (8.3)	6	0.792	0.497	0.353	0.911	0.996	**0.031**	1	0.097	1
Temporal_Inf_R_37	76				54 (4.6)	-54 (7.7)	-11 (5.7)	8	0.794	0.453	0.743	0.529	0.978	0.097	0.466	0.543	0.528
SupraMarginal_R_48	90				61 (4)	-20 (4.8)	33 (5.2)	7	0.671	0.623	0.059	1	0.151	1	1	1	1
Occipital_Mid_R_19	93				37 (3.1)	-87 (2.3)	11 (1.2)	3	0.926	0.381	0.298	1	0.858	0.556	1	1	1
Fusiform_R_20	95				32 (1.8)	-26 (5.5)	-22 (3.8)	8	0.547	0.725	0.743	0.529	0.978	0.097	1	1	0.528
Caudate head/Nucleus Accumbens_L_25	99	-7 (5.5)	14 (8.6)	-9 (6.4)				8	0.937	0.206	0.981	0.087	0.903	0.289	0.505	1	**0.031**
Postcentral_L_48	101	-50 (7)	-16 (4.4)	18 (4.3)				7	0.883	0.329	0.993	**0.045**	0.478	0.849	1	1	1

Region	ID	x	y	z	x	y	z	N									
Thalamus_R_0	103				14 (4.1)	-14 (3.4)	0 (5.5)	9	**0.007**	1	0.999	**0.008**	0.637	0.667	1	1	0.107
Insula_L_48	104	-39 (4)	-4 (5.6)	6 (5.4)				16	0.92	0.183	0.168	0.94	**0.013**	1	1	1	1
SupraMarginal_R_40	106				46 (4.5)	-35 (4.5)	39 (3)	8	0.937	0.206	0.471	0.803	0.401	0.885	0.466	1	1
Hippocampus_R_37	110				35 (5.5)	-30 (5.8)	-3 (5.5)	15	0.547	0.657	0.913	0.201	0.957	0.121	0.109	0.596	0.614
Temporal_Pole_Sup_R_48	111				43 (6.5)	8 (3.9)	-16 (5.1)	13	0.955	0.126	0.325	0.86	0.936	0.174	0.242	1	1
Rolandic_Oper_R_48	113				60 (3.9)	-2 (5.6)	16 (6.5)	9	**0.007**	1	1	**0.001**	0.961	0.142	1	1	1
Frontal_Inf_Tri_L_45	115	-42 (4.8)	38 (5.7)	7 (6.4)				12	0.185	0.936	0.935	0.176	0.689	0.568	0.516	1	1
Anterior Insula/Frontal Operculum_L	116	-38 (5.7)	13 (6.4)	-19 (7.2)				10	0.997	**0.017**	**0.018**	1	0.565	0.725	1	0.509	1
Brainstem	118				4 (5.9)	-34 (3.4)	-42 (4.6)	7	0.671	0.623	0.059	1	0.151	1	1	1	1

Supplementary File 2 - How the Harm of Drugs and Their Availability Affect Brain Reactions to Drug Cues: a Meta-analysis of 64 Neuroimaging Activation Studies

Supplementary File 2

1. Supplementary Methods

2. Supplementary Tables

3. Supplementary Figures

1. Supplementary Methods

1.1. Sample characteristics of the included studies

In the end, the final dataset was based on 1558 substance-dependent individuals (mean age: 36.9 years) with an average history of abuse of 11.56 years (information about the history of abuse was not available for 20 studies). In the majority of the studies, the sample included only males (24 studies, 37.5 %), or the majority of male participants (25 studies, 39.1%), whereas in the minority of the studies the sample included only females (3 studies, 4.7%) or the majority of female participants (1 study, 1.6%). In 9 studies (14.1%) gender of the participants was balanced, whereas in 2 studies (3%) this information was not available. Studies on legal (M = 22, SD = 17) and illegal substances (M = 23, SD = 10), on average, **did not differ significantly with respect to sample size** (Wilcoxon test, W = 448.5, p = .12). TS (M = 25, SD = 16) and NST individuals (M = 21, SD = 12), on average, **did not differ significantly with respect to sample size** (Wilcoxon test, W = 502.5, p = .71).

Subjects from studies on legal (M = 35.4 years, SD = 8.6 years, NA = 1 study) and illegal substances (M = 38.5 years, SD = 6.2 years, NA = 0 studies), on average, **did not differ significantly with respect to age** (Wilcoxon test, W = 630, p = .07). TS (M = 36.3 years, SD = 5.9 years, NA = 0 studies) and NST individuals (M = 37.8 years, SD = 9.3 years, NA = 1 study) **did not differ significantly in terms of mean age** of the participants (Wilcoxon test, W = 472, p = .81). Studies on legal (M = 13.2 years, SD = 7.4 years, NA = 15 studies) and illegal substances (M = 10.8 years, SD = 4.9 years, NA = 5 studies) **did not differ significantly in terms of history of abuse** (Wilcoxon test, W = 235.5, p = .29), whereas studies with **treatment-seeking participants on average had a briefer history of abuse** (M = 10.6 years, SD = 4.6 years, NA = 8 studies) compared to not-seeking treatment participants (M = 15 years, SD = 7.2 years, NA = 12 studies; Wilcoxon test, W = 129, p = .03).

2. Supplementary Tables

2.1. Table S3.1.

Author(s)	Drug of Primary Abuse	Cue-reactivity Paradigm	Sample size	Sample characteristics	Drug cue	Baseline condition	Cue-induced craving assessment	Abstinence	Main route of administration	History of abuse	Additional substances	Treatment status
Bach et al., 2019	**Alcohol**	- *Imaging:* fMRI. - *Modality:* Visual (Pictures). - *Design:* Block. Participants were instructed to watch and attend to the stimuli.	**DA**: 50 **HC**: 35	**Sex** *DA:* all men HC: all men **Co-occurring disorders** No other axis I psychiatric condition other than alcohol abuse or dependence, except nicotine dependence **Socio-economic status** *DA- education* • 2 post-secondary education • 14 apprenticeship only • 32 attended college or higher *HC- education* • 0 post-secondary education • 5 apprenticeship only • 30 attended college or higher	*Alcohol:* Alcohol-related pictures (wine, beer, spirit).	*Neutral:* Neutral objects.	No assessment of cue-induced craving.	17.2 days (averaged between the groups)	Ingestion	17.56 years (averaged between the groups)	Cigarettes	TS (in-patient treatment)
Cortese et al., 2015	**Nicotine**	- *Imaging:* fMRI. - *Modality:* Visual (Pictures). - *Design:* Block. Participants were instructed to watch and attend to the stimuli.	*DA*:17	**Sex** *DA:* 13 men, 4 women **Co-occurring disorders** No other axis I psychiatric condition other than nicotine and caffeine abuse or dependence **Socio-economic status** Not reported	*Nicotine:* Smoking-related pictures (advertisement or digital photos).	*Neutral:* Neutral images matched for intensity, color and complexity.	*Assessment:* Before fMRI. *Scale:* Three 11-point Likert scales to measure craving amount [0 = 'very little'; 10 = 'a great deal], craving intensity [0 = 'none', 10 = 'irresistible'] and craving control [0 = 'no control', 10 = 'complete control']. *Results:* Amount: mean = 7.6 (2.6); Intensity: mean = 6.5 (2.7); Control: mean = 6.5 (3.1).	12 hours (minimum)	Smoking	12.2 ± 6.5 years	Not specified	NST

Study	Drug	Imaging	DA	Demographics	Drug cue	Neutral/Control	Craving assessment	Abstinence	Route	Age	Other drugs	Sample
Courtney et al., 2014	**Nicotine**	- *Imaging:* fMRI. - *Modality:* Visual (Videos). - *Design:* Block. Participants were instructed to watch and attend to the stimuli.	*DA*:39	**Sex** *DA:* 25 men,15 women **Co-occurring disorders** No other axis I psychiatric condition other than nicotine abuse or dependence. **Socio-economic status** Education DA: 14.55 years (± 3.73) Race • 28 Caucasian • 7 African American • 2 Asian • 3 Latino	*Nicotine:* Smoking-related videos filmed in a first-person point of view (i.e. writing a letter and smoking a cigarette or standing outside of a nightclub smoking a cigarette).	*Neutral:* Neutral videos matched for similar content except for the absence of smoking cues.	*Assessment:* During fMRI. *Scale:* During the urge-rating period, participants were asked to rate their current urge to smoke using Likert scale ranging from 1 [No urge] to 4 [Very high urge]. *Results:* Cigarette cues were found to be effective in eliciting greater self-reported craving compared to the neutral cues.	Not specified (abstinence not required prior to scanning)	Smoking	Not specified	Alcohol	NST
David et al., 2007	**Nicotine**	- *Imaging:* fMRI. - *Modality:* Visual (Pictures). - *Design:* Event-related. Participants were instructed to watch and attend to indicate with a keypress the gender of the subject in each photograph.	*DA*:8	**Sex** *DA:* all women **Co-occurring disorders** No other axis I psychiatric condition other than nicotine abuse or dependence. **Socio-economic status** Not reported	*Nicotine:* Smoking-related pictures (i.e. images of humans smoking cigarettes) taken from the International Smoking Image Series (ISIS).	*Control:* Neutral pictures (i.e. images of humans holding pens or glasses in their hands and mouths) of the same size as smoking-related pictures.	*Assessment:* Before and after stimulus presentation during fMRI. *Scale:* The Shiffman-Jarvik Craving Scale (SJCS) consists of five items; subjects are asked to rate each item from 0–100 (total 500 maximum). *Results:* Average SJCS scores were not significantly different before and after the scans.	Abstinence: 12 hours (minimum) Smoking = prior to scanning	Smoking	38 ± 7.1 years	Not specified	NST
De Pirro et al., 2018	**Cocaine and heroin**	- *Imaging:* fMRI. - *Modality:* Imagery. - *Design:* Block. Participants were instructed to recall a typical drug experience and to rate the affective state produced by heroin versus cocaine in two settings (at home vs outside the home).	*DA:* 20	**Sex** *DA:* all men. **Co-occurring disorders** No other axis I psychiatric condition other than cocaine or heroin abuse or dependence. **Socio-economic status** Employment: 17 employed, 3 unemployed. Education: 13.6 years (± 3.31).	*Cocaine:* Scripts of situations in which cocaine is used (at home/outside home). *Heroin:* Scripts of situations in which heroin is used (at home/outside home).	*Neutral:* Scripts of relaxing situations (at home or in their usual club).	No assessment of cue-induced craving. Only vividness of imagery during fMRI is assessed.	Not specified	Cocaine and heroin: intranasal, smoking, intravenously	Cocaine: 15.25 years Heroin: 13.20 years	Methadone, heroin, cocaine	TS (recruited from drug rehabilitation center)

Duncan et al., 2007	Cocaine	- *Imaging:* fMRI. - *Modality:* Imagery. - *Design:* Block. Participants were told to mentally reenact personalized scripts about cocaine use and a neutral experience both with and without a stressor present (anticipation of electrical shock).	*DA:* 10	**Sex** *DA:* all men. **Co-occurring disorders** No other axis I psychiatric condition other than cocaine abuse or dependence, with the exception of substance-induced mood disorder or substance-induced mood disorder with psychotic features. **Socio-economic status** Education: 14.2 years (± 1.5).	*Cocaine:* Produced from a self-reported sensations checklist and from narratives of environmental contexts of personal drug use experiences.	*Neutral:* Script consisting of an emotion- and drug-neutral experience (getting up and dressing in the morning).	*Assessment:* During fMRI Scans, at the end of each baseline period, immediately after completion of the neutral scripts, and again after completion of the cocaine scripts. *Scale:* 100-point visual analogue scale ranging from 1 [Not at all] to 100 [The most I've ever felt] assessing the craving level. *Results:* Craving responses were higher after cocaine scripts compared to baseline and compared to the neutral scripts.	8 ± 4.9 days	Smoking (freebase, crack)	15.9 ± 6.2 years	Not specified	TS
Elton et al., 2015	Cocaine	- *Imaging:* fMRI. - *Modality:* Imagery. - *Design:* Block. Subjects were instructed to relate to previous personal experiences associated with the personalized script.	*DA:* 38	**Sex** *DA:* all men. **Co-occurring disorders** No other axis I psychiatric condition other than cocaine abuse or dependence. **Socio-economic status** Education: • patients with a history of childhood maltreatment: 12.7 years (± 1.7); • patients without a history of childhood maltreatment: 12.2 years (± 1.1).	*Cocaine:* Personalized drug use script.	*Neutral:* Script describing nature scenes (beach, forest, lake, river).	*Assessment:* After each imagery script. *Scale:* Participant rated their cocaine craving and the vividness of the mental image on a scale ranging from 0 to 10. *Results:* The average reported urge to use cocaine did not meet the statistical significance for cocaine craving compared to neutral scripts. The cocaine script condition produced significantly greater ratings of vividness of the related mental image compared to the neutral script condition.	Urine screening detected recent use of cocaine and other drugs of abuse	Not specified	14 years (averaged between maltreated and non-maltreated)	Cigarettes, alcohol, marijuana,	NST
Falcone et al., 2016	Nicotine	- *Imaging:* fMRI. - *Modality:* Visual (Pictures). - *Design:* Event-related. Participants were instructed to watch and attend to the stimuli.	*DA* SlowMetab: 30 NormalMetab: 39	**Sex** *DA_ SlowMetab*: 19 men, 11 women DA_ NormalMetab: 19 men, 20 women **Co-occurring disorders** No other axis I psychiatric condition other than nicotine abuse or dependence. **Socio-economic status** *DA SlowMetab* Post- secondary education: 22/30	*Nicotine:* Smoking-related pictures (i.e. images of people smoking or images of smoking-related objects, such as cigarettes or ashtrays).	*Neutral:* Neutral pictures (i.e. images of people engaged in everyday tasks or unrelated objects, such as pencils) matched for visual features such as size, shape, and luminosity.	*Assessment:* Before, during and after fMRI. *Scale:* A two-item subjective craving questionnaire was administered: participants were asked to rate the degree of craving on a scale ranging from 0 [Not at all] to 10 [Extremely]. *Results:* Slow metabolizers reported significantly less craving in both satiety and abstinence conditions compared to normal metabolizers, but increases in craving between the smoking session and the abstinence session were not different between slow and normal metabolizers.	Abstinence: 24 hours Smoking = 1 hour	Smoking	Not specified	None	TS

				DA NormalMetab Post- secondary education: 26/39 *DA SlowMetab* Race • 21 African American • 7 Caucasian • 2 Other *DA NormalMetab* Race • 18 African American • 19 Caucasian • 1 Other • 1 Not reported								
Garavan et al., 2000	**Cocaine**	- *Imaging:* fMRI. - *Modality:* Visual (Videos). - *Design:* Block. Participants were instructed to watch and attend to the stimuli. After each video, subjects performed a working memory task unrelated to cue-reactivity.	*DA:* 17 *HC:* 14	**Sex** *DA:* 14 men, 3 women; *HC:* 9 men, 5 women. **Co-occurring disorders** No other axis I psychiatric condition other than cocaine abuse or dependence. **Socio-economic status** Not reported.	*Cocaine:* People engaged in drug-specific dialogue while smoking "crack cocaine" and "drinking alcohol".	*Nature:* Scenic outdoor images. *Sex:* Explicit group heterosexual activity.	*Assessment:* Inside MRI scanner, after each movie. *Scale:* Questions focusing on subjects' responses to the movie. *Results:* DA showed significant higher craving composite scores compared to HC.	Not reported	Smoking (freebase, crack)	11 years (range:2-25)	Not specified	NST
George et al., 2001	**Alcohol**	- *Imaging:* fMRI. - *Modality:* Visual (Pictures). - *Design:* Block. Participants were instructed to watch and attend to the stimuli.	*DA:* 10 *HC:* 10	**Sex** *DA:* 8 men, 2 women. HC: 8 men, 2 women **Co-occurring disorders** No other axis I psychiatric condition other than alcohol abuse or dependence **Socio-economic status** Not reported.	*Alcohol:* Alcohol-related pictures (wine, beer, liquor).	*Non-alcoholic beverages:* Pictures of non-alcoholic beverages. *Control:* Blurred alcohol-related pictures.	*Assessment:* Before and after the sip of alcohol (before fMRI), during cue-reactivity and after fMRI. *Scale:* Assessment of current craving using a visual analogue scale ranging from 0 to 100. *Results:* Alcoholic subjects had a higher self-reported of urge to drink alcohol compared to HC at all time points. Significant increase of craving levels across time points for both alcoholic subjects and social drinkers	3.4 ± 2.2 days	Ingestion	Not specified	Not specified (negative urine drug screening)	NST

Goudriaan et al., 2010	Nicotine	- *Imaging:* fMRI. - *Modality:* Visual (Pictures). - *Design:* Event-related. Participants were instructed to watch and attend to the stimuli. To ensure attentional focus, participants had to press a response button with their left index finger when a face was present in the picture and they had to press a response button with their right index finger when no face was present.	*DA:*18 - *FTDN-High: 10* - *FTDN-Low:8* *HC*: 17	**Sex** *DA:* all men *HC*: all men **Co-occurring disorders** No other axis I psychiatric condition other than nicotine abuse or dependence **Socio-economic status** *DA* Education: 4.1 level (± 1.1) *HC* Education: 4.3 level (± 1.2)	*Nicotine:* Smoking-related pictures (i.e. several persons smoking, detailed image of a hand with a cigarette).	*Neutral:* Neutral pictures matched for complexity and similar content except for the absence of smoking cues (i.e. a hand with a magazine, persons talking).	*Assessment:* Before and after fMRI. *Scale:* Smoking Urge Questionnaire [range 1-7]. *Results:* Craving for smoking before scanning was higher in the smoking group compared with healthy controls. No differences between smoking craving before and after the cue reactivity task in the group.	16-18 hours	Smoking	Not specified	None	TS
Goudriann et al., 2013	Cocaine	- *Imaging:* fMRI. - *Modality:* Visual (Pictures). - *Design:* Block. Participants were instructed to pay attention to the images and press a button when a target image (picture of an animal) is presented.	*DA:* 13 *HC:* 16	**Sex** *DA:* not reported; *HC:* not reported. **Co-occurring disorders** No other axis I psychiatric condition other than cocaine abuse or dependence. **Socio-economic status** Not reported.	*Cocaine:* Individuals preparing for cocaine use, individuals using cocaine, or cocaine user-related objects, cocaine paraphernalia, different ways of administration (snorting, crack use).	*Neutral:* Not specified.	*Assessment:* Before and after scanning. *Scale:* Craving Urge Questionnaire (CUQ): 8 items with a 7-point Likert scale ranging from 1 [Strongly disagree] to 7 [Strongly agree]. *Results:* No change in craving scores across conditions.	At least 3 weeks	Not specified	Not specified	Cigarettes	TS (in treatment)
Grusser et al., 2004	Alcohol	- *Imaging:* fMRI. - *Modality:* Visual (Pictures). - *Design:* Block. Participants were instructed to watch and attend to the stimuli.	*DA:*10 *HC:*10	**Sex** *DA:* 5 men, 5 women HC:5 men, 5 women **Co-occurring disorders** No other axis I psychiatric condition other than alcohol abuse or dependence (and axis-II disorders in HC). **Socio-economic status** Not reported	*Alcohol:* Alcohol-related pictures.	*Neutral:* Affectively-neutral pictures. *Control:* Scrambled alcohol-related pictures.	*Assessment:* Before fMRI. *Scale:* Alcohol craving was measured using the Alcohol-Craving Questionnaire (ACQ). *Results:* No significant differences were detected between alcohol-dependent individuals and healthy controls.	9 ± 9 weeks (range: 1-25)	Ingestion	Alcohol dependence onset: 31 years Mean age: 36 years	None	TS

Study	Drug	Methods	Sample	Sex / Co-occurring disorders / Socio-economic status	Drug stimuli	Neutral / Control stimuli	Cue-induced craving assessment	Abstinence	Route	Duration of use	Urine screen	Treatment status
Hassani-Abharian et al., 2015	**Heroin**	- *Imaging:* fMRI. - *Modality:* Visual (Pictures). - *Design:* Block. Participants were instructed to watch drug-related and neutral pictures.	*DA:* 25	**Sex** *DA:* all men. **Co-occurring disorders** No other axis I psychiatric condition other than cocaine abuse or dependence. **Socio-economic status** Education: 8.57 years (± 2.6) Marital status: • married: 15; • single: 5; • separated: 3; • divorced: 2.	*Heroin:* 24 pictures of heroin-related pictures (e.g., crystallized-heroin, paraphernalia, preparation, smoking, and co-smoking related cues).	*Neutral:* 24 pictures of neutral stimuli.	*Assessment and Scale:* During trial intervals, subjects verbally reported their subjective feeling of cue induced craving (CIC). After fMRI procedure, participants reported the intensity of their "need for drug use" and "drug use imagination" on a 0-100 visual analog scale. Afterwards, they completed positive and negative affect scale (PANAS) and desire for drug questionnaire (DDQ) with 3 components of "desire and intention to drug use", "negative reinforcement" and "loss of control". *Results:* Average verbally reported intensity of craving slightly increased during scanning. Correlation analysis among different self-reported variables exhibited no significant relationship except between the intensity of "drug use imagination" and "need for heroin use", as well as between the intensity of "drug use imagination" and "verbal self-report of cue-induced craving".	4-6 hours	Not specified	3 ± 1.9 years	Not specified	TS (in-patient treatment)
He et al., 2018	**Cocaine**	- *Imaging:* fMRI. - *Modality:* Visual (Pictures). - *Design:* Block. Participants performed a cue task in the scanner to measure their brain activity when watching two categories of stimuli: cocaine-related pictures and natural scene pictures. Participants were asked to passively view the images.	*DA:* 32 *HC:* 7	**Sex** *DA:* all men; *HC:* all men. **Co-occurring disorders** No other axis I psychiatric condition other than cocaine abuse or dependence. **Socio-economic status** Not reported.	*Cocaine:* Cocaine-related pictures (e.g., cocaine lines, cocaine crystals).	*Neutral:* Natural scenes (e.g., a garden, a tree).	No assessment of cue-induced craving.	USERS: < 1 years ABS1: 1-5 years ABS2: 6-10 years ABS3: > 10 years	Not specified	Not specified	Not specified	NST
Hermann et al., 2006	**Alcohol**	- *Imaging:* fMRI. - *Modality:* Visual (Pictures). - *Design:* Block. Participants were instructed to watch and attend to the stimuli	*DA:* 10 *HC:* 10	**Sex** *DA:* all men *HC:* all men **Co-occurring disorders** No other axis I psychiatric condition other than alcohol abuse or dependence **Socio-economic status** Not reported	*Alcohol:* Alcohol-related pictures.	*Neutral:* Affectively-neutral pictures; *Control:* Scrambled alcohol-related pictures.	*Assessment:* Before and after fMRI. *Scale:* Alcohol wanting, the intention to consume alcohol, expected positive effects of alcohol consumption and whether alcohol could now improve negative feelings were assessed with 4 VAS [0-100 mm]. *Results:* No pre/post difference in any VAS.	15 ± 5 days (range: 8-21)	Ingestion	19 ± 10 years	Not specified (negative urine drug screening)	TS (in-patient treatment)

		Imaging/Modality/Design		Sex / Co-occurring disorders / SES	Drug cue	Control cue	Craving assessment	Abstinence	Route	Severity	Other drug	Group
Holla et al., 2014	Alcohol	- *Imaging:* fMRI. - *Modality:* Visual (Pictures). - *Design:* Block. Participants were instructed to watch and attend to the stimuli, and to indicate by means of button presses whether they experienced craving for alcohol after seeing the picture or not.	DA:5	**Sex** *DA:* all men **Co-occurring disorders** No other axis I psychiatric condition other than alcohol abuse or dependence, except nicotine dependence. **Socio-economic status** *DA* Education: 11.2 years	*Alcohol*: Alcohol-related pictures in 5 scenarios (i.e. liquor stores, alcoholic beverage containers, glasses filled with alcohol, scenes of people sipping alcoholic beverages).	*Non-alcoholic beverages:* Neutral pictures (i.e. bar stores, bottles, glasses filled with non-alcoholic beverages, scene of people sipping non-alcoholic beverages).	*Assessment:* During fMRI. *Scale:* Button presses. *Results:* Not specified.	12-15 days	Ingestion	Alcohol dependence onset: 21.4 years Mean age: 34.2 years	Cigarettes	TS
Hong et al. 2017	Nicotine	- *Imaging:* fMRI. - *Modality:* Visual (Pictures). - *Design:* Block. Participants were instructed to watch and attend to the stimuli.	*DA*:15 *HC*:15	**Sex** *DA:* all men HC: all men **Co-occurring disorders** No other axis I psychiatric condition other than nicotine abuse or dependence. **Socio-economic status** *DA* Education: 11.9 years (± 3.1) *HC* Education: 12.0 years (± 3.7)	*Nicotine:* Smoking-related pictures downloaded from Google with the search terms: 'positive smoking', 'negative smoking'.	*Control:* Pictures obtained as mosaic modification of tobacco-related images.	No assessment of cue-induced craving.	Not specified	Smoking	16.8 ± 7.4 pack years	Alcohol	NST
Huang et al. 2018	Alcohol	- *Imaging:* fMRI. - *Modality:* Visual (Pictures). - *Design:* Block. Participants were instructed to watch and attend to the stimuli.	*DA*:11	**Sex** *DA:* 8 men, 3 women **Co-occurring disorders** No other axis I psychiatric condition other than alcohol abuse or dependence. **Socio-economic status** Not reported	*Alcohol:* Alcohol-related pictures.	*Non-alcoholic beverages:* Pictures of non-alcoholic beverages. *Control:* Blurred pictures.	*Assessment:* Before fMRI. *Scale:* Assessment of current craving using a Numeric Rating Scale (question: "How much do you desire for alcohol?"). The range of the scale is not reported. *Results:* No statistics is provided. Mean subjective alcohol craving reported in Table 1 is 8.32 (standard deviation: 1.87).	24 hours (minimum)	Ingestion	Not specified	Not specified	NST
Janes et al. 2015	Nicotine	- *Imaging:* fMRI. - *Modality:* Visual (Pictures). - *Design:* Event-related. Participants were instructed to watch and attend to the stimuli. To ensure attentional focus, participants were instructed to press a button when they see a	*DA*:17	**Sex** *DA:* 8 men, 9 women **Co-occurring disorders** No other axis I psychiatric condition other than nicotine abuse or dependence. **Socio-economic status** Education DA: 15.3 years (± 2.1)	*Nicotine:* Smoking-related pictures comprised of 3 categories: people smoking, people holding cigarettes and smoking-related items such as cigarettes.	*Neutral:* Neutral pictures matched for content with respect to people, body parts and manipulated objects (i.e. pens or paint brushes).	*Assessment:* Before the fMRI. *Scale:* Brief Questionnaire for Smoking Urges (Brief-QSU). *Results:* Data not reported.	1.5 hours	Smoking	9.5 ± 5.5 pack years	None	NST

Study	Drug	Imaging/Modality/Design	Sample	Sex / Co-occurring disorders / Socio-economic status	Drug stimuli	Neutral stimuli	Assessment/Scale/Results	Abstinence	Route	Duration of use	Other drugs	Treatment
		target image to ensure attention to the task.										
Janse Van Rensburg et al., 2009	**Nicotine**	- *Imaging:* fMRI. - *Modality:* Visual (Pictures). - *Design:* Crossover. Participants were instructed to watch and attend to the stimuli. Participants were asked to press a button to ensure attentional focus.	*DA:*10	**Sex** *DA:* 6 men, 4 women **Co-occurring disorders** No other axis I psychiatric condition other than nicotine abuse or dependence **Socio-economic status** Not reported	*Nicotine:* Smoking-related pictures (i.e. images of humans smoking cigarettes) taken from the International Smoking Image Series (ISIS).	*Neutral:* Neutral pictures (i.e. images of humans holding pens or glasses in their hands and mouths) of the same size as smoking-related pictures.	*Assessment:* Before fMRI. *Scale:* Three times before fMRI session the participants verbally rated their agreement to the statement 'I have a desire to smoke' [1 = 'strongly disagree', 7 = 'strongly agree']. *Results:* Baseline 'desire to smoke' was 4.4 (0.58) in the control condition.	15 hours	Smoking	8.2 ± 5.5 years	Not specified	NST
Kaag et al., 2018	**Cocaine**	- *Imaging:* fMRI. - *Modality:* Visual (Pictures). - *Design:* Event-related. Participants were instructed to watch and attend to the stimuli. To ensure participants' attention, they were instructed to press a key on a response box when they see a picture of an animal.	*DA:* 59 *HC:* 58	**Sex** *DA:* all men; *HC:* all men. **Co-occurring disorders** No other axis I psychiatric condition other than cocaine abuse or dependence. **Socio-economic status** Not reported.	*Cocaine:* Photos of cocaine and individuals snorting cocaine.	*Neutral:* Photos of individuals and objects visually matched to the cocaine pictures on color, composition and type of gesture.	*Assessment:* Inside MRI scanner, at baseline and at the end of the experimental paradigm. *Scale:* Visual analogue scale ("How much do you crave for cocaine right now?") ranging from 0 [Not at all] to 10 [Extremely]. *Results:* Only in DA, and not in HC, craving for cocaine significantly increased during the cue-reactivity task.	33/59 positive on drug urine screening	Intranasal	6 ± 12 years	Cannabis, MDMA, alcohol	NST
Kilts et al., 2001	**Cocaine**	- *Imaging:* PET (O[15]). - *Modality:* Imagery. - *Design:* Block. Participants are instructed to mentally rehearse the situation illustrated by the individual imagery script.	*DA:* 8	**Sex** *DA:* all men. **Co-occurring disorders** No other axis I and II psychiatric condition other than cocaine abuse or dependence; 1 subject fulfilled DSM-IV criteria for nicotine dependence and 1 subject fulfilled DSM-IV criteria for marijuana abuse. **Socio-economic status** Not reported.	*Cocaine:* Script-guided imagery of autobiographical memories. Participants described vivid episodic memories of ritualistic acts of cocaine use and anticipatory arousal.	*Neutral:* Neutral episodic memory recall, selected from either a beach or forest scene. *Anger:* Anger-episodic memory recall, selected from either a beach or forest scene.	*Assessment:* Following offset of the scanner. *Scale:* The inductive properties of the imagery scripts were evaluated for each condition using 0 to 10 visual analogue scales. For the cocaine scripts, subjects self-rated the vividness of the mental image ("how vivid was the image?") and the experience of drug craving ("how strong was the urge to use?"). *Results:* Anger-related script imagery was associated with mild to absent self-rated cocaine craving and it was significantly less compared to cocaine use scripts.	3-30 days (negative urine screening before fMRI)	Smoking (freebase, crack)	10 ± 6 years	Cigarettes (1/8 subjects), marijuana (1/8 subjects)	TS (inpatient treatment)

Kim et al., 2014	**Alcohol**	- *Imaging:* fMRI. - *Modality:* Visual (Videos). - *Design:* Block. Participants were instructed to watch and attend to the stimuli.	*DA*: 38 *HC*: 26	**Sex** *DA:* 27 men, 11 women HC:20 men, 6 women **Co-occurring disorders** No other axis I psychiatric condition other than alcohol abuse or dependence (DA group) or nicotine (both groups). **Socio-economic status** *DA* Education: 11.6 years (± 2.5) *HC* Education: 12.9 years (± 3.5)	*Alcohol:* Video depicting alcohol-related scenes to induce craving.	*Control:* Blurred video segment.	*Assessment*: Before fMRI. *Scale*: Korean Alcohol Urge Questionnaire (AUQ-K). *Results*: Alcoholic subjects had higher AUQ-K scores compared to healthy controls.	3-21 days	Ingestion	15.9 ± 9.5 years	Cigarettes	TS
Kober et al., 2016	**Cocaine**	- *Imaging:* fMRI. - *Modality:* Visual (Videos). - *Design:* Block. Participants were instructed to view six videos depicting cocaine, gambling, and sad scenarios.	*DA*: 30	**Sex** *DA:* 18 men, 12 women. **Co-occurring disorders** No other axis I psychiatric condition other than cocaine abuse or dependence. **Socio-economic status** Education: • men: 13.06 years (± 1.14); • women: 12.30 years (± 1.06).	*Cocaine:* Videos including cocaine use (e.g., presentation of cocaine and paraphernalia, preparation of a "crack hit," repeated smoking, and getting a rush with a description of how good it was).	*Gambling:* Videos including gambling experiences (e.g., spinning slot machines, rolling a dice). *Sad:* Videos describing sad experiences (e.g., death of a close family member, divorce).	*Assessment:* After each run during fMRI. *Scale:* Urge to use cocaine and to gamble rated on a scale ranging from 1 [Not at all] to 10 [A lot]. *Results:* Gambling videos were associated with the most intense responses compared to cocaine videos and sad videos. Cocaine videos were associated with more intense urges compared to the sad videos.	Not specified	Not specified	Not specified	Cigarettes, alcohol, marijuana	NST
Koopmann et al., 2018	**Alcohol**	- *Imaging:* fMRI. - *Modality:* Visual (Pictures). - *Design:* Block. Participants were instructed to watch and attend to the stimuli.	*DA*: 41	**Sex** *DA:* 30 men, 11 women **Co-occurring disorders** No other axis I psychiatric condition other than alcohol abuse or dependence, except from nicotine dependence in the last 12 months **Socio-economic status** Not reported	*Alcohol:* Alcohol-related pictures (wine, beer, spirit).	*Neutral:* Neutral objects.	*Assessment:* During fMRI, after each block. *Scale:* Assessment of current craving using a visual analogue scale ranging from 0 [No craving at all] to 100 [Very intense craving]. *Results:* No statistics is provided. Mean subjective alcohol cue-induced craving reported in Table 1 is 8.1 (standard deviation: 12.0).	10.1 ± 5.6 days	Ingestion	Not specified	Cigarettes	TS (inpatient treatment)
Kosten et al., 2006	**Cocaine**	- *Imaging:* fMRI. - *Modality:* Visual (Videos). - *Design:* Block. Participants were instructed to watch the	*DA:* 17	**Sex** *DA:* 12 men, 5 women. **Co-occurring disorders** No other axis I psychiatric condition	*Cocaine:* Videos of an actor pretending to smoke cocaine and get a rush.	*Neutral:* Videos describing vegetable prices.	*Assessment:* During fMRI, immediately after each video. *Scale:* Numbered scale ranging from 0 to 10 to rate craving intensity. *Results:* No significant correlation between brain activity and craving ratings.	10 days	Not specified	6 years	Cigarettes, alcohol	TS (participating in a clinical trial)

Author	Substance	Imaging / Design	Sample	Participant characteristics	Alcohol stimuli	Control	Assessment / Results		Route	Duration of use	Smoking	Treatment
		videos and rate their craving.		other than cocaine abuse or dependence. **Socio-economic status** Employment: • patients who relapsed from outpatient treatment: 5 employed, 4 unemployed; • patients who didn't relapse from outpatient treatment: 6 employed, 2 unemployed. Education: • patients who relapsed from outpatient treatment: 12 years (± 1.4); • patients who didn't relapse from outpatient treatment: 13 years (± 1.0).								
Krienke et al. 2014	**Alcohol**	- **Imaging:** fMRI. - **Modality:** Visual (Videos). - **Design:** Block. Participants were instructed to watch and attend to the stimuli.	**DA**:30	**Sex** *DA:* 23 men, 7 women **Co-occurring disorders** No other axis I psychiatric condition other than alcohol abuse or dependence. **Socio-economic status** Not reported	**Alcohol:** Alcohol-related videos tailored on the participant's preference (beer, wine or hard liquor).	**Control**: neutral videos (i.e. two hands folding and coloring a paper boat; a person soldering).	**Assessment:** During fMRI. **Scale:** The current craving level was assessed using a VAS ranging from 0 [No craving] to 10 [Heavy craving]. **Results:** There was a statistically significant increase in craving levels after the presentation of the alcohol-related compared to the control videos.	27.4 days (range: 4-70)	Ingestion	171.9 months	Cigarettes	NST
Lee et al., 2013	**Alcohol**	- **Imaging:** fMRI. - **Modality:** Visual (Pictures). - **Design:** Event-related. Participants were instructed to watch and attend to the stimuli. Participants reported craving in response to alcohol-related stimuli by means of a button press.	**DA**: 17 **HC**: 25	**Sex** *DA:* 12 men, 5 women HC: 18 men, 5 women **Co-occurring disorders** No other axis I psychiatric condition other than alcohol abuse or dependence (except nicotine- or caffeine-related disorders) **Socio-economic status** *DA* Education: 14.6 years (± 2.1)	**Alcohol:** Alcohol-related pictures (i.e. advertisements for alcoholic beverages and pictures of bottles of beer and soju).	**Control**: Non-alcoholic beverage pictures (similar to the alcohol-related cues with respect to size, color and other physical properties).	**Assessment:** Before and after fMRI. **Scale:** Participants were instructed: 'For each of the following pictures, if you crave alcohol, press the left button. If you don't crave alcohol, press the right button'. **Results:** During the craving paradigm, the patient group reported higher craving in response to alcohol-related stimuli compared to the control group.	39 ± 44 days	Ingestion	8.4 ± 5.9 years	Not specified	TS (out-patient treatment)

Study	Drug	Methods	Sample	Participants	Drug cue	Neutral/Stress cue	Craving assessment	Abstinence		Duration	Other substance	Treatment
				HC Education: 16.7 years (± 1.7)								
Li et al., 2005	**Cocaine**	- *Imaging:* fMRI. - *Modality:* Imagery. - *Design:* Block. Participants were told to mentally reenact personalized scripts about cocaine use, about neutral experiences and about acceptable stressful situations.	*DA:* 11	**Sex** *DA:* 5 men; 6 women. **Co-occurring disorders** No other axis I psychiatric condition other than cocaine abuse or dependence. **Socio-economic status** Education: • men: 13.4 years (± 2.8); • women: 11.8 years (± 1.0).	*Cocaine:* Scripts about drug-use situations included meeting with a friend to use drugs together after being paid at work.	*Stress:* Acceptable stressful situations included a breakup with a significant other, a verbal argument with a significant other or family member, and employment-related stress (e.g., being fired or laid off from work). *Neutral:* Include a beach scene, reading on a Sunday afternoon, an autumn day in the park.	*Assessment:* Before and after each trial during fMRI. *Scale:* Rate your craving for cocaine on a Likert scale ranging from 0 [None] to 10 [The highest level of craving ever experienced]. *Results:* Drug cue trials elicited a greater change in craving rating compared with stress trials.	2 weeks (minimum)	Not specified	12.6 years (averaged between males and females)	Not specified	TS (inpatient treatment)
Li et al., 2012	**Heroin**	- *Imaging:* fMRI. - *Modality:* Visual (Pictures). - *Design:* Event-related. Participants were instructed to watch drug-related and neutral pictures passively.	*DA:* 24 *HC:* 20	**Sex** *DA:* all men; *HC:* all men. **Co-occurring disorders** No other axis I psychiatric condition other than cocaine abuse or dependence. **Socio-economic status** *DA* Education: 10.9 years (± 3.1) *HC* Education: 10.1 years (± 2.3)	*Heroin:* Images of heroin injection, preparation, and paraphernalia	*Neutral:* Images of household objects or chores.	*Assessment:* Pre and post cue presentation. *Scale:* Subjective heroin craving was evaluated with a visual analogue scale ranging from 0 [Least craving] to 10 [Strongest craving] using the question "To what extent do you feel the urge to use heroin?". *Results:* Subjective craving scores after cue presentation were significantly higher than before cue presentation for the heroin-dependent patients.	21.7 ± 16 days	Not specified	78.6 ± 50.1 months	Cigarettes	TS (in-patient treatment)
Li et al., 2013a	**Heroin**	- *Imaging:* fMRI. - *Modality:* Visual (Pictures). - *Design:* Event-related. Participants were instructed to watch and attend to the stimuli.	*DA* *ST* :19 *LT:* 18	**Sex** *DA:* all men **Co-occurring disorders** No other axis I psychiatric condition other than heroin abuse or dependence except nicotine dependence. **Socio-economic status** *ST* Education: 9.7 years (±2.2) *LT*	*Heroin:* Heroin-related pictures.	*Neutral:* Neutral drug-unrelated pictures.	*Assessment:* Before and after the cue-reactivity run. *Scale:* craving was assessed using a visual analogue scale ranging from 0 to 10 answering to the question "To what extent do you feel the urge to use heroin?". *Results:* Subjective craving scores after cue exposure were significantly higher than before cue exposure for the short-term abstinence group, but not for the long-term abstinence group.	Protracted abstinence: 193.3 days Short abstinence: 23.6 days	Not specified	Protracted abstinence: 96.3 months Short abstinence: 80.5 months	Methadone	TS (in-patient treatment)

					Education: 8.8 years (±2.3)							
Li et al., 2013b	**Heroin**	- *Imaging:* fMRI. - *Modality:* Visual (Pictures). - *Design:* Event-related. Participants were instructed to watch and attend to the stimuli.	**DA** :14 **HC**: 15	**Sex** *DA:* all men *HC:* all men **Co-occurring disorders** No other axis I psychiatric condition other than heroin abuse or dependence. **Socio-economic status** *DA* Education: 9.4 years (± 2.6) *HC* Education: 9.2 years (± 2.4)	*Heroin:* Heroin-related pictures.	*Neutral:* Neutral pictures.	*Assessment:* Before and after fMRI. *Scale:* Assessment of current craving using a visual analogue scale ranging from 0 to 10. *Results:* The heroin-dependent group had a higher level of subjective craving after performing the cue-induced craving task, compared to controls.	17.6 ± 5.7 days	Not specified	89.3 ± 50.5 months	None	TS (recruited from drug rehabilitation center)
Li et al., 2015	**Heroin**	- *Imaging:* fMRI. - *Modality:* Visual (Pictures). - *Design:* Event-related. Participants were instructed to watch drug-related and neutral pictures.	*DA:* 44 *HC:* 20	**Sex** *DA:* all men; *HC:* all men. **Co-occurring disorders** No other axis I psychiatric condition other than cocaine abuse or dependence. **Socio-economic status** *DA* Education: • patients who relapsed: 9.5 years (± 2.3); • patients who didn't relapse: 9.2 years (± 1.9). *HC* Education: 10.0 years (± 2.3).	*Heroin:* Pictures of heroin injection, preparation and paraphernalia.	*Neutral:* Pictures of household objects or chores.	*Assessment:* Pre- and post- scan. *Scale:* Subjective heroin craving was evaluated with a visual analogue scale ("To what extent do you feel the urge to use heroin?") ranging from 0 to 10. *Results:* Subjects who relapsed showed significantly higher craving ratings after cue exposure compared to subjects who did not relapse.	12 hours (minimum)	Not specified	Relapsers: 69.2 months Non-relapsers: 92.3 months	Cigarettes, methadone	TS (recruited from drug rehabilitation center)

Study	Substance	Imaging/Design	Sample	Participant characteristics	Drug stimuli	Control/Neutral stimuli	Craving assessment	Abstinence	Consumption	Duration of use	Tobacco	Treatment
Li et al., 2019	**Nicotine**	- *Imaging:* fMRI. - *Modality:* Visual (Pictures). - *Design:* Block. Participants were instructed to watch and attend to the stimuli.	*DA*: 24	**Sex** *DA:* 23 men, 1 woman **Co-occurring disorders** No other axis I psychiatric condition other than nicotine abuse or dependence **Socio-economic status** Not reported	*Nicotine:* Smoking-related pictures.	*Control:* Neutral pictures.	*Assessment:* Before and after fMRI in each state. *Scale:* Tobacco Craving Questionnaire (TCQ). *Results:* The TCQ scores were significantly decreased after the scan in the hypnotic state (hypnotic state was not included in our meta-analysis).	2 hours (minimum)	Smoking	17.92 ± 6.83 years	Not specified	TS
Liberman et al., 2018	**Nicotine**	- *Imaging:* fMRI. - *Modality:* Visual (Pictures). - *Design:* Block. Participants were instructed to watch and attend to the stimuli. To ensure participants attention, a yellow dot was randomly presented once during each stimulus block. When the dot appeared, participants were asked to press on the reaction button.	*DA*: 5 *HC*: 5	**Sex** *DA:* 1 man, 4 women *HC:* 1 man, 4 women **Co-occurring disorders** No other axis I psychiatric condition other than nicotine abuse or dependence. Participants were excluded if they had alcohol or other drugs dependence. **Socio-economic status** Not reported	*Nicotine:* Smoking-related pictures (i.e. smoking persons, lit up cigarettes and hands holding cigarettes) taken from the International Smoking Image Series (ISIS).	*Control*: Scrambled smoking-related pictures..	*Assessment:* Before and after fMRI. *Scale:* Brief Questionnaire for Smoking Urges (Brief-QSU). *Results:* Smoking participants showed a significant increase of craving after fMRI.	Overnight abstinence	Smoking	Not specified	None	NST
Lou et al., 2012	**Heroin**	- *Imaging:* fMRI. - *Modality:* Visual (Pictures). - *Design:* Block. Participants were instructed to watch drug-related and neutral pictures passively.	*DA* *ST*:17 *LT*:17	**Sex** *DA:* all men **Co-occurring disorders** No other axis I psychiatric condition other than heroin abuse or dependence. **Socio-economic status** *ST* Education: 7.7 years (± 0.7) *LT* Education: 8.1 years (±0.4)	*Heroin:* Pictures of people using heroin.	*Neutral:* Pictures of people engaged in everyday activities.	*Assessment:* Before and after each block. *Scale:* The current craving level was assessed using a Likert scale ranging from 0 [Not at all] to 4 [Extremely]. *Results:* Craving significantly increased after heroin cues presentation in short- and long-term abstinence groups. Abstinence significantly increased craving ratings across cue types.	Short-term abstinence: 1.2 months Long-term abstinence: 13.6 months	Not specified	Short-term abstinence: 7 years Long-term abstinence: 8.2 years	Cigarettes	TS (in-patient treatment)
Mann et al., 2014	**Alcohol**	- *Imaging:* fMRI. - *Modality:* Visual (Pictures). - *Design:* Block. Participants were instructed to watch and attend to the stimuli.	*DA*: 73	**Sex** *DA:* 51 men, 22 women **Co-occurring disorders** No other axis I psychiatric condition other than alcohol abuse or dependence (apart from alcohol, nicotine and cannabis). **Socio-economic status**	*Alcohol:* Alcohol-related pictures.	*Neutral:* Affectively neutral pictures. *Control:* Scrambled alcohol-related pictures (comparable in color distribution, contrast, and complexity).	*Assessment:* Before and after fMRI. *Scale:* Alcohol craving was assessed by means of a VAS. *Results:* VAS results not reported.	Range: 14-21 days	Ingestion	Not specified	Cigarettes	TS (clinical trial)

Study	Substance	Task	Sample	Sex / Co-occurring disorders / Socio-economic status	Cue	Neutral/Control	Assessment / Scale / Results	Abstinence	Route	Use	Medication	
				Not reported								
McBride et al., 2006	**Nicotine**	- *Imaging:* fMRI. - *Modality:* Visual (Videos). - *Design:* Block. Participants were instructed to watch and attend to the stimuli.	DA:19	**Sex** *DA:* 10 men, 9 women **Co-occurring disorders** No other axis I psychiatric condition other than nicotine abuse or dependence **Socio-economic status** Not reported	*Nicotine:* Smoking-related videos (i.e. people lighting cigarettes, smoking while socializing, blowing smoke rings)	*Neutral:* Neutral videos (i.e. people getting their hair cut). Videos were similar in degree of facial exposure, movement, and physical characteristics of the actors.	*Assessment:* During fMRI. *Scale:* The craving questionnaire consisted of 7 items taken from a larger battery (Tiffany and Drobes, 1991); participants rated their agreement with each question on a VAS ranging from 0 [Not at all] to 10 [Extremely]. *Results:* Smoking videos were successful in significantly increasing subjective reports of craving.	Abstinence: 12 hours (minimum) Smoking = smoke as usual	Smoking	Not specified	None	NST
Moran et al., 2017	**Nicotine**	- *Imaging:* fMRI. - *Modality:* Visual (Pictures). - *Design:* Event-related. Participants were instructed to watch and attend to the stimuli. To ensure participants attention, an occasional target stimulus (picture of animal) was presented and subjects were required to press a button in response to the target.	DA: 19	**Sex** *DA:* 9 men, 10 women **Co-occurring disorders** No other axis I psychiatric condition other than nicotine abuse or dependence. **Socio-economic status** DA Education: 14.4 years (± 2.4)	*Nicotine:* Smoking-related pictures comprised of 3 categories: people smoking, people holding cigarettes and smoking-related items such as cigarettes.	*Neutral:* Neutral pictures (i.e. a person with pen in mouth, a hand holding a paintbrush and neutral items such as pens).	*Assessment:* Before and after fMRI. *Scale:* Questionnaire for Smoking Urges (QSU). *Results:* Control smokers had significantly greater increase of craving than smokers with schizophrenia after fMRI (schizophrenic patients were not included in our meta-analysis).	1.5 hours	Smoking	9.5 ± 5.2 pack years	None	NST
Myrick et al. 2008	**Alcohol**	- *Imaging:* fMRI. - *Modality:* Visual (Pictures). - *Design:* Block. Participants were instructed to watch and attend to the stimuli.	DA:24	**Sex** *DA:* 18 men, 6 women **Co-occurring disorders** No other axis I psychiatric condition other than alcohol abuse or dependence **Socio-economic status** DA Education: 13.25 years (± 2.07)	*Alcohol:* Alcohol-related pictures (i.e. wine, beer, spirits).	*Non-alcoholic beverages:* Pictures of non-alcoholic beverages. *Control:* Pictures matching the alcohol cues in color and hue but lack any object recognition.	*Assessment:* During fMRI. *Scale:* Alcohol craving was assessed by means of a VAS ranging from 0 [No craving at all] to 100 [Severe craving] after each block. *Results:* Placebo-treated participants reported higher craving compared to both participants treated with the combination of naltrexone and ondansetron hydrochloride and social drinking controls.	Not specified	Ingestion	Not specified	Not specified	NST
Myrick et al., 2004	**Alcohol**	- *Imaging:* fMRI. - *Modality:* Visual (Pictures). - *Design:* Block. Participants were instructed to watch	DA: 10 HC: 10	**Sex** *DA:* 8 men, 2 women HC:8 men, 2 women **Co-occurring disorders** No other axis I psychiatric condition	*Alcohol:* Alcohol-related pictures.	*Control*: Non-alcoholic beverage pictures.	*Assessment:* Before and during fMRI. *Scale:* Obsessive Compulsive Drinking Scale (OCDS) before scan and a VAS [0-100 mm] for real-time craving after each block. *Results:* At baseline, the alcoholic group reported a higher OCDS score compared to	24 hours (minimum)	Ingestion	Not specified	Not specified	NST

Study	Substance	Methodology	Sample	Participant characteristics	Cue	Control/Comparison	Assessment & Results	Abstinence	Route	Duration	Other substances	Treatment
		and attend to the stimuli.		other than alcohol abuse or dependence (excluding caffeine). **Socio-economic status** *DA* Education: 15.15 years (± 1.73) *HC* Education: 16.30 years (± 1.57) DA Race: 7 Caucasian HC Race: 10 Caucasian			the control group, and alcoholic subjects showed higher ratings of craving during viewing of alcohol pictures compared to non-alcoholic and control pictures.					
Park et al., 2007	**Alcohol**	- **Imaging:** fMRI. - **Modality:** Visual (Pictures). - **Design:** Block. Participants were instructed to watch and attend to the stimuli, and to indicate their craving levels after each block.	*DA*: 9 *HC*: 9	**Sex** *DA:* 8 men, 1 woman HC:7 men, 2 women **Co-occurring disorders** No other axis I psychiatric condition other than alcohol abuse or dependence **Socio-economic status** *DA* Education: 14.00 years (± 1.25) *HC* Education: 12.9 years (± 3.5) DA and HC: never married	*Alcohol*: Alcohol-related pictures (Korean beer and mild liquor).	*Control:* Duplications of liquor pictures with blurred distortions.	**Assessment:** Before and after the sip of alcohol (before fMRI), during fMRI. **Scale:** Obsessive Compulsive Drinking Scale (OCDS) before scan (pre- and post-sip), and a one-item Likert scale (range from 1 to 7 points) before and after scan. **Results:** Alcohol-dependent individuals had higher craving levels than controls pre- and post-sip. Alcoholic subjects showed higher levels of craving during visual cue compared with controls.	24 hours (minimum)	Ingestion	Not specified	Cigarettes	NST
Potenza et al., 2012	**Cocaine**	- **Imaging:** fMRI. - **Modality:** Imagery. - **Design:** Block. Participants were told to mentally reenact individualized drug-associated scripts and neutral relaxing scripts were generated in agreement with the clinical interview session.	*DA:* 30 *HC:* 36	**Sex** *DA:* 14 men,16 women; *HC:* 18 men, 18 women. **Co-occurring disorders** No other axis I psychiatric condition other than cocaine abuse or dependence, with the exception of alcohol or tobacco dependence. **Socio-economic status** Education: • men: 12.1 years (± 1.8); • women: 12.6 years (± 1.1).	*Cocaine:* Involved descriptions of anticipation and consummatory phases of substance use (e.g., being at a bar and being offered cocaine, using cocaine with a drug-using buddy).	*Stress:* Including familial conflicts and work-related stress. *Neutral:* Including resting on a beach or a fall day in the park.	**Assessment:** During scanning, pre- and post-trial. **Scale:** Likert scale ranging from 0 to 10. **Results:** Significant higher craving (and anxiety) ratings increase in cocaine scripts in cocaine addicted individuals compared to comparison subjects.	2 weeks (minimum)	Not specified	9.85 years (averaged between males and females)	Cigarettes, alcohol	TS (inpatient treatment)

| Prisciandaro et al., 2013a | Cocaine | - *Imaging:* fMRI.
- *Modality:* Visual (Pictures).
- *Design:* Block.

Participants were instructed to watch and attend to the stimuli. | *DA:* 30 | **Sex**
DA:
• with cocaine positive Urine Drug Screen (UDS+): 5 men, 1 woman;
• with cocaine negative Urine Drug Screen (UDS-): 20 men, 4 women.

Co-occurring disorders
No other axis I psychiatric condition other than cocaine abuse or dependence. Patients were excluded if they met DSM-IV criteria for non-cocaine substance dependence (except caffeine, nicotine, marijuana or alcohol).

Socio-economic status
Employment:
• UDS+: 1 employed, 5 unemployed;
• UDS-: 2 employed, 22 unemployed.

Education:
• UDS+: 4 graduated from high school, 2 didn't;
• UDS-: 21 graduated from high school, 3 didn't.

Marital status:
• UDS+: all married;
• UDS-: 18 married, 6 unmarried. | *Cocaine:* Pictures of cocaine and related objects (e.g., crack pipe). | *Neutral:* Objects (e.g., furniture).
Control: Images that lack object recognition processes, but matched by color and brightness. | *Assessment:* Inside MRI scanner, after each block.
Scale: Rate their craving, from 0 [None] to 4 [Severe], using a handpad.
Results: Participants with positive urine screening at one-week follow-up did not significantly differ from those with negative urine screening at follow-up in terms of subjective craving to cocaine minus neutral cues during the cue-reactivity task. | Participants were required to provide negative alcohol breath and urine drug screens for all drugs of abuse expect marijuana. | Not specified | Not reported | Cigarettes, marijuana, alcohol | TS (participating in a clinical trial) |

Prisciandaro et al., 2013b	**Cocaine**	- *Imaging:* fMRI. - *Modality:* Visual (Pictures). - *Design:* Block. Subjects were instructed to look at the pictures and to rate their craving.	*DA:* 25	**Sex** *DA:* • patients treated with d-cycloserine (DCS): all men; • patients treated with placebo: 13 men, 2 women. **Co-occurring disorders** No other axis I psychiatric condition other than cocaine abuse or dependence. Patients were excluded if they met DSM-IV criteria for non-cocaine substance dependence (except caffeine, nicotine, marijuana or alcohol). **Socio-economic status** Education: • patients treated with d-cycloserine (DCS): 9 graduated from high school, 1 didn't; • patients treated with placebo: 13 graduated from high school, 2 didn't. Marital status: • patients treated with d-cycloserine (DCS): 1 married, 9 unmarried; • patients treated with placebo: 4 married, 11 unmarried.	*Cocaine:* Fourteen of the 30 pictures contained both cocaine and cocaine paraphernalia (e.g., lighter, crack pipe, rolled paper money, razor), 12 contained cocaine only, and 4 depicted cocaine use.	*Neutral:* Pictures of neutral objects (e.g. furniture).	*Assessment:* During the task, after each block using a handpad. *Scale:* On a scale ranging from 0 [None] to 4 [Severe]. *Results:* Higher craving during cocaine versus neutral pictures. No significant change in craving pre- to post-fMRI.	72 hours	Not specified	Cocaine dependence onset: 33.5 years Mean age: 48.8 years	Cigarettes, marijuana	TS (participating in a clinical trial)
Prisciandaro et al., 2014	**Cocaine**	- *Imaging:* fMRI. - *Modality:* Visual (Pictures). - *Design:* Block. Participants were instructed to watch and attend to the stimuli.	*DA:* 33	**Sex** *DA:* 33 men, 5 women. **Co-occurring disorders** No other axis I psychiatric condition other than cocaine abuse or dependence. Patients were excluded if they met DSM-IV criteria for non-cocaine substance dependence (except	*Cocaine:* Pictures of cocaine and related objects (e.g., crack pipe).	*Neutral:* Objects (e.g., furniture) *Control:* Images that lack object recognition processes, but matched by color and brightness.	*Assessment:* Inside MRI scanner during the task, after each block. *Scale:* Rate their craving, from 0 [None] to 4 [Severe], using a handpad. *Results:* Subjective craving was significantly higher following cocaine pictures vs neutral objects blocks.	72 hours	Not specified	TS = 18.11 ± 9.31 years NST = 17.5 ± 5.79 years	Cigarettes	TS (outpatient treatment) and NST

Study	Drug	Imaging/Modality/Design	N	Demographics	Drug cue	Neutral cue	Craving assessment	Abstinence	Route	Years of use	Other substances	Treatment
				caffeine, nicotine, marijuana or alcohol). **Socio-economic status** Education: 18 attended college, 20 didn't. Marital status: 7 married, 31 unmarried.								
Ray et al., 2015	**Cocaine**	- *Imaging:* fMRI. - *Modality:* Visual (Videos). - *Design:* Block. Participants were instructed to watch and attend to the stimuli.	*DA:* 20 *HC:* 17	**Sex** *DA:* 15 men, 5 women; *HC:* 13 men, 4 women. **Co-occurring disorders** No other axis I psychiatric condition other than cocaine abuse or dependence. **Socio-economic status** Not reported.	*Cocaine:* Pictures of smokable cocaine, paraphernalia, and people smoking cocaine.	*Neutral:* Nature scenes.	*Assessment:* Inside MRI scanner, after the presentation of the first cocaine cue and neutral cue blocks. Craving ratings were collected also post-fMRI using the 10-item CCQ-Brief. *Scale:* Three-item version of the cocaine-craving questionnaire (CCQ-Brief). The items appeared one at a time on the screen, and participants had to press a button to rate their craving for cocaine on a seven-point scale from 1 [Strongly Disagree] to 7 [Strongly Agree]. *Results:* During the cue exposure task DA showed higher craving ratings to the cocaine cues compared to HC. Post-fMRI ratings showed that DA had a higher craving rating compared to HC.	72 hours	Smoking (freebase, crack)	16 years (range:3-34)	Cigarettes, alcohol	NST
Tabatabaei-Jafari et al., 2014	**Heroin**	- *Imaging:* fMRI. - *Modality:* Visual (Pictures). - *Design:* Block. Participants were instructed to watch and attend to the stimuli.	*DA* MMT:20 ABT:20 *HC:*20	**Sex** *DA:* all men; *HC:* all men **Co-occurring disorders** No other axis I psychiatric condition other than heroin abuse or dependence. Patients were excluded if they had a history of multidrug use except nicotine, alcohol, and benzodiazepines. **Socio-economic status** Not reported	*Heroin:* Heroin-related pictures.	*Neutral:* Neutral drug-unrelated pictures.	*Assessment:* Before and after fMRI. *Scale:* Desires for Drugs Questionnaire (DDQ): answer the questions on a 7-point Likert scale. *Results:* No significant change in craving levels after cue presentation in either group.	Abstinence: 9.2 months Methadone: 11.61 months	Smoking	Abstinence: 11.35 years Methadone: 11.05 years	Methadone, cigarettes	TS (recruited from drug rehabilitation center)

Study	Drug	Methods	Sample	Demographics	Drug cue	Control cue	Craving	Abstinence	Route	Duration	Other	
Tang et al., 2012	**Nicotine**	- *Imaging:* fMRI. - *Modality:* Visual (Videos). - *Design:* Block. Participants were instructed to watch and attend to the stimuli.	*DA Met-Fast:*15 *DA Met-Slow:*16	**Sex** DA Met-Fast*:* 11 men, 4 women DA Met-Slow: 12 men, 4 women **Co-occurring disorders** No other axis I psychiatric condition other than nicotine abuse or dependence. **Socio-economic status** Race *DA Met-Fast* • 8 Caucasian • 3 Asian • 4 Latin/Hispanic *DA Met-Slow* • 8 Caucasian • 6 Asian • 2 Latin/Hispanic	*Nicotine:* Smoking-related videos (i.e. lighting cigarettes, smoking while socializing).	*Neutral:* Neutral videos (except for the absence of smoking cues, i.e. getting hair cut), similar in terms of facial exposure, movement, and physical characteristics of the actors and did not include audio.	*Assessment:* Before and during fMRI. *Scale:* The craving questionnaire consisted of 3 items taken from a larger battery (Tiffany and Drobes, 1991); participants rated their agreement with each question by means of a Likert scale ranging from 0 [Not at all] to 20 [Extremely]. *Results:* Craving scores were calculated by subtracting craving levels before scanning from craving after scanning. There were no significant differences between fast and slow nicotine metabolism groups, and normal and reduced genotype groups in changes in craving scores.	Smoking as usual	Smoking	12 ± 5.2 years	None	NST
Tomasi et al., 2015	**Cocaine**	- *Imaging:* fMRI. - *Modality:* Visual (Videos). - *Design:* Block. Participants were instructed to watch the screen continuously and to press a response button with their right thumb whenever they liked the features of the scene.	*DA:* 20	**Sex** *DA:* all men. **Co-occurring disorders** No other axis I psychiatric condition other than cocaine abuse or dependence. **Socio-economic status** Not reported.	*Cocaine:* Scenes that simulated purchase, preparation, and smoking of cocaine.	*Neutral:* Scenes about routine administrative/technical work. *Food:* Scenes portraying scenes of serving and consuming ready to eat foods (i.e., meatballs, pasta, omelets, burger, and pancakes).	*Assessment:* During fMRI. *Scale:* The more the subjects pressed the response button during the food, cocaine, and neutral epochs the more they liked the features displayed in the respective scenes. The number of button presses was used to compute relative valences in a scale from 0 to 10. *Results:* The valences were lower for neutral cues than for food or cocaine cues but did not differ for food and cocaine cues.	Positive urine testing (cocaine use within 72 hours)	Smoking (freebase, crack) and/or intravenously	19.4 years (computed with "Enauguge Digitalizer"(Mitchell et al.) from the upper plot in Figure 8)	Cigarettes	NST
Volkow et al., 2010	**Cocaine**	- *Imaging:* PET (^{18}FDG). - *Modality:* Visual (Videos). - *Design:* Block. Participants are instructed to look at the videos and rate their craving.	*DA:* 24	**Sex** *DA:* 21 men; 3 women. **Co-occurring disorders** No other axis I psychiatric condition other than cocaine abuse or dependence. **Socio-economic status** Education: 13 years (± 2).	*Cocaine:* Cocaine-cue video with no instruction to inhibit craving responses, portraying scenes that simulated purchase, preparation, and smoking of cocaine.	*Baseline:* Eyes open, no video exposure.	*Assessment:* Pre and post video exposure. *Scale:* Visual analogue scale ranging from 1 to 10 for self-reports of "cocaine craving" and CCQ-brief. *Results:* Significant increase of craving from pre to post cocaine video exposure in the no-inhibition condition.	2.5 ± 2 days	Smoking (freebase, crack)	17 ± 6 years	Cigarettes	NST

Study	Substance	Method	N	Participants	Substance cues	Control stimuli	Craving assessment					
Vollstädt-Klein et al., 2010	Alcohol	- *Imaging:* fMRI. - *Modality:* Visual (Pictures). - *Design:* Block. Participants were instructed to watch and attend to the stimuli.	*DA*:21	**Sex** *DA:* 12 men, 9 women **Co-occurring disorders** No other axis I psychiatric condition other than alcohol abuse or dependence (and tobacco) **Socio-economic status** Not reported	*Alcohol:* Alcohol-related pictures (i.e. wine, beer, spirits).	*Control:* Neutral stimuli taken from the International Affective Picture Series (IAPS) and were matched for color distribution and complexity to the alcohol cues.	*Assessment:* During fMRI after each block. *Scale:* Alcohol craving was assessed by means of a VAS ranging from 0 [No craving at all] to 100 [Severe craving] after each block. *Results:* VAS results not reported.	1.2 ± 0.9 days	Ingestion	Not specified	Not specified	NST
Vollstädt-Klein et al., 2011	Nicotine	- *Imaging:* fMRI. - *Modality:* Visual (Pictures). - *Design:* Block. Participants were instructed to watch and attend to the stimuli. After the scanning session participants performed an unannounced recognition task, to test whether they paid sufficient attention to the stimuli during the fMRI session.	*DA*:22 *HC*:21	**Sex** *DA:* all men *HC:* all men **Co-occurring disorders** No other axis I psychiatric condition other than nicotine abuse or dependence **Socio-economic status** Not reported	*Nicotine:* Smoking-related advertisements taken from print media.	*Neutral:* Neutral advertisements taken from print media (i.e. areas household, personal hygiene and clothing) and matched to tobacco advertisings regarding complexity, colors and content.	*Assessment:* During fMRI. *Scale:* After each block, the participants were asked to rate their craving on a VAS ranging from 0 [No craving at all] to 100 [Extreme craving]. *Results:* Smokers reported substantially more subjective craving after presentation of tobacco advertisement (mean □= 41.3) □ than after control advertisement (mean = 27.8).	Prior to scanning	Smoking	14.6 ± 7.2 years	None	NST
Wang et al., 2014	Heroin	- *Imaging:* fMRI. - *Modality:* Visual (Pictures). - *Design:* Event-related. Participants were instructed to watch and attend to the stimuli.	*DA* A: 15 B: 15 *HC*: 17	**Sex** *DA:* all men; HC: all men **Co-occurring disorders** No other axis I psychiatric condition other than heroin abuse or dependence, except nicotine. **Socio-economic status** *DA* education*:* • A: 9.2 years (± 1.6) • B: 9.47 years (± 2.7) *HC* education: 10.6 ± 2.4	*Heroin:* Images of heroin injection, preparation, and paraphernalia.	*Neutral:* Images of household objects or chores.	*Assessment:* Before and after fMRI. *Scale:* Assessment of current craving using a visual analogue scale ranging from 0 to 10. *Results:* No significant change in craving levels after cue presentation in either group. No significant different craving levels between the groups.	Group A: 7.92 months Group B: 29.62 months	Not specified	Group A: 48.6 months Group B: 49.64 months	Methadone	TS (out-patient treatment)

Study	Drug	Imaging	Sample	Sex / Co-occurring disorders / Socio-economic status	Drug-related stimuli	Neutral stimuli	Craving assessment	Abstinence	Route	Duration	Tobacco	TS
Wang et al., 2015	**Heroin**	- *Imaging:* fMRI. - *Modality:* Visual (Pictures). - *Design:* Event-related. Participants were instructed to watch and attend to the stimuli.	**DA**: 32	**Sex** *DA:* 17 men, 15 women. **Co-occurring disorders** No other axis I psychiatric condition other than heroin abuse or dependence with the exception of opioid and nicotine dependence, non-dependent cocaine abuse and depressive disorders. **Socio-economic status** Education: 13.2 years (±1.9) Race: • 28 Caucasian • 2 African American • 2 Asian	*Heroin:* Images of heroin injection, paraphernalia and preparation.	*Neutral:* Household objects or chores, graphically and contextually matched to the heroin-related stimuli.	*Assessment:* Pre and post cue reactivity task. *Scale:* Craving for heroin were assessed on a scale ranging from 0 [Not at all] to 9 [Extremely]. *Results:* A significant increase of craving scores was observed across treatment groups. The magnitude of cue-induced craving was significantly reduced in the treatment group after the last drug administration.	Not specified (fMRI after detoxification)	Intravenous	Not specified	Not specified	TS (participating in a clinical trial)
Wei et al., 2019	**Heroin**	- *Imaging:* fMRI. - *Modality:* Visual (Pictures). - *Design:* Event-related. Participants were instructed to watch and attend to the stimuli.	*DA MMT:18* *PA:23* *HC: 20*	**Sex** *DA:* all men; HC: all men **Co-occurring disorders** No other axis I psychiatric condition other than heroin abuse or dependence. Patients were excluded if they met a drug abuse history other than heroin dependence. **Socio-economic status** *HC* Education: 11.1 years (± 2.3) *MMT* Education :10.3 years (±2.2) *PA* Education :10.4 years (±2.0)	*Heroin:* Images of heroin injection, paraphernalia and preparation.	*Neutral:* Household objects or chores.	*Assessment:* Pre and post fMRI scan. *Scale:* Craving was assessed using a Likert scale ranging from 0 [Least craving] to 10 [Strongest craving] answering to the question "To what extent do you feel the urge to use heroin?". *Results:* No significant increase in craving was observed in the short- nor long-abstinence groups.	Methadone: 5.6 months Protracted abstinence: 6 months	Not specified	Methadone :88.86 months Protracted abstinence: 99.3 months	Cigarettes	TS (recruited from drug rehabilitation center)
Wrase et al., 2007	**Alcohol**	- *Imaging:* fMRI. - *Modality:* Visual (Pictures). - *Design:* Event-related. Participants were instructed to passively view the stimuli.	*DA*:13 *HC*:16	**Sex** *DA:* all men HC: all men **Co-occurring disorders** No other axis I psychiatric condition other than alcohol abuse or dependence **Socio-economic status**	*Alcohol:* Alcohol-related pictures.	*Control*: Neutral stimuli all inanimate and matched for complexity and color with the alcohol cues.	No assessment of cue-induced craving.	11.5 ± 7.5 days (range: 5-37)	Ingestion	12.69 ± 7.09 years	Cigarettes	TS (in-patient treatment)

Study	Drug	Method	Sample	Participant characteristics	Drug stimuli	Neutral stimuli	Craving assessment					Setting
		Participants had to confirm every viewed picture with a button press with the right thumb.		DA Education: 9.06 years (± 1.69) HC Education: 11.69 years (± 1.54)								
Xiao et al., 2006	**Heroin**	- *Imaging:* fMRI. - *Modality:* Visual (Pictures). - *Design:* Block. Participants were instructed to watch drug-related and neutral pictures passively for future recognition. Eye-tracking to ensure attention to the stimuli.	*DA:* 14	**Sex** *DA:* all men. **Co-occurring disorders** No other axis I psychiatric condition other than cocaine abuse or dependence. **Socio-economic status** Not reported.	*Heroin:* Drug-related pictures.	*Neutral:* Neutral scenes pictures.	*Assessment:* Only pre-fMRI interview. *Scale:* Craving measured on a scale ranging from 1 to 5. *Results:* The interview indicated that participants showed a moderate (3.5) level of craving.	8.5 hours	Not specified	7.1 years (range: 2-16)	Not specified	TS (in-patient treatment)
Yalachkov, Kaiser, Naumer, 2009	**Nicotine**	- *Imaging:* fMRI. - *Modality:* Visual (Pictures). - *Design:* Block. Participants were instructed to watch and attend to the stimuli.	*DA:*15 *HC:*15	**Sex** *DA:* 6 men, 9 women *HC:* 6 men, 9 women **Co-occurring disorders** No other axis I psychiatric condition other than nicotine abuse or dependence. **Socio-economic status** Not reported	*Nicotine:* Smoking-related pictures (i.e. images of humans smoking cigarettes) taken from the International Smoking Image Series (ISIS).	*Neutral:* Neutral pictures (i.e. images of humans holding pens or glasses in their hands and mouths) of the same size as smoking-related pictures.	No assessment of cue-induced craving.	Smoking as usual	Smoking	Not specified	Not specified	NST
Zanchi et al., 2015	**Nicotine**	- *Imaging:* fMRI. - *Modality:* Visual (Videos). - *Design:* Block. Participants were instructed to watch and attend to the stimuli.	*DA:*14 *HC:*18	**Sex** *DA:* 4 men, 10 women *HC:* 7 men, 11 women **Co-occurring disorders** No other axis I psychiatric condition other than nicotine abuse or dependence. **Socio-economic status** Not reported	*Nicotine:* Smoking-related videos filmed in a first-person point of view (i.e. writing a letter and smoking a cigarette or standing outside of a nightclub smoking a cigarette).	*Neutral:* Neutral videos matched for similar content except for the absence of smoking cues.	*Assessment:* During fMRI. *Scale:* After each video participants were asked to rate the degree of craving by means of a Likert scale ranging from 0 [No craving] to 7 [High craving]. *Results:* Smoking videos induced higher craving in smokers than in non-smokers.	15 minutes	Smoking	29.3 ± 6 years	Not specified	NST
Zeng et al., 2018	**Heroin**	- *Imaging:* fMRI. - *Modality:* Visual (Pictures). - *Design:* Block. Participants were instructed to watch drug-related and neutral pictures (in isolation, with tool	*DA:* 37 *HC:* 29	**Sex** *DA:* 24 men, 13 women; *HC:* 19 men, 10 women. **Co-occurring disorders** No other axis I psychiatric condition other than cocaine abuse or dependence.	*Heroin:* Drug images containing only the drug itself, drug use tool images consisting of pictures of a syringe and other tools for using heroin and drug	*Neutral:* Including granular material pictures, daily life manipulable object pictures and pictures of people engaged in activities using manipulable objects.	*Assessment:* Pre- and post-fMRI. *Scale:* Visual Analogue Scale ranging from 0 to 7 to rate the current craving for heroin. *Results:* No significant increase in craving ratings from pre- to post-fMRI.	42.11 ± 21.65 months	Nor specified	21.32 ± 47.32 months	Cigarettes, alcohol	TS (recruited from drug rehabilitation center)

		Cue-reactivity paradigm	Sample size	Sample characteristics	Drug cue	Baseline condition	Cue-induced craving assessment	Abstinence	Main route of administration	History of abuse		Treatment status
		present, with body parts engaged in drug-taking actions) and to press a button to declare that they have seen the picture clearly.		**Socio-economic status** *DA* Education: 9.83 years (± 1.8). *HC* Education: 10.41 years (± 1.16).	using action images containing people engaged in the activities of using tools to absorb or inject heroin.							
Zhang et al., 2018	**Cocaine**	- *Imaging:* fMRI. - *Modality:* Visual (Pictures). - *Design:* Block. Participants were asked to look at the pictures and think about how they may relate to the scenes.	*DA:* 23	**Sex** *DA:* 17 men, 6 women. **Co-occurring disorders** No other axis I psychiatric condition other than cocaine abuse or dependence. **Socio-economic status** Not reported.	*Cocaine:* Pictures displaying people preparing and snorting/smoking cocaine.	*Neutral:* Scenes of people performing various acts with similar color and complexity as inspected visually.	*Assessment:* Inside scanner, at the end of each block. *Scale:* After each block it was assessed by means of visual analogue scale ranging from 0 [No craving] to 10 [Highest craving ever]. *Results:* DA reported higher craving when viewing cocaine pictures as compared with viewing neutral pictures.	12.1 ± 5.8 days	Not specified	16 ± 9.7 years	Cigarettes	TS (inpatient treatment)
Zijlstra et al., 2009	**Heroin**	- *Imaging:* fMRI. - *Modality:* Visual (Pictures). - *Design:* Block. Participants were instructed to watch and attend to the stimuli.	*DA:* 12	**Sex** *DA:* all men **Co-occurring disorders** No other axis I psychiatric condition other than heroin abuse or dependence. **Socio-economic status** Not reported	*Heroin:* Pictures depicting drug preparation and objects used for the preparation for a dose of heroin for inhalation.	*Baseline:* Black screen with a centered white crosshair.	*Assessment:* Desires for Drugs Questionnaire (DDQ) at baseline during the intake, and at the end of fMRI. *Scale:* DDQ for desire and intention to take drugs: 7 questions with response on a 7-point Likert scale. *Results:* No significant increase of heroin craving was observed after cue presentation.	8.8 weeks	Intranasal	16 ± 6.8 years	Cigarettes	TS (in-patient treatment)

Table S3.1 | Studied included in the meta-analysis. Brief description of the experimental paradigms included and of the population involved in the included studies. The column '*Cue-reactivity paradigm'* contains information about the imaging modality, type of stimuli used (pictures, videos, imagery scripts), fMRI task design (block, event-related), and instructions given to the participants. The columns *'Sample size'* and *'Sample characteristics'* report basic information about the sample (number of participants, sex distribution, co-occurring disorders, and socio-economic status). The columns '*Drug cue'* and '*Baseline condition'* contain information about the content of the experimental and control stimuli, respectively (only [cue > baseline] contrasts were included). The column '*Cue-induced craving assessment'* contains a summary of the craving assessments and eventual changes in craving due to the cue-reactivity paradigm. The column '*Abstinence'* reports the average time (if not otherwise specified) of abstinence before the fMRI session. The column '*Main route of administration'* contains information about the preferred route of administration of the substance. The column '*History of abuse'* report the average (if not otherwise specified) time of substance use; pack years = numbers of packs of cigarettes smoked per day * number of years smoking. The column '*Treatment status'* reports whether participants were treatment-seeking (TS) or not-seeking treatment (NST) at the time of the study. fMRI, functional Magnetic Resonance Imaging; PET, Positron Emission Tomography; VAS, Visual Analogue Scale. Taken from: Devoto et al. *Transl. Psych.*

2.2. Table S3.2

Cluster ID	Centroid label (BA)	Left hemisphere			Right hemisphere			N	# of contributing studies	CoS		TR		CoSxTR
		X (SD)	Y (SD)	Z (SD)	X (SD)	Y (SD)	Z (SD)			L	IL	TS	NST	
2	Putamen				23 (2.4)	5 (1.9)	-4 (5.6)	8	8	.316	.881	.664	.618	.313
6	Superior medial frontal gyrus (10)	-4 (9)	58 (3.7)	24 (4.9)				9	3	.062	.987	.931	.206	1
7	Amygdala (34)				25 (3.8)	1 (3.5)	-20 (2.8)	9	5	.891	.313	.559	.707	1
8	Hippocampus (35)				23 (5.4)	-10 (2.5)	-18 (6.1)	14	8	.928	.197	.771	.419	1
18	Precuneus (23)				9 (3.6)	-52 (4.9)	35 (5.2)	8	7	.316	.881	.967	.13	.313
19	Middle temporal gyrus (37)				52 (3.6)	-57 (3.4)	1 (6.2)	9	5	.891	.313	.293	.901	1
20	Inferior temporal gyrus (37)				51 (5.2)	-66 (3.2)	-6 (4.6)	22	10	.861	.267	.239	.879	.581
21	Inferior occipital gyrus (19)	-46 (4.5)	-70 (3.8)	-8 (3.9)				17	4	.616 [a]	.583 [a]	.552	.645	.102
22	Inferior temporal gyrus (37)	-51 (3.4)	-63 (4.2)	-5 (5.8)				17	8	.995	.027 [b]	.076	.977	1
27	Caudate	-10 (3)	5 (2.9)	7 (4.6)				12	9	.964	.134	.121	.968	1
28	Caudate	-13 (6.7)	17 (3.8)	2 (4)				9	7	.687	.582	.794	.441	.032 [b]
29	Ventral striatum (25)				12 (3.6)	-1 (3.2)	-13 (2.8)	8	5	.972	.154	.382	.858	1
30	Nucleus accumbens				8 (3.4)	8 (5.6)	-6 (6.1)	19	10	.986	.049 [b]	.597	.59	1

37	Precuneus (23)	-9 (3.7)	-57 (3.6)	33 (3.4)				12	8	.098	.969	.742	.474	.052
38	Posterior cingulum (23)	-4 (3)	-50 (4.9)	26 (3.7)				19	15	.735	.443	.41	.762	.225
42	Inferior parietal lobule(40)				37 (4.7)	-50 (5.2)	51 (4)	16	10	.74	.454	.627	.576	.513
47	Middle occipital gyrus (19)				49 (3.7)	-77 (4.9)	4 (4.3)	6	5	.7 [a]	.626 [a]	.607	.716	1
50	Posterior cingulum (23)	-4 (6.8)	-32 (4.6)	31 (3.3)				12	10	.447	.764	.742	.474	1
51	Inferior frontal gyrus, pars opercularis (44)				47 (3.4)	9 (2.1)	25 (4.6)	10	9	.989	.076	.461	.779	1
60	Middle cingulum (24)				1 (4.4)	3 (8.7)	34 (4.4)	11	8	.947	.181	.165	.953	1
61	Cuneus	0 (4.3)	-71 (3.4)	29 (2.4)				5	3	.252	.94	.934	.266	1
62	Calcarine scissure/Precuneus (17/30)	0 (6.3)	-59 (5.1)	15 (4)				12	6	.995	.036 [b]	.032 [b]	.996	1
68	Lingual gyrus (27)	-15 (5.3)	-35 (4.8)	-6 (5.3)				10	9	.515 [a]	.728 [a]	.461	.779	1
69	Midbrain (ventral tegmental area)	-5 (2.8)	-23 (6.7)	-9 (4.7)				12	9	.995	.036 [b]	.032 [b]	.996	.438
82	Hippocampus (30)				17 (6)	-24 (3.3)	-7 (6.3)	11	10	.36	.833	.982	.067	.343
92	Medial orbitofrontal gyrus (10)	-5 (5.6)	52 (4.7)	-4 (4.9)				15	11	.47	.726	.701	.5	.006 [c]
95	Caudate				13 (5)	14 (5.4)	9 (5.8)	21	17	.923	.174	.153	.934	1
96	Anterior cingulate cortex (32)	-5 (5.9)	45 (4.5)	18 (5.8)				20	9	.622 [a]	.562 [a]	.087	.97	.54

ID	Label	x	y	z	x	y	z	Foci	Studies	p	p	p	p	p
97	Hippocampus/amygdala (35/28)	-21 (4.2)	-5 (3.7)	-21 (3.3)				17	9	1	.005 [c]	.076	.977	1
101	Nucleus accumbens	-7 (4)	11 (4.9)	-10 (5.3)				18	10	.934	.165	.293	.854	.506
103	Perigenual anterior cingulate cortex (32)				2 (4.5)	40 (3.5)	5 (7)	16	12	.344	.817	.908	.204	.045 [b]
107	Inferior occipital gyrus (19)				37 (5)	-78 (4.2)	-12 (3.3)	10	8	.989	.076	.221	.932	1
114	Dorsal anterior cingulate cortex (24)	0 (2.3)	29 (4.2)	22 (6.1)				13	7	.003 [c]	1	.999	.004 [c]	1
116	Thalamus				1 (3.6)	-11 (3.7)	4 (4.7)	24	10	.913	.181	.158	.927	.04 [b]

Table S3.2 | Results of the cluster composition analysis for all the clusters overlapping with the ALE map. For each cluster, the following information are reported: cluster ID, anatomical label according to the AAL (and Brodmann area, BA), centroid coordinates (standard deviation) in MNI, number of contributing foci, number of contributing studies, p-values for the binomial tests (class of substances, treatment status) and for the Fisher's exact tests (class of substances-by-treatment status interactions). [a], undifferentiated clusters; [b], $p < .05$; [c], $p < .01$.

2.3. Table S3.3

Table S3.3 | Full list of words identified by Neurosynth. Full list of 100 terms identified by Neurosynth for all the CCA maps. Each term is clickable and redirects to the corresponding Neurosynth page.
[a], words considered for discussion. In brackets are semantic complements taken from the exploration of the papers contributing to the term.

Undifferentiated		Class of substances		Treatment status		Class of substances-by-treatment status	
Word	**r-value**	**Word**	**r-value**	**Word**	**r-value**	**Word**	**r-value**
traits (personality) [a]	0.09	tools [a]	0.098	midbrain	0.098	engagement [a]	0.238
medial prefrontal	0.088	ventral	0.089	substantia	0.09	cortex vmpfc	0.236
mpfc	0.081	motivational [a]	0.078	gyrus cerebellum	0.082	vmpfc	0.23
cingulate cortex	0.077	midbrain	0.076	periaqueductal	0.079	ventromedial prefrontal	0.188
mentalizing [a]	0.075	anticipation [a]	0.076	parietal occipital	0.077	ventromedial	0.184
beliefs [a]	0.074	nucleus accumbens	0.075	cortex precuneus	0.066	referential (self) [a]	0.161
anterior cingulate	0.071	accumbens	0.072	dmn	0.056	mpfc	0.151
medial	0.069	addiction [a]	0.072	aversive [a]	0.056	connectivity	0.15
anterior	0.068	reward anticipation [a]	0.071	reversal (learning) [a]	0.055	midline	0.141
cortex acc	0.066	nucleus	0.07	network dmn	0.054	self referential	0.14
cingulate	0.066	outcome [a]	0.069	pcc	0.052	cortex mpfc	0.138
trait	0.064	hypothalamus	0.069	anticipatory [a]	0.052	cingulate cortex	0.138
acc	0.063	ventral striatum	0.068	ventral tegmental	0.049	anterior cingulate	0.129
craving [a]	0.059	substantia	0.068	hypothalamus	0.049	medial prefrontal	0.129
cortex mpfc	0.058	striatum	0.066	tegmental	0.048	default mode	0.129
visual stimuli [a]	0.057	motivation	0.066	heart (rate) [a]	0.047	default	0.128

214

Term	Value	Term	Value	Term	Value	Term	Value
contexts [a]	0.055	mesolimbic	0.064	precuneus	0.045	cingulate	0.122
autobiographical [a]	0.053	subjective [a]	0.061	intense (emotion) [a]	0.043	medial	0.118
moral (decision-making) [a]	0.052	behavior [a]	0.061	posterior cingulate	0.041	prefrontal cortex	0.117
prefrontal cortex	0.051	monetary reward [a]	0.06	default mode	0.039	posterior cingulate	0.112
emotion regulation [a]	0.051	reward	0.059	brainstem	0.038	network dmn	0.104
stress [a]	0.05	complex [a]	0.058	episodic memory [a]	0.038	dmn	0.103
prefrontal	0.049	lateral occipital	0.057	dopaminergic	0.038	functional connectivity	0.103
cortex anterior	0.048	dopaminergic	0.057	default	0.037	pcc	0.099
emotional	0.045	monetary	0.055	nucleus	0.037	cortex posterior	0.095
oscillations [a]	0.045	gyrus cerebellum	0.054	episodic	0.036	anterior	0.092
posterior cingulate	0.041	rewarding	0.054	autobiographical [a]	0.035	ventral striatum	0.091
occipital cortex	0.039	behaviors	0.052	ventral	0.033	prefrontal	0.09
personality	0.039	periaqueductal	0.051	cognitive emotional [a]	0.032	acc	0.088
object recognition [a]	0.039	parietal occipital	0.051	medial frontal	0.032	value [a]	0.085
placebo [a]	0.039	probabilistic [a]	0.051	amnestic	0.03	rostral	0.083
lateral occipital	0.038	ventral tegmental	0.05	thalamus	0.03	medial orbitofrontal	0.082
attended [a]	0.037	tegmental	0.049	cortex pcc	0.029	rostral anterior	0.081
occipital temporal	0.035	objects [a]	0.049	force [a]	0.028	reward [a]	0.079
dorsal medial	0.035	object	0.048	anticipation	0.028	medial pfc	0.078
abuse [a]	0.034	incentive delay [a]	0.048	junction tpj	0.028	cortex acc	0.076
selective	0.033	rewards	0.047	fear [a]	0.026	traits (personality) [a]	0.074
default mode	0.033	form [a]	0.047	reward [a]	0.026	rest	0.072
dmn	0.032	incentive	0.044	cortex posterior	0.025	dorsal attention	0.07
referential	0.032	sighted [a]	0.043	heart rate	0.024	ventral anterior	0.067

personality traits	0.032	cortex precuneus	0.043	mild cognitive [a]	0.023	personality	0.064
mt	0.031	monetary incentive	0.042	striatum	0.023	choose [a]	0.063
spectrum disorder	0.031	modality	0.042	resting state	0.022	cortex pcc	0.062
preferences	0.031	visual motion	0.041	pain [a]	0.022	arousal [a]	0.062
object	0.03	self report	0.041	tpj	0.022	striatum	0.061
default	0.029	lexical	0.04	posterior	0.022	task positive [a]	0.058
stream	0.029	abstract	0.038	medial	0.021	autobiographical [a]	0.058
resting state	0.028	posterior	0.038	personal [a]	0.02	default network	0.055
familiar	0.028	multisensory	0.038	sensation [a]	0.019	rewards	0.054
social	0.027	aversive	0.037	motivational	0.019	monetary [a]	0.05
resting	0.027	stream	0.037	autobiographical memory	0.019	moral (decision-making) [a]	0.047
passively	0.027	reversal	0.037	skin conductance	0.017	contexts [a]	0.044
readers	0.026	dmn	0.036	painful	0.017	resting	0.043
word pairs	0.026	striatal	0.036	autonomic	0.017	hubs	0.042
ventral visual	0.026	reinforcement	0.036	midline	0.016	monetary incentive [a]	0.042
mesolimbic	0.026	inferior temporal	0.035	rewards	0.016	expectations [a]	0.042
chinese	0.025	network dmn	0.035	mesolimbic	0.015	resting state	0.041
objects	0.025	money	0.034	reward anticipation	0.015	valence [a]	0.041
encoding	0.025	occipitotemporal	0.034	retrosplenial cortex	0.014	remembering	0.04
characters	0.025	anticipatory	0.034	vmpfc	0.014	risky	0.039
emotion	0.024	medial lateral	0.033	basal ganglia	0.014	solving	0.039
extrastriate	0.023	pcc	0.033	ganglia	0.014	nucleus	0.037
parahippocampal gyrus	0.023	value	0.032	video clips	0.014	striatal	0.037
color	0.022	preferences	0.032	electrical	0.014	ventral medial	0.037

occipito temporal	0.022	vision	0.032	resting	0.012	personal	0.036
visual cortex	0.022	risky	0.032	insular cortex	0.011	anticipation	0.036
personal	0.021	risk taking	0.032	conditioning	0.011	motivational	0.036
occipitotemporal	0.021	occipito temporal	0.031	subcortical	0.011	caudate	0.036
insula anterior	0.021	sexual	0.03	mentalizing	0.01	thinking	0.035
functional connectivity	0.021	heart	0.03	nociceptive	0.01	gains	0.034
gestures	0.02	early visual	0.03	memories	0.01	incentive	0.034
orthographic	0.02	prediction error	0.029	striatal	0.009	dmpfc	0.034
emotional valence	0.02	intense	0.029	retrosplenial	0.009	caudate nucleus	0.034
medial frontal	0.02	familiar	0.029	ventromedial	0.008	cognitive emotional	0.033
visual word	0.02	precuneus	0.028	neutral	0.008	mental states	0.033
learning	0.019	delay	0.028	ventral striatum	0.008	retrosplenial	0.033
occipital	0.019	reinforcement learning	0.027	monetary	0.008	orbitofrontal	0.032
category	0.019	dorsolateral pfc	0.026	cingulate cortex	0.007	nucleus accumbens	0.031
parahippocampal	0.019	words	0.026	amygdala	0.007	social interactions	0.03
self referential	0.018	action	0.026	nuclei	0.006	retrosplenial cortex	0.029
reactions	0.018	recognition	0.026	noxious	0.006	thalamus	0.029
word form	0.018	occipito	0.026	basal	0.006	dorsal striatum	0.028
ratings	0.018	perceptual	0.025	medial prefrontal	0.006	intense	0.028
learning task	0.017	posterior cingulate	0.025	cingulate	0.006	incentive delay	0.027
matching	0.017	conceptual	0.025	prefrontal cortex	0.005	construction	0.027
motion	0.017	word form	0.025	semantic	0.005	cortico	0.027
visual motion	0.017	eating	0.025	vi	0.004	dopamine	0.027
form	0.017	gambling	0.025	retrieval	0.004	accumbens	0.026

lobe mtl	0.017	avoidance	0.024	memory	0.003	memory retrieval	0.026
network dmn	0.017	brainstem	0.024	prefrontal	0.002	sexual	0.025
lobe	0.017	unfamiliar	0.024	insula	0.002	emotion	0.025
valence	0.016	verbs	0.024	controls	0.001	rewarding	0.025
temporal cortex	0.016	visual word	0.024	disorder	0.001	mesolimbic	0.025
cortex hippocampus	0.016	default mode	0.024	chronic	0	risk taking	0.024
tools	0.016	speakers	0.023	cerebral cortex	0	posterior	0.023
mtl	0.016	episodic memory	0.023	questionnaire	0	regulate	0.022
visual	0.016	default	0.022	reference	0	limbic	0.022
pseudowords	0.016	dorsal striatum	0.022	categorization	0	confidence	0.022
watching	0.015	languages	0.022	correction	0	losses	0.022
visuo	0.015	animal	0.022	rt	0	autobiographical memory	0.021
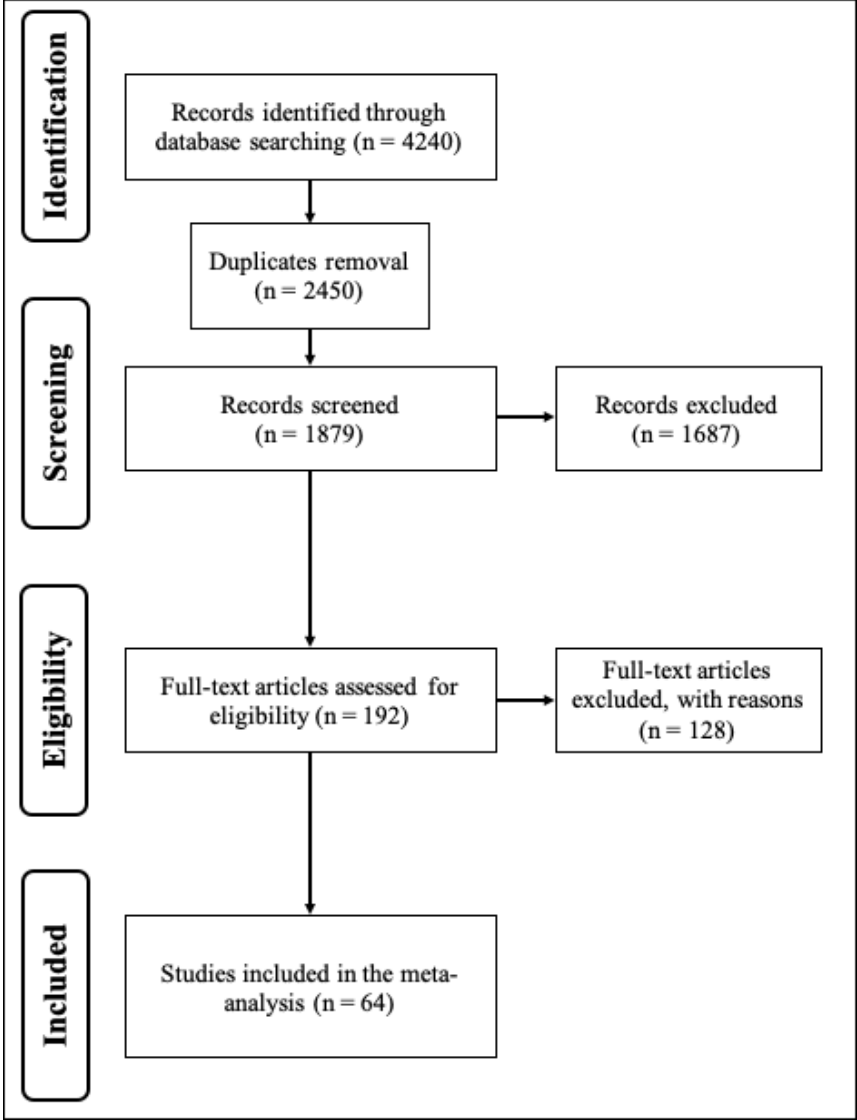
Figure S3.1 | Paper selection strategy. Flowchart of the study search and selection process that led to the identification of 64 final studies.
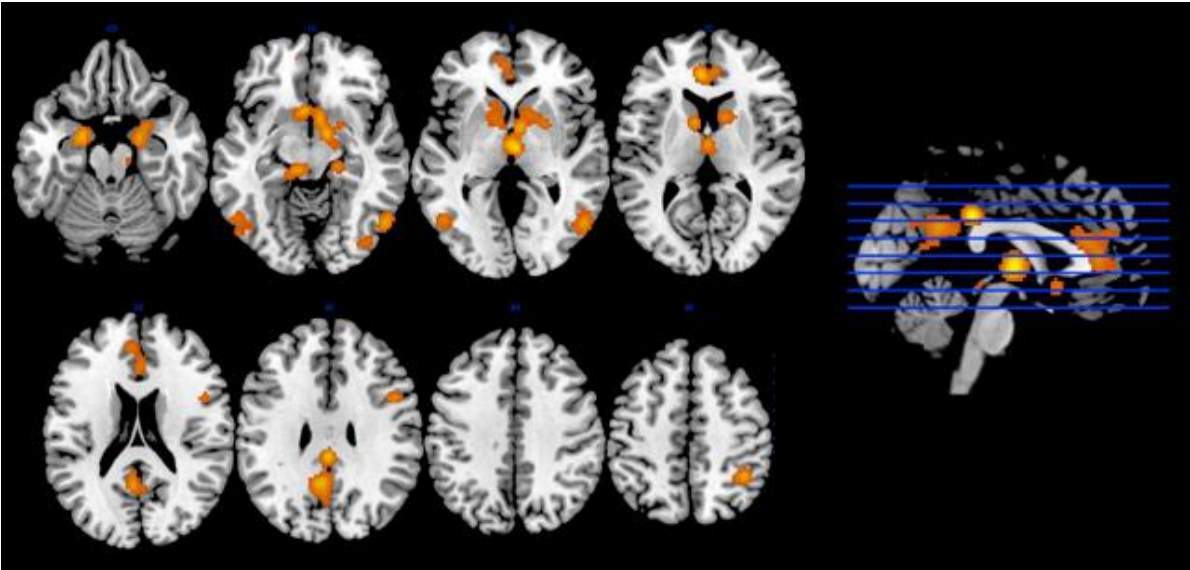
Figure S3.2 | Results of the ALE meta-analysis. The results of the ALE meta-analysis are overlaid on a structural template in MNI space. This map was used to perform the cross-validation method described in the methods section.

Supplementary File 3 - Repetitive Deep TMS for the Reduction of Body Weight: Bimodal Effect on the Functional Brain Connectivity in Obese Individuals

Supplementary File 3

1. Supplementary Methods

2. Supplementary Results

1. Supplementary Methods

1.1. Randomization code

The randomization code was made accessible (by an independent investigator not involved with any other aspects of the trial) only to the treating investigator at the first treatment session. The independent investigator could be contacted at any time to unblind the randomization code, but only in the case of serious adverse events. Participants and other investigators were unaware of the type of treatment to which they were assigned, and the magnetic stimulation coil for active and sham treatments (dTMS sessions) was the same. Magnetic cards encoding for real or sham stimulation were used to activate the dTMS device or not, according to the randomization sequence. Both real and sham stimulation produced identical sounds and scalp sensations during the sessions. In the cue condition, each daily repetitive dTMS session was preceded by showing the patients pictures of their favourite food, identified during the interview with the subjects at the Screening visit. In the cue condition, each daily repetitive dTMS session was preceded by showing the patients pictures of their favourite food, identified during the interview with the subjects at the Screening visit. Since all subjects but one (in the realTMS group) were exposed to food cues prior to the daily stimulation, the factor cue-condition was not taken into account in data analysis.

1.2. Diet and lifestyle recommendations

The energy requirement was calculated by the dietitian based on the measured basal metabolic rate (via indirect calorimetry) and the physical activity of each subject identified at the Screening visit. 300 kcal/day were subtracted from this amount of energy to obtain the recommended hypocaloric diet. The daily dietary intake included approximately 45% to 50% calorie intake from carbohydrates, up to 30% of calories from fats, and 20% to 25% of calories from proteins. At each follow-up visit, the dietitian confirmed the reduction of food intake with a direct interview. The participants were also instructed to engage in moderate-intensity physical activity (e.g., 30-minute walking every day) during the study.

2. Supplementary results

2.1. Drop-out patients

In the real stimulation group, one patient reported an asymptomatic incidentaloma diagnosed while performing the fMRI, the study was discontinued to allow the patient to proceed with the necessary therapeutic itinerary; another patient decided to stop the study after the first session

due to treatment intolerance; the last patient decided to voluntarily withdraw from the studio, immediately after randomization, for personal reasons.

In the sham stimulation group, three patients decided to voluntarily withdraw from the studio, immediately after randomization, for personal reasons; one patient decided to stop the study after the first 5 sessions due to treatment ineffectiveness.

2.2. Table S4.1

Table S4.1. Complete results of the Neurosynth analysis | Full list of 50 terms and correlation values resulted from the Neurosynth analysis for the **(A)** mOFC and **(B)** occipital pole rsFC maps. Anatomical-related terms are highlighted in bold.

A) mOFC		B) Occipital pole	
Term	*Correlation*	*Term*	*Correlation*
medial orbitofrontal	0.464	**v1**	0.508
ventromedial	0.438	**primary visual**	0.397
ventromedial prefrontal	0.425	**visual cortex**	0.353
orbitofrontal	0.419	**lingual gyrus**	0.341
vmpfc	0.410	early visual	0.311
orbitofrontal cortex	0.409	**cuneus**	0.268
ofc	0.359	**lingual**	0.266
cortex ofc	0.352	visual	0.230
cortex vmpfc	0.337	**occipital**	0.187
subgenual	0.294	sighted	0.147
ventral medial	0.260	**visual cortices**	0.142
value	0.199	**occipital cortex**	0.130
medial	0.197	mental imagery	0.124
reward	0.180	metabolism	0.100
medial prefrontal	0.171	visual stimulus	0.096
reinforcement	0.133	eye movement	0.091
anterior cingulate	0.126	vision	0.069
cingulate	0.123	**occipito**	0.056
prefrontal cortex	0.121	**mt**	0.054
ventral striatum	0.119	sensory information	0.047
orbital	0.118	erp	0.044
social	0.115	visual field	0.038
medial lateral	0.114	negativity	0.037
spectrum disorder	0.114	invasive	0.034
food	0.113	naturalistic	0.034
prefrontal	0.112	category	0.033
striatum	0.106	**occipital lobe**	0.031
anterior	0.106	**occipital temporal**	0.031

amygdala	0.100		agent	0.031
cingulate cortex	0.099		navigation	0.029
valence	0.097		low level	0.028
rewards	0.093		integrative	0.027
rostral anterior	0.089		**visual stream**	0.026
olfactory	0.089		eye movements	0.026
positive negative	0.089		pair	0.026
arousal	0.083		categorization	0.025
autonomic	0.083		**parietal lobules**	0.025
suffering	0.080		imagery	0.025
mentalizing	0.078		**extrastriate**	0.024
decision	0.077		**middle occipital**	0.024
affective	0.077		add	0.024
implicit	0.076		competition	0.024
pleasant	0.073		blind	0.023
computation	0.071		modalities	0.022
choices	0.070		**temporal frontal**	0.022
conductance	0.068		**inferior superior**	0.021
skin conductance	0.068		concept	0.021
taste	0.065		**v5**	0.021
emotional	0.065		remembering	0.021
subjective	0.064		**retrosplenial**	0.021

Supplementary File 4

1. Supplementary Tables

1. Supplementary Tables

1.1. Table SA1.1

Table SA1.1 | Results of CluB with User's Spatial Criterion set to 7 mm. For each cluster, the anatomical label according with the AAL the mean centroid coordinates in MNI stereotaxic space, the standard deviation along the three axes and the cardinality (N) are reported. Taken from: Berlingeri et al. 2019.

	Left Hemisphere							Right Hemisphere						
	μx	μy	μz	SDx	SDy	SDz	N	μx	μy	μz	SDx	SDy	SDz	N
Inferior Frontal Gyrus, pars Orbitalis	-40	23	-13	5.31	8.16	8.50	12	52	34	-2	4.88	5.03	5.15	10
Inferior Frontal Gyrus, pars Triangularis	-42	32	29	4.27	4.08	11.08	6	57	34	16	3.21	7.21	5.09	7
	-46	37	3	6.72	5.11	6.64	14							
Inferior Frontal Gyrus, pars Opercularis	-47	12	18	4.63	5.47	8.65	19							
Rolandic Operculum								60	9	6	8.32	8.33	11.06	12
Middle Frontal Gyrus								39	39	40	3.06	3.06	6.93	3
Middle Frontal Gyrus, pars Orbitalis	-36	51	-7	5.18	4.15	8.79	5	37	45	-15	8.64	8.01	4.22	10
Superior Frontal Gyrus	-14	57	38	6.00	5.76	8.00	5							
Superior Medial Frontal Gyrus								10	58	36	9.59	4.75	7.13	8
								7	38	58	8.08	1.91	4.43	4

Region	x	y	z				n	x	y	z				n
Gyrus Rectus	-3	50	-19	4.16	7.21	4.16	3							
Anterior Cingulum	-9	22	25	7.55	10.56	12.12	10							
Supplementary Motor Area	-7	7	67	8.59	10.70	6.24	12							
Precentral Gyrus	-45	4	55	5.75	6.89	3.91	10	36	-10	58	2.61	8.29	10.77	5
	-39	5	38	4.93	7.87	3.40	11	49	10	43	4.60	8.65	3.03	5
	-27	-25	73	8.33	8.33	1.15	3							
Postcentral Gyrus	-60	-10	33	2.31	10.55	11.53	7							
Paracentral Lobule								5	-27	60	8.25	3.83	6.32	4
Superior Parietal Lobule	-31	-63	60	3.03	3.90	6.16	5							
Inferior Parietal Lobule	-50	-42	57	4.29	5.90	7.42	9	48	-42	56	8.29	9.63	4.97	6
Supramarginal Gyrus								65	-39	26	4.76	5.51	8.49	4
Superior Temporal Gyrus	-53	-44	24	7.12	7.86	6.36	10							
	-58	4	-10	2.63	5.96	7.71	10							
Superior Temporal Pole	-28	8	-29	5.17	8.17	5.20	9	48	15	-19	7.13	5.29	8.16	12

Region														
Middle Temporal Gyrus	-57	-45	4	4.98	9.55	4.55	15	55	-26	-12	7.17	4.45	6.81	14
	-62	-20	-7	4.78	6.77	8.53	15	62	-45	-4	3.71	7.69	10.58	16
Inferior Temporal Gyrus	-62	-41	-15	4.63	2.73	8.45	6							
Fusiform Gyrus	-42	-47	-24	1.98	5.35	7.29	8							
Precuneus	-10	-53	71	11.35	6.72	7.95	5	6	-51	9	9.32	5.02	8.79	5
Cuneus								7	-92	24	4.73	5.26	8.06	4
Lingual Gyrus								25	-98	-13	7.48	3.99	5.64	15
								10	-76	-10	7.27	9.50	6.20	6
Superior Occipital Gyrus								20	-103	5	3.58	2.76	4.84	6
								27	-63	37	1.15	3.06	4.16	3
Middle Occipital Gyrus	-25	-100	2	5.61	4.18	4.25	12	38	-90	3	6.62	6.69	6.02	6
	-32	-73	34	6.36	7.01	9.91	10							
Inferior Occipital Gyrus	-18	-102	-11	4.86	3.24	3.66	12							
	-30	-93	-11	5.95	5.06	4.75	14							
	-43	-69	-14	5.25	9.10	7.93	10							

228

Region	x	y	z				n	x	y	z				n
Parahippocampal Gyrus	-26	-12	-24	4.87	5.18	5.18	8							
	-14	-27	-10	9.10	5.93	6.54	5							
Hippocampus								25	-20	-7	7.08	5.43	9.17	9
								22	-4	-17	8.97	9.02	9.09	10
Vermis								5	-61	-38	5.85	7.48	10.05	8
Cerebellum, Crus I								29	-83	-25	5.13	4.43	4.43	7
								38	-60	-26	6.89	10.36	5.53	10
Cerebellum, Crus II	-23	-81	-42	12.25	5.49	5.46	9	30	-76	-45	9.59	4.54	4.13	8
Thalamus	-7	-6	1	5.38	10.09	9.30	7							
No Region	-26	-45	24	3.65	10.06	13.95	7							

1.2. Table SA1.2

Table SA1.2 | Results of CluB with User's Spatial Criterion set to 8 mm. For each cluster, the anatomical label according with the AAL the mean centroid coordinates in MNI stereotaxic space, the standard deviation along the three axes and the cardinality (N) are reported. Taken from: Berlingeri et al. 2019.

	Left Hemisphere							Right Hemisphere						
	μx	μy	μz	SDx	SDy	SDz	N	μx	μy	μz	SDx	SDy	SDz	N
Inferior Frontal Gyrus, pars Orbitalis	-40	23	-13	5.31	8.16	8.50	12							
Inferior Frontal Gyrus, pars Triangularis	-42	32	29	4.27	4.08	11.08	6	54	34	5	4.86	5.81	10.44	17
	-43	40	1	7.54	8.01	8.35	19							
Inferior Frontal Gyrus, pars Opercularis	-47	12	18	4.63	5.47	8.65	19							
Rolandic Operculum								60	9	6	8.32	8.33	11.06	12
Medial Frontal Gyrus, pars Orbitalis								37	45	-15	8.64	8.01	4.22	10
Medial Frontal Gyrus								46	21	42	6.39	16.80	4.66	8
Superior Frontal Gyrus								1	57	37	14.71	4.93	7.23	13
								7	38	58	8.08	1.91	4.43	4
Gyrus Rectus	-3	50	-19	4.16	7.21	4.16	3							

Region														
Anterior Cingulum	-9	22	25	7.55	10.56	12.12	10							
Supplementary Motor Area	-7	7	67	8.59	10.70	6.24	12							
Precentral Gyrus	-27	-25	73	8.33	8.33	1.15	3	36	-10	58	2.61	8.29	10.77	5
	-42	4	46	6.06	7.26	9.22	21							
Postcentral Gyrus	-60	-10	33	2.31	10.55	11.53	7							
Postcentral Lobe								5	-27	60	8.25	3.83	6.32	4
Superior Parietal Lobule	-20	-58	65	13.64	7.39	8.80	10							
Inferior Parietal Lobule	-50	-42	57	4.29	5.90	7.42	9	48	-42	56	8.29	9.63	4.97	6
Supramarginal Gyrus								65	-39	26	4.76	5.51	8.49	4
Superior Temporal Gyrus	-53	-44	24	7.12	7.86	6.36	10							
	-58	4	-10	2.63	5.96	7.71	10							
Superior Temporal Pole	-28	8	-29	5.17	8.17	5.20	9	48	15	-19	7.13	5.29	8.16	12
Medial Temporal Gyrus	-59	-43	-2	5.15	8.30	10.19	21	55	-26	-12	7.17	4.45	6.81	14
	-62	-20	-7	4.78	6.77	8.53	15	62	-45	-4	3.71	7.69	10.58	16

Region	x	y	z	t1	t2	t3	k	x	y	z	t1	t2	t3	k
Precuneus								6	-51	9	9.32	5.02	8.79	5
Cuneus								7	-92	24	4.73	5.26	8.06	4
Lingual Gyrus								10	-76	-10	7.27	9.50	6.20	6
								25	-98	-13	7.48	3.99	5.64	15
Fusiform Gyrus	-42	-47	-24	1.98	5.35	7.29	8							
Superior Occipital Gyrus								27	-63	37	1.15	3.06	4.16	3
Medial Occipital Gyrus	-32	-73	34	6.36	7.01	9.91	10	29	-97	4	10.53	8.36	5.26	12
Inferior Occipital Gyrus	-25	-98	-7	7.27	5.83	7.56	38							
	-43	-69	-14	5.25	9.10	7.93	10							
Hippocampus	-21	-18	-18	8.82	9.04	9.01	13	23	-12	-12	8.08	11.17	10.44	19
Vermis								5	-61	-38	5.85	7.48	10.05	8
Cerebellum, Crus I								38	-60	-26	6.89	10.36	5.53	10
Cerebellum, Crus II	-23	-81	-42	12.25	5.49	5.46	9	29	-79	-36	7.61	5.50	11.44	15
Thalamus	-7	-6	1	5.38	10.09	9.30	7							
No Region	-26	-45	24	3.65	10.06	13.95	7							

1.3. Table SA1.3

Table SA1.3 | Results of CluB with User's Spatial Criterion set to 9 mm. For each cluster, the anatomical label according with the AAL the mean centroid coordinates in MNI stereotaxic space, the standard deviation along the three axes and the cardinality (N) are reported. Taken from: Berlingeri et al. 2019.

	Left Hemisphere							**Right Hemisphere**						
	μx	**μy**	**μz**	**SDx**	**SDy**	**SDz**	**N**	**μx**	**μy**	**μz**	**SDx**	**SDy**	**SDz**	**N**
Inferior Frontal Gyrus, pars Orbitalis	-40	35	-2	4.90	1.03	6.07	6	47	20	-11	5.26	4.32	4.12	4
								46	40	-17	1.63	5.00	2.58	4
								52	34	-2	4.88	5.03	5.15	10
Inferior Frontal Gyrus, pars Triangularis	-43	32	23	5.26	5.00	5.00	4	57	34	16	3.21	7.21	5.09	7
	-50	38	7	3.92	6.50	3.69	8							
Inferior Frontal Gyrus, pars Opercularis	-45	11	24	5.01	5.89	5.99	11	43	12	17	7.07	0.00	7.07	2
	-49	14	10	2.60	4.46	2.14	8	62	17	2	1.00	2.58	4.90	4
Middle Frontal Gyrus	-37	15	57	1.41	4.24	7.07	2	39	39	40	3.06	3.06	6.93	3
	-42	32	42	2.83	2.83	5.66	2							
	-36	9	36	3.27	5.50	1.38	7							

Region	x	y	z				n	x	y	z				n
Middle Frontal Gyrus, pars Orbitalis	-36	51	-7	5.18	4.15	8.79	5	32	49	-13	5.85	7.76	4.52	6
Superior Frontal Gyrus	-16	19	63	6.00	5.03	7.02	3	21	57	38	6.43	3.06	6.00	3
	-14	57	38	6.00	5.76	8.00	5							
Superior Medial Frontal Gyrus								4	58	34	3.16	5.83	8.05	5
								7	38	58	8.08	1.91	4.43	4
Gyrus Rectus	-3	50	-19	4.16	7.21	4.16	3							
Anterior Cingulum	-17	38	19	4.24	0.00	1.41	2							
Middle Cingulum	-6	22	39	3.65	8.39	6.19	4							
Supplementary Motor Area	-9	-3	71	4.38	6.87	3.03	5	3	9	64	3.42	4.76	6.53	4
Precentral Gyrus	-27	-25	73	8.33	8.33	1.15	3	36	-10	58	2.61	8.29	10.77	5
	-47	1	54	4.41	3.70	3.28	8	49	10	43	4.60	8.65	3.03	5
	-44	-3	42	2.31	3.83	3.42	4	65	6	20	1.41	5.66	8.49	2
Postcentral Gyrus	-45	-37	65	3.06	6.43	4.16	3							
	-59	-16	43	1.15	8.17	1.91	4							

Region	x	y	z				x	y	z			
	-61	-3	21	3.06	9.02	3.06	3					
Paracentral Lobule	5	-27	60	8.25	3.83	6.32	4					
Insula	-37	16	-4	5.93	6.84	4.77	5					
Superior Parietal Lobule	-17	-49	71	8.33	4.16	11.02	3	41	-50	57	2.31	5.29	7.02	3
	-31	-63	60	3.03	3.90	6.16	5					
Inferior Parietal Lobule	-53	-45	52	2.07	3.01	3.67	6	55	-34	54	5.77	3.46	2.00	3
Supramarginal Gyrus	-58	-44	28	3.67	9.16	3.67	6	65	-39	26	4.76	5.51	8.49	4
Superior Temporal Pole	-58	4	-10	2.63	5.96	7.71	10	43	15	-28	5.29	2.00	2.83	4
	-41	28	-19	4.43	4.00	4.43	7					
	-29	17	-30	5.00	4.43	5.16	4					
Middle Temporal Pole	56	10	-18	4.43	3.65	3.65	4					
Superior Temporal Gyrus	-45	-45	19	1.15	6.63	6.22	4	63	2	-4	3.46	8.06	4.32	4
Middle Temporal Gyrus	-57	-52	5	6.23	6.23	5.45	8	60	-53	3	3.74	4.60	3.63	5
	-58	-36	2	3.55	2.83	2.83	7	65	-38	-1	3.21	3.55	7.46	7
	-63	-22	-2	5.01	6.31	4.60	10	55	-26	-9	7.87	3.90	2.43	11

Region	x	y	z			n	x	y	z			n
	-60	-16	-16	4.34	6.39	4.98	5						
Inferior Temporal Gyrus	-62	-41	-15	4.63	2.73	8.45	6	61	-47	-19	2.58	5.74	4.16	4
								57	-24	-24	4.62	6.93	2.00	3
Fusiform Gyrus	-43	-63	-18	3.50	3.50	5.85	6						
	-42	-47	-24	1.98	5.35	7.29	8						
Precuneus	-27	-49	14	3.46	7.02	5.26	4	1	-59	70	1.41	4.24	2.83	2
								10	-48	15	10.00	3.46	3.06	3
Cuneus								7	-92	24	4.73	5.26	8.06	4
Lingual Gyrus								16	-84	-6	3.46	3.46	6.00	3
								16	-102	-15	4.34	2.61	4.82	5
Superior Occipital Gyrus								27	-63	37	1.15	3.06	4.16	3
								20	-103	5	3.58	2.76	4.84	6
Middle Occipital Gyrus	-33	-73	39	7.47	8.46	3.80	7	38	-90	3	6.62	6.69	6.02	6
	-30	-74	22	2.00	2.00	10.00	3						
	-25	-100	2	5.61	4.18	4.25	12						

Region	x	y	z				x	y	z			
Inferior Occipital Gyrus	-43	-79	-7	7.90	5.26	4.43	4	30	-96	-11	3.75	3.05	5.82	10
	-18	-102	-11	4.86	3.24	3.66	12						
	-30	-93	-11	5.95	5.06	4.75	14						
Amygdala	-28	2	-28	5.90	1.41	5.55	5						
Parahippocampal Gyrus	-20	-25	-14	3.46	6.11	3.46	3	21	-27	-16	1.15	1.15	4.00	3
	-26	-12	-24	4.87	5.18	5.18	8	18	-7	-22	5.59	8.38	4.68	7
Vermis	-1	-55	0	1.41	4.24	2.83	2	4	-69	-14	3.46	6.11	3.46	3
								2	-54	-31	5.51	2.83	7.72	4
Cerebellum, Crus I								41	-69	-25	3.35	5.22	5.02	5
								29	-83	-25	5.13	4.43	4.43	7
Cerebellum, Crus II	-13	-82	-41	5.97	4.90	3.42	4	25	-79	-44	7.01	3.03	3.85	5
	-32	-80	-44	7.87	6.32	6.63	5	39	-71	-48	5.03	1.15	3.46	3
Cerebellum VI								34	-52	-28	8.17	6.16	6.23	5
Cerebellum VIII	8	-68	-45	4.62	1.00	6.00	4						
Thalamus	-3	-13	8	1.91	4.12	5.97	4						

Region														
Caudate	-9	15	15	9.85	5.29	1.15	4							
Putamen								27	-17	-2	7.87	3.03	7.04	6
								30	5	-6	11.14	1.15	5.29	3
Pallidum	-12	3	-7	2.00	8.08	4.16	3							
No Region	-25	-39	38	4.16	12.22	5.29	3							
	-4	-30	-3	0.00	5.66	1.41	2							

1.4. Table SA1.4

Table SA1.4 | Results of CluB with User's Spatial Criterion set to 10 mm. For each cluster, the anatomical label according with the AAL the mean centroid coordinates in MNI stereotaxic space, the standard deviation along the three axes and the cardinality (N) are reported. Taken from: Berlingeri et al. 2019.

	Left Hemisphere							Right Hemisphere						
	μx	μy	μz	SDx	SDy	SDz	n	μx	μy	μz	SDx	SDy	SDz	n
Inferior Frontal Gyrus, pars Triangularis	-43	40	1	7.54	8.01	8.35	19	54	34	5	4.86	5.81	10.44	17
Inferior Frontal Gyrus, pars Opercularis	-46	17	21	4.85	9.85	10.17	25							
Anterior Cingulum	-9	22	25	7.55	10.56	12.12	10							
Superior Medial Frontal Gyrus								2	53	42	13.48	9.72	11.24	17
Middle Frontal Gyrus, pars Opercularis								28	46	-16	19.44	7.85	4.41	13
Supplementary Motor Area	-7	7	67	8.59	10.70	6.24	12							
Precentral Gyrus	-46	1	43	9.63	10.27	11.12	28	42	9	48	7.16	20.89	10.82	13
Paracentral Lobule	-9	-26	65	18.86	5.59	8.14	7							
Superior Parietal Lobe	-20	-58	65	13.64	7.39	8.80	10							
Inferior Parietal Lobule	-50	-42	57	4.29	5.90	7.42	9							
Supramarginal Gyrus	-42	-44	24	14.68	8.53	9.78	17	55	-41	44	11.08	8.06	16.50	10
Superior Temporal Pole	-35	17	-20	7.66	10.80	10.79	21	54	12	-7	9.48	7.45	15.64	24
Middle Temporal Gyrus	-59	-43	-2	5.15	8.30	10.19	21	59	-36	-8	6.53	11.64	9.79	30
	-61	-10	-8	4.38	13.39	8.19	25							
Fusiform Gyrus	-42	-59	-18	4.03	13.50	9.06	18							
Cuneus								15	-79	29	11.31	15.95	9.37	7
Lingual Gyrus								8	-65	-1	8.15	15.26	12.27	11
Middle Occipital Gyrus	-32	-73	34	6.36	7.01	9.91	10							
Inferior Occipital Gyrus	-25	-98	-7	7.27	5.83	7.56	38	27	-97	-5	8.97	6.21	10.00	27
Hippocampus								23	-12	-12	8.08	11.17	10.44	19
Vermis								5	-61	-38	5.85	7.48	10.05	8

Region	x	y	z				N	x	y	z				N
Cerebellum, Crus I								33	-72	-32	8.31	12.04	10.49	25
Cerebellum, Crus II	-23	-81	-42	12.25	5.49	5.46	9							
Thalamus	-16	-14	-12	10.37	10.91	13.01	20							
No region	-16	-14	-12	10.37	10.91	13.01	20							

Table SA1.5 | Results of CluB with User's Spatial Criterion set to 11 mm. For each cluster, the anatomical label according with the AAL the mean centroid coordinates in MNI stereotaxic space, the standard deviation along the three axes and the cardinality (N) are reported. Taken from: Berlingeri et al. 2019.

	Left Hemisphere							Right Hemisphere						
	μx	μy	μz	SDx	SDy	SDz	N	μx	μy	μz	SDx	SDy	SDz	N
Inferior Frontal Gyrus, pars Orbitalis								54	21	-2	7.82	12.89	14.78	41
Inferior Frontal Gyrus, pars Triangularis	-43	40	1	7.54	8.01	8.35	19							
Inferior Frontal Gyrus, pars Opercularis	-46	17	21	4.85	9.85	10.17	25							
Middle Frontal Gyrus, pars Orbitalis								28	46	-16	19.44	7.85	4.41	13
Superior Medial Frontal Gyrus								2	53	42	13.48	9.72	11.24	17
Supplementary Motor Area	-7	7	67	8.59	10.70	6.24	12							
Precentral Gyrus	-46	1	43	9.63	10.27	11.12	28	42	9	48	7.16	20.89	10.82	13
Inferior Parietal Lobule	-50	-42	57	4.29	5.90	7.42	9							
Supramarginal Gyrus	-42	-44	24	14.68	8.53	9.78	17	55	-41	44	11.08	8.06	16.50	10
Superior Temporal Pole	-35	17	-20	7.66	10.80	10.79	21							
Middle Temporal Gyrus	-59	-43	-2	5.15	8.30	10.19	21	59	-36	-8	6.53	11.64	9.79	30
	-61	-10	-8	4.38	13.39	8.19	25							
Fusiform Gyrus	-42	-59	-18	4.03	13.50	9.06	18							
Precuneus	-16	-45	65	16.47	17.26	8.27	17							
Middle Occipital Gyrus	-32	-73	34	6.36	7.01	9.91	10							
Inferior Occipital Gyrus	-25	-98	-7	7.27	5.83	7.56	38	27	-97	-5	8.97	6.21	10.00	27
Calcarine Sulcus								11	-70	11	9.85	16.71	18.77	18
Hippocampus								23	-12	-12	8.08	11.17	10.44	19
Cerebellum, Crus I								33	-72	-32	8.31	12.04	10.49	25

Cerebellum, 7b	-10	-71	-40	17.28	12.12	8.06	17
Thalamus	-16	-14	-12	10.37	10.91	13.01	20
Caudate	-9	22	25	7.55	10.56	12.12	10

1.6. Table SA1.6

Table SA1.6 | Results of CluB with User's Spatial Criterion set to 12 mm. For each cluster, the anatomical label according with the AAL the mean centroid coordinates in MNI stereotaxic space, the standard deviation along the three axes and the cardinality (N) are reported. Taken from: Berlingeri et al. 2019.

	Left Hemisphere							Right Hemisphere						
	μx	μy	μz	SDx	SDy	SDz	N	μx	μy	μz	SDx	SDy	SDz	N
Inferior Frontal Gyrus, pars Orbitalis								54	21	-2	7.82	12.89	14.78	41
Inferior Frontal Gyrus, pars Triangularis	-43	40	1	7.54	8.01	8.35	19							
Inferior Frontal Gyrus, pars Opercularis	-46	17	21	4.85	9.85	10.17	25							
Middle Frontal Gyrus, pars Orbitalis								28	46	-16	19.44	7.85	4.41	13
Superior Medial Frontal Gyrus	-2	41	35	12.80	17.95	13.90	27							
Supplementary Motor Area	-7	7	67	8.59	10.70	6.24	12							
Precentral Gyrus	-46	1	43	9.63	10.27	11.12	28	42	9	48	7.16	20.89	10.82	13
Superior Parietal Lobule	-28	-44	62	21.51	14.25	8.91	26							
Supramarginal Gyrus	55	-41	44	11.08	8.06	16.50	10							

Region	x	y	z				k	x	y	z				k
Angular Gyrus	-38	-55	28	12.97	16.09	10.75	27							
Superior Temporal Pole	-35	17	-20	7.66	10.80	10.79	21							
Middle Temporal Gyrus	-61	-10	-8	4.38	13.39	8.19	25	59	-36	-8	6.53	11.64	9.79	30
Inferior Temporal Gyrus	-51	-51	-9	9.40	13.47	12.68	39							
Inferior Occipital Gyrus	-25	-98	-7	7.27	5.83	7.56	38	27	-97	-5	8.97	6.21	10.00	27
Calarine Sulcus	11	-70	11	9.85	16.71	18.77	18							
Hippocampus	-16	-14	-12	10.37	10.91	13.01	20	23	-12	-12	8.08	11.17	10.44	19
Cerebellum, Crus I	33	-72	-32	8.31	12.04	10.49	25							
Cerebellum VIIb	-10	-71	-40	17.28	12.12	8.06	17							

244

1.7. Table SA1.7

Table SA1.7 | Results of CluB with User's Spatial Criterion set to 13 mm. For each cluster, the anatomical label according with the AAL the mean centroid coordinates in MNI stereotaxic space, the standard deviation along the three axes and the cardinality (N) are reported. Taken from: Berlingeri et al. 2019.

	Left Hemisphere							Right Hemisphere						
	μx	μy	μz	SDx	SDy	SDz	N	μx	μy	μz	SDx	SDy	SDz	N
Inferior Frontal Gyrus, pars Orbtalis	-39	28	-10	8.65	15.24	13.99	40	54	21	-2	7.82	12.89	14.78	41
Middle Frontal Gyrus, pars Orbitalis	28	46	-16	19.44	7.85	4.41	13							
Superior Medial Frontal Gyrus	-2	41	35	12.8	17.95	13.90	27							
Supplementary Motor Area	-7	7	67	8.59	10.70	6.24	12							
Precentral Gyrus	-46	8	33	7.69	12.91	15.34	53	42	9	48	7.16	20.89	10.82	13
Superior Parietal Lobule	-28	-44	62	21.51	14.25	8.91	26							
Supramarginal Gyrus								55	-41	44	11.08	8.05	16.51	10
Angular Gyrus	-38	-55	28	12.97	16.90	10.75	27							
Middle Temporal Gyrus	-61	-10	-8	4.38	13.39	8.19	25	59	-36	-8	6.53	11.64	9.79	30

Inferior Temporal Gyrus	-51	-51	-9	9.40	13.47	12.68	39							
Inferior Occipital Grus	-25	-98	-7	7.27	5.83	7.56	38							
Calcarine Sulcus								20	-86	1	12.17	17.54	16.02	45
Hippocampus	-16	-14	-12	10.37	10.91	13.01	20	23	-12	-12	8.08	11.17	10.44	19
Cerebelum, Crus I								33	-72	-32	8.31	12.04	10.49	25
Cerebellum VIIb	-10	-71	-40	17.28	12.12	8.06	17							

1.8. Table SA1.8

Table SA1.8 | Results of CluB with User's Spatial Criterion set to 14 mm. For each cluster, the anatomical label according with the AAL the mean centroid coordinates in MNI stereotaxic space, the standard deviation along the three axes and the cardinality (N) are reported. Taken from: Berlingeri et al. 2019.

	Left Hemisphere							Right Hemisphere						
	μx	μy	μz	SDx	SDy	SDz	N	μx	μy	μz	SDx	SDy	SDz	N
Inferior Frontal Gyrus, pars Orbitalis	-39	28	-10	8.65	15.24	13.99	40	48	27	-5	15.99	15.97	14.30	54
Superior Medial Frontal Gyrus	-2	41	35	12.80	17.95	13.90	27							
Supplementary Motor Area	-7	7	67	8.59	10.70	6.24	12							
Precentral Gyrus	-46	8	33	7.69	12.91	15.34	53	42	9	48	7.16	20.89	10.82	13
Superior Parietal Lobule	-28	-44	62	21.51	14.25	8.91	26							
Supramarginal Gyrus								55	-41	44	11.08	8.06	16.51	10
Angular Gyrus	-38	-55	28	12.97	16.90	10.75	27							
Middle Temporal Gyrus	-61	-10	-8	4.39	13.39	8.19	25	59	-36	-8	6.53	11.64	9.79	30
Inferior Temporal Gyrus	-51	-51	-9	9.40	13.47	12.68	39							

Inferior Occipital Gyrus	-25	-98	-7	7.27	5.83	7.56	38						
Calcarine Sulcus								20	-86	1	12.17	17.54	16.02	45
Hippocampus	-16	-14	-12	10.37	10.91	13.01	20	23	-12	-12	8.08	11.17	10.44	19
Cerebellum. Crus I								33	-72	-32	8.31	12.04	10.49	25
Cerebellum VIIb	-10	-71	-40	17.28	12.12	8.06	17						

References

Aiello M, Ambron E, Situlin R, Foroni F, Biolo G and Rumiati Ri (2018) Body weight and its association with impulsivity in middle and old age individuals. *Brain Cogn,* **123,** 103-109.

Ambrose Lm, Unterwald Em and Van Bockstaele Ej (2004) Ultrastructural evidence for co-localization of dopamine D2 and micro-opioid receptors in the rat dorsolateral striatum. *Anat Rec A Discov Mol Cell Evol Biol,* **279,** 583-91.

Armstrong Cc, Moody Td, Feusner Jd, Mccracken Jt, Chang S, Levitt Jg, Piacentini Jc and O'neill J (2016) Graph-theoretical analysis of resting-state fMRI in pediatric obsessive-compulsive disorder. *J Affect Disord,* **193,** 175-84.

Bach P, Weil G, Pompili E, Hoffmann S, Hermann D, Vollstädt-Klein S, Mann K, Perez-Ramirez U, Moratal D, Canals S, Dursun Sm, Greenshaw Aj, Kirsch P, Kiefer F and Sommer Wh (2019) Incubation of neural alcohol cue reactivity after withdrawal and its blockade by naltrexone. *Addict Biol,* **25,** e12717.

Baek K, Morris Ls, Kundu P and Voon V (2017) Disrupted resting-state brain network properties in obesity: decreased global and putaminal cortico-striatal network efficiency. *Psychol Med,* **47,** 585-596.

Baessler A, Hasinoff Mj, Fischer M, Reinhard W, Sonnenberg Ge, Olivier M, Erdmann J, Schunkert H, Doering A, Jacob Hj, Comuzzie Ag, Kissebah Ah and Kwitek Ae (2005) Genetic linkage and association of the growth hormone secretagogue receptor (ghrelin receptor) gene in human obesity. *Diabetes,* **54,** 259-67.

Baik Jh (2013) Dopamine signaling in reward-related behaviors. *Front Neural Circuits,* **7,** 152.

Barker At (1991) An introduction to the basic principles of magnetic nerve stimulation. *J Clin Neurophysiol,* **8,** 26-37.

Barry Ma, Gatenby Jc, Zeiger Jd and Gore Jc (2001) Hemispheric dominance of cortical activity evoked by focal electrogustatory stimuli. *Chem Senses,* **26,** 471-82.

Barth Ks, Rydin-Gray S, Kose S, Borckardt Jj, O'neil Pm, Shaw D, Madan A, Budak A and George Ms (2011) Food cravings and the effects of left prefrontal repetitive transcranial magnetic stimulation using an improved sham condition. *Front Psychiatry,* **2,** 9.

Bassareo V and Di Chiara G (1999) Differential responsiveness of dopamine transmission to food-stimuli in nucleus accumbens shell/core compartments. *Neuroscience,* **89,** 637-41.

Batterink L, Yokum S and Stice E (2010) Body mass correlates inversely with inhibitory control in response to food among adolescent girls: an fMRI study. *Neuroimage,* **52,** 1696-703.

Baumgartner R, Somorjai R, Summers R and Richter W (2001) Ranking fMRI time courses by minimum spanning trees: assessing coactivation in fMRI. *Neuroimage,* **13,** 734-42.

Bechara A, Damasio H, Tranel D and Anderson Sw (1998) Dissociation Of working memory from decision making within the human prefrontal cortex. *J Neurosci,* **18,** 428-37.

Bechara A, Tranel D and Damasio H (2000) Characterization of the decision-making deficit of patients with ventromedial prefrontal cortex lesions. *Brain,* **123 (Pt 11),** 2189-202.

Behzadi Y, Restom K, Liau J and Liu Tt (2007) A component based noise correction method (CompCor) for BOLD and perfusion based fMRI. *Neuroimage,* **37,** 90-101.

Berlingeri M, Devoto F, Gasparini F, Saibene A, Corchs Se, Clemente L, Danelli L, Gallucci M, Borgoni R, Borghese Na and Paulesu E (2019) Clustering the Brain With "CluB": A New Toolbox for Quantitative Meta-Analysis of Neuroimaging Data. *Front Neurosci,* **13,** 1037.

Berlingeri M, Losasso D, Girolo A, Cozzolino E, Masullo T, Scotto M, Sberna M, Bottini G and Paulesu E (2017) Resting state brain connectivity patterns before eventual relapse into cocaine abuse. *Behav Brain Res,* **327,** 121-132.

Berridge Kc, Ho Cy, Richard Jm and Difeliceantonio Ag (2010) The tempted brain eats: pleasure and desire circuits in obesity and eating disorders. *Brain Res,* **1350,** 43-64.

Berridge Kc and Kringelbach Ml (2015) Pleasure systems in the brain. *Neuron,* **86,** 646-64.

Berthoud Hr, Münzberg H and Morrison Cd (2017) Blaming the Brain for Obesity: Integration of Hedonic and Homeostatic Mechanisms. *Gastroenterology,* **152,** 1728-1738.

Biswal B, Yetkin Fz, Haughton Vm and Hyde Js (1995) Functional connectivity in the motor cortex of resting human brain using echo-planar MRI. *Magn Reson Med,* **34,** 537-41.

Blechert J, Feige B, Hajcak G and Tuschen-Caffier B (2010) To eat or not to eat? Availability of food modulates the electrocortical response to food pictures in restrained eaters. *Appetite,* **54,** 262-8.

Blechert J, Klackl J, Miedl Sf and Wilhelm Fh (2016) To eat or not to eat: Effects of food availability on reward system activity during food picture viewing. *Appetite,* **99,** 254-261.

Bonato Dp and Boland Fj (1983) Delay of gratification in obese children. *Addict Behav,* **8,** 71-4.

Bonson Kr, Grant Sj, Contoreggi Cs, Links Jm, Metcalfe J, Weyl Hl, Kurian V, Ernst M and London Ed (2002) Neural systems and cue-induced cocaine craving. *Neuropsychopharmacology,* **26,** 376-86.

Borowitz Ma, Yokum S, Duval Er and Gearhardt An (2020) Weight-Related Differences in Salience, Default Mode, and Executive Function Network Connectivity in Adolescents. *Obesity (Silver Spring),* **28,** 1438-1446.

Bragulat V, Dzemidzic M, Bruno C, Cox Ca, Talavage T, Considine Rv and Kareken Da (2010) Food-related odor probes of brain reward circuits during hunger: a pilot FMRI study. *Obesity (Silver Spring),* **18,** 1566-71.

Brand M, Snagowski J, Laier C and Maderwald S (2016) Ventral striatum activity when watching preferred pornographic pictures is correlated with symptoms of Internet pornography addiction. *Neuroimage,* **129,** 224-232.

Breiter Hc, Gollub Rl, Weisskoff Rm, Kennedy Dn, Makris N, Berke Jd, Goodman Jm, Kantor Hl, Gastfriend Dr, Riorden Jp, Mathew Rt, Rosen Br and Hyman Se (1997) Acute effects of cocaine on human brain activity and emotion. *Neuron,* **19,** 591-611.

Brooks Sj, Cedernaes J and Schiöth Hb (2013) Increased prefrontal and parahippocampal activation with reduced dorsolateral prefrontal and insular cortex activation to food images in obesity: a meta-analysis of fMRI studies. *PLoS One,* **8,** e60393.

Buka Sl, Shenassa Ed and Niaura R (2003) Elevated risk of tobacco dependence among offspring of mothers who smoked during pregnancy: a 30-year prospective study. *Am J Psychiatry,* **160,** 1978-84.

Burger Ks and Berner La (2014) A functional neuroimaging review of obesity, appetitive hormones and ingestive behavior. *Physiol Behav,* **136,** 121-7.

Burger Ks and Stice E (2011) Variability in reward responsivity and obesity: evidence from brain imaging studies. *Curr Drug Abuse Rev,* **4,** 182-9.

Burger Ks and Stice E (2014) Greater striatopallidal adaptive coding during cue-reward learning and food reward habituation predict future weight gain. *Neuroimage,* **99,** 122-8.

Butler Ab and Hodos W (2005) *Comparative Vertebrate Neuroanatomy,* Hoboken, New Jersey, John Wiley & Sons, Inc.

Calvo-Merino B, Grèzes J, Glaser De, Passingham Re and Haggard P (2006) Seeing or doing? Influence of visual and motor familiarity in action observation. *Curr Biol,* **16,** 1905-10.

Carpenter Pa and Just Ma (1999) Modeling the mind: very-high-field functional magnetic resonance imaging activation during cognition. *Top Magn Reson Imaging,* **10,** 16-36.

Carter Bl and Tiffany St (1999) Meta-analysis of cue-reactivity in addiction research. *Addiction,* **94,** 327-40.

Carter Bl and Tiffany St (2001) The cue-availability paradigm: the effects of cigarette availability on cue reactivity in smokers. *Exp Clin Psychopharmacol,* **9,** 183-90.

Carter Rm, Meyer Jr and Huettel Sa (2010) Functional neuroimaging of intertemporal choice models: A review. *of Neuroscience, Psychology, and Economics,* **3,** 27-45.

Cattinelli I, Borghese Na, Gallucci M and Paulesu E (2013a) Reading the reading brain: A new meta-analysis of functional imaging data on reading. *Journal of Neurolinguistics,* **26,** 214-238.

Cattinelli I, Valentini G, Paulesu E and Borghese Na (2013b) A novel approach to the problem of non-uniqueness of the solution in hierarchical clustering. *IEEE Trans Neural Netw Learn Syst,* **24,** 1166-73.

Cauda F, Costa T, Torta Dm, Sacco K, D'agata F, Duca S, Geminiani G, Fox Pt and Vercelli A (2012) Meta-analytic clustering of the insular cortex: characterizing the meta-analytic connectivity of the insula when involved in active tasks. *Neuroimage,* **62,** 343-55.

Cauda F, D'agata F, Sacco K, Duca S, Geminiani G and Vercelli A (2011) Functional connectivity of the insula in the resting brain. *Neuroimage,* **55,** 8-23.

Caulkins Jp and Reuter P (1998) What price data tell us about drug markets.

Cavanna Ae and Trimble Mr (2006) The precuneus: a review of its functional anatomy and behavioural correlates. *Brain,* **129,** 564-83.

Cerf-Ducastel B, Van De Moortele Pf, Macleod P, Le Bihan D and Faurion A (2001) Interaction of gustatory and lingual somatosensory perceptions at the cortical level in the human: a functional magnetic resonance imaging study. *Chem Senses,* **26,** 371-83.

Cerit H, Davidson P, Hye T, Moondra P, Haimovici F, Sogg S, Shikora S, Goldstein Jm, Evins Ae, Whitfield-Gabrieli S, Stoeckel Le and Holsen Lm (2019) Resting-State Brain Connectivity Predicts Weight Loss and Cognitive Control of Eating Behavior After Vertical Sleeve Gastrectomy. *Obesity (Silver Spring),* **27,** 1846-1855.

Chase Hw, Eickhoff Sb, Laird Ar and Hogarth L (2011) The neural basis of drug stimulus processing and craving: an activation likelihood estimation meta-analysis. *Biol Psychiatry,* **70,** 785-93.

Chen Ey, Eickhoff Sb, Giovannetti T and Smith Dv (2020) Obesity is associated with reduced orbitofrontal cortex volume: A coordinate-based meta-analysis. *Neuroimage Clin,* **28,** 102420.

Childress Ar, Hole Av, Ehrman Rn, Robbins Sj, Mclellan At and O'brien Cp (1993) Cue reactivity and cue reactivity interventions in drug dependence. *NIDA Res Monogr,* **137,** 73-95.

Claus Ed, Ewing Sw, Filbey Fm, Sabbineni A and Hutchison Ke (2011) Identifying neurobiological phenotypes associated with alcohol use disorder severity. *Neuropsychopharmacology,* **36,** 2086-96.

Colquitt Jl, Pickett K, Loveman E and Frampton Gk (2014) Surgery for weight loss in adults. *Cochrane Database Syst Rev***,** CD003641.

Colquitt Jl, Picot J, Loveman E and Clegg Aj (2009) Surgery for obesity. *Cochrane Database Syst Rev***,** CD003641.

Conklin Ca and Tiffany St (2002) Applying extinction research and theory to cue-exposure addiction treatments. *Addiction,* **97,** 155-67.

Contreras-Rodríguez O, Vilar-López R, Andrews Zb, Navas Jf, Soriano-Mas C and Verdejo-García A (2017) Altered cross-talk between the hypothalamus and non-homeostatic regions linked to obesity and difficulty to lose weight. *Sci Rep,* **7,** 9951.

Cook Jb, Hendrickson Lm, Garwood Gm, Toungate Km, Nania Cv and Morikawa H (2017) Junk food diet-induced obesity increases D2 receptor autoinhibition in the ventral tegmental area and reduces ethanol drinking. *PLoS One,* **12,** e0183685.

Coricelli C, Toepel U, Notter Ml, Murray Mm and Rumiati Ri (2019) Distinct brain representations of processed and unprocessed foods. *Eur J Neurosci,* **50,** 3389-3401.

Cornier Ma, Mcfadden Kl, Thomas Ea, Bechtell Jl, Eichman Ls, Bessesen Dh and Tregellas Jr (2013) Differences in the neuronal response to food in obesity-resistant as compared to obesity-prone individuals. *Physiol Behav,* **110-111,** 122-8.

Cornier Ma, Melanson El, Salzberg Ak, Bechtell Jl and Tregellas Jr (2012) The effects of exercise on the neuronal response to food cues. *Physiol Behav,* **105,** 1028-34.

Cornier Ma, Salzberg Ak, Endly Dc, Bessesen Dh, Rojas Dc and Tregellas Jr (2009) The effects of overfeeding on the neuronal response to visual food cues in thin and reduced-obese individuals. *PLoS One,* **4,** e6310.

Cornier Ma, Shott Me, Thomas Ea, Bechtell Jl, Bessesen Dh, Tregellas Jr and Frank Gk (2015) The effects of energy balance, obesity-proneness and sex on the neuronal response to sweet taste. *Behav Brain Res,* **278,** 446-52.

Cortese Bm, Uhde Tw, Brady Kt, Mcclernon Fj, Yang Qx, Collins Hr, Lematty T and Hartwell Kj (2015) The fMRI BOLD response to unisensory and multisensory smoking cues in nicotine-dependent adults. *Psychiatry Res,* **234,** 321-7.

Costafreda Sg (2009) Pooling FMRI data: meta-analysis, mega-analysis and multi-center studies. *Front Neuroinform,* **3,** 33.

Courtney Ke, Ghahremani Dg, London Ed and Ray La (2014) The association between cue-reactivity in the precuneus and level of dependence on nicotine and alcohol. *Drug Alcohol Depend,* **141,** 21-6.

Courtney Ke, Schacht Jp, Hutchison K, Roche Dj and Ray La (2016) Neural substrates of cue reactivity: association with treatment outcomes and relapse. *Addict Biol,* **21,** 3-22.

Crepaldi D, Berlingeri M, Cattinelli I, Borghese Na, Luzzatti C and Paulesu E (2013) Clustering the lexicon in the brain: a meta-analysis of the neurofunctional evidence on noun and verb processing. *Front Hum Neurosci,* **7,** 303.

Dagher A (2012) Functional brain imaging of appetite. *Trends Endocrinol Metab,* **23,** 250-60.

Dagher A, Tannenbaum B, Hayashi T, Pruessner Jc and Mcbride D (2009) An acute psychosocial stress enhances the neural response to smoking cues. *Brain Res,* **1293,** 40-8.

Damoiseaux Js, Rombouts Sa, Barkhof F, Scheltens P, Stam Cj, Smith Sm and Beckmann Cf (2006) Consistent resting-state networks across healthy subjects. *Proc Natl Acad Sci U S A,* **103,** 13848-53.

Danelli L, Berlingeri M, Bottini G, Borghese Na, Lucchese M, Sberna M, Price Cj and Paulesu E (2017) How many deficits in the same dyslexic brains? A behavioural and fMRI assessment of comorbidity in adult dyslexics. *Cortex,* **97,** 125-142.

David Sp, Munafò Mr, Johansen-Berg H, Mackillop J, Sweet Lh, Cohen Ra, Niaura R, Rogers Rd, Matthews Pm and Walton Rt (2007) Effects of Acute Nicotine Abstinence on Cue-elicited Ventral Striatum/Nucleus Accumbens Activation in Female Cigarette Smokers: A Functional Magnetic Resonance Imaging Study. *Brain Imaging Behav,* **1,** 43-57.

David Sp, Ware Jj, Chu Im, Loftus Pd, Fusar-Poli P, Radua J, Munafò Mr and Ioannidis Jp (2013) Potential reporting bias in fMRI studies of the brain. *PLoS One,* **8,** e70104.

Davis C (2014) Evolutionary and neuropsychological perspectives on addictive behaviors and addictive substances: relevance to the "food addiction" construct. *Subst Abuse Rehabil,* **5,** 129-37.

Davis C, Strachan S and Berkson M (2004) Sensitivity to reward: implications for overeating and overweight. *Appetite,* **42,** 131-8.

Davis Jf, Tracy Al, Schurdak Jd, Tschöp Mh, Lipton Jw, Clegg Dj and Benoit Sc (2008) Exposure to elevated levels of dietary fat attenuates psychostimulant reward and mesolimbic dopamine turnover in the rat. *Behav Neurosci,* **122,** 1257-63.

De Pirro S, Galati G, Pizzamiglio L and Badiani A (2018) The Affective and Neural Correlates of Heroin versus Cocaine Use in Addiction Are Influenced by Environmental Setting But in Opposite Directions. *J Neurosci,* **38,** 5182-5195.

De Silva A, Salem V, Long Cj, Makwana A, Newbould Rd, Rabiner Ea, Ghatei Ma, Bloom Sr, Matthews Pm, Beaver Jd and Dhillo Ws (2011) The gut hormones PYY 3-36 and GLP-1 7-36 amide reduce food intake and modulate brain activity in appetite centers in humans. *Cell Metab,* **14,** 700-6.

Del Parigi A, Gautier Jf, Chen K, Salbe Ad, Ravussin E, Reiman E and Tataranni Pa (2002) Neuroimaging and obesity: mapping the brain responses to hunger and satiation in humans using positron emission tomography. *Ann N Y Acad Sci,* **967,** 389-97.

Demonet Jf, Fiez Ja, Paulesu E, Petersen Se and Zatorre Rj (1996) PET Studies of Phonological Processing: A Critical Reply to Poeppel. *Brain Lang,* **55,** 352-79.

Devoto F, Zapparoli L, Bonandrini R, Berlingeri M, Ferrulli A, Luzi L, Banfi G and Paulesu E (2018) Hungry Brains: A Meta-Analytical Review of Brain Activation Imaging Studies On Food Perception and Appetite in Obese Individuals. *Neurosci Biobehav Rev.*

Dewitt Sj, Ketcherside A, Mcqueeny Tm, Dunlop Jp and Filbey Fm (2015) The hyper-sentient addict: an exteroception model of addiction. *Am J Drug Alcohol Abuse,* **41,** 374-81.

Di Chiara G and Imperato A (1988) Drugs abused by humans preferentially increase synaptic dopamine concentrations in the mesolimbic system of freely moving rats. *Proc Natl Acad Sci U S A,* **85,** 5274-8.

Di Chiara G, Tanda G, Frau R and Carboni E (1993) On the preferential release of dopamine in the nucleus accumbens by amphetamine: further evidence obtained by vertically implanted concentric dialysis probes. *Psychopharmacology (Berl),* **112,** 398-402.

Dimitropoulos A, Tkach J, Ho A and Kennedy J (2012) Greater corticolimbic activation to high-calorie food cues after eating in obese vs. normal-weight adults. *Appetite,* **58,** 303-12.

Dinur-Klein L, Dannon P, Hadar A, Rosenberg O, Roth Y, Kotler M and Zangen A (2014) Smoking cessation induced by deep repetitive transcranial magnetic stimulation of the prefrontal and insular cortices: a prospective, randomized controlled trial. *Biol Psychiatry,* **76,** 742-9.

Eickhoff Sb, Bzdok D, Laird Ar, Kurth F and Fox Pt (2012) Activation likelihood estimation meta-analysis revisited. *Neuroimage,* **59,** 2349-61.

Eickhoff Sb, Laird Ar, Grefkes C, Wang Le, Zilles K and Fox Pt (2009) Coordinate-based activation likelihood estimation meta-analysis of neuroimaging data: a random-effects approach based on empirical estimates of spatial uncertainty. *Hum Brain Mapp,* **30,** 2907-26.

Eiler Wj, Dzemidzic M, Case Kr, Considine Rv and Kareken Da (2012) Correlation between Ventromedial Prefrontal Cortex Activation to Food Aromas and Cue-driven Eating: An fMRI Study. *Chemosens Percept,* **5,** 27-36.

Elton A, Smitherman S, Young J and Kilts Cd (2015) Effects of childhood maltreatment on the neural correlates of stress- and drug cue-induced cocaine craving. *Addict Biol,* **20,** 820-31.

Engelmann Jm, Versace F, Robinson Jd, Minnix Ja, Lam Cy, Cui Y, Brown Vl and Cinciripini Pm (2012) Neural substrates of smoking cue reactivity: a meta-analysis of fMRI studies. *Neuroimage,* **60,** 252-62.

Epstein Lh, Dearing Kk, Temple Jl and Cavanaugh Md (2008) Food reinforcement and impulsivity in overweight children and their parents. *Eat Behav,* **9,** 319-27.

Evans Gw, Fuller-Rowell Te and Doan Sn (2012) Childhood cumulative risk and obesity: the mediating role of self-regulatory ability. *Pediatrics,* **129,** e68-73.

Everitt Bj, Parkinson Ja, Olmstead Mc, Arroyo M, Robledo P and Robbins Tw (1999) Associative processes in addiction and reward. The role of amygdala-ventral striatal subsystems. *Ann N Y Acad Sci,* **877,** 412-38.

Everitt Bj and Robbins Tw (2005) Neural systems of reinforcement for drug addiction: from actions to habits to compulsion. *Nat Neurosci,* **8,** 1481-9.

Everitt Bj and Robbins Tw (2013) From the ventral to the dorsal striatum: devolving views of their roles in drug addiction. *Neurosci Biobehav Rev,* **37,** 1946-54.

Falcone M, Cao W, Bernardo L, Tyndale Rf, Loughead J and Lerman C (2016) Brain Responses to Smoking Cues Differ Based on Nicotine Metabolism Rate. *Biol Psychiatry,* **80,** 190-7.

Feldstein Ewing Sw, Filbey Fm, Chandler Ld and Hutchison Ke (2010) Exploring the relationship between depressive and anxiety symptoms and neuronal response to alcohol cues. *Alcohol Clin Exp Res,* **34,** 396-403.

Ferrulli A, Macrì C, Terruzzi I, Ambrogi F, Milani V, Adamo M and Luzi L (2019a) High frequency deep transcranial magnetic stimulation acutely increases β-endorphins in obese humans. *Endocrine,* **64,** 67-74.

Ferrulli A, Macrì C, Terruzzi I, Massarini S, Ambrogi F, Adamo M, Milani V and Luzi L (2019b) Weight loss induced by deep transcranial magnetic stimulation in obesity: A randomized, double-blind, sham-controlled study. *Diabetes Obes Metab,* **21,** 1849-1860.

Filbey Fm, Ray L, Smolen A, Claus Ed, Audette A and Hutchison Ke (2008) Differential neural response to alcohol priming and alcohol taste cues is associated with DRD4 VNTR and OPRM1 genotypes. *Alcohol Clin Exp Res,* **32,** 1113-23.

Finlayson G (2017) Food addiction and obesity: unnecessary medicalization of hedonic overeating. *Nat Rev Endocrinol,* **13,** 493-498.

Fiocchi S, Chiaramello E, Luzi L, Ferrulli A, Bonato M, Roth Y, Zangen A and Ravazzani P (2018) Deep Transcranial Magnetic Stimulation for the Addiction Treatment: Electric Field Distribution Modeling. *IEEE Journal of Electromagnetics, RF and Microwaves in Medicine and Biology,* **2,** 242-248.

Fiore Mc (2000) US public health service clinical practice guideline: treating tobacco use and dependence. *Respir Care,* **45,** 1200-62.

Firat O, Ozay M, Onal I, Oztekin I and Yarman Vural Ft (2013) Representation of cognitive processes using the minimum spanning tree of local meshes. *Conf Proc IEEE Eng Med Biol Soc,* **2013,** 6780-3.

Fisher Ra (1970) *Statistical methods for research workers,* Edimburgh, Oliver and Boyd.

Fisher Rj (1993a) Social Desirability Bias and the Validity of Indirect Questioning. *Journal of consumer research*.

Fisher Rj (1993b) Social desirability bias and the validity of indirect questioning. *Journal of consumer research,* **20,** 303-315.

Flandin G and Friston Kj (2019) Analysis of family-wise error rates in statistical parametric mapping using random field theory. *Hum Brain Mapp,* **40,** 2052-2054.

Fletcher Pc and Kenny Pj (2018) Food addiction: a valid concept? *Neuropsychopharmacology,* **43,** 2506-2513.

Fornara Ga, Papagno C and Berlingeri M (2017) A neuroanatomical account of mental time travelling in schizophrenia: A meta-analysis of functional and structural neuroimaging data. *Neurosci Biobehav Rev,* **80,** 211-222.

Fox Md and Raichle Me (2007) Spontaneous fluctuations in brain activity observed with functional magnetic resonance imaging. *Nat Rev Neurosci,* **8,** 700-11.

Fox Md, Snyder Az, Vincent Jl, Corbetta M, Van Essen Dc and Raichle Me (2005) The human brain is intrinsically organized into dynamic, anticorrelated functional networks. *Proc Natl Acad Sci U S A,* **102,** 9673-8.

Fregni F, Orsati F, Pedrosa W, Fecteau S, Tome Fa, Nitsche Ma, Mecca T, Macedo Ec, Pascual-Leone A and Boggio Ps (2008) Transcranial direct current stimulation of the prefrontal cortex modulates the desire for specific foods. *Appetite,* **51,** 34-41.

Frey S and Petrides M (1999) Re-examination of the human taste region: a positron emission tomography study. *Eur J Neurosci,* **11,** 2985-8.

Friston Kj, Holmes A, Poline Jb, Price Cj and Frith Cd (1996) Detecting activations in PET and fMRI: levels of inference and power. *Neuroimage,* **4,** 223-35.

Fryer Sl, Jorgensen Kw, Yetter Ej, Daurignac Ec, Watson Td, Shanbhag H, Krystal Jh and Mathalon Dh (2013) Differential brain response to alcohol cue distractors across stages of alcohol dependence. *Biol Psychol,* **92,** 282-91.

Fulton S, Pissios P, Manchon Rp, Stiles L, Frank L, Pothos En, Maratos-Flier E and Flier Js (2006) Leptin regulation of the mesoaccumbens dopamine pathway. *Neuron,* **51,** 811-22.

Führer D, Zysset S and Stumvoll M (2008) Brain activity in hunger and satiety: an exploratory visually stimulated FMRI study. *Obesity (Silver Spring),* **16,** 945-50.

Gallus S, Lugo A, Murisic B, Bosetti C, Boffetta P and La Vecchia C (2015) Overweight and obesity in 16 European countries. *Eur J Nutr,* **54,** 679-89.

Garavan H, Pankiewicz J, Bloom A, Cho Jk, Sperry L, Ross Tj, Salmeron Bj, Risinger R, Kelley D and Stein Ea (2000) Cue-induced cocaine craving: neuroanatomical specificity for drug users and drug stimuli. *Am J Psychiatry,* **157,** 1789-98.

García-García I, Horstmann A, Jurado Ma, Garolera M, Chaudhry Sj, Margulies Ds, Villringer A and Neumann J (2014) Reward processing in obesity, substance addiction and non-substance addiction. *Obes Rev,* **15,** 853-69.

García-García I, Jurado M, Garolera M, Marqués-Iturria I, Horstmann A, Segura B, Pueyo R, Sender-Palacios Mj, Vernet-Vernet M, Villringer A, Junqué C, Margulies Ds and Neumann J (2015) Functional network centrality in obesity: A resting-state and task fMRI study. *Psychiatry Res,* **233,** 331-8.

García-García I, Jurado M, Garolera M, Segura B, Sala-Llonch R, Marqués-Iturria I, Pueyo R, Sender-Palacios Mj, Vernet-Vernet M, Narberhaus A, Ariza M and Junqué C (2013) Alterations of the salience network in obesity: a resting-state fMRI study. *Hum Brain Mapp,* **34,** 2786-97.

Garrison Ka and Potenza Mn (2014) Neuroimaging and biomarkers in addiction treatment. *Curr Psychiatry Rep,* **16,** 513.

Gautier Jf, Chen K, Salbe Ad, Bandy D, Pratley Re, Heiman M, Ravussin E, Reiman Em and Tataranni Pa (2000) Differential brain responses to satiation in obese and lean men. *Diabetes,* **49,** 838-46.

Gautier Jf, Chen K, Uecker A, Bandy D, Frost J, Salbe Ad, Pratley Re, Lawson M, Ravussin E, Reiman Em and Tataranni Pa (1999) Regions of the human brain affected during a liquid-meal taste perception in the fasting state: a positron emission tomography study. *Am J Clin Nutr,* **70,** 806-10.

Gautier Jf, Del Parigi A, Chen K, Salbe Ad, Bandy D, Pratley Re, Ravussin E, Reiman Em and Tataranni Pa (2001) Effect of satiation on brain activity in obese and lean women. *Obes Res,* **9,** 676-84.

Gearhardt An, Yokum S, Stice E, Harris Jl and Brownell Kd (2014) Relation of obesity to neural activation in response to food commercials. *Soc Cogn Affect Neurosci,* **9,** 932-8.

Geliebter A, Pantazatos Sp, Mcouatt H, Puma L, Gibson Cd and Atalayer D (2013) Sex-based fMRI differences in obese humans in response to high vs. low energy food cues. *Behav Brain Res,* **243,** 91-6.

Gelperin A (1986) Complex associative learning in small neural networks. *Trends in Neurosciences,* **9,** 323-328.

George Ms, Anton Rf, Bloomer C, Teneback C, Drobes Dj, Lorberbaum Jp, Nahas Z and Vincent Dj (2001) Activation of prefrontal cortex and anterior thalamus in alcoholic subjects on exposure to alcohol-specific cues. *Arch Gen Psychiatry,* **58,** 345-52.

Giuliani Nr, Merchant Js, Cosme D and Berkman Et (2018) Neural predictors of eating behavior and dietary change. *Ann N Y Acad Sci,* **1428,** 208-220.

Goldman Rl, Borckardt Jj, Frohman Ha, O'neil Pm, Madan A, Campbell Lk, Budak A and George Ms (2011) Prefrontal cortex transcranial direct current stimulation (tDCS) temporarily reduces food cravings and increases the self-reported ability to resist food in adults with frequent food craving. *Appetite,* **56,** 741-6.

Goldstein Rz and Volkow Nd (2002) Drug addiction and its underlying neurobiological basis: neuroimaging evidence for the involvement of the frontal cortex. *Am J Psychiatry,* **159,** 1642-52.

Gordon Cm, Dougherty Dd, Rauch Sl, Emans Sj, Grace E, Lamm R, Alpert Nm, Majzoub Ja and Fischman Aj (2000) Neuroanatomy of human appetitive function: A positron emission tomography investigation. *Int J Eat Disord,* **27,** 163-71.

Goudriaan Ae, De Ruiter Mb, Van Den Brink W, Oosterlaan J and Veltman Dj (2010) Brain activation patterns associated with cue reactivity and craving in abstinent problem gamblers, heavy smokers and healthy controls: an fMRI study. *Addict Biol,* **15,** 491-503.

Goudriaan Ae, Veltman Dj, Van Den Brink W, Dom G and Schmaal L (2013) Neurophysiological effects of modafinil on cue-exposure in cocaine dependence: a randomized placebo-controlled cross-over study using pharmacological fMRI. *Addict Behav,* **38,** 1509-1517.

Goutte C, Hansen Lk, Liptrot Mg and Rostrup E (2001) Feature-space clustering for fMRI meta-analysis. *Hum Brain Mapp,* **13,** 165-83.

Graham Rl and Hell P (1985) On The History of the Minimum Spanning Tree Problem. *Annals of the History of Computing,* **7,** 43-57.

Grahn Ja, Parkinson Ja and Owen Am (2008) The cognitive functions of the caudate nucleus. *Prog Neurobiol,* **86,** 141-55.

Grant S, London Ed, Newlin Db, Villemagne Vl, Liu X, Contoreggi C, Phillips Rl, Kimes As and Margolin A (1996) Activation of memory circuits during cue-elicited cocaine craving. *Proc Natl Acad Sci U S A,* **93,** 12040-5.

Green E, Jacobson A, Haase L and Murphy C (2011) Reduced nucleus accumbens and caudate nucleus activation to a pleasant taste is associated with obesity in older adults. *Brain Res,* **1386,** 109-17.

Greenwald Ag, Banaji Mr, Rudman La, Farnham Sd, Nosek Ba and Mellott Ds (2002) A unified theory of implicit attitudes, stereotypes, self-esteem, and self-concept. *Psychol Rev,* **109,** 3-25.

Greicius Md, Krasnow B, Reiss Al and Menon V (2003) Functional connectivity in the resting brain: a network analysis of the default mode hypothesis. *Proc Natl Acad Sci U S A,* **100,** 253-8.

Grüsser Sm, Wrase J, Klein S, Hermann D, Smolka Mn, Ruf M, Weber-Fahr W, Flor H, Mann K, Braus Df and Heinz A (2004) Cue-induced activation of the striatum and medial prefrontal cortex is associated with subsequent relapse in abstinent alcoholics. *Psychopharmacology (Berl),* **175,** 296-302.

Haase L, Cerf-Ducastel B and Murphy C (2009) Cortical activation in response to pure taste stimuli during the physiological states of hunger and satiety. *Neuroimage,* **44,** 1008-21.

Haase L, Green E and Murphy C (2011) Males and females show differential brain activation to taste when hungry and sated in gustatory and reward areas. *Appetite,* **57,** 421-34.

Hanlon Ca, Dowdle Lt, Gibson Nb, Li X, Hamilton S, Canterberry M and Hoffman M (2018) Cortical substrates of cue-reactivity in multiple substance dependent populations: transdiagnostic relevance of the medial prefrontal cortex. *Transl Psychiatry,* **8,** 186.

Hanlon Ca, Dowdle Lt, Naselaris T, Canterberry M and Cortese Bm (2014) Visual cortex activation to drug cues: a meta-analysis of functional neuroimaging papers in addiction and substance abuse literature. *Drug Alcohol Depend,* **143,** 206-12.

Hartwell Kj, Johnson Ka, Li X, Myrick H, Lematty T, George Ms and Brady Kt (2011) Neural correlates of craving and resisting craving for tobacco in nicotine dependent smokers. *Addict Biol,* **16,** 654-66.

Hassani-Abharian P, Ganjgahi H, Tabatabaei-Jafari H, Oghabian Ma, Mokri A and Ekhtiari H (2015) Exploring Neural Correlates of Different Dimensions in Drug Craving Self-Reports among Heroin Dependents. *Basic Clin Neurosci,* **6,** 271-84.

Haxby Jv, Horwitz B, Ungerleider Lg, Maisog Jm, Pietrini P and Grady Cl (1994) The functional organization of human extrastriate cortex: a PET-rCBF study of selective attention to faces and locations. *J Neurosci,* **14,** 6336-53.

Hayashi T, Ko Jh, Strafella Ap and Dagher A (2013) Dorsolateral prefrontal and orbitofrontal cortex interactions during self-control of cigarette craving. *Proc Natl Acad Sci U S A,* **110,** 4422-7.

He Q, Huang X, Turel O, Schulte M, Huang D, Thames A, Bechara A and Hser Yi (2018) Presumed structural and functional neural recovery after long-term abstinence from cocaine in male military veterans. *Prog Neuropsychopharmacol Biol Psychiatry,* **84,** 18-29.

Hendrick Om, Luo X, Zhang S and Li Cs (2012) Saliency processing and obesity: a preliminary imaging study of the stop signal task. *Obesity (Silver Spring),* **20,** 1796-802.

Hermann D, Smolka Mn, Wrase J, Klein S, Nikitopoulos J, Georgi A, Braus Df, Flor H, Mann K and Heinz A (2006) Blockade of cue-induced brain activation of abstinent alcoholics by a single administration of amisulpride as measured with fMRI. *Alcohol Clin Exp Res,* **30,** 1349-54.

Hermann P, Gál V, Kóbor I, Kirwan Cb, Kovács P, Kitka T, Lengyel Z, Bálint E, Varga B, Csekő C and Vidnyánszky Z (2019) Efficacy of weight loss intervention can be

predicted based on early alterations of fMRI food cue reactivity in the striatum. *Neuroimage Clin,* **23,** 101803.

Herremans Sc, Van Schuerbeek P, De Raedt R, Matthys F, Buyl R, De Mey J and Baeken C (2015) The Impact of Accelerated Right Prefrontal High-Frequency Repetitive Transcranial Magnetic Stimulation (rTMS) on Cue-Reactivity: An fMRI Study on Craving in Recently Detoxified Alcohol-Dependent Patients. *PLoS One,* **10,** e0136182.

Hietala J, West C, Syvälahti E, Någren K, Lehikoinen P, Sonninen P and Ruotsalainen U (1994) Striatal D2 dopamine receptor binding characteristics in vivo in patients with alcohol dependence. *Psychopharmacology (Berl),* **116,** 285-90.

Ho A, Kennedy J and Dimitropoulos A (2012) Neural correlates to food-related behavior in normal-weight and overweight/obese participants. *PLoS One,* **7,** e45403.

Holla B, Viswanath B, Agarwal Sm, Kalmady Sv, Maroky As, Jayarajan D, Bharath Rd, Venkatasubramanian G and Benegal V (2014) Visual Image-Induced Craving for Ethanol (VICE): Development, Validation, and a Pilot fMRI Study. *Indian J Psychol Med,* **36,** 164-9.

Holsen Lm, Savage Cr, Martin Le, Bruce As, Lepping Rj, Ko E, Brooks Wm, Butler Mg, Zarcone Jr and Goldstein Jm (2012) Importance of reward and prefrontal circuitry in hunger and satiety: Prader-Willi syndrome vs simple obesity. *Int J Obes (Lond),* **36,** 638-47.

Hong Js, Kim Sm, Jung Hy, Kang Kd, Min Kj and Han Dh (2017) Cognitive avoidance and aversive cues related to tobacco in male smokers. *Addict Behav,* **73,** 158-164.

Hsu Js, Wang Pw, Ko Ch, Hsieh Tj, Chen Cy and Yen Jy (2017) Altered brain correlates of response inhibition and error processing in females with obesity and sweet food addiction: A functional magnetic imaging study. *Obes Res Clin Pract,* **11,** 677-686.

Huang As, Mitchell Ja, Haber Sn, Alia-Klein N and Goldstein Rz (2018a) The thalamus in drug addiction: from rodents to humans. *Philos Trans R Soc Lond B Biol Sci,* **373.**

Huang Y, Mohan A, De Ridder D, Sunaert S and Vanneste S (2018b) The neural correlates of the unified percept of alcohol-related craving: a fMRI and EEG study. *Sci Rep,* **8,** 923.

Huerta Ci, Sarkar Pr, Duong Tq, Laird Ar and Fox Pt (2014) Neural bases of food perception: coordinate-based meta-analyses of neuroimaging studies in multiple modalities. *Obesity (Silver Spring),* **22,** 1439-46.

Hussain Ss and Bloom Sr (2013) The regulation of food intake by the gut-brain axis: implications for obesity. *Int J Obes (Lond),* **37,** 625-33.

Hutchison Ke, Lachance H, Niaura R, Bryan A and Smolen A (2002) The DRD4 VNTR polymorphism influences reactivity to smoking cues. *J Abnorm Psychol,* **111,** 134-43.

Innamorati M, Imperatori C, Balsamo M, Tamburello S, Belvederi Murri M, Contardi A, Tamburello A and Fabbricatore M (2014) Food Cravings Questionnaire-Trait (FCQ-T) discriminates between obese and overweight patients with and without binge eating tendencies: the Italian version of the FCQ-T. *J Pers Assess,* **96,** 632-9.

Jacobson A, Green E, Haase L, Szajer J and Murphy C (2019) Differential Effects of BMI on Brain Response to Odor in Olfactory, Reward and Memory Regions: Evidence from fMRI. *Nutrients,* **11.**

Jain Ak, Morty Mn and Flynn Pj (1999) Data Clustering: a Review. *ACM Computing Surveys,* **31,** 264-323.

Janes Ac, Farmer S, Peechatka Al, Frederick Beb and Lukas Se (2015) Insula-Dorsal Anterior Cingulate Cortex Coupling is Associated with Enhanced Brain Reactivity to Smoking Cues. *Neuropsychopharmacology,* **40,** 1561-8.

Janes Ac, Pizzagalli Da, Richardt S, Deb Frederick B, Chuzi S, Pachas G, Culhane Ma, Holmes Aj, Fava M, Evins Ae and Kaufman Mj (2010) Brain reactivity to smoking cues prior to smoking cessation predicts ability to maintain tobacco abstinence. *Biol Psychiatry,* **67,** 722-9.

Janse Van Rensburg K, Taylor A, Hodgson T and Benattayallah A (2009) Acute exercise modulates cigarette cravings and brain activation in response to smoking-related images: an fMRI study. *Psychopharmacology (Berl),* **203,** 589-98.

Jansen Jm, Daams Jg, Koeter Mw, Veltman Dj, Van Den Brink W and Goudriaan Ae (2013) Effects of non-invasive neurostimulation on craving: a meta-analysis. *Neurosci Biobehav Rev,* **37,** 2472-80.

Jasinska Aj, Stein Ea, Kaiser J, Naumer Mj and Yalachkov Y (2014) Factors modulating neural reactivity to drug cues in addiction: a survey of human neuroimaging studies. *Neurosci Biobehav Rev,* **38,** 1-16.

Jastreboff Am, Sinha R, Lacadie C, Small Dm, Sherwin Rs and Potenza Mn (2013) Neural correlates of stress- and food cue-induced food craving in obesity: association with insulin levels. *Diabetes Care,* **36,** 394-402.

Jauch-Chara K, Kistenmacher A, Herzog N, Schwarz M, Schweiger U and Oltmanns Km (2014) Repetitive electric brain stimulation reduces food intake in humans. *Am J Clin Nutr,* **100,** 1003-9.

Jeffery Rw, Drewnowski A, Epstein Lh, Stunkard Aj, Wilson Gt, Wing Rr and Hill Dr (2000) Long-term maintenance of weight loss: current status. *Health Psychol,* **19,** 5-16.

Jiang G, Wen X, Qiu Y, Zhang R, Wang J, Li M, Ma X, Tian J and Huang R (2013) Disrupted topological organization in whole-brain functional networks of heroin-dependent individuals: a resting-state FMRI study. *PLoS One,* **8,** e82715.

Jobard G, Crivello F and Tzourio-Mazoyer N (2003) Evaluation of the dual route theory of reading: a metanalysis of 35 neuroimaging studies. *Neuroimage,* **20,** 693-712.

Kaag Am, Reneman L, Homberg J, Van Den Brink W and Van Wingen Ga (2018) Enhanced Amygdala-Striatal Functional Connectivity during the Processing of Cocaine Cues in Male Cocaine Users with a History of Childhood Trauma. *Front Psychiatry,* **9,** 70.

Kahnt T, Heinzle J, Park Sq and Haynes Jd (2010) The neural code of reward anticipation in human orbitofrontal cortex. *Proc Natl Acad Sci U S A,* **107,** 6010-5.

Kalisch R, Wiech K, Critchley Hd and Dolan Rj (2006) Levels of appraisal: a medial prefrontal role in high-level appraisal of emotional material. *Neuroimage,* **30,** 1458-66.

Kalivas Pw and Volkow Nd (2005) The neural basis of addiction: a pathology of motivation and choice. *Am J Psychiatry,* **162,** 1403-13.

Kanno M, Matsumoto M, Togashi H, Yoshioka M and Mano Y (2004) Effects of acute repetitive transcranial magnetic stimulation on dopamine release in the rat dorsolateral striatum. *J Neurol Sci,* **217,** 73-81.

Karoly Hc, Schacht Jp, Meredith Lr, Jacobus J, Tapert Sf, Gray Km and Squeglia Lm (2019) Investigating a novel fMRI cannabis cue reactivity task in youth. *Addict Behav,* **89,** 20-28.

Karra E, O'daly Og, Choudhury Ai, Yousseif A, Millership S, Neary Mt, Scott Wr, Chandarana K, Manning S, Hess Me, Iwakura H, Akamizu T, Millet Q, Gelegen C, Drew Me, Rahman S, Emmanuel Jj, Williams Sc, Rüther Uu, Brüning Jc, Withers Dj, Zelaya Fo and Batterham Rl (2013) A link between FTO, ghrelin, and impaired brain food-cue responsivity. *J Clin Invest,* **123,** 3539-51.

Kekic M, Mcclelland J, Campbell I, Nestler S, Rubia K, David As and Schmidt U (2014) The effects of prefrontal cortex transcranial direct current stimulation (tDCS) on food

craving and temporal discounting in women with frequent food cravings. *Appetite,* **78,** 55-62.

Kelly B, Halford Jc, Boyland Ej, Chapman K, Bautista-Castaño I, Berg C, Caroli M, Cook B, Coutinho Jg, Effertz T, Grammatikaki E, Keller K, Leung R, Manios Y, Monteiro R, Pedley C, Prell H, Raine K, Recine E, Serra-Majem L, Singh S and Summerbell C (2010) Television food advertising to children: a global perspective. *Am J Public Health,* **100,** 1730-6.

Kennedy J and Dimitropoulos A (2014) Influence of feeding state on neurofunctional differences between individuals who are obese and normal weight: a meta-analysis of neuroimaging studies. *Appetite,* **75,** 103-9.

Kennerley Sw, Walton Me, Behrens Te, Buckley Mj and Rushworth Mf (2006) Optimal decision making and the anterior cingulate cortex. *Nat Neurosci,* **9,** 940-7.

Killgore Wd, Young Ad, Femia La, Bogorodzki P, Rogowska J and Yurgelun-Todd Da (2003) Cortical and limbic activation during viewing of high- versus low-calorie foods. *Neuroimage,* **19,** 1381-94.

Kilts Cd, Schweitzer Jb, Quinn Ck, Gross Re, Faber Tl, Muhammad F, Ely Td, Hoffman Jm and Drexler Kp (2001) Neural activity related to drug craving in cocaine addiction. *Arch Gen Psychiatry,* **58,** 334-41.

Kim Sh, Chung Jh, Kim Th, Lim Sh, Kim Y, Eun Ym and Lee Ya (2019a) The effects of repetitive transcranial magnetic stimulation on body weight and food consumption in obese adults: A randomized controlled study. *Brain Stimul,* **12,** 1556-1564.

Kim Sh, Chung Jh, Kim Th, Lim Sh, Kim Y, Lee Ya and Song Sw (2018) The effects of repetitive transcranial magnetic stimulation on eating behaviors and body weight in obesity: A randomized controlled study. *Brain Stimul,* **11,** 528-535.

Kim Sh, Park By, Byeon K, Park H, Kim Y, Eun Ym and Chung Jh (2019b) The effects of high-frequency repetitive transcranial magnetic stimulation on resting-state functional connectivity in obese adults. *Diabetes Obes Metab,* **21,** 1956-1966.

Kim Sm, Han Dh, Min Kj, Kim Bn and Cheong Jh (2014) Brain activation in response to craving- and aversion-inducing cues related to alcohol in patients with alcohol dependence. *Drug Alcohol Depend,* **141,** 124-31.

Kishinevsky Fi, Cox Je, Murdaugh Dl, Stoeckel Le, Cook Ew and Weller Re (2012) fMRI reactivity on a delay discounting task predicts weight gain in obese women. *Appetite,* **58,** 582-92.

Knight Rt, Grabowecky Mf and Scabini D (1995) Role of human prefrontal cortex in attention control. *Adv Neurol,* **66,** 21-34; discussion 34-6.

Kober H, Lacadie Cm, Wexler Be, Malison Rt, Sinha R and Potenza Mn (2016) Brain Activity During Cocaine Craving and Gambling Urges: An fMRI Study. *Neuropsychopharmacology,* **41,** 628-37.

Kober H, Mende-Siedlecki P, Kross Ef, Weber J, Mischel W, Hart Cl and Ochsner Kn (2010) Prefrontal-striatal pathway underlies cognitive regulation of craving. *Proc Natl Acad Sci U S A,* **107,** 14811-6.

Koob Gf (1992) Drugs of abuse: anatomy, pharmacology and function of reward pathways. *Trends Pharmacol Sci,* **13,** 177-84.

Koob Gf (1996) Drug addiction: the yin and yang of hedonic homeostasis. *Neuron,* **16,** 893-6.

Koob Gf and Volkow Nd (2016) Neurobiology of addiction: a neurocircuitry analysis. *Lancet Psychiatry,* **3,** 760-773.

Koopmann A, Bach P, Schuster R, Bumb Jm, Vollstädt-Klein S, Reinhard I, Rietschel M, Witt Sh, Wiedemann K and Kiefer F (2019) Ghrelin modulates mesolimbic reactivity

to alcohol cues in alcohol-addicted subjects: a functional imaging study. *Addict Biol,* **24,** 1066-1076.

Kosten Tr, Scanley Be, Tucker Ka, Oliveto A, Prince C, Sinha R, Potenza Mn, Skudlarski P and Wexler Be (2006) Cue-induced brain activity changes and relapse in cocaine-dependent patients. *Neuropsychopharmacology,* **31,** 644-50.

Koyama S, Kawaharada M, Terai H, Ohkurano M, Mori M, Kanamaru S and Hirose S (2013) Obesity decreases excitability of putative ventral tegmental area GABAergic neurons. *Physiol Rep,* **1,** e00126.

Krakowski M, Czobor P and Citrome L (2009) Weight gain, metabolic parameters, and the impact of race in aggressive inpatients randomized to double-blind clozapine, olanzapine or haloperidol. *Schizophr Res,* **110,** 95-102.

Krienke Uj, Nikesch F, Spiegelhalder K, Hennig J, Olbrich Hm and Langosch Jm (2014) Impact of alcohol-related video sequences on functional MRI in abstinent alcoholics. *Eur Addict Res,* **20,** 33-40.

Kringelbach Ml (2005) The human orbitofrontal cortex: linking reward to hedonic experience. *Nat Rev Neurosci,* **6,** 691-702.

Kringelbach Ml, De Araujo Ie and Rolls Et (2004) Taste-related activity in the human dorsolateral prefrontal cortex. *Neuroimage,* **21,** 781-8.

Kullmann S, Heni M, Linder K, Zipfel S, Häring Hu, Veit R, Fritsche A and Preissl H (2014) Resting-state functional connectivity of the human hypothalamus. *Hum Brain Mapp,* **35,** 6088-96.

Kullmann S, Heni M, Veit R, Ketterer C, Schick F, Häring Hu, Fritsche A and Preissl H (2012) The obese brain: association of body mass index and insulin sensitivity with resting state network functional connectivity. *Hum Brain Mapp,* **33,** 1052-61.

Kullmann S, Pape Aa, Heni M, Ketterer C, Schick F, Häring Hu, Fritsche A, Preissl H and Veit R (2013) Functional network connectivity underlying food processing: disturbed salience and visual processing in overweight and obese adults. *Cereb Cortex,* **23,** 1247-56.

Kühn S and Gallinat J (2011) Common biology of craving across legal and illegal drugs - a quantitative meta-analysis of cue-reactivity brain response. *Eur J Neurosci,* **33,** 1318-26.

Lancaster Jl, Tordesillas-Gutiérrez D, Martinez M, Salinas F, Evans A, Zilles K, Mazziotta Jc and Fox Pt (2007) Bias between MNI and Talairach coordinates analyzed using the ICBM-152 brain template. *Hum Brain Mapp,* **28,** 1194-205.

Lapenta Om, Sierve Kd, De Macedo Ec, Fregni F and Boggio Ps (2014) Transcranial direct current stimulation modulates ERP-indexed inhibitory control and reduces food consumption. *Appetite,* **83,** 42-8.

Lauritzen Tz, D'esposito M, Heeger Dj and Silver Ma (2009) Top-down flow of visual spatial attention signals from parietal to occipital cortex. *J Vis,* **9,** 18.1-14.

Lee E, Ku J, Jung Yc, Lee H, An Sk, Kim Kr, Yoon Kj and Namkoong K (2013) Neural evidence for emotional involvement in pathological alcohol craving. *Alcohol Alcohol,* **48,** 288-94.

Lee Mr, Caparelli Ec, Leff M, Steele Vr, Maxwell Am, Mccullough K and Salmeron Bj (2020) Repetitive Transcranial Magnetic Stimulation Delivered With an H-Coil to the Right Insula Reduces Functional Connectivity Between Insula and Medial Prefrontal Cortex. *Neuromodulation,* **23,** 384-392.

Lewis Jw (2006) Cortical networks related to human use of tools. *Neuroscientist,* **12,** 211-31.

Li Cs, Kemp K, Milivojevic V and Sinha R (2005) Neuroimaging study of sex differences in the neuropathology of cocaine abuse. *Gend Med,* **2,** 174-82.

Li P, Shan H, Liang S, Nie B, Liu H, Duan S, Huang Q, Zhang T, Dong G, Guo Y, Du J, Gao H, Ma L, Li D and Shan B (2018) Sleeve Gastrectomy Recovering Disordered Brain Function in Subjects with Obesity: a Longitudinal fMRI Study. *Obes Surg,* **28,** 2421-2428.

Li Q, Li W, Wang H, Wang Y, Zhang Y, Zhu J, Zheng Y, Zhang D, Wang L, Li Y, Yan X, Chang H, Fan M, Li Z, Tian J, Gold Ms, Wang W and Liu Y (2015) Predicting subsequent relapse by drug-related cue-induced brain activation in heroin addiction: an event-related functional magnetic resonance imaging study. *Addict Biol,* **20,** 968-78.

Li Q, Wang Y, Zhang Y, Li W, Yang W, Zhu J, Wu N, Chang H, Zheng Y, Qin W, Zhao L, Yuan K, Liu J, Wang W and Tian J (2012) Craving correlates with mesolimbic responses to heroin-related cues in short-term abstinence from heroin: an event-related fMRI study. *Brain Res,* **1469,** 63-72.

Li Q, Wang Y, Zhang Y, Li W, Zhu J, Zheng Y, Chen J, Zhao L, Zhou Z, Liu Y, Wang W and Tian J (2013a) Assessing cue-induced brain response as a function of abstinence duration in heroin-dependent individuals: an event-related fMRI study. *PLoS One,* **8,** e62911.

Li Q, Yang Wc, Wang Yr, Huang Yf, Li W, Zhu J, Zhang Y, Zhao Ly, Qin W, Yuan K, Von Deneen Km, Wang W and Tian J (2013b) Abnormal function of the posterior cingulate cortex in heroin addicted users during resting-state and drug-cue stimulation task. *Chin Med J (Engl),* **126,** 734-9.

Li X, Chen L, Ma R, Wang H, Wan L, Wang Y, Bu J, Hong W, Lv W, Vollstädt-Klein S, Yang Y and Zhang X (2019) The top-down regulation from the prefrontal cortex to insula via hypnotic aversion suggestions reduces smoking craving. *Hum Brain Mapp,* **40,** 1718-1728.

Liakakis G, Nickel J and Seitz Rj (2011) Diversity of the inferior frontal gyrus--a meta-analysis of neuroimaging studies. *Behav Brain Res,* **225,** 341-7.

Liberman K, Van Schuerbeek P, Herremans S, Meysman M, De Mey J and Buls N (2018) The effect of nicotine patches on craving in the brain: A functional MRI study on heavy smokers. *Medicine (Baltimore),* **97,** e12415.

Lieberman Md and Cunningham Wa (2009) Type I and Type II error concerns in fMRI research: re-balancing the scale. *Soc Cogn Affect Neurosci,* **4,** 423-8.

Lim Sl, O'doherty Jp and Rangel A (2013) Stimulus value signals in ventromedial PFC reflect the integration of attribute value signals computed in fusiform gyrus and posterior superior temporal gyrus. *J Neurosci,* **33,** 8729-41.

Limbrick-Oldfield Eh, Mick I, Cocks Re, Mcgonigle J, Sharman Sp, Goldstone Ap, Stokes Pr, Waldman A, Erritzoe D, Bowden-Jones H, Nutt D, Lingford-Hughes A and Clark L (2017) Neural substrates of cue reactivity and craving in gambling disorder. *Transl Psychiatry,* **7,** e992.

Liotti M, Brannan S, Egan G, Shade R, Madden L, Abplanalp B, Robillard R, Lancaster J, Zamarripa Fe, Fox Pt and Denton D (2001) Brain responses associated with consciousness of breathlessness (air hunger). *Proc Natl Acad Sci U S A,* **98,** 2035-40.

Liu Cm and Kanoski Se (2018) Homeostatic and non-homeostatic controls of feeding behavior: Distinct vs. common neural systems. *Physiol Behav*.

Liu X, Banich Mt, Jacobson Bl and Tanabe Jl (2004) Common and distinct neural substrates of attentional control in an integrated Simon and spatial Stroop task as assessed by event-related fMRI. *Neuroimage,* **22,** 1097-106.

Logothetis Nk (2008) What we can do and what we cannot do with fMRI. *Nature,* **453,** 869-78.

Lou M, Wang E, Shen Y and Wang J (2012) Cue-elicited craving in heroin addicts at different abstinent time: an fMRI pilot study. *Subst Use Misuse,* **47,** 631-9.

Lundgren Jd, Patrician Tm, Breslin Fj, Martin Le, Donnelly Je and Savage Cr (2013) Evening hyperphagia and food motivation: a preliminary study of neural mechanisms. *Eat Behav,* **14,** 447-50.

Luo S, Romero A, Adam Tc, Hu Hh, Monterosso J and Page Ka (2013) Abdominal fat is associated with a greater brain reward response to high-calorie food cues in Hispanic women. *Obesity (Silver Spring),* **21,** 2029-36.

Mann K, Vollstädt-Klein S, Reinhard I, Leménager T, Fauth-Bühler M, Hermann D, Hoffmann S, Zimmermann Us, Kiefer F, Heinz A and Smolka Mn (2014) Predicting naltrexone response in alcohol-dependent patients: the contribution of functional magnetic resonance imaging. *Alcohol Clin Exp Res,* **38,** 2754-62.

Mann T, Tomiyama Aj, Westling E, Lew Am, Samuels B and Chatman J (2007) Medicare's search for effective obesity treatments: diets are not the answer. *Am Psychol,* **62,** 220-33.

Mantel N and Haenszel W (1959) Statistical aspects of the analysis of data from retrospective studies of disease. *J Natl Cancer Inst,* **22,** 719-48.

Martens Mj, Born Jm, Lemmens Sg, Karhunen L, Heinecke A, Goebel R, Adam Tc and Westerterp-Plantenga Ms (2013) Increased sensitivity to food cues in the fasted state and decreased inhibitory control in the satiated state in the overweight. *Am J Clin Nutr,* **97,** 471-9.

Martin Le, Holsen Lm, Chambers Rj, Bruce As, Brooks Wm, Zarcone Jr, Butler Mg and Savage Cr (2010) Neural mechanisms associated with food motivation in obese and healthy weight adults. *Obesity (Silver Spring),* **18,** 254-60.

Martuzzi R, Ramani R, Qiu M, Shen X, Papademetris X and Constable Rt (2011) A whole-brain voxel based measure of intrinsic connectivity contrast reveals local changes in tissue connectivity with anesthetic without a priori assumptions on thresholds or regions of interest. *Neuroimage,* **58,** 1044-50.

Maumet C and Nichols Te (2016) Minimal data needed for valid & accurate image-based fMRI meta-analysis. *BioRxiv   048249*.

Mazziotta Jc, Toga Aw, Evans A, Fox P and Lancaster J (1995) A probabilistic atlas of the human brain: theory and rationale for its development. The International Consortium for Brain Mapping (ICBM). *Neuroimage,* **2,** 89-101.

Mcbride D, Barrett Sp, Kelly Jt, Aw A and Dagher A (2006) Effects of expectancy and abstinence on the neural response to smoking cues in cigarette smokers: an fMRI study. *Neuropsychopharmacology,* **31,** 2728-38.

Mcclernon Fj, Hiott Fb, Huettel Sa and Rose Je (2005) Abstinence-induced changes in self-report craving correlate with event-related FMRI responses to smoking cues. *Neuropsychopharmacology,* **30,** 1940-7.

Mcclernon Fj, Hutchison Ke, Rose Je and Kozink Rv (2007) DRD4 VNTR polymorphism is associated with transient fMRI-BOLD responses to smoking cues. *Psychopharmacology (Berl),* **194,** 433-41.

Mcclernon Fj, Kozink Rv, Lutz Am and Rose Je (2009) 24-h smoking abstinence potentiates fMRI-BOLD activation to smoking cues in cerebral cortex and dorsal striatum. *Psychopharmacology (Berl),* **204,** 25-35.

Mcclernon Fj, Kozink Rv and Rose Je (2008) Individual differences in nicotine dependence, withdrawal symptoms, and sex predict transient fMRI-BOLD responses to smoking cues. *Neuropsychopharmacology,* **33,** 2148-57.

Mcfadden Kl, Cornier Ma, Melanson El, Bechtell Jl and Tregellas Jr (2013) Effects of exercise on resting-state default mode and salience network activity in overweight/obese adults. *Neuroreport,* **24,** 866-71.

Mcfarland K and Kalivas Pw (2001) The circuitry mediating cocaine-induced reinstatement of drug-seeking behavior. *J Neurosci,* **21,** 8655-63.

Mclaughlin J and See Re (2003) Selective inactivation of the dorsomedial prefrontal cortex and the basolateral amygdala attenuates conditioned-cued reinstatement of extinguished cocaine-seeking behavior in rats. *Psychopharmacology (Berl),* **168,** 57-65.

Mclellan At, Lewis Dc, O'brien Cp and Kleber Hd (2000) Drug dependence, a chronic medical illness: implications for treatment, insurance, and outcomes evaluation. *JAMA,* **284,** 1689-95.

Meany G, Conceição E and Mitchell Je (2014) Binge eating, binge eating disorder and loss of control eating: effects on weight outcomes after bariatric surgery. *Eur Eat Disord Rev,* **22,** 87-91.

Mitchell M, Baurzhan M and Tobias W "Engauge Digitizer Software". Webpage: http://markummitchell.github.io/engauge-digitizer.

Montenegro Ra, Okano Ah, Cunha Fa, Gurgel Jl, Fontes Eb and Farinatti Pt (2012) Prefrontal cortex transcranial direct current stimulation associated with aerobic exercise change aspects of appetite sensation in overweight adults. *Appetite,* **58,** 333-8.

Montorsi F, Perani D, Anchisi D, Salonia A, Scifo P, Rigiroli P, Zanoni M, Heaton Jp, Rigatti P and Fazio F (2003) Apomorphine-induced brain modulation during sexual stimulation: a new look at central phenomena related to erectile dysfunction. *Int J Impot Res,* **15,** 203-9.

Moran Lv, Betts Jm, Ongur D and Janes Ac (2018) Neural Responses to Smoking Cues in Schizophrenia. *Schizophr Bull,* **44,** 525-534.

Murdaugh Dl, Cox Je, Cook Ew and Weller Re (2012) fMRI reactivity to high-calorie food pictures predicts short- and long-term outcome in a weight-loss program. *Neuroimage,* **59,** 2709-21.

Murphy K and Garavan H (2004) An empirical investigation into the number of subjects required for an event-related fMRI study. *Neuroimage,* **22,** 879-85.

Murray E, Brouwer S, Mccutcheon R, Harmer Cj, Cowen Pj and Mccabe C (2014) Opposing neural effects of naltrexone on food reward and aversion: implications for the treatment of obesity. *Psychopharmacology (Berl),* **231,** 4323-35.

Myrick H, Anton Rf, Li X, Henderson S, Drobes D, Voronin K and George Ms (2004) Differential brain activity in alcoholics and social drinkers to alcohol cues: relationship to craving. *Neuropsychopharmacology,* **29,** 393-402.

Myrick H, Anton Rf, Li X, Henderson S, Randall Pk and Voronin K (2008) Effect of naltrexone and ondansetron on alcohol cue-induced activation of the ventral striatum in alcohol-dependent people. *Arch Gen Psychiatry,* **65,** 466-75.

Müller Vi, Cieslik Ec, Laird Ar, Fox Pt, Radua J, Mataix-Cols D, Tench Cr, Yarkoni T, Nichols Te, Turkeltaub Pe, Wager Td and Eickhoff Sb (2018) Ten simple rules for neuroimaging meta-analysis. *Neurosci Biobehav Rev,* **84,** 151-161.

Naqvi Nh and Bechara A (2009) The hidden island of addiction: the insula. *Trends Neurosci,* **32,** 56-67.

Naqvi Nh, Rudrauf D, Damasio H and Bechara A (2007) Damage to the insula disrupts addiction to cigarette smoking. *Science,* **315,** 531-4.

Nederkoorn C, Braet C, Van Eijs Y, Tanghe A and Jansen A (2006a) Why obese children cannot resist food: the role of impulsivity. *Eat Behav,* **7,** 315-22.

Nederkoorn C, Smulders Ft, Havermans Rc, Roefs A and Jansen A (2006b) Impulsivity in obese women. *Appetite,* **47,** 253-6.

Nesse Rm and Berridge Kc (1997) Psychoactive drug use in evolutionary perspective. *Science,* **278,** 63-6.

Niaura Rs, Rohsenow Dj, Binkoff Ja, Monti Pm, Pedraza M and Abrams Db (1988) Relevance of cue reactivity to understanding alcohol and smoking relapse. *J Abnorm Psychol,* **97,** 133-52.

Nitsche Ma, Cohen Lg, Wassermann Em, Priori A, Lang N, Antal A, Paulus W, Hummel F, Boggio Ps, Fregni F and Pascual-Leone A (2008) Transcranial direct current stimulation: State of the art 2008. *Brain Stimul,* **1,** 206-23.

Nummenmaa L, Hirvonen J, Hannukainen Jc, Immonen H, Lindroos Mm, Salminen P and Nuutila P (2012) Dorsal striatum and its limbic connectivity mediate abnormal anticipatory reward processing in obesity. *PLoS One,* **7,** e31089.

Nutt D, King La, Saulsbury W and Blakemore C (2007) Development of a rational scale to assess the harm of drugs of potential misuse. *Lancet,* **369,** 1047-53.

Ochsner Kn, Ray Rd, Cooper Jc, Robertson Er, Chopra S, Gabrieli Jd and Gross Jj (2004) For better or for worse: neural systems supporting the cognitive down- and up-regulation of negative emotion. *Neuroimage,* **23,** 483-99.

Park Ms, Sohn Jh, Suk Ja, Kim Sh, Sohn S and Sparacio R (2007) Brain substrates of craving to alcohol cues in subjects with alcohol use disorder. *Alcohol Alcohol,* **42,** 417-22.

Paulesu E, Danelli L and Berlingeri M (2014) Reading the dyslexic brain: multiple dysfunctional routes revealed by a new meta-analysis of PET and fMRI activation studies. *Front Hum Neurosci,* **8,** 830.

Pelchat Ml, Johnson A, Chan R, Valdez J and Ragland Jd (2004) Images of desire: food-craving activation during fMRI. *Neuroimage,* **23,** 1486-93.

Pohjalainen T, Rinne Jo, Någren K, Lehikoinen P, Anttila K, Syvälahti Ek and Hietala J (1998) The A1 allele of the human D2 dopamine receptor gene predicts low D2 receptor availability in healthy volunteers. *Mol Psychiatry,* **3,** 256-60.

Potenza Mn, Hong Ki, Lacadie Cm, Fulbright Rk, Tuit Kl and Sinha R (2012) Neural correlates of stress-induced and cue-induced drug craving: influences of sex and cocaine dependence. *Am J Psychiatry,* **169,** 406-14.

Prisciandaro Jj, Mcrae-Clark Al, Myrick H, Henderson S and Brady Kt (2014) Brain activation to cocaine cues and motivation/treatment status. *Addict Biol,* **19,** 240-9.

Prisciandaro Jj, Myrick H, Henderson S, Mcrae-Clark Al and Brady Kt (2013a) Prospective associations between brain activation to cocaine and no-go cues and cocaine relapse. *Drug Alcohol Depend,* **131,** 44-9.

Prisciandaro Jj, Myrick H, Henderson S, Mcrae-Clark Al, Santa Ana Ej, Saladin Me and Brady Kt (2013b) Impact of DCS-facilitated cue exposure therapy on brain activation to cocaine cues in cocaine dependence. *Drug Alcohol Depend,* **132,** 195-201.

Pursey Km, Stanwell P, Callister Rj, Brain K, Collins Ce and Burrows Tl (2014) Neural responses to visual food cues according to weight status: a systematic review of functional magnetic resonance imaging studies. *Front Nutr,* **1,** 7.

Puzziferri N, Zigman Jm, Thomas Bp, Mihalakos P, Gallagher R, Lutter M, Carmody T, Lu H and Tamminga Ca (2016) Brain imaging demonstrates a reduced neural impact of eating in obesity. *Obesity (Silver Spring),* **24,** 829-36.

Raichle Me (2015) The brain's default mode network. *Annu Rev Neurosci,* **38,** 433-47.

Rajan I, Murthy Pj, Ramakrishnan Ag, Gangadhar Bn and Janakiramaiah N (1998) Heart rate variability as an index of cue reactivity in alcoholics. *Biol Psychiatry,* **43,** 544-6.

Raschpichler M, Straatman K, Schroeter Ml, Arelin K, Schlögl H, Fritzsch D, Mende M, Pampel A, Böttcher Y, Stumvoll M, Villringer A and Mueller K (2013) Abdominal fat distribution and its relationship to brain changes: the differential effects of age on cerebellar structure and function: a cross-sectional, exploratory study. *BMJ Open,* **3**.

Ray S, Haney M, Hanson C, Biswal B and Hanson Sj (2015) Modeling Causal Relationship Between Brain Regions Within the Drug-Cue Processing Network in Chronic Cocaine Smokers. *Neuropsychopharmacology,* **40,** 2960-8.

Reinhard I, Leménager T, Fauth-Bühler M, Hermann D, Hoffmann S, Heinz A, Kiefer F, Smolka Mn, Wellek S, Mann K and Vollstädt-Klein S (2015) A comparison of region-of-interest measures for extracting whole brain data using survival analysis in alcoholism as an example. *J Neurosci Methods,* **242,** 58-64.

Ritchie T and Noble Ep (2003) Association of seven polymorphisms of the D2 dopamine receptor gene with brain receptor-binding characteristics. *Neurochem Res,* **28,** 73-82.

Robinson Jl, Laird Ar, Glahn Dc, Blangero J, Sanghera Mk, Pessoa L, Fox Pm, Uecker A, Friehs G, Young Ka, Griffin Jl, Lovallo Wr and Fox Pt (2012) The functional connectivity of the human caudate: an application of meta-analytic connectivity modeling with behavioral filtering. *Neuroimage,* **60,** 117-29.

Robinson Mj, Warlow Sm and Berridge Kc (2014) Optogenetic excitation of central amygdala amplifies and narrows incentive motivation to pursue one reward above another. *J Neurosci,* **34,** 16567-80.

Robinson Te and Berridge Kc (1993) The neural basis of drug craving: an incentive-sensitization theory of addiction. *Brain Res Brain Res Rev,* **18,** 247-91.

Rolls Et (2008) Functions of the orbitofrontal and pregenual cingulate cortex in taste, olfaction, appetite and emotion. *Acta Physiol Hung,* **95,** 131-64.

Rolls Et (2015) Taste, olfactory, and food reward value processing in the brain. *Prog Neurobiol,* **127-128,** 64-90.

Rolls Et (2019) The cingulate cortex and limbic systems for emotion, action, and memory. *Brain Struct Funct,* **224,** 3001-3018.

Rolls Et, Grabenhorst F and Deco G (2010) Choice, difficulty, and confidence in the brain. *Neuroimage,* **53,** 694-706.

Rorden C and Brett M (2000) Stereotaxic display of brain lesions. *Behav Neurol,* **12,** 191-200.

Roseberry Ag, Painter T, Mark Gp and Williams Jt (2007) Decreased vesicular somatodendritic dopamine stores in leptin-deficient mice. *J Neurosci,* **27,** 7021-7.

Roth Y, Amir A, Levkovitz Y and Zangen A (2007) Three-dimensional distribution of the electric field induced in the brain by transcranial magnetic stimulation using figure-8 and deep H-coils. *J Clin Neurophysiol,* **24,** 31-8.

Rothemund Y, Preuschhof C, Bohner G, Bauknecht Hc, Klingebiel R, Flor H and Klapp Bf (2007) Differential activation of the dorsal striatum by high-calorie visual food stimuli in obese individuals. *Neuroimage,* **37,** 410-21.

Rubinov M and Sporns O (2010) Complex network measures of brain connectivity: uses and interpretations. *Neuroimage,* **52,** 1059-69.

Salimi-Khorshidi G, Smith Sm, Keltner Jr, Wager Td and Nichols Te (2009) Meta-analysis of neuroimaging data: a comparison of image-based and coordinate-based pooling of studies. *Neuroimage,* **45,** 810-23.

Salvador R, Suckling J, Coleman Mr, Pickard Jd, Menon D and Bullmore E (2005) Neurophysiological architecture of functional magnetic resonance images of human brain. *Cereb Cortex,* **15,** 1332-42.

Sanz-Arigita Ej, Schoonheim Mm, Damoiseaux Js, Rombouts Sa, Maris E, Barkhof F, Scheltens P and Stam Cj (2010) Loss of 'small-world' networks in Alzheimer's disease: graph analysis of FMRI resting-state functional connectivity. *PLoS One,* **5,** e13788.

Schacht Jp, Anton Rf and Myrick H (2013) Functional neuroimaging studies of alcohol cue reactivity: a quantitative meta-analysis and systematic review. *Addict Biol,* **18,** 121-33.

Scharmüller W, Übel S, Ebner F and Schienle A (2012) Appetite regulation during food cue exposure: a comparison of normal-weight and obese women. *Neurosci Lett,* **518,** 106-10.

Schlam Tr, Wilson Nl, Shoda Y, Mischel W and Ayduk O (2013) Preschoolers' delay of gratification predicts their body mass 30 years later. *J Pediatr,* **162,** 90-3.

Schmidt U and Campbell Ic (2013) Treatment of eating disorders can not remain 'brainless': the case for brain-directed treatments. *Eur Eat Disord Rev,* **21,** 425-7.

Seeyave Dm, Coleman S, Appugliese D, Corwyn Rf, Bradley Rh, Davidson Ns, Kaciroti N and Lumeng Jc (2009) Ability to delay gratification at age 4 years and risk of overweight at age 11 years. *Arch Pediatr Adolesc Med,* **163,** 303-8.

Self Dw (2004) Regulation of drug-taking and -seeking behaviors by neuroadaptations in the mesolimbic dopamine system. *Neuropharmacology,* **47 Suppl 1,** 242-55.

Shao C, Li Y, Jiang K, Zhang D, Xu Y, Lin L, Wang Q, Zhao M and Jin L (2006) Dopamine D4 receptor polymorphism modulates cue-elicited heroin craving in Chinese. *Psychopharmacology (Berl),* **186,** 185-90.

Shehzad Z, Kelly Am, Reiss Pt, Gee Dg, Gotimer K, Uddin Lq, Lee Sh, Margulies Ds, Roy Ak, Biswal Bb, Petkova E, Castellanos Fx and Milham Mp (2009) The resting brain: unconstrained yet reliable. *Cereb Cortex,* **19,** 2209-29.

Shott Me, Cornier Ma, Mittal Va, Pryor Tl, Orr Jm, Brown Ms and Frank Gk (2015) Orbitofrontal cortex volume and brain reward response in obesity. *Int J Obes (Lond),* **39,** 214-21.

Siep N, Roefs A, Roebroeck A, Havermans R, Bonte M and Jansen A (2012) Fighting food temptations: the modulating effects of short-term cognitive reappraisal, suppression and up-regulation on mesocorticolimbic activity related to appetitive motivation. *Neuroimage,* **60,** 213-20.

Silvers Ja, Insel C, Powers A, Franz P, Weber J, Mischel W, Casey Bj and Ochsner Kn (2014) Curbing craving: behavioral and brain evidence that children regulate craving when instructed to do so but have higher baseline craving than adults. *Psychol Sci,* **25,** 1932-42.

Sinha R (2008) Chronic stress, drug use, and vulnerability to addiction. *Ann N Y Acad Sci,* **1141,** 105-30.

Small Dm, Jones-Gotman M, Zatorre Rj, Petrides M and Evans Ac (1997a) A role for the right anterior temporal lobe in taste quality recognition. *J Neurosci,* **17,** 5136-42.

Small Dm, Jones-Gotman M, Zatorre Rj, Petrides M and Evans Ac (1997b) Flavor processing: more than the sum of its parts. *Neuroreport,* **8,** 3913-7.

Small Dm, Zald Dh, Jones-Gotman M, Zatorre Rj, Pardo Jv, Frey S and Petrides M (1999) Human cortical gustatory areas: a review of functional neuroimaging data. *Neuroreport,* **10,** 7-14.

Smolka Mn, Bühler M, Klein S, Zimmermann U, Mann K, Heinz A and Braus Df (2006) Severity of nicotine dependence modulates cue-induced brain activity in regions involved in motor preparation and imagery. *Psychopharmacology (Berl),* **184,** 577-88.

Sobhany Ms and Rogers Cs (1985) External responsiveness to food and non-food cues among obese and non-obese children. *Int J Obes,* **9,** 99-106.

Song S, Zilverstand A, Gui W, Li Hj and Zhou X (2019) Effects of single-session versus multi-session non-invasive brain stimulation on craving and consumption in individuals with drug addiction, eating disorders or obesity: A meta-analysis. *Brain Stimul,* **12,** 606-618.

St-Onge Mp, Wolfe S, Sy M, Shechter A and Hirsch J (2014) Sleep restriction increases the neuronal response to unhealthy food in normal-weight individuals. *Int J Obes (Lond),* **38,** 411-6.

Stevenson M, Nunes T, Sanchez J, Thornton R, Reiczigel J, Robison-Cox J and Sebastiani P (2013) epiR: An R package for the analysis of epidemiological data. R *package version 0.9-43* .

Stice E, Burger Ks and Yokum S (2015a) Reward Region Responsivity Predicts Future Weight Gain and Moderating Effects of the TaqIA Allele. *J Neurosci,* **35,** 10316-24.

Stice E and Dagher A (2010) Genetic variation in dopaminergic reward in humans. *Forum Nutr,* **63,** 176-85.

Stice E, Spoor S, Bohon C and Small Dm (2008a) Relation between obesity and blunted striatal response to food is moderated by TaqIA A1 allele. *Science,* **322,** 449-52.

Stice E, Spoor S, Bohon C, Veldhuizen Mg and Small Dm (2008b) Relation of reward from food intake and anticipated food intake to obesity: a functional magnetic resonance imaging study. *J Abnorm Psychol,* **117,** 924-35.

Stice E and Yokum S (2014) Brain reward region responsivity of adolescents with and without parental substance use disorders. *Psychol Addict Behav,* **28,** 805-15.

Stice E and Yokum S (2016) Neural vulnerability factors that increase risk for future weight gain. *Psychol Bull,* **142,** 447-71.

Stice E, Yokum S, Blum K and Bohon C (2010a) Weight gain is associated with reduced striatal response to palatable food. *J Neurosci,* **30,** 13105-9.

Stice E, Yokum S, Bohon C, Marti N and Smolen A (2010b) Reward circuitry responsivity to food predicts future increases in body mass: moderating effects of DRD2 and DRD4. *Neuroimage,* **50,** 1618-25.

Stice E, Yokum S, Burger K, Epstein L and Smolen A (2012) Multilocus genetic composite reflecting dopamine signaling capacity predicts reward circuitry responsivity. *J Neurosci,* **32,** 10093-100.

Stice E, Yokum S, Burger K, Rohde P, Shaw H and Gau Jm (2015b) A pilot randomized trial of a cognitive reappraisal obesity prevention program. *Physiol Behav,* **138,** 124-32.

Stice E, Yokum S, Burger Ks, Epstein Lh and Small Dm (2011a) Youth at risk for obesity show greater activation of striatal and somatosensory regions to food. *J Neurosci,* **31,** 4360-6.

Stice E, Yokum S, Veling H, Kemps E and Lawrence Ns (2017) Pilot test of a novel food response and attention training treatment for obesity: Brain imaging data suggest actions shape valuation. *Behav Res Ther,* **94,** 60-70.

Stice E, Yokum S, Zald D and Dagher A (2011b) Dopamine-based reward circuitry responsivity, genetics, and overeating. *Curr Top Behav Neurosci,* **6,** 81-93.

Stoeckel Le, Weller Re, Cook Ew, Twieg Db, Knowlton Rc and Cox Je (2008) Widespread reward-system activation in obese women in response to pictures of high-calorie foods. *Neuroimage,* **41,** 636-47.

Strafella Ap, Paus T, Barrett J and Dagher A (2001) Repetitive transcranial magnetic stimulation of the human prefrontal cortex induces dopamine release in the caudate nucleus. *J Neurosci,* **21,** RC157.

Subramaniapillai M and Mcintyre Rs (2017) A review of the neurobiology of obesity and the available pharmacotherapies. *CNS Spectr,* **22,** 29-38.

Sun X, Kroemer Nb, Veldhuizen Mg, Babbs Ae, De Araujo Ie, Gitelman Dr, Sherwin Rs, Sinha R and Small Dm (2015) Basolateral amygdala response to food cues in the absence of hunger is associated with weight gain susceptibility. *J Neurosci,* **35,** 7964-76.

Szalay C, Aradi M, Schwarcz A, Orsi G, Perlaki G, Németh L, Hanna S, Takács G, Szabó I, Bajnok L, Vereczkei A, Dóczi T, Janszky J, Komoly S, Örs Horváth P, Lénárd L and Karadi Z (2012) Gustatory perception alterations in obesity: an fMRI study. *Brain Res,* **1473,** 131-40.

Tabatabaei-Jafari H, Ekhtiari H, Ganjgahi H, Hassani-Abharian P, Oghabian Ma, Moradi A, Sadighi N and Zarei M (2014) Patterns of brain activation during craving in heroin dependents successfully treated by methadone maintenance and abstinence-based treatments. *J Addict Med,* **8,** 123-9.

Talairach J and Tournoux P (1988) Co-planar Stereotaxic Atlas of the Human Brain: 3-D Proportional System: An Approach to Cerebral Imaging. New York, NY: Thieme Medical Publishers.

Tang Dw, Fellows Lk, Small Dm and Dagher A (2012a) Food and drug cues activate similar brain regions: a meta-analysis of functional MRI studies. *Physiol Behav,* **106,** 317-24.

Tang Dw, Hello B, Mroziewicz M, Fellows Lk, Tyndale Rf and Dagher A (2012b) Genetic variation in CYP2A6 predicts neural reactivity to smoking cues as measured using fMRI. *Neuroimage,* **60,** 2136-43.

Tapert Sf, Brown Gg, Baratta Mv and Brown Sa (2004) fMRI BOLD response to alcohol stimuli in alcohol dependent young women. *Addict Behav,* **29,** 33-50.

Tataranni Pa, Gautier Jf, Chen K, Uecker A, Bandy D, Salbe Ad, Pratley Re, Lawson M, Reiman Em and Ravussin E (1999) Neuroanatomical correlates of hunger and satiation in humans using positron emission tomography. *Proc Natl Acad Sci U S A,* **96,** 4569-74.

Tian L, Meng C, Jiang Y, Tang Q, Wang S, Xie X, Fu X, Jin C, Zhang F and Wang J (2016) Abnormal functional connectivity of brain network hubs associated with symptom severity in treatment-naive patients with obsessive-compulsive disorder: A resting-state functional MRI study. *Prog Neuropsychopharmacol Biol Psychiatry,* **66,** 104-11.

Tomasi D, Wang Gj, Wang R, Caparelli Ec, Logan J and Volkow Nd (2015) Overlapping patterns of brain activation to food and cocaine cues in cocaine abusers: association to striatal D2/D3 receptors. *Hum Brain Mapp,* **36,** 120-36.

Torres Sj and Nowson Ca (2007) Relationship between stress, eating behavior, and obesity. *Nutrition,* **23,** 887-94.

Toschke Am, Ehlin Ag, Von Kries R, Ekbom A and Montgomery Sm (2003) Maternal smoking during pregnancy and appetite control in offspring. *J Perinat Med,* **31,** 251-6.

Tuominen L, Tuulari J, Karlsson H, Hirvonen J, Helin S, Salminen P, Parkkola R, Hietala J, Nuutila P and Nummenmaa L (2015) Aberrant mesolimbic dopamine-opiate interaction in obesity. *Neuroimage,* **122,** 80-6.

Turkeltaub Pe, Eden Gf, Jones Km and Zeffiro Ta (2002) Meta-analysis of the functional neuroanatomy of single-word reading: method and validation. *Neuroimage,* **16,** 765-80.

Turkeltaub Pe, Eickhoff Sb, Laird Ar, Fox M, Wiener M and Fox P (2012) Minimizing within-experiment and within-group effects in Activation Likelihood Estimation meta-analyses. *Hum Brain Mapp,* **33,** 1-13.

Tuulari Jj, Karlsson Hk, Hirvonen J, Salminen P, Nuutila P and Nummenmaa L (2015) Neural circuits for cognitive appetite control in healthy and obese individuals: an fMRI study. *PLoS One,* **10,** e0116640.

Uher R, Yoganathan D, Mogg A, Eranti Sv, Treasure J, Campbell Ic, Mcloughlin Dm and Schmidt U (2005) Effect of left prefrontal repetitive transcranial magnetic stimulation on food craving. *Biol Psychiatry,* **58,** 840-2.

Uhl Gr, Liu Qr and Naiman D (2002) Substance abuse vulnerability loci: converging genome scanning data. *Trends Genet,* **18,** 420-5.

Unger Jw, Livingston Jn and Moss Am (1991) Insulin receptors in the central nervous system: localization, signalling mechanisms and functional aspects. *Prog Neurobiol,* **36,** 343-62.

Val-Laillet D, Aarts E, Weber B, Ferrari M, Quaresima V, Stoeckel Le, Alonso-Alonso M, Audette M, Malbert Ch and Stice E (2015) Neuroimaging and neuromodulation approaches to study eating behavior and prevent and treat eating disorders and obesity. *Neuroimage Clin,* **8,** 1-31.

Van Bloemendaal L, Ijzerman Rg, Ten Kulve Js, Barkhof F, Konrad Rj, Drent Ml, Veltman Dj and Diamant M (2014) GLP-1 receptor activation modulates appetite- and reward-related brain areas in humans. *Diabetes,* **63,** 4186-96.

Van Der Kloot Wa, Spaans Am and Heiser Wj (2005) Instability of hierarchical cluster analysis due to input order of the data: the PermuCLUSTER solution. *Psychol Methods,* **10,** 468-76.

Van Der Laan Ln, De Ridder Dt, Viergever Ma and Smeets Pa (2011) The first taste is always with the eyes: a meta-analysis on the neural correlates of processing visual food cues. *Neuroimage,* **55,** 296-303.

Van Meer F, Van Der Laan Ln, Adan Ra, Viergever Ma and Smeets Pa (2015) What you see is what you eat: an ALE meta-analysis of the neural correlates of food viewing in children and adolescents. *Neuroimage,* **104,** 35-43.

Veldhuizen Mg, Albrecht J, Zelano C, Boesveldt S, Breslin P and Lundström Jn (2011) Identification of human gustatory cortex by activation likelihood estimation. *Hum Brain Mapp,* **32,** 2256-66.

Volkow Nd, Fowler Js, Wang Gj, Hitzemann R, Logan J, Schlyer Dj, Dewey Sl and Wolf Ap (1993) Decreased dopamine D2 receptor availability is associated with reduced frontal metabolism in cocaine abusers. *Synapse,* **14,** 169-77.

Volkow Nd, Fowler Js, Wang Gj, Telang F, Logan J, Jayne M, Ma Y, Pradhan K, Wong C and Swanson Jm (2010) Cognitive control of drug craving inhibits brain reward regions in cocaine abusers. *Neuroimage,* **49,** 2536-43.

Volkow Nd and O'brien Cp (2007) Issues for DSM-V: should obesity be included as a brain disorder? *Am J Psychiatry,* **164,** 708-10.

Volkow Nd, Wang Gj, Telang F, Fowler Js, Logan J, Childress Ar, Jayne M, Ma Y and Wong C (2006) Cocaine cues and dopamine in dorsal striatum: mechanism of craving in cocaine addiction. *J Neurosci,* **26,** 6583-8.

Volkow Nd, Wang Gj, Telang F, Fowler Js, Thanos Pk, Logan J, Alexoff D, Ding Ys, Wong C, Ma Y and Pradhan K (2008) Low dopamine striatal D2 receptors are associated with prefrontal metabolism in obese subjects: possible contributing factors. *Neuroimage,* **42,** 1537-43.

Volkow Nd, Wang Gj, Tomasi D and Baler Rd (2013) Obesity and addiction: neurobiological overlaps. *Obes Rev,* **14,** 2-18.

Volkow Nd and Wise Ra (2005) How can drug addiction help us understand obesity? *Nat Neurosci,* **8,** 555-60.

Vollstädt-Klein S, Kobiella A, Bühler M, Graf C, Fehr C, Mann K and Smolka Mn (2011) Severity of dependence modulates smokers' neuronal cue reactivity and cigarette craving elicited by tobacco advertisement. *Addict Biol,* **16,** 166-75.

Vollstädt-Klein S, Wichert S, Rabinstein J, Bühler M, Klein O, Ende G, Hermann D and Mann K (2010) Initial, habitual and compulsive alcohol use is characterized by a shift of cue processing from ventral to dorsal striatum. *Addiction,* **105,** 1741-9.

Voon V, Mole Tb, Banca P, Porter L, Morris L, Mitchell S, Lapa Tr, Karr J, Harrison Na, Potenza Mn and Irvine M (2014) Neural correlates of sexual cue reactivity in individuals with and without compulsive sexual behaviours. *PLoS One,* **9,** e102419.

Walker Rj, Brooks Hl and Holden-Dye L (1996) Evolution and overview of classical transmitter molecules and their receptors. *Parasitology,* **113 Suppl,** S3-33.

Wang Al, Elman I, Lowen Sb, Blady Sj, Lynch Kg, Hyatt Jm, O'brien Cp and Langleben Dd (2015a) Neural correlates of adherence to extended-release naltrexone pharmacotherapy in heroin dependence. *Transl Psychiatry,* **5,** e531.

Wang Gj, Volkow Nd and Fowler Js (2002) The role of dopamine in motivation for food in humans: implications for obesity. *Expert Opin Ther Targets,* **6,** 601-9.

Wang Gj, Volkow Nd, Fowler Js, Logan J, Abumrad Nn, Hitzemann Rj, Pappas Ns and Pascani K (1997) Dopamine D2 receptor availability in opiate-dependent subjects before and after naloxone-precipitated withdrawal. *Neuropsychopharmacology,* **16,** 174-82.

Wang Gj, Volkow Nd, Logan J, Pappas Nr, Wong Ct, Zhu W, Netusil N and Fowler Js (2001) Brain dopamine and obesity. *Lancet,* **357,** 354-7.

Wang Y and Lobstein T (2006) Worldwide trends in childhood overweight and obesity. *Int J Pediatr Obes,* **1,** 11-25.

Wang Y, Wang H, Li W, Zhu J, Gold Ms, Zhang D, Wang L, Li Y, Yan X, Cheng J, Li Q and Wang W (2014) Reduced responses to heroin-cue-induced craving in the dorsal striatum: effects of long-term methadone maintenance treatment. *Neurosci Lett,* **581,** 120-4.

Wang Z, Suh J, Li Z, Li Y, Franklin T, O'brien C and Childress Ar (2015b) A hyper-connected but less efficient small-world network in the substance-dependent brain. *Drug Alcohol Depend,* **152,** 102-8.

Ward J (1963) Hierarchical grouping to optimize an objective function. . *Journal of the American Statistical Association,* **Volume 58,** 236-244.

Warlow Sm, Robinson Mjf and Berridge Kc (2017) Optogenetic Central Amygdala Stimulation Intensifies and Narrows Motivation for Cocaine. *J Neurosci,* **37,** 8330-8348.

Wei X, Li W, Chen J, Li Y, Zhu J, Shi H, Liu J, Xue J, Liu W, Wang F, Liu Y, Dang S, Li Q and Wang W (2019) Assessing drug cue-induced brain response in heroin dependents treated by methadone maintenance and protracted abstinence measures. *Brain Imaging Behav*.

Wesley Mj and Bickel Wk (2014) Remember the future II: meta-analyses and functional overlap of working memory and delay discounting. *Biol Psychiatry,* **75,** 435-48.

Westbrook C, Creswell Jd, Tabibnia G, Julson E, Kober H and Tindle Ha (2013) Mindful attention reduces neural and self-reported cue-induced craving in smokers. *Soc Cogn Affect Neurosci,* **8,** 73-84.

Weygandt M, Mai K, Dommes E, Leupelt V, Hackmack K, Kahnt T, Rothemund Y, Spranger J and Haynes Jd (2013) The role of neural impulse control mechanisms for dietary success in obesity. *Neuroimage,* **83,** 669-78.

Whitfield-Gabrieli S and Nieto-Castanon A (2012) Conn: a functional connectivity toolbox for correlated and anticorrelated brain networks. *Brain Connect,* **2,** 125-41.

Wijngaarden Ma, Veer Im, Rombouts Sa, Van Buchem Ma, Willems Van Dijk K, Pijl H and Van Der Grond J (2015) Obesity is marked by distinct functional connectivity in brain networks involved in food reward and salience. *Behav Brain Res,* **287,** 127-34.

Wilson Sj, Sayette Ma, Delgado Mr and Fiez Ja (2005) Instructed smoking expectancy modulates cue-elicited neural activity: a preliminary study. *Nicotine Tob Res,* **7,** 637-45.

Wilson Sj, Sayette Ma and Fiez Ja (2004) Prefrontal responses to drug cues: a neurocognitive analysis. *Nat Neurosci,* **7,** 211-4.

Wilson Sj, Sayette Ma and Fiez Ja (2012) Quitting-unmotivated and quitting-motivated cigarette smokers exhibit different patterns of cue-elicited brain activation when anticipating an opportunity to smoke. *J Abnorm Psychol,* **121,** 198-211.

Wise Ra (1996) Addictive drugs and brain stimulation reward. *Annu Rev Neurosci,* **19,** 319-40.

Wrase J, Schlagenhauf F, Kienast T, Wüstenberg T, Bermpohl F, Kahnt T, Beck A, Ströhle A, Juckel G, Knutson B and Heinz A (2007) Dysfunction of reward processing correlates with alcohol craving in detoxified alcoholics. *Neuroimage,* **35,** 787-94.

Xiao Z, Lee T, Zhang Jx, Wu Q, Wu R, Weng X and Hu X (2006) Thirsty heroin addicts show different fMRI activations when exposed to water-related and drug-related cues. *Drug Alcohol Depend,* **83,** 157-62.

Yalachkov Y, Kaiser J, Görres A, Seehaus A and Naumer Mj (2013) Sensory modality of smoking cues modulates neural cue reactivity. *Psychopharmacology (Berl),* **225,** 461-71.

Yalachkov Y, Kaiser J and Naumer Mj (2009) Brain regions related to tool use and action knowledge reflect nicotine dependence. *J Neurosci,* **29,** 4922-9.

Yalachkov Y, Kaiser J and Naumer Mj (2010) Sensory and motor aspects of addiction. *Behav Brain Res,* **207,** 215-22.

Yalachkov Y, Kaiser J and Naumer Mj (2012) Functional neuroimaging studies in addiction: multisensory drug stimuli and neural cue reactivity. *Neurosci Biobehav Rev,* **36,** 825-35.

Ye M, Yang T, Qing P, Lei X, Qiu J and Liu G (2015) Changes of Functional Brain Networks in Major Depressive Disorder: A Graph Theoretical Analysis of Resting-State fMRI. *PLoS One,* **10,** e0133775.

Yokum S, Gearhardt An, Harris Jl, Brownell Kd and Stice E (2014) Individual differences in striatum activity to food commercials predict weight gain in adolescents. *Obesity (Silver Spring),* **22,** 2544-51.

Yokum S and Stice E (2013) Cognitive regulation of food craving: effects of three cognitive reappraisal strategies on neural response to palatable foods. *Int J Obes (Lond),* **37,** 1565-70.

Yu C, Zhou Y, Liu Y, Jiang T, Dong H, Zhang Y and Walter M (2011) Functional segregation of the human cingulate cortex is confirmed by functional connectivity based neuroanatomical parcellation. *Neuroimage,* **54,** 2571-81.

Zanchi D, Brody Al, Montandon Ml, Kopel R, Emmert K, Preti Mg, Van De Ville D and Haller S (2015) Cigarette smoking leads to persistent and dose-dependent alterations of brain activity and connectivity in anterior insula and anterior cingulate. *Addict Biol,* **20,** 1033-41.

Zangen A, Roth Y, Voller B and Hallett M (2005) Transcranial magnetic stimulation of deep brain regions: evidence for efficacy of the H-coil. *Clin Neurophysiol,* **116,** 775-9.

Zapparoli L, Seghezzi S and Paulesu E (2017) The What, the When, and the Whether of Intentional Action in the Brain: A Meta-Analytical Review. *Front Hum Neurosci,* **11,** 238.

Zeng H, Su D, Wang P, Wang M, Vollstädt-Klein S, Chen Q and Ye H (2018) The Action Representation Elicited by Different Types of Drug-Related Cues in Heroin-Abstinent Individuals. *Front Behav Neurosci,* **12,** 123.

Zhang J, Berridge Kc, Tindell Aj, Smith Ks and Aldridge Jw (2009) A neural computational model of incentive salience. *PLoS Comput Biol,* **5,** e1000437.

Zhang J, Wang J, Wu Q, Kuang W, Huang X, He Y and Gong Q (2011) Disrupted brain connectivity networks in drug-naive, first-episode major depressive disorder. *Biol Psychiatry,* **70,** 334-42.

Zhang P, Liu Y, Lv H, Li My, Yu Fx, Wang Z, Ding Hy, Wang Lx, Zhao Kx, Zhang Zy, Zhao Pf, Li J, Yang Zh, Zhang Zt and Wang Zc (2019) Integration of Neural Reward Processing and Appetite-Related Signaling in Obese Females: Evidence From Resting-State fMRI. *J Magn Reson Imaging,* **50,** 541-551.

Zhang S, Zhornitsky S, Angarita Ga and Li Cr (2018) Hypothalamic response to cocaine cues and cocaine addiction severity. *Addict Biol,* **25,** e12682.

Zhao X, Liu Y, Wang X, Liu B, Xi Q, Guo Q, Jiang H, Jiang T and Wang P (2012) Disrupted small-world brain networks in moderate Alzheimer's disease: a resting-state FMRI study. *PLoS One,* **7,** e33540.

Ziauddeen H, Farooqi Is and Fletcher Pc (2012) Obesity and the brain: how convincing is the addiction model? *Nat Rev Neurosci,* **13,** 279-86.

Ziauddeen H and Fletcher Pc (2013) Is food addiction a valid and useful concept? *Obes Rev,* **14,** 19-28.

Zijlstra F, Veltman Dj, Booij J, Van Den Brink W and Franken Ih (2009) Neurobiological substrates of cue-elicited craving and anhedonia in recently abstinent opioid-dependent males. *Drug Alcohol Depend,* **99,** 183-92.

Acknowledgements

spent together, from the breaks at the vending machines to the Saturday afternoons at the hospital.

This whole experience would have had a different flavor without you.

Thank you Desirèe for breaking the Guinness World Record for the longest Skype calls with me: thanks for being always *with* me and *for* me, for your precious friendship, and for your patience in dealing with my wild, doubtful mind. Thank you Gianluca for having shared with me not only the funniest, but also the most insightful moments of my PhD. Thanks for your hospitality in Zurich, and for being an important part of my personal and professional growth.

I am also extremely grateful to my friend, and flat mate, Luigi Praino: thank you for appreciating the best and the worst parts of me, day after day. I am truly lucky to have met you. Thank you to also to all of my friends that contributed to the most unforgettable moments of my PhD, outside of the lab: thank you Nicolò, Federico, Guenda, Stefano, Paolino, Massimone, Tanaya, Marco Crevani, Marco Malfichindemi, and Federica.

Finally, to Andrea. Thank you for being with me through the highs and lows of the past two years, and for always having a kind word to tell me; for all the time you spent watching and listening to my Power Point presentations, or to the clicking noise of my keyboard, at odd hours.

Thank you for taking part to this journey with me.